

TECHNISCHE UNIVERSITÄT MÜNCHEN

Lehrstuhl für Strahlenbiologie

Fakultät für Medizin

Low- and high-dose irradiation effects on microvascular endothelial cells of different origin (tumor and normal tissues)

Jos Philipp

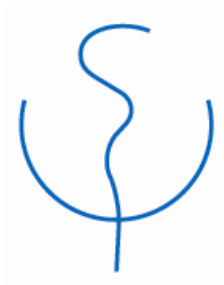
Vollständiger Abdruck der von der Technischen Universität München zur Erlangung des akademischen Grades eines Doktors der Naturwissenschaften (Dr. rer. nat.) genehmigten Dissertation.

Vorsitzende*r: Prof. Dr. Wolfgang Weber

Prüfer*innen der Dissertation:

1. Priv.-Doz. Dr. Soile Tapio
2. Prof. Dr. Gabriele Multhoff

Die Dissertation wurde am 30.03.2021 bei der Technischen Universität München eingereicht und durch die Fakultät für Medizin am 13.07.2021 angenommen.



Doctoral Thesis

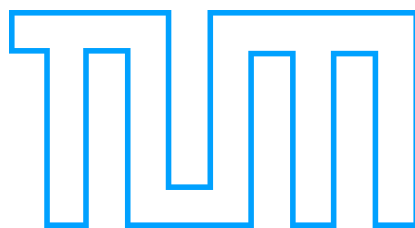
TECHNISCHE UNIVERSITÄT MÜNCHEN

Chair of Radiation Biology

Faculty of Medicine

Low- and high-dose irradiation effects on microvascular endothelial cells of different origin (tumor and normal tissues)

Jos Philipp



Diese Arbeit ist meinem Bruder Adrian gewidmet.

This work is dedicated to my brother Adrian.

This PhD thesis was written at the Institute of Radiation Biology of the Helmholtz Center Munich. Therefore I would like to thank all persons involved for their help.

Special thanks go to my supervisor and mentor PD Dr. Soile Tapio, who gave me the opportunity to do my PhD at the ISB. She supported me personally, never tired of pushing me to turn my studies into publications. Rather, she also supported me in attending further education and training courses. I also thank her for her initiative, so that I was able to present my projects in talks at two international congresses and to cooperate internationally.

I would also like to thank the director of the institute, Prof. Dr. Michael J. Atkinson, to give me the opportunity for the PhD study at the ISB and for his suggestions, corrections and criticism of projects. Furthermore, he was always at hand with advice.

I also have a lot to thank my research group. Especially Dr. Omid Azimzadeh, Daniela Hladik and Dr. Prabal Subedi, I had many constructive discussions to set up studies and discuss results. As a result, the studies and projects gained in sharpness and content.

Furthermore, I would like to thank my second supervisor Prof. Dr. Gabriele Multhoff, who was always available for help and advice in the Thesis Committee meetings and who was able to help in a pragmatic way.

I would also like to thank the group leaders of the ISB Dr. Michael Rosemann, PD Dr. Simone Mörtl, Dr. Natascha Anastasov, as well as the cooperation partners Dr. Juliane Merl-Pham and Dr. Christine von Törne for their scientific support and advice.

Special thanks go to my colleagues Martina Matjanovski, Daniela Hladik, Prabal Subedi and Michael Schneider for relax and fun time moments in and outside the laboratory.

Last but not least, I would also like to thank the ISB technical staff Rosemarie Kell, Stefanie Winkler and Klaudia Winkler. It was a pleasure to work with you and I was very grateful for all your help.

Zusammenfassung.....	7
Summary.....	10
Table of abbreviations.....	13
List of figures.....	17
1. Introduction	19
1.1 Ionizing radiation	19
1.1.1 X- and γ -rays.....	19
1.1.2 Reactive oxygen species (ROS) generation.....	20
1.2 Atomic bombing and nuclear accidents.....	22
1.2.1 Occupational radiation exposure.....	23
1.2.2 Clinical radiation exposure.....	23
1.3 Endothelial cells.....	24
1.3.1 Historical classification	24
1.3.2 Shape and structure.....	25
1.3.3 Function	27
1.3.4 Radiation-induced endothelial dysfunction.....	28
1.3.5 Radiation-induced inflammation.....	29
1.3.6 Radiation-induced senescence.....	31
1.3.7 Irradiation-induced bystander effect.....	32
1.4 Proteomics and mass spectrometry.....	32
1.4.1 Data dependent acquisition (DDA).....	35
1.4.2 Data independent acquisition (DIA).....	35
1.4.3 Label free quantification	36
1.4.4 Endothelial irradiation proteomics.....	36
1.5 Scientific classification and working hypothesis.....	37
2. Methodological aspects for the analysis of radiation-induced effects on endothelial cells.....	38
2.1 Cell culture irradiation	38
2.1.1 Mouse irradiation.....	39
2.1.2 Protein preparation.....	40
2.2 LC-MS/MS measurement.....	41
2.2.1 Label-free quantification of generated MS/MS data	42
2.2.2 Statistical analysis of the generated proteomics data	43
2.2.3 Bioinformatics data interpretation	44

2.3 Evaluation of proteomics data	44
2.3.1 Protein targeting with immunoblotting.....	45
2.3.2 Luminex® based antibody detection.....	45
2.3.3 Gene expression analysis.....	45
3. Results and Publications	47
3.1 Radiation-Induced Endothelial Inflammation Is Transferred via the Secretome to Recipient Cells in a STAT-Mediated Process.....	47
3.1.1 Aim and Summary.....	47
3.1.2 Contribution to the study	48
3.1.3 Publication.....	49
3.2 Data-independent acquisition mass spectrometry of irradiated mouse lung endothelial cells reveals a STAT-associated inflammatory response	64
3.2.1 Aim and Summary.....	64
3.2.2 Contribution to the study	64
3.2.3 Publication.....	65
3.3 Radiation response in HCECest2 revealed a central role for cGAS/STING pathway in the development of chronic inflammation.....	76
3.3.1 Aim and Summary.....	76
3.3.2 Contribution to the study	76
3.3.3 Publication.....	77
4. Conclusion and Discussion	95
4.1 Direct irradiation damage on endothelial cells	96
4.2 Irradiation-induced inflammation	96
4.2.1 Innate immune response via cGAS/STING-pathway	97
4.2.2 Type I Interferon response and its consequences.....	99
4.2.3 Role of STAT1 and STAT3.....	101
4.2.4 ISG15 a potential biomarker for radiation-induced inflammation?.....	102
4.3 Bystander effects in human endothelial coronary artery endothelial cells after irradiation.....	103
4.4 Irradiation induces senescence by chronic inflammation.....	105
4.5 Oxidative stress after irradiation.....	106
4.6 Low dose effects on endothelial cells.....	106
4.7 How DNA damage, senescence and inflammation come together	108
Bibliography	110

Zusammenfassung

Ionisierende Strahlung ist ein Bestandteil des menschlichen Seins. Verstärkt tritt sie in der Luft- und Raumfahrtindustrie oder an Orten schwerer Unfälle auf. Gleichzeitig wird sie in der Medizin zur Diagnose mittels bildgebender Verfahren und zur Behandlung schwerer Krankheiten wie Krebs eingesetzt. Hierbei steht ihr Nutzen außer Frage. Nichtsdestotrotz zeigen sich bei der erfolgreichen Behandlung der entsprechenden Tumore lange nach Bestrahlung vermehrt Nebenwirkungen wie sekundäre Tumorerkrankungen und kardiovaskuläre Erkrankungen. Sie sind eine Folge der Bestrahlung gesunden Normalgewebes mit moderaten bis hohen Dosen um noch vorhandenes malignes Gewebe abzutöten. Diese Nebenwirkungen werden durch bessere Behandlungsmethoden und geringere aber effektivere Strahlendosen reduziert. Dennoch zeigen auch epidemiologische Studien zum Beispiel an den Überlebenden der Atombombenabwürfe über Japan bei sehr geringen Dosen Folgeerkrankungen des kardiovaskulären Systems. Die molekularen Hintergründe dieser Entwicklungen sind sowohl für moderate und hohe Dosen als auch für niedrige Dosen weitgehend unbekannt.

Das Ziel der vorgelegten Arbeit ist die Auswirkungen radioaktiver Strahlung auf Endothelzellen zu untersuchen. Diese Zellen bilden die Wand eines Blutgefäßes in malignem und gesundem Gewebe aus und sind für den vaskulären Tonus verantwortlich. Sie sind passiv und aktiv am Austausch von Stoffen zwischen Blut und Gewebe beteiligt, leiten Immunzellen zu geschädigtem Gewebe und sezernieren verschiedenste Proteine in parakriner und endokriner Art und Weise. Schädigungen wie durch Bestrahlung können zu dysfunktionalen Verhalten der Zellen führen und sind damit mitverantwortlich für die Genese der kardiovaskulären Erkrankungen. Der Fokus dieser Arbeit liegt auf der Aufklärung molekularer Mechanismen der dysfunktionalen Entwicklung bestrahlter Endothelzellen.

Die Ergebnisse der folgenden Studien lassen einen entzündungsfördernden Effekt nach einmaliger moderater oder hoher Dosis eine bzw. zwei Wochen nach Bestrahlung im Proteom einer humanen Endothelzelllinie erkennen. Gleichzeitig geht die Zahl der Endothelzellen unmittelbar nach Bestrahlung zurück und die überlebenden Endothelzellen vergrößern ihren Zellkörper. Studien haben gezeigt,

dass Endothelzellen zwei Wochen nach Bestrahlung mit einer hohen Dosis von 10 Gy seneszent sind. In dieser Arbeit konnte zusätzlich gezeigt werden, dass eine Herunterregulierung der oxidativen Stressproteine, sowie eine Hochregulierung von hemmenden Zellzyklusproteinen stattfindet. Die Entzündungsmarker zeigen, dass die angeborene Immunantwort, der sogenannte cGAS/STING-Signalweg, etwa eine Woche nach Bestrahlung der Endothelzellen hochreguliert ist und damit eine tragende Rolle in der Entzündungsbildung spielen könnte. Weiterhin zeigen verschiedene Marker eine Hochregulierung der Typ I Interferon-Antwort insbesondere mit den Proteinen ISG15, ICAM1 und STAT1. Die frühzeitige Seneszenz und Indizierung einer Entzündung kann in einen chronischen Verlauf übergehen. Beides kann dann zur Dysfunktion der Endothelzellen führen.

Ein wichtiges Merkmal seneszenter Endothelzellen sind sekretierte Proteine wie IL-6, IL-8 und MCP1. Diese Marker konnten wir im Sekretom bestrahlter Endothelzellen zwei Wochen nach einer Hochdosis-Bestrahlung (10 Gy) feststellen. Weiterhin zeigte das Sekretom der Endothelzellen immun-modulatorische Signalwege. Nach Inkubation dieses Sekretoms mit nicht bestrahlten, allerdings gleich alten Endothelzellen konnten wir feststellen, dass in den Empfänger-Zellen der STAT3-Signalweg aktiviert wurde, welcher in die Immunantwort involviert ist. Somit konnten wir zeigen, dass mit einer hohen Dosis bestrahlte, seneszente Endothelzellen durch sekretierte Proteine eine Immunantwort in endokriner und parakriner Art und Weise in weitere nicht-bestrahlte Endothelzellen transferiert werden kann.

Die Indizierung dieser entzündlichen Signalwege konnten wir nach einer Woche und 10 Gy Bestrahlung des Thorax in isolierten und kultivierten Lungenendothelzellen der Maus bestätigen. Auch hier fanden wir die vorgenannten Entzündungsmarker hochreguliert vor. Gleichzeitig waren auch die oxidativen Stressproteine herunterreguliert.

In der mit niedrigen Dosen von 0,25 Gy und 0,5 Gy bestrahlten Endothelzelllinie konnten wir allerdings keine Deregulierung der vorgenannten Proteine nach einer Woche feststellen. Dies lässt aber keine Aussage über längerfristige Effekte der niedrigen Dosen zu.

Alles in allem zeigen diese Daten, dass hohe Dosen von 2 Gy und 10 Gy ionisierender Strahlung Endothelzelllinien und primäre Endothelzellen schädigen.

Sie entwickeln Seneszenz und einen pro-entzündlichen Phänotyp. Weiterhin induzieren sie eine angeborene Immunantwort, welche durch sekretierte Proteine auf weitere Zellen übertragbar ist. Daher ist es wichtig die frühzeitige Indizierung der Entzündung zu verhindern um den Schaden auf die Endothelzellen zu verringern. Gleichzeitig kann so das umliegende nicht bestrahlte Gewebe geschützt werden. Dies kann auch mögliche chronische Schäden verringern und somit die Dysfunktion des Endotheliums reduzieren oder gar verhindern.

Die Erforschung der niedrigen Dosen muss nichtsdestotrotz verstärkt werden um Fragen im Strahlenschutz zum Beispiel über mögliche Schwellenwerte zu beantworten.

Summary

Ionizing radiation is a part of human existence. It is increasingly encountered in the aerospace industry or at sites of serious nuclear accidents. At the same time, it is used in medicine for diagnosis by means of imaging procedures and for the treatment of serious diseases such as cancer. Here, its usefulness is beyond question. Nevertheless, long after successful tumor treatment with irradiation, side effects such as secondary tumor diseases and cardiovascular diseases become increasingly apparent. They are a consequence of irradiation not only of the malignant tissue but also of the adjacent healthy normal tissue with moderate to high doses. These side effects are reduced by better treatment methods and lower but more effective radiation doses. Nevertheless, epidemiological studies, for example, on the survivors of the atomic bombings over Japan, also show secondary diseases of the cardiovascular system at very low doses. The molecular background of these developments is largely unknown for moderate and high doses as well as for low doses.

The aim of the presented work is to study the effects of ionizing radiation on endothelial cells. These cells form the wall of a blood vessel in malignant and healthy tissue and are responsible for vascular tone. They are passively and actively involved in the exchange of substances between blood and tissue, direct immune cells to damaged tissue, and secrete a wide variety of proteins in a paracrine and endocrine manner. Damage such as that caused by irradiation can lead to dysfunctional behavior of the cells and is thus partly responsible for the genesis of cardiovascular disease. The focus of this work is to elucidate molecular mechanisms of dysfunctional development of irradiated endothelial cells.

The results of the following studies indicate a pro-inflammatory effect after a single moderate or high dose one or two weeks after irradiation in the proteome of a human endothelial cell line. At the same time, the number of endothelial cells decreases immediately after irradiation and the surviving endothelial cells increase their cell body size. Studies have shown that endothelial cells are senescent two weeks after irradiation with a high dose of 10 Gy. In this work, it was additionally shown that there is a downregulation of oxidative stress proteins, as well as an upregulation of

inhibitory cell cycle proteins. The inflammatory markers show that the innate immune response, the so-called cGAS/STING pathway, is upregulated approximately one week after irradiation of endothelial cells and thus might play a major role in inflammation formation. Furthermore, several markers of the type I interferon response, in particular the proteins ISG15, ICAM1, and STAT1, show upregulation. Early senescence and induction of inflammation may progress to a chronic progression. Both can then lead to endothelial cell dysfunction.

An important feature of senescent endothelial cells is the secretion of proteins such as IL-6, IL-8, and MCP1. We detected these markers in the secretome of irradiated endothelial cells two weeks after high-dose irradiation (10 Gy). Furthermore, the secretome of endothelial cells indicated induction of immunomodulatory signaling pathways. After incubation of this secretome with non-irradiated but equally aged endothelial cells, we found that the STAT3 signaling pathway, which is involved in the immune response, was activated in the recipient cells. Thus, we could show that high-dose irradiated senescent endothelial cells can transfer an immune response in an endocrine and paracrine manner into further non-irradiated endothelial cells by secreted proteins.

We were able to confirm the induction of these inflammatory signaling pathways in isolated and cultured mouse lung endothelial cells one week after irradiation of the thorax using 10 Gy (X-ray). Here, too, we found the aforementioned inflammatory markers to be upregulated. At the same time, oxidative stress proteins were also downregulated.

However, in the endothelial cell line irradiated with low doses of 0.25 Gy and 0.5 Gy, we could not detect any deregulation of the aforementioned proteins after one week. However, this does not allow any conclusion on long-term effects of the low doses.

All in all, these data show that high doses of ionizing radiation (2 Gy, 10 Gy) damage endothelial cell lines and primary endothelial cells. They develop senescence and a pro-inflammatory phenotype. Furthermore, they induce an innate immune response, which is transmissible to other cells by secreted proteins. Therefore, it is important to prevent the early induction of inflammation and thus reduce the damage to the endothelial cells. At the same time, the surrounding non-irradiated tissue can be protected in this way. This may also reduce potential chronic damage and reduce

associated dysfunction of the endothelium. Nevertheless, research on low doses needs to be intensified in order to answer questions in radiation protection, e.g. about possible threshold values.

Table of abbreviations

ACN	Acetonitrile
AGC	Automatic gain control
AHF	Anti-hemophilic factor
Al	Aluminium
AMP	Adenosine monophosphate
ANOVA	Analysis of variance
ApoE	Apolipoprotein E
ATP	Adenosine triphosphate
BCA	Bicinchoninic assay
CAM	Cell adhesion molecule
CAT	Catalase
CCL2	C-C motif chemokine 2 (same as MCP1)
CD31	Cluster of differentiation 31 (PECAM1)
CD44	CD (Cluster of differentiation) 44 antigen
cGAMP	Cyclic guanosine monophosphate-adenosine monophosphate
cGAS	Cyclic GMP-AMP synthase
CID	Collision-induced dissociation
Cu	Copper
CVD	Cardiovascular disease
DAMP	Damage associated molecular pattern
DDA	Data dependent acquisition
DDR	DNA damage response
DIA	Data independent acquisition
DNA	Deoxyribonucleic acid
DSB	Double strand breaks
dsDNA	Double stranded Deoxyribonucleic Acid
EA.hy926	Fusion product of HUVEC cells with epithelial lung tumor cell line A549-8
EC	Endothelial cell
ECL	Enhanced chemiluminescence
ER	Endoplasmic reticulum

FASP	Filter-aided sample preparation
FDR	False discovery rate
FLASH	Ultra-high dose rate radiotherapy
G-CSF	Granulocyte colony stimulating factor
GMP	Guanosine monophosphate
GPX	Glutathione peroxidase
GTP	Guanosine triphosphate
Gy	Gray
HCAEC/	Human coronary endothelial cell line
HCECest2	
HCD	Higher-energy collision dissociation
HLA	Human leukocyte antigen
HLA-B, C	HLA class I histocompatibility antigen (human leukocyte antigen B, C)
HMEC-1	Human dermal microvascular endothelial cell line
HR	Homologous recombination
HRM	Hyper reaction monitoring
HUVEC	Human umbilical vein endothelial cells
H2-D1	H-2 class I histocompatibility antigen D (mouse homolog to human HLA-B)
ICAM1	Intercellular adhesion molecule 1
IFN- γ	Interferon- γ
IL-6, 8, 10	Interleukin 6, 8, 10
IPA	Ingenuity pathway analysis
IRF3	Interferon regulatory factor 3
ISG15	Ubiquitin-like protein ISG15 (Interferon-induced 15 kDa protein)
JAK	Tyrosine protein kinase (Janus kinase)
LC-MS/MS	Liquid chromatography-tandem mass spectrometry
LDL	Low density lipoprotein
MAVS	Mitochondrial antiviral-signaling protein
MCP1	Monocyte chemoattractant protein 1 (same as CCL2)
MHC	Major histocompatibility complex
m/z	Mass to charge ratio
MS	Mass spectrometry

MX1	Interferon-induced GTP-binding protein MX1 (Myxoma resistance protein 1)
NF- κ B	Nuclear factor kappa-light-chain-enhancer of activated B cells
NHEJ	Non-homologous end joining
NK cell	Natural killer cell
NO	Nitric oxide
PCR	Polymerase chain reaction
PDGF-BB	Platelet derived growth factor, 2 subunits B
PECAM1	Platelet endothelial cell adhesion molecule 1
PET	Positron emission tomography
PMF	Peptide mass fingerprint
PRDX	Peroxiredoxin
PRDXN	Peroxiredoxin 5
p16 ^{INK4a}	Cyclin-dependent kinase inhibitor 2A
p21 ^{Cip1}	Cyclin-dependent kinase inhibitor 1
p38/MAPK	p38 mitogen-activated protein kinases
p53	Cellular tumor antigen p53 (tumor protein p53)
RB1	Retinoblastoma-associated protein
RIBE	Radiation-induced bystander effect
RNA	Ribonucleic Acid
ROS	Reactive oxygen species
SAHF	Senescence-associated heterochromatin foci
SASP	Senescence associated secretory phenotype
SOD	Superoxide dismutase
SOD	Superoxide dismutase 1
SSB	Single strand breaks
STAT	Signal transducer and activator of transcription
STAT1, 3	Signal transducer and activator of transcription 1, 3
STIM1	Stromal interaction molecule 1
STING	Stimulator of interferon genes protein
TBK1	Serine/threonine protein kinase TBK1 (TANK binding kinase1)
TLR	Toll-like receptor
TNF- α	Tumor necrosis factor α

TRX

Thioredoxin

vWF

von Willebrand factor

List of figures

Figure 1: Direct and indirect DNA damage by ionizing radiation. Radiation causes direct DNA damage by causing different types of breaks. Indirectly, the generation of radicals by hydrolysis of water as a consequence of irradiation leads to secondary DNA damage. Free radicals can be transferred via gap junctions to neighboring cells. The cells react to direct DNA damage by inducing DNA damage response (DDR) pathways and to indirect reactive oxygen species (ROS) damage by inducing oxidative stress response.

Figure 2: The uranium and thorium decay series. The radon isotope is marked in red to illustrate its intermediate state.

Figure 3: The structure of a healthy and radiation-damaged vessel. A illustrates the structure of a healthy endothelial layer with an intact endothelial layer. B illustrates radiation-induced damage on the structural components of the endothelial cells. The main characteristics in both cases are pointed out.

Figure 4: Visualization of the different steps of the rolling process enabling monocyte penetration through the endothelial layer.

Figure 5: The metamorphosis of the butterfly swallowtail symbolizing the difference between the genome and the proteome. The genome stays the same throughout all steps of development while the proteome changes step by step. Pictures of the developmental stages of the swallowtail were taken from.

Figure 6: The principle of mass spectrometry is an ion source followed by mass analyzer and a detector.

Figure 7: Design and conducted experiments of the three studies.

Figure 8: Response of endothelial cells on irradiation. Ionizing radiation induces DNA double strand breaks resulting in dsDNA fragments in the cytoplasm. The protein cGAS recognizes the dsDNA fragments initiating a cascade by producing cGAMP after dimerization. The protein STING is

activated by cGAMP and gets phosphorylated by TBK1. The phosphorylated STING in turn leads to the phosphorylation of IRF3 that translocates to the nucleus and initiates transcription of type I interferon responsive genes. Some target proteins are secreted or presented on the cell surface.

Figure 9: A damaged endothelial cell in a senescent state as a consequence of irradiation. After initiation of apoptosis the cell produces great amounts of signaling molecules such as IL-6 and DNA fragments that become released. IL-6 is then recognized by a receptor on an intact endothelial cell inducing a signaling cascade of p38/STAT3. STAT3 is translocated to the nucleus to initiate a type I interferon response. Furthermore, second messengers as cGAMP and ROS might influence directly neighboring endothelial cells by gap junction-mediated transport.

The images of the basic structure for cells, the blood vessel, mitochondria, and junction proteins were taken from Reactome icon library by a Creative Commons Attribution 4.0 International (CC BY 4.0) license (<https://reactome.org/icon-lib>, on 23.02.2021).

1. Introduction

Ionizing radiation is still the most common treatment for cancer and especially breast cancer (Early Breast Cancer Trialists' Collaborative Group (EBCTCG) 2005). Nevertheless, epidemiological studies on breast cancer patients reveal an increase of cardiovascular diseases long after radiotherapy (Hoening et al. 2007). The understanding and molecular reasons for this increased risk are not well understood. One potential mechanism might be chronic inflammation resulting in and from endothelial dysfunction of cardiac micro- and macrovasculature. Therefore, the induction, response and activation of the inflammatory immune response have been investigated. Thus, aim of the following cumulative doctoral thesis is to understand molecular inflammatory mechanisms as a consequence of ionizing radiation focusing on the inflammatory character of the proteome of endothelial cells. In the first study radiation-induced inflammatory markers in endothelial cells, their secretome and bystander cells were investigated. The second publication aimed to understand and identify radiation-induced inflammatory pathways in primary mouse lung endothelial cells. In the third manuscript the objective was to further elucidate the inflammatory pathways of the previous two studies, especially their time and radiation dose-dependency using a human coronary artery endothelial cell line. So, this cumulative thesis describes the results based on the proteomics data and discusses the possible mechanisms of the innate immune response after irradiation.

1.1 Ionizing radiation

1.1.1 X- and γ -rays

Ionizing radiation includes electromagnetic and particle radiation. Gamma- (γ) and x-rays are electromagnetic waves (photons) differing in their origin: γ -rays originate from the nuclear decay of radioactive isotopes, whereas x-rays are produced by electron collisions and rearrangements on the outer atomic shells. Consequently, they differ in their wavelength and energy: x-rays typically have a wavelength in the order of 10^{-9} m to 10^{-12} m (Atkins 2010), whereas γ -rays cover lower wavelengths of the length of approximately 10^{-13} m. Both x- and γ -rays can directly damage both normal and cancer cells and tissues. The amount of the radiation damage depends not only on the source and the total number of photons emitted in time, defined as

dose and dose rate but also on the nature of the target cells and tissues. The probability of damaging events increases with the radiation dose and dose rates of mGy/s but not for dose rates in as high as hundreds of Gy/s *in vivo*, which is called ultra-high dose rate (FLASH) radiotherapy (Vozenin, Hendry, and Limoli 2019). Whereas γ -rays can completely penetrate the human body thereby leading to deep radiation injury, the x-rays deliver their radiation damage 2-4 cm after entry in the body. Thereafter, a decrease in the delivered energy occurs in a nearly exponential manner.

In contrast to electromagnetic radiation, that has a negligible mass and no electric charge, severe local damage is caused by particle radiation that is able to induce secondary electron build up. Comparing the consequences induced by α -particles to x-rays, the damage to endothelial cells was measured to be 14 times higher in the former case by comparing the effectiveness of ^{210}Po exposure versus the effect of the same dose of x-rays in bovine endothelial cells (Thomas et al. 2003). However, since photon radiation penetrates tissues much deeper than particle radiation and shows a low correlation to a linear scattering, the damage is spread to a much larger area (Pouget and Mather 2001). The dose and the deposited energy are the central parameters when cellular damage is evaluated. In this thesis, I have used the unit Gray (Gy) which is defined as absorbed kinetic energy within a defined mass (Joule/kg).

1.1.2 Reactive oxygen species (ROS) generation

Ionizing radiation can directly damage macromolecules such as DNA, RNA, proteins and lipids. Radiation directly accounts for 30-40 % of damaging effects, whereas radicals induced by radiation-generated hydrolysis account for the other 60-70 % (Ward 1988). The radiation-induced DNA damage comprise double strand breaks (DSB), single strand breaks (SSB), and base and sugar damages. If not repaired, the DNA damage will induce impending cell death or incorrect repair leading to carcinogenic DNA mutations. The main pathways for DNA repair are homologous recombination (HR), mainly responsible for SSBs, and non-homologous end joining (NHEJ) that mainly corrects DSBs. Homologous recombination is based on the stretch of the sister chromatid that serves as a template for the broken one. Therefore, non-homologous end joining is not as accurate and is based on the ligation of the two broken ends. The survival of irradiated cells depends highly on the

phase of DNA replication. Further, the state of DNA replication also affects the type of DNA repair after irradiation (Hinz et al. 2005).

Since the cells contain mainly water, the exposure to electromagnetic waves such as x- and γ-rays leads to the excitation of water molecules, starting the radiolysis process thereby producing reactive radicals like $\cdot\text{OH}$, free electrons and $\text{H}\cdot$. In the second step, those free radicals and electrons attack water molecules and oxygen which leads to the production of the superoxide radical $\text{O}_2^{\cdot-}$, H_2O_2 , $\text{OH}\cdot$, $^1\text{O}_2$ and other reactive oxygen species (ROS; Figure 1). Most likely, the strand breaks occur due to the transfer of the radical to the sugar moiety (Osman et al. 1991). Direct DNA damage and ROS formed by hydrolysis are immediate effects of radiation in cells and tissues. However, these can't explain the permanently increased ROS levels and the presence of oxidized lipids and proteins several weeks and months after the radiation exposure (Azimzadeh et al. 2015).

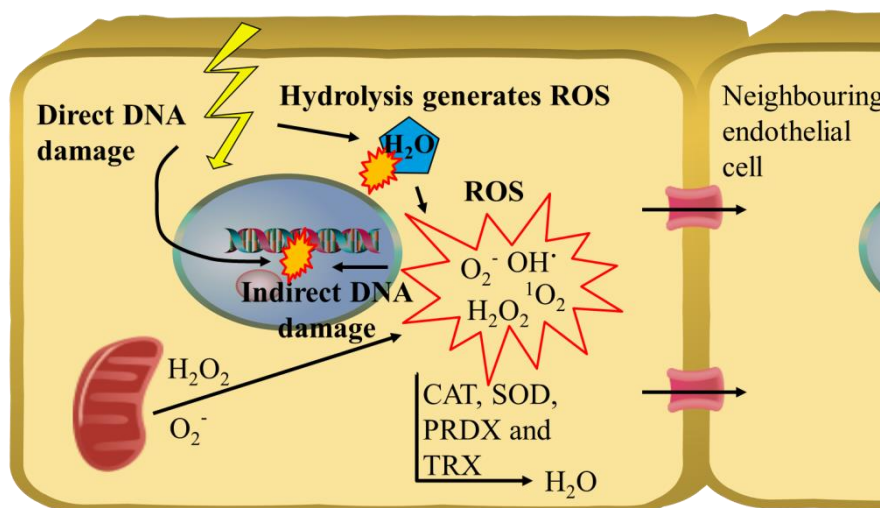


Figure 1: Direct and indirect DNA damage by ionizing radiation. Radiation causes direct DNA damage by causing different types of breaks. Indirectly, the generation of radicals by hydrolysis of water as a consequence of irradiation leads to secondary DNA damage. Free radicals can be transferred via gap junctions to neighboring cells. The cells react to direct DNA damage by inducing DNA damage response (DDR) pathways and to indirect reactive oxygen species (ROS) damage by inducing oxidative stress response.

One possible mechanism for permanently increased levels of ROS is the continuous production of free radicals by mitochondria (Figure 1) (Barjaktarovic et al. 2011). Mitochondrial ROS is mainly produced by the electron transport chain (Turrens 2003). Main product thereby is the $\text{O}_2^{\cdot-}$ (Chance, Sies, and Boveris 1979). This ROS production results in reduced mitochondrial function and lesions in the mitochondrial

DNA (Kawamura, Qi, and Kobayashi 2018). Particularly in endothelial cells the ROS can be transferred to neighboring cells via gap junctions (Hoorelbeke et al. 2020). To keep the level of free radicals low, cellular signaling pathways are activated to neutralize ROS. This is called oxidative stress response. Among proteins so induced are superoxide dismutases (SOD), glutathione peroxidases (GPX), catalase (CAT), peroxiredoxins (PRDX), and thioredoxins (TRX). However, after high radiation dose the cellular amount of these enzymes may become depleted due to high ROS levels and their expression seems to be downregulated (Han et al. 2018). It is yet unclear if they are upregulated immediately after the high-dose radiation but downregulated due to such depletion or later on.

1.2 Atomic bombing and nuclear accidents

We are constantly exposed to ionizing radiation in the form of so called background radiation. Background radiation is composed of terrestrial and cosmic radiation and varies depending, for instance, on the soil composition. Nuclear decay of elements naturally occurring in soil, rock, and water such as thorium and, uranium results in the release of Radon and isotopes (Marsac et al. 2016) (Figure 2).

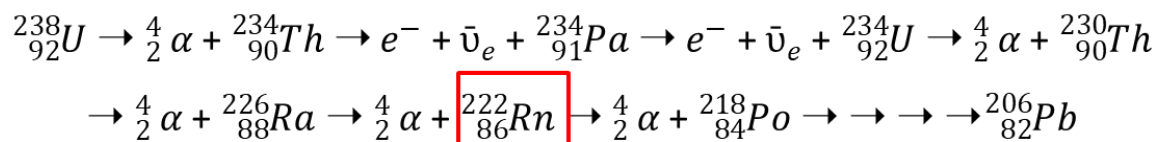


Figure 2: The uranium and thorium decay series. The radon isotope is marked in red to illustrate its intermediate state.

In a few occasions, large amounts of nuclear isotopes greatly exceeding the background radiation levels have been released into the atmosphere. Incidents such as the atomic bombings of Hiroshima and Nagasaki or accidents in nuclear power stations (Chernobyl and Fukushima) have resulted in elevated radiation exposure levels of large populations. Tragically, the epidemiological monitoring of these populations has been a great tool in understanding radiation effects in large cohorts. These data show that, in addition to linear dose-dependent increase in the incidence of several cancers, heart disease and stroke were the most relevant non-cancer-related causes of death (Shimizu et al. 2010; Yamada et al. 2005). So far, the causal

relationship between radiation exposure and these health outcomes is still unclear. One possible reason for this causality is radiation-induced inflammation, which has been shown in the cohorts (Neriishi, Nakashima, and DeLongchamp 2001; Hayashi et al. 2003).

1.2.1 Occupational radiation exposure

The nuclear workers at the Russian Mayak plutonium enrichment facility show an increased risk for ischemic heart disease in response to chronic low-dose-rate irradiation (Tamara V Azizova et al. 2015; Tamara V. Azizova et al. 2016; T. V. Azizova et al. 2018; T. Azizova et al. 2019). It has been suggested that disturbed heart metabolism could contribute to the disease (Azimzadeh et al. 2017). Furthermore, additional studies focusing on the risk for hypertension, atherosclerosis and lower extremity artery disease revealed a significant induction by radiation exposure (Simonetto et al. 2017) suggesting that radiation-induced damage of the endothelium plays an important role in the vascular abnormalities found in these cohorts.

In radiation facilities of hospitals, private doctor's offices and nuclear laboratories, medical and laboratory staff working with x-ray units, sealed high-radioactive sources and unsealed radioactive substances are exposed to chronic low-dose-rate radiation (Carnicer et al. 2011). Imaging methods such as positron-emission tomography (PET) result in low radiation exposure situation in medical staff as well (Bar-Ad et al. 2019). Similarly, radiological tracers for imaging purposes and in linear accelerators expose the working force to low-dose radiation (Keehan et al. 2016). Increased risk for cardiovascular disease has been found in these populations (Little et al. 2012; Little 2016; Boaventura et al. 2018; Tapio et al. 2021).

1.2.2 Clinical radiation exposure

Radiotherapy is one of the most common techniques to treat cancer. In contrast to medical staff, cancer patients are still receive local high dose radiation (Wennstig et al. 2020; Darby et al. 2013). Although highly effective in treating cancer, radiotherapy may result in adverse health outcomes by increasing incidence of secondary cancers and coronary artery diseases (Wennstig et al. 2019). Epidemiological evidence of radiation-induced cardiovascular disease by exposure to modern medical diagnostics is scarce. In addition, developments and constant improvements in

medical devices lead to lower doses during usage, which means that the additional dose is about as high as the background radiation (Baker, Moulder, and Hopewell 2011). Lifelong risk estimations, therefore, might need the time of the first generations that were permanently exposed to these medical devices. Thus, a proper knowledge of risks of these clinical implications concerning the very low doses needs to be assessed.

1.3 Endothelial cells

1.3.1 Historical classification

The endothelium has been investigated for a long time. Still, its function and role was for long unclear (Jones 1887). Rudolf Wagner observed already in 1839 that leukocytes or as he called them “lymph-corpuses” were slower moving and became “adhesive”, when close to the vessel wall in a grass frog (Wagner 1839). On the one hand, the endothelium was early identified as the layer of cells that forms the vessels (Kettle 1918). On the other hand, at that time the endothelium was defined as “a sheet of nucleated cellophane” as the Nobel laureate Lord Florey (Florey 1966) stated. Shortly after that, the first cell culture of human umbilical vein endothelial cells (HUVECs) derived from the umbilical cord was established and published by Jaffe et al. (Jaffe et al. 1973). This enabled the discovery of the so called anti-hemophilic factor (AHF) and one year later its binding partner von Willebrand factor (vWF) that are expressed in endothelial cells (Hoyer, de los Santos, and Hoyer 1973). These findings lead to the identification of endothelial cells in several human tissues. Furthermore, the discoveries of prostacyclin synthesis in endothelial cells (Moncada, Higgs, and Vane 1977), its role in vasodilation and blood pressure (Furchgott and Zawadzki 1980) and the expression of interleukin-1 receptors on their surface (McEver et al. 1989) demonstrated that the endothelium is an active tissue in general and it participates especially in inflammatory and immune response.

However, it took a long time to discover the causal relationship between radiation-induced endothelial cell damage and cardiovascular disease (CVD). Although it was recognized that radiotherapy of Hodgkin’s lymphoma resulted in increased incidence of CVD (Fajardo, Stewart, and Cohn 1968), a connection to the endothelium was not made. First experiments conducted on radiation and endothelial cells observed a reduced number of capillaries in the hamster cheek (Hopewell 1975). Thereby, a

loss of small but not large capillaries and arteries was observed after 22.5 and 25 Gy x-radiation. In parallel, experiments were conducted to measure the repair capacity, proliferation and, radiosensitivity of endothelial cells by metabolic labeling. In all investigated tissues, kidney, liver, brain, heart and skin, the proliferation rate was slow and the authors concluded no differences between the turnover-rate of endothelial cells of different origin (Hobson and Denekamp 1984). First, in the 90's long-term studies on Hodgkin's lymphoma patients and Japanese atomic bombing survivors revealed an increased rate of CVD, especially myocardial infarction (Reinders et al. 1999). Similar findings were published in breast cancer patients long after radiotherapy (Early Breast Cancer Trialists' Collaborative Group (EBCTCG) 2005). The mixture of experimental and epidemiological data made the endothelium an interesting target tissue for radiation-induced CVD research.

1.3.2 Shape and structure

“The main type of cell found in the inside lining of blood vessels, lymph vessels, and the heart”, is the definition for endothelial cells by the National Cancer Institute (NCI Dictionaries 2020). Endothelial cells are generated early in life via vasculogenesis or via angiogenesis, for the terminology describing the growth of vessels from embryo to the aged human. However, there are big differences between endothelial cells of different origin, in their shape, but also in their structural and functional characteristics depending on the organ and the location (Aird 2007). Nevertheless, all endothelial cells have two aspects in common. They are polarized and base their energy metabolism on glycolysis. This is characterized by a reduced number of mitochondria (Groschner et al. 2012). In the human body, there is an endothelial surface area of more than 1000 m² in total (Jaffe 1987), including the structure of the vessels up to 3000-6000 m² (Krüger-Genge et al. 2019) formed by estimated 1 to 6x10¹³ endothelial cells. The differences in endothelial cells of different origin start with their thickness, which ranges from around 0.1 µm in the capillaries to around 1 µm in the arteries (Florey 1966). Therefore, they are called micro- and macrovascular endothelial cells. In addition, the length of endothelial cells is greater in the aorta as in the veins, whereas the endothelial cells in the veins are broader. Furthermore, also a different alignment according to the blood flow has been observed, very strong in the aorta and in the veins whilst nearly no alignment has been found in the pulmonary trunk (Kibria et al. 1980).

Radiation exposure triggers changes in the endothelial cell shape and structure. In human coronary artery endothelial cells, a radiation-induced alteration in the morphology has been shown leading to increased cell size (Lowe and Raj 2014). Yet, an overall reduction of the cell number was observed after a dose of 10 Gy (X-ray) two weeks post radiation (Lowe and Raj 2014). In addition to morphological changes, surface markers are greatly altered by irradiation. High radiation doses mimicking those received by the normal tissue in radiotherapy (X-ray, 8 Gy) trigger an increased expression of several adhesion proteins on the endothelial surface in mouse heart and lung microvascular endothelial cells 10, 15 and 20 weeks after the exposure (Sievert et al. 2015). In ApoE knockout mice, which are prone to atherosclerosis, lesions in the carotid artery vessels were found 22-35 weeks post radiation using a single 14 Gy x-ray dose to the neck region (Stewart et al. 2006). Receptors of the MHC class I, important in the immediate immune response, were overexpressed in macrovascular HUVEC and EA.hy926 cells, result of a fusion of HUVEC cells with the epithelial lung tumor cell line A549-8 (Edgell, McDonald, and Graham 1983), after a 4 Gy x-ray dose leading to a reduction of NK cell activation and thereby to increased survival (Riederer et al. 2010). In contrast, Riederer et al. could not find this effect in microvascular HMEC-1 cells, immortalized human dermal microvascular ECs (Ades et al. 1992). Similarly, TLR receptor expression that are of importance in the signaling of the innate immune system is induced by irradiation (Ratikan et al. 2015). At lower doses between 0.1 Gy and 2 Gy (X-ray) an increased expression of adhesive surface markers such as ICAM1 and others inducing leukocyte attachment was observed *in vitro* in HUVECs (Cervelli et al. 2014). Importantly, this suggested an increased adhesiveness of leukocytes to endothelial cells even at this dose range. These results indicate an increased adhesion after irradiation independent of the applied dose. However, low dose studies on adhesiveness after radiation exposure *in vivo* are scarce but are important to investigate the adhesion including the environment of the endothelial cells. Interestingly, in an experiment using label-free data-independent proteomics and stereotactic radiosurgery of brain arteriovenous malformations in mice, cytosolic and mitochondrial proteins were found located on the surface of brain endothelial cells after the dose of 20 Gy γ -radiation; these were later validated *in vitro* experiments (McRobb et al. 2017). All these radiation-induced changes in the shape and surface

structure of endothelial cells may result in their malfunctions and thereby contribute to the onset of CVD.

1.3.3 Function

As described previously, endothelial cells are lining vessels as a single monolayer, which forms the barrier between blood and every tissue in the body. As such, they are critically involved in signaling, adhesion and permeability. The main function of endothelial cells is keeping the blood flow constant by modulating the so-called vascular tone. This was the first described function for the endothelial layer (Furchgott and Zawadzki 1980). In order to fulfill this function, endothelial cells produce nitric oxide (NO) (Furchgott and Zawadzki 1980) by nitric oxide synthase. Together with Louis J. Ignarro and Ferid Murad, Robert F. Furchgott was awarded the Nobel Prize in 1998 for the discovery of NO. In tandem with other vasoactive metabolites such as prostacyclin (Moncada and Vane 1981), NO affects the smooth muscle cells and leads to vasodilation in large conduit vessels. In a similar fashion, the endothelium also secretes proteins to induce the narrowing of blood vessels vasoconstriction. Furthermore, the vascular tone is also affected by ROS produced by endothelial cells. The main player of ROS is H₂O₂ which is mainly produced in resistance arteries (Matoba et al. 2000).

Another main function of the endothelium is its permeability. It allows various molecules and even cells coming with the blood flow to pass the endothelium. While small molecules under 70 kDa and gases are able to diffuse *in vivo* (Egawa et al. 2013), proteins and molecules of higher molecular weight are actively transported. Therefore, two transport mechanisms have been observed: the transcellular mechanism via caveolae-mediated vesicular uptake and the paracellular mechanism through interendothelial junctions (Komarova and Malik 2010). In the transcellular pathway, proteins like albumin or LDL act as tracer molecules within vesicles (Tiruppathi et al. 1997; Ghitescu et al. 1988). The paracellular pathway is used for the transit of different types of immune cells but also for passive transport of small molecules.

Another functional aspect of endothelial cells is the recruitment of immune cells. For this function, the endothelium produces chemokines, type-I-interferon-responding proteins and interleukins (Slany et al. 2016; Philipp et al. 2017) to send signals in a

paracrine, autocrine and endocrine manner. To bind immune cells, cells adhesion molecules (CAM) are expressed on the cellular surface. The CAMs are strongly adhesive and allow arrest and crawling of immune cells through the endothelial barrier either in para- or transcellular way (Gerhardt and Ley 2015).

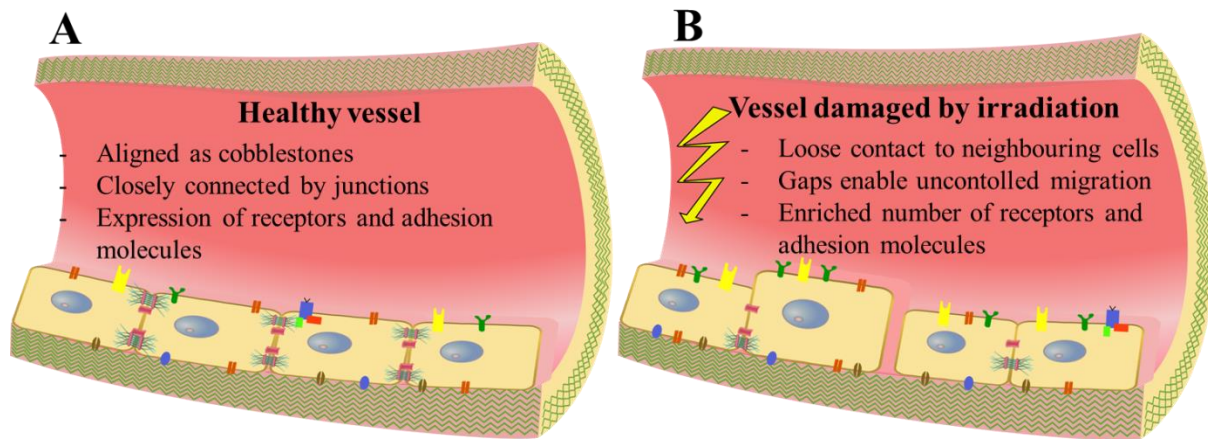


Figure 3: The structure of a healthy and radiation-damaged vessel. A illustrates the structure of a healthy endothelial layer with an intact endothelial layer. B illustrates radiation-induced damage on the structural components of the endothelial cells. The main characteristics in both cases are pointed out.

1.3.4 Radiation-induced endothelial dysfunction

Endothelial dysfunction is a non-obstructive pathological state of the endothelium preceding the development of CVD. This state is characterized by reduced vasodilation and production of pro-inflammatory and pro-thrombotic factors. On the molecular level, it is associated with reduced bioavailability of NO and increased oxidative stress, and production of inflammatory factors such as NF- κ B and STAT-proteins. This leads to enhanced expression of type I interferons and adhesion molecules presented on the cellular surface. Furthermore, endothelial cells secrete increasingly chemokines and interleukins and show increased permeability and a reduced number of gap junctions (Figure 3). The high number of adhesion molecules leads to increased docking of immune on the endothelial layer (Halcox 2012; Endemann 2004).

Radiation exposure is a risk factor for developing endothelial dysfunction. At high radiation doses, endothelial cells undergo cell cycle arrest and initiate apoptosis that may lead to cell death. Typically, however, many endothelial cells can escape

apoptotic death by developing premature senescence (Yingying Wang, Boerma, and Zhou 2016). As a consequence of radiation exposure, the endothelial layer loses its barrier function and gets increasingly permeable. In addition, dying and damaged endothelial cells release large numbers of immune-modulatory factors such as chemokines, cytokines and interferons, extracellular vesicles and damage associated molecular patterns (DAMPs) (Shan et al. 2007). The pro-inflammatory state itself is not toxic to the endothelial cell. However, a strong activation of the pro-inflammatory system by irradiation characterized by the immune system, and increased oxidative stress, can lead to excessive and uncontrolled release of immune-modulatory, pro-inflammatory factors contributing to endothelial dysfunction. A key consequence of the chronic pro-inflammatory state is an impairment of vasodilation (Beckman et al. 2001), coupled to reduced bioavailability of NO that has been shown in cardiac endothelial cells 16 weeks after local heart x-radiation with 8 or 16 Gy in C57Bl/6 mice (Azimzadeh et al. 2015). Endothelial dysfunction in general promotes atherosclerosis, thrombus formation, hypertension and artery and venous diseases leading to CVD (Moncada and Vane 1981). A similar mechanism can be valid in the case of radiation-induced CVD.

1.3.5 Radiation-induced inflammation

Inflammation is known as a process of reconstitution of diseased tissue using cells, cell compartments and biological and chemical molecules to combat pathogens and endogenous aberrations. In 2001, a study among A-bomb survivors suggested a statistically significant association between chronic inflammation and radiation dose (Neriishi, Nakashima, and Delongchamp 2001).

As mentioned earlier, irradiated endothelial cells are actively participating in the inflammatory response by releasing DAMPs and cytokines and chemokines. This induces migration of immune cells through the endothelial cell layer (N. Wu et al. 1994). The adhesion is mediated by cell adhesion molecule ICAM1 (Hallahan, Kuchibhotla, and Wyble 1996) and CD44 (Lowe and Raj 2014), that are both overexpressed in reaction to radiation-induced inflammation even long after radiation exposure (Azimzadeh et al. 2015; Sievert et al. 2015; Lowe and Raj 2014). Upstream mediators might be the NF- κ B pathway (Min et al. 2005) and the type I

interferon response (Philipp et al. 2017). This enables increased attachment of leukocytes and monocytes to the endothelial surface. Simultaneously, the endothelial barrier becomes leaky.

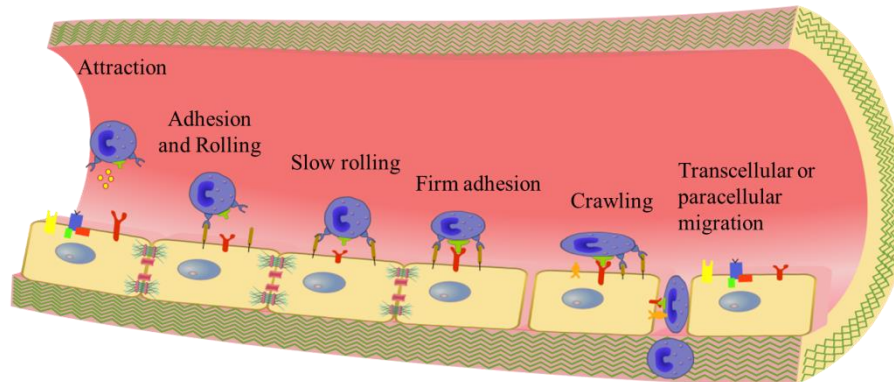


Figure 4: Visualization of the different steps of the rolling process enabling monocyte penetration through the endothelial layer.

Besides the activation of immune cells, increasing amount of data suggest an activation of the innate immune system after irradiation. The cGAS/STING-pathway is critically involved in the cellular response of the cytosolic double stranded DNA (dsDNA) recognition after irradiation (Li et al. 2013). Binding of dsDNA to cGAS leads to its oligomerization (Li et al. 2013). In turn, such oligo-cGAS-dsDNA complexes lead to the production of cyclic guanosine monophosphate-adenosine monophosphate (cGAMP) originating from ATP and GTP. This cGAMP then acts as a second messenger recognized by the target protein STING (J. Wu et al. 2013). STING is a protein embedded in the endoplasmic reticulum (ER) that dimerizes and gets activated by the binding of cGAMP, then translocating to the intermediate compartment between the ER and the Golgi together with the protein kinase TBK1 (Ishikawa and Barber 2008). Subsequently, the cGAMP-TBK1 phosphorylates IRF3 that dimerizes and translocates to the nucleus, activating the transcription of type I interferon related proteins (Ahn et al. 2012). The type I interferon response also includes proteins regulated by the JAK/STAT-pathway (Furusawa et al. 2016; Philipp et al. 2017). In addition, proteins of the type I interferon response such as ISG15, IL-6 and IL-8 are released into the blood stream by endothelial cells as a part of senescence associated secretory phenotype (SASP) (Bogunovic, Boisson-Dupuis, and Casanova 2013; Kojima et al. 2013). These findings suggest that there is a

close connection between innate immune signaling and DNA damage after irradiation.

1.3.6 Radiation-induced senescence

The term “senescence” was first coined by Hayflick in 1965, as an endpoint of the limited number of replications of *in vitro* cultured cells (Hayflick 1965). In this occasion, the term “replicative senescence” is used (Martin, Sprague, and Epstein 1970). After the last division the cell enters a cell cycle arrest but stays metabolically active.

In living organisms, we use the term “cellular senescence” (López-Otín et al. 2013). Cellular senescence is characterized by (1) a resistance towards apoptosis (E. Wang 1995), (2) an increased expression of tumor suppressors p53, RB1 and DNA damage-dependent and independent cell cycle inhibitors p16^{INK4a} and p21^{Cip1} (Serrano et al. 1997; Vogt et al. 1998; Shay 1991), (3) a cell growth up to a doubling of their size (Hayflick 1965), (4) an increased production of senescence-associated β-galactosidase (Dimri et al. 1995), (5) development of senescence-associated heterochromatin foci (SAHF) (Narita et al. 2003), and occurrence of DNA damage nuclear foci called DNA segments with chromatin alterations reinforcing senescence (Rodier et al. 2009) and (6) the SASP. SASP includes a vast number of proteins that are secreted in response to DNA damage (Lasry and Ben-Neriah 2015). In addition, several other pathways are induced that are not only relevant for the DNA damage response but also play a pivotal role in the senescence activation.

Senescence can also be triggered prematurely by ionizing radiation but also other factors (Rodier and Campisi 2011). Radiation-induced senescence is defined by an irreversible, permanent growth arrest in response to damaging and stress stimuli such as DNA damage, oxidative stress and others (Hernandez-Segura, Nehme, and Demaria 2018). Radiation induces senescence in a dose-dependent manner: The higher the dose the earlier the senescent state can be measured. The dose of 10 Gy (X-ray) results in a senescent state after 1-2 weeks in endothelial cell culture (Lowe and Raj 2014). It is important to understand the mechanism of radiation-induced SASP production and the effect of SASP in neighboring non-irradiated cells in order to prevent the spreading of pro-senescent and pro-inflammatory state in the endothelium.

1.3.7 Irradiation-induced bystander effect

SASP is one potential way of communication between irradiated and non-irradiated cells. The release of SASP components such as cytokines, chemokines, NO and other secreted molecules affect target cells in a remote non-irradiated tissue. This influence of irradiated cells and tissues on non-irradiated cells/tissues is called radiation-induced bystander effect (RIBE). The first observation of RIBE was made with α -particles in Chinese hamster ovary cells. Only 1 % of the cell nuclei were directly hit by α -particles but more than 30 % of all cells exhibited sister chromatid exchanges (Nagasawa and Little 1992). In addition to SASP, gap junctions have shown to play an important role in RIBE (see also Figure 1) (Zhou et al. 2001; Ramadan et al. 2020). Reactive oxygen and nitrogen species and NO in particular have been suggested as cellular mediators (Havaki et al. 2015; Iyer, Lehnert, and Svensson 2000). Recently, extracellular vesicles have been found to induce RIBE (Schey, Luther, and Rose 2015). The bystander cells are often dysfunctional and show increased inflammation, chromosomal aberrations, genomic instability, apoptosis and DNA damage (Morgan and Sowa 2007; Gaugler et al. 2007). Although of importance, the possible mechanisms of RIBE are still not fully understood.

1.4 Proteomics and mass spectrometry

Proteomics is a relatively new research field dedicated to the analysis of the proteome, all proteins which are expressed from the genome at a certain time point. It was coined in 1994 by Mark Wilkins (Wasinger et al. 1995). The same genome can express several different proteomes. This becomes clear when looking at different developmental stages of animals or insects.

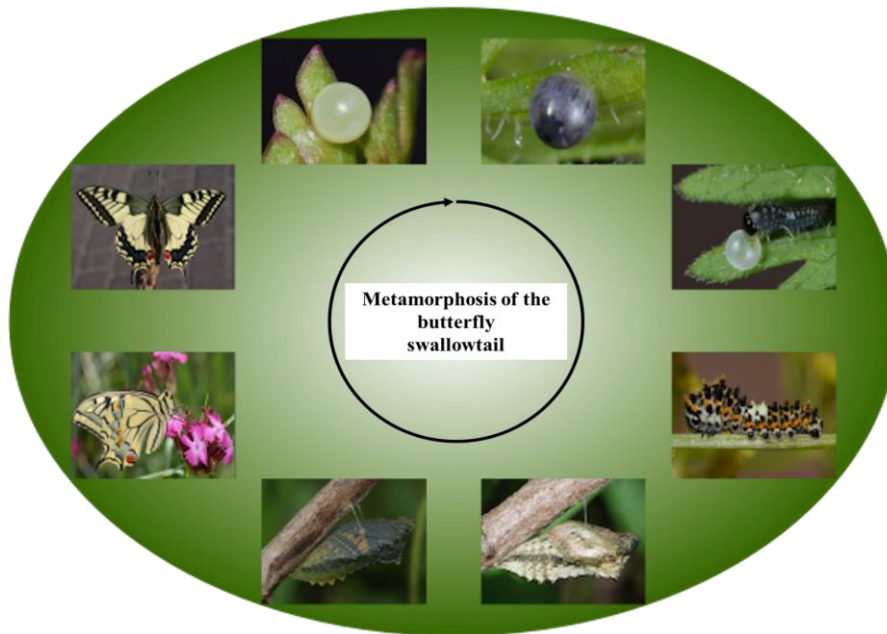


Figure 5: The metamorphosis of the butterfly swallowtail symbolizing the difference between the genome and the proteome. The genome stays the same throughout all steps of development while the proteome changes step by step. Pictures of the developmental stages of the swallowtail were taken from (BUND 2020).

As illustrated in figure 5, the development of the butterfly initially leads to a caterpillar which pupates. Hereafter, the actual butterfly hatches from this cocoon. During all these steps, the genome remains the same, whereas the proteome changes continuously and controls numerous biological processes. Here, for responsible are the different parameters such as dynamics, size and changes in the quantity of the proteome are responsible for the visible alterations (Wasinger et al. 1995).

Two main strategies are used for the quantitative analysis of the proteome. Firstly, the so-called top-down approach describes the analysis of the proteome based on intact proteins (Kelleher et al. 1998). Secondly, the so-called bottom-up approach involves an analysis on the peptide level (Andersen, Svensson, and Roepstorff 1996). In both techniques, tandem mass spectrometry coupled to liquid chromatographic separation has become the method of choice. Mass spectrometry is an analytical tool based on determining the mass of particles, which can be determined by the so-called mass-to-charge ratio (m/z) of the analyzed ions. Irrespective of the type of mass spectrometer used, it makes use of the fact that ions with different charges behave differently depending on their mass in an electric field and can therefore be analyzed selectively (Figure 6). Preceding the mass

spectrometry run, the proteins are cleaved so that it is known where the cleavage sites are located. A common approach for the lysis is to use the enzyme trypsin, which cleaves after arginine and lysine residues. The peptides are then separated *via* liquid chromatography according to their size and hydrophobicity. The peptides elute from the column after a certain time, the so-called retention time. This is followed by ionization. For this purpose, an electric field is applied to the tip of the capillary, in which first charged droplets are formed. They decay into ever smaller droplets in a reaction called Coulomb explosion until individual ions finally enter the gas phase. This behavior is triggered by the permanent evaporation of the solvent.

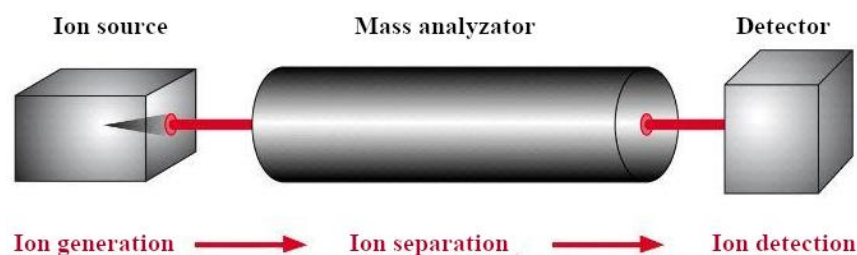


Figure 6: The principle of mass spectrometry is an ion source followed by mass analyzer and a detector (Friedrich Lottspeich and Joachim W. Engels 2006).

The ions are getting separated from impurities, will be focused in a quadrupole and a downstream ion trap. Thereafter, the peptides will be selected for fragmentation by several methods of which collision induced dissociation (CID) with helium and higher-energy collision dissociation (HCD) with nitrogen are the most common ones and becoming stored in ion traps. Finally, the fragments will be scanned with two consecutive scans in an Orbitrap mass analyzer (Hu et al. 2005). Thereby, the ions are oscillating around a frequently changing alternating and direct current. In this way, the ions can be selectively separated according to their m/z . Out of their oscillation characteristics the mass of the fragments can be calculated. The acquired spectra of the m/z characteristics are unique for the combination of protein and enzyme and therefore is called peptide mass fingerprint (PMF) (Henzel et al. 1989). The spectra are transferred to a peak list, analyzed by *de novo* sequencing and the resulting sequences are then searched against a protein sequence database. Verified by statistical methods, probabilities for matches with proteins are provided.

1.4.1 Data dependent acquisition (DDA)

In data dependent acquisition all ions of a certain m/z will be fragmented. In a first scan (MS1), the most abundant ions are selected for fragmentation. By reading out the resulting fragment ions using the Orbitrap in a second scan (MS2), a MS/MS spectrum is generated for each of the peptide ions. Subsequent database analysis or *de novo* sequencing allows the determination of the peptide sequences and the assignment to proteins. Since the information about the peptides is generated based on the MS1 scan and therefore on data, this method is called data dependent acquisition. DDA has the disadvantage, that it is limited in the precursor ion abundance, thus making it difficult to detect proteins of low abundance.

1.4.2 Data independent acquisition (DIA)

In contrast to DDA, a second method exists that scans the MS2 level independently of the existence of their precursor ions in the MS1 scan, which is called data independent acquisition DIA (Masselon et al. 2000). First of all, a spectral library of mass spectrometric and chromatographic parameters of peptides is generated by repeated DDA runs. For the DIA runs, selected narrow windows of a defined m/z range are then focused. All precursor ions detected within the particular window are fragmented and parallel analyzed. Systematically, the instrument goes window by window over the entire m/z range. Afterwards, the generated MS/MS data are queried against the generated library. Based on several vendors in the field of mass spectrometry instrumentation a couple of names for DIA-based approaches have been developed and due to trademarking issues have complicated the situation for the term DIA (Ludwig et al. 2018). However, the term described here is the so called hyper reaction monitoring (HRM) (Bruderer et al. 2015). This method combines the advantages of targeted proteomic approaches based on known mass spectrometric and chromatographic parameters in retention-time-normalized spectral libraries (Escher et al. 2012). For this purpose, 12 non-naturally occurring artificial peptides are spiked into the digested protein extract of choice at known absolute concentrations. The generated spectra are then realigned on these spiked in peptides, enabling a quantitation and quantification. Due to the window-based

screening and the independency of the MS1 level, DIA is more precise and accurate than DDA and has the advantage of unlimited protein detection.

1.4.3 Label free quantification

DDA dependent label free quantification is based on the peptide ion intensities. Here, identification only takes place at MS1 level (Megger et al. 2013). DIA in contrast, uses the same parameters for both, MS1 and MS2, levels. Nevertheless, the measured values are the maximum intensity or the area under the chromatographic peaks of the peptide ions. Each peptide has a mono-isotopic peak in the MS1 spectrum at a specific m/z ratio. The intensity of this peak as a function of retention time gives a chromatogram for the corresponding peptide ion (Extracted ion chromatogram). From the area below the chromatographic peak the abundance of the peptide can then be quantitatively determined. This is made possible by linear correlation of the intensity with the peptide abundance (Bondarenko, Chelius, and Shaler 2002). To make different samples comparable, the retention times must be adjusted due to experimental deviations of the chromatographic peaks. Deviations in the intensities can then be compensated for by normalization.

1.4.4 Endothelial irradiation proteomics

Research on irradiated endothelial cells, which use proteomics to unravel the mechanisms behind the radiation-induced damage, is a comparatively young field within the radiation biology. Main focus of the proteomics based endothelial radiation research is the heart in concern of cardiovascular disease as a consequence of radiotherapy. Since mechanisms are difficult to detect with non-omics methods, proteomics enables the identification of mechanisms on the level of action leading to the observed phenotypes. Results of proteomics studies revealed stress and senescence after induced DNA damage repair (Sriharshan et al. 2012). Chronic low dose irradiation (γ , 4.1 mGy/h) lead to the development of premature senescence with an activated p53-pathway as a result of the DNA damage response and the associated oxidative stress (Yentrapalli, Azimzadeh, Barjaktarovic, et al. 2013). Similarly, premature senescence was found in a long-term study after high dose irradiation on the heart of C57Bl/6 mice (X-ray, 8 and 16 Gy) (Azimzadeh et al.

2015). The same study also found lower NO availability, increased oxidative stress and an enhanced inflammatory response. All these discoveries were only possible through the use of proteomics. They enable to investigate the interaction of different malfunctions after irradiation simultaneously. Based on this, endothelial dysfunction could also be defined more precisely as a function of several malfunctions together.

The studies presented in this thesis follow this pattern and were conducted for the elucidation of the mechanisms behind radiation-induced inflammation and DNA damage. In addition, the inflammatory impact on paracrine and endocrine effects on neighboring cells was investigated. However, more studies using proteomics technology to identify potential pathways, mechanisms and the overall constitution of endothelial cells are necessary to provide approaches for in-depth analyses.

1.5 Scientific classification and working hypothesis

Irradiation is widely used to treat cancer such as breast cancer. Unfortunately years after successful treatment of breast cancer, patients develop several kinds of cardiovascular diseases. One of the main challenges long after irradiation is the development of endothelial senescence and dysfunction. To address this issue, this work was conducted using endothelial cell culture as well as mouse models with a global proteome analysis of the endothelial cells. Therefore low and high doses were used to identify and quantify possible pathways in addition to an integration of these data into structural biology. Thereby, certain pathways or proteins are becoming activated by irradiation and either stay chronically activated or lead to chronic activation of downstream targets. The assumption is that the chronic activation of these pathways and/or proteins induces endothelial senescence and later on endothelial dysfunction. Further, the paracrine and autocrine signaling is enhanced by irradiation in endothelial cells involving also the surrounding endothelial cells of damaged endothelial cells towards endothelial senescence and dysfunction. In addition, it is assumed that the paracrine pathway enables the identification of potential biomarkers, which can be used to determine the state of the endothelial dysfunction after irradiation.

2. Methodological aspects for the analysis of radiation-induced effects on endothelial cells

The undergone investigations in this thesis were executed in the expectation to explore radiation-induced effects on endothelial cells in mice and *in vitro*. Thereby, human coronary artery endothelial cell line (HCAEC) was used in case of the first and the third study. For both studies time and dose schedules were made in advance. The second conducted study used primary mouse endothelial cells obtained from the lung after *in vivo* irradiation. The focus of all studies was a global analysis of the protein alterations. On top of these proteomics-based studies, further experiments were used to determine the expression alterations on single protein candidates indicated by the global analysis. Additional bioinformatics evaluations were performed to classify the obtained results into pathways and functions within an organism. Within the following chapters, the methods, workflows and bioinformatics tools used are described.

2.1 Cell culture irradiation

The human coronary artery endothelial cell line was obtained from the Raj lab at Public Health England (PHE) (Lowe and Raj 2014). We performed two studies using this cell line. The first was a comparison study on the effects of 10 Gy vs 0 Gy x-rays after two weeks. In this study not only direct effects were measured but we analyzed also the secretome content and the impact of the secretome on non-irradiated cells (Philipp et al. 2017). The second study elucidated time- and dose-related effects (Philipp, Le Gleut, et al. 2020).

In the first study, the cells were incubated at 37 °C with 5 % CO₂. They were grown until confluency. The irradiation with the 10 Gy dose was performed on an AGO HS320/250 X-ray cabinet (250 kV, 13 mA, 1.5 mm Al, 1.2 mm Cu, 3 keV/μm). Control cells were not irradiated (0 Gy dose). The cells were not passaged but received fresh media every day except the weekends until harvesting. The analysis of the secretome was done by changing media on day 13 to serum-free media to prevent albumin. The serum-free media was taken when harvesting. In parallel, cells were cultured without any treatment to provide non-irradiated bystander cells of the

same passage and culture conditions. The serum-free media from irradiated and control cells was diluted 1:1 with fresh serum containing media and put on the non-irradiated bystander cells for 24 h.

In the second study, irradiation was done at 0 Gy for the controls and 0.25 Gy, 0.5 Gy, 2 Gy and 10 Gy for the irradiated cells with a Caesium-137 γ -source in a closed cabinet (HWM-D-2000, dose rate: 400 mGy/min). Cells were not passaged but the media was changed every two days. Cells were then harvested after 4 h, 24 h, 48 h and one week post irradiation.

2.1.1 Mouse irradiation

Female C57Bl/6 mice (Charles River laboratories) of 4-5 weeks age were irradiated on the whole thorax with 10 Gy using a Small Animal Radiation Research Platform [SARRP, Xstrahl, 220 kV and 13 mA X-ray beam filtered with copper (0.15 mm)]. The thorax of all mice including controls was first visualized by CBCT to identify the required radiation field (60 kV and 0.8 mA photons filtered with aluminium 1 mm). Lungs were dissected from the animals 24 h thereafter. Primary microvascular CD31 positive endothelial cells were isolated using an established protocol (Sievert et al. 2014), grown in ibidi® chamber for six days and harvested one week after irradiation.

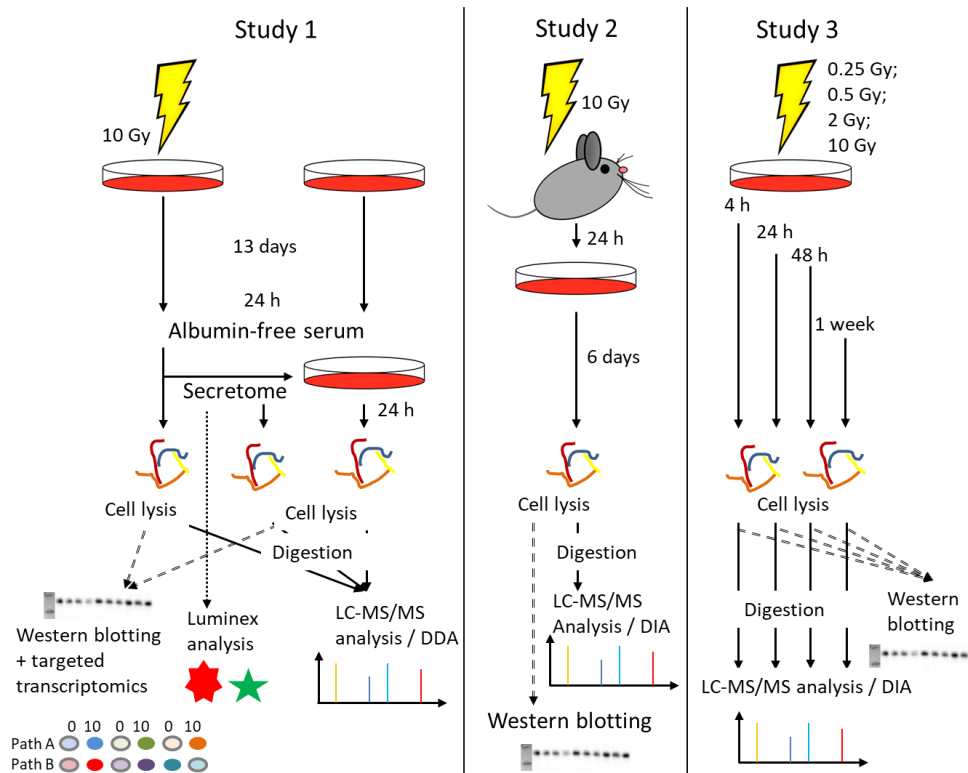


Figure 7: Design and conducted experiments of the three studies.

2.1.2 Protein preparation

In the first study (Philipp et al. 2017) cell pellets were lysed by using the mirVana Paris Kit (Ambion, Thermo Fisher) according to the manufacturer's instructions to gain both proteins and RNA. The protein concentration was determined by Bradford assay (Sigma Aldrich) and measured at 595 nm on an Infinite M200 (Tecan). The obtained RNA concentration was measured on a NanoDrop (PqLab) with a ratio of 260/280 nm of more than 2. For proteome analysis 10 µg protein and 1 µl for the secretome of each treatment group and replicate were provided for proteomic analysis.

In the second and third study (Philipp, Sievert, et al. 2020; Philipp, Le Gleut, et al. 2020) only lysis for protein isolation was done. For this purpose, RIPA buffer (Thermo Fisher) was enriched with protease and phosphatase inhibitor (Roche) and added to the cell pellets. In the second study, the slides containing the grown cells were frozen for 10 min at -20 °C after RIPA application. All following steps were similar for studies two and three. For better cell disruption the mixture was sonicated and the lysate was shaken for 30 min at 4 °C. After centrifugation the pellets were

dissolved in water and measured with bicinchoninic assay (BCA, Thermo Fisher) at 562 nm on an Infinite M200 (Tecan). For each replicate 10 µg protein lysate was used for proteome measurement. The third study included an additional mastermix to guarantee the same quality throughout all 80 measurements.

Samples were stored at -80 °C until further usage.

2.2 LC-MS/MS measurement

In the studies 2 and 3 that were based on DIA, one injection unit of the HRM calibration kit (Biognosys) was added to each sample. The HRM calibration kit is a protein mixture the composition of which is known. In the first study a filter-aided sample preparation (FASP) method (Wiśniewski et al. 2009) was used, whereas a slightly modified version was used in the second and third study. The modified FASP included more washing steps before digestion (Grosche et al. 2016). In FASP, proteins were reduced and alkylated. After washing steps they were digested first with the endoproteinase Lys-C, which cleaves on the c-terminal side of the lysine residues and thereafter with trypsin, which in addition to C-terminal side of lysine residues cleaves after all arginine residues. All these steps were performed within a filter device. This improved the isolation and digestion of membrane proteins.

For negative charging the peptide solution was acidified. Applying organic gradients was necessary to enable elution of peptides with different hydrophobic values. In addition, it sharpened the peaks generated with the MS/MS measurement and the increasing gradient of organic solvent improved the elution by time reducing the risk of losing peptides in the column.

All proteomics measurements were performed by the injection of approximately 0.5 µg of protein. In the first study, peptides were enriched on a trap column and then separated on a C18 column with a gradient of the organic phase from 5-25 % of acetonitrile (ACN) over 90 min and 25-40 % ACN for 5 min and 40 °C. The Orbitrap mass spectrometer QExactive HF (Thermo Fisher) was coupled to the liquid chromatography column with an elution flow rate set to 300 nl/min. At a resolution of 60,000 the m/z range was set to 300-1500. From the MS-scan, the top 10 most abundant peptides were selected in an isolation window of 1.6 m/z for fragmentation with HCD. The analysis of the MS/MS was performed at a resolution of 15,000 m/z .

In the second publication, a different method for peptide separation was used. After enriching the peptides, the peptides were eluted with an organic gradient from 3-40 % over 45 min at a temperature of 40 °C with an elution flow rate of 250 nl/min. For the DIA analysis, a survey scan was performed at a 120,000 resolution from 300-1500 *m/z*. The precursor peptides were analyzed in 17 variable windows from 300-1500 *m/z* and fragmented with HCD.

In the third study, a gradient of 105 min length and 3-41 % ACN with similar column preparations at 40 °C was used for peptide separation. A survey scan was performed from 300-1650 *m/z* at a 120,000 resolution. The precursor ions were analyzed in 37 variable windows across the range of 300-1650 *m/z* at a 30,000 resolution. HCD was used for fragmentation.

In all experiments, ACN was prepared in 0.1 % formic acid. The automatic gain control (AGC) was set for all conducted MS measurements to $3 \cdot 10^6$.

2.2.1 Label-free quantification of generated MS/MS data

In the first study, the DDA label-free MS/MS data were loaded into Progenesis QI software (version 2.0, Nonlinear Dynamics) for quantification. For that purpose, peak models were created, which contained all relevant information of the LC-MS/MS run including peak *m/z* values, intensities, width and areas under the curve (abundance). The different runs were aligned by retention time referenced to one sample or a sample collection. After charge exclusion, all MS/MS-data were exported to Mascot files (version 2.5.1) for *de novo* sequencing and peptide identification. The generated peptides were searched against the Ensembl human protein database (release 83, 31,286,148 residues, 83,462 sequences). To provide an intermediate path between false-positive and false-negative results, 10 ppm peptide mass tolerance and 20 mmu fragment mass tolerance were applied. In addition, one missed cleavage was allowed. The ionizing modification of carbamidomethylation was set as a fixed modification and methionine oxidation as well as asparagine or glutamine deamidation were allowed as variable modifications. With an average false discovery of < 1 % for search statistics and the usage of a decoy-based score cut-off of 13 including a significance threshold, false positive and false negative identifications were reduced to a minimum. After reimport into the Progenesis QI software the

abundances of all peptides allocated to each protein were summed up. All proteins were analyzed that have been identified with at least two unique peptides.

The DIA approach of the second and third study contained label-free data analysis in an almost similar manner. A spectral library was generated in both studies. In the case of the second study, 164 DDA raw files of mouse data were analyzed with Proteome Discoverer (2.1, Thermo Fisher) with 1 % FDR on peptide and protein level using Byonic (2.0, Proteinmetrics) search engine node. Thereof, the spectral library was generated using Spectronaut with default settings using the Proteome Discoverer result file. By applying the Swiss-Prot mouse database (release 2017.02, 16,869 sequences) 11,184 protein groups and 349,634 peptide precursors were included in the spectral library. The third study contained 43 DDA generated raw files of human data to generate the spectral library. The human Swiss-Prot database (Release 2017.02, 20,194 sequences) was used to merge the spectral data to human peptide and protein sequences. This resulted in 11,505 protein groups and 417,843 peptide precursors. The so generated Spectronaut data were processed with Spectronaut 10 in study two, and 12 in study three. The applied settings were the default ones, except that the quantification was limited to proteotypic peptides. The filtering was done with a q-value of 50 % percentile in study two and 20 % percentile in study three, no protein FDR was applied in the third study and summing up peptide abundances was performed in both studies.

2.2.2 Statistical analysis of the generated proteomics data

Statistical analysis for the first study was performed with the Progenesis software, whereby, the normalized protein abundances were used for calculation of fold-changes and significance values (p) and the false discovery rate-correction (FDR, q) for each protein. For selection of deregulated proteins a fold change of ± 1.3 was applied with a Storey corrected p -value of < 0.05 (Storey 2002).

The statistical analysis for the DIA studies was done with self-written R scripts (<https://www.R-project.org/>). In the second study, protein expression was analyzed in the normalized dataset by an one-way ANOVA approach using the limma package. Here, proteins were considered deregulated with a fold change of ± 2.0 and a Benjamini-Hochberg corrected q -value of < 0.05 .

In the third study, the conducted statistical analysis was complex due to the large amount of data gathered. Here, protein normalized abundances were filtered in those proteins with more than one unique peptide using the vsn-package (version 3.52.0). Log₂ transformation of the normalized abundances and batch effect correction were done with the random effect model included in the limma-package (version 3.40.2) and the duplicate correction function was applied on the replicate factor. Fold changes and p-values were calculated based on dose- and time-dependency comparing with the values either at 0 Gy (radiation effect) or at the time point 4 h (time effect). Dose, time and replicate were treated as separate factors. Proteins having the Storey corrected p-values of < 0.05 and a fold change of ± 1.3 were considered as significantly deregulated.

2.2.3 Bioinformatics data interpretation

The significantly deregulated proteins were further analyzed in databases such as Ingenuity® pathway analysis (IPA®, Qiagen) and STRING-database (<https://string-db.org/>). IPA® is based on peer-reviewed literature. We used to integrate the proteomics data into a biological context. It was also used to determine potentially activated or inhibited pathways that the significantly proteins were involved in. Furthermore, the proteomics dataset was examined for up- and downstream regulators, potential biomarker candidates and nodes of a class of proteins. Furthermore, it was used to elucidate the association of the significantly deregulated proteins with functional and dysfunctional aspects of biological systems. STRING-database was in addition to IPA® utilized to identify networks and nodes to classify checkpoint proteins. Additionally, functional integration of selected proteins was assessed to account their biological role.

2.3 Evaluation of proteomics data

As mentioned, the bioinformatics analysis of the proteomics data revealed information about the up- and downstream regulators, node proteins and potential biomarkers. Such proteins were further validated and evaluated by immunological methods or on the transcript level (Figure 7).

2.3.1 Protein targeting with immunoblotting

Immunoblotting is based on the antibody detection of the protein of interest where the primary antibody detects the protein and the secondary on the primary antibody. The secondary antibody has a modification which enables a chemical or chemo luminescence based visualization of the first antibody. We used in this study enhanced chemiluminescence-based detection (ECL) (Hawkins and Cumming 1990). In the first and third study, a chemiluminescence reader from Alpha Innotec (Biozym Scientific GmbH) and in the second study a reader ChemiDoc™ MP (Bio-Rad) were used to measure the light intensity. The images were processed with the image J software (Schneider, Rasband, and Eliceiri 2012). The measured intensities were normalized to Ponceau staining (Studies 1 and 3) and to total protein staining based on Stainfree™ technology (Rivero-Gutiérrez et al. 2014) (Bio-Rad) (Study 2).

2.3.2 Luminex® based antibody detection

Luminex® was used to determine the levels of IL-6, IL-8, MCP1 and IFN-γ in the secretome in the first study. Luminex® is based on the multiplexed flow-cytometric detection of antibodies coupled to fluorescent magnetic beads (Fulton et al. 1997). The harvested medium was diluted 1:2 and centrifuged. The multiplex analysis was performed with a Milliplex MAP Kit (EMD Millipore Corporation) according to the manufacturer's instructions. The fluorescent intensities were measured on a Bio-Rad Luminex 100 (Bio-Rad). The analysis including standardization was done on a Bioplex Manager (Version 6.1, Bio-Rad). Standard curves were generated of a range from 14,000–23,000 pg/ml for IL-6, IL-8, and MCP-1 and 14,000–15,000 pg/ml for IFN-γ. The lowest limit of quantification was 3 pg/ml and the highest limit of quantification 10,000 pg/ml.

2.3.3 Gene expression analysis

To validate the findings of proteomics pathways, three main pathways (oxidative stress, JAK/STAT signaling, type I interferon response) were investigated on the gene expression level. The transcripts were therefore measured in real time. The three RT² profiler polymerase chain reaction (PCR) arrays were purchased from Qiagen (Oxidative Stress, PAHS-065Z, JAK/STAT Signaling Pathway, PAHS-039Y,

and Interferon Type I Response, PAHS-016Z). The implementation was performed according to the manufacturer's instructions. The needed amount of RNA (350 ng) was prepared using the RT2 First Strand Kit (Qiagen) with the Cyclone Gradient Cycler (PEQLAB). The amplification as real-time PCR was done on a StepOnePlus Real-time PCR System (Applied Biosystems). The fold change ($2^{-\Delta\Delta \text{ Cycle threshold (Ct)}}$) was calculated from the normalized gene expression ($2^{-\Delta \text{ Ct}}$) in the test sample divided by the normalized gene expression ($2^{-\Delta \text{ Ct}}$) in the control sample. The final analysis of the Ct data was done in the Data Analysis Center (Qiagen). Transcripts with a fold change of ± 2 and a p-value of < 0.05 were considered as significantly deregulated.

3. Results and Publications

3.1 Radiation-Induced Endothelial Inflammation Is Transferred via the Secretome to Recipient Cells in a STAT-Mediated Process

3.1.1 Aim and Summary

Ionizing radiation is a common treatment of cancer, whereby the health benefit clearly outweighs the damage to healthy tissue. However, damage to the vascular endothelium should be minimized to reduce the risk of late occurring CVD. The knowledge about the radiation effects on the vessels and on the endothelial cells in particular is limited. Therefore, it is necessary to investigate the effects of high-dose radiation on vascular endothelial cells. Endothelial cells form a monolayer where the cells are able to communicate in a paracrine manner (Xiao et al. 2014). How they signal and what this effect induces is only marginally investigated. Endothelial senescence may change the cellular communication in a pivotal manner. The aim of this study was to analyze direct and indirect radiation effects on the endothelium and to investigate the mechanisms of signal transduction from irradiated to non-irradiated endothelial cells by means of secreted proteins. Therefore, a label-free proteome analysis of human coronary artery endothelial cell line (HCECest2), that was known to undergo senescence two weeks after the exposure to 10 Gy X-rays *in vitro* (Lowe and Raj 2014), was carried out to elucidate which signal pathways are affected in the irradiated cells. For this purpose, the proteome changes were compared to the changes in the non-irradiated control. In addition, the secreted proteins (secretome) of the irradiated cells vs. non-irradiated cells and their effects on non-irradiated HCECest2 were examined using proteomics analysis. The non-irradiated “bystander” cells were exposed to the secretome of the irradiated vs. non-irradiated cells for 24 hours before analyzed. Based on the proteomics and bioinformatics data of the irradiated and bystander endothelial cells, key changes were validated by immunoblotting and targeted transcriptome analyses. In addition, a bead-based multiplex analysis of the secretome to study radiation-induced pro-inflammatory markers was performed. In the irradiated cells, their secretome and the non-irradiated recipient cells, we observed a pro-inflammatory interferon type I-related response with ISG15 and MX1 as the most upregulated proteins. These are classical antiviral proteins and expressed against invading pathogens. In addition, an

activation of the STAT3 and the downstream target p38/MAPK was observed in the “bystander” recipient cells. This “bystander” activation was presumably mediated by the secretion of IL-6, IL-8 and MCP1 from the irradiated endothelial cells. These data indicate that irradiated endothelial cells are able to develop an inflammatory state that affects non-irradiated surrounding cells *via* the senescence-associated secretory phenotype. These data contribute to an improved understanding of the pathological background of radiation-induced CVD.

3.1.2 Contribution to the study

This study was designed by Dr. Omid Azimzadeh, PD Dr. Soile Tapio from the institute of Radiation Biology, HMGU, and Dr. Ken Raj from Biological Effects Department, Centre for Radiation, Chemicals and Environmental Hazards at Public Health England (PHE). The cell culture and irradiation was performed by Donna Lowe from the group of Dr. Ken Raj at the PHE. The protein and RNA isolation, protein lysis, concentration measurements and the preparation for the LC-MS/MS runs were performed by me. The LC-MS/MS runs were performed by Dr. Juliane Merl-Pham from the Research Unit Protein Science at HMGU. The bioinformatics analysis, immunoblotting and the targeted transcriptomics assays were performed by me. Dr. Vikram Subramanian and Omid Azimzadeh supported the performance of the immunoblotting. Dr. Nadine Erbeldinger, Dr. Svetlana Kitareva, and Prof. Dr. Claudia Fournier from the GSI delivered supportive data to initiate the secretome analysis. The Luminex-based multiplex assay was performed by me with spatial, technical and advisory support by the Core Facility Immunoanalytics, HMGU. Daniela Hladik helped with the analysis of the immunoblotting data. I did the figures, statistical analysis and the first version of the manuscript. Omid Azimzadeh, Soile Tapio and Prof. Dr. Michael J. Atkinson provided me with advice, scientific discussions throughout the study and especially Soile Tapio did proofreading of the manuscript.

3.1.3 Publication

I presented the data in orally on September, 27th, 2016 at the GBS in Erlangen, and they were published as an original research paper on August, 29th, 2017 in the Journal of Proteome Research:

Reprinted (adapted) with permission from:

Radiation-Induced Endothelial Inflammation Is Transferred via the Secretome to Recipient Cells in a STAT-Mediated Process.

Jos Philipp, Omid Azimzadeh, Vikram Subramanian, Juliane Merl-Pham, Donna Lowe, Daniela Hladik, Nadine Erbdinger, Svetlana Ktitareva, Claudia Fournier, Michael J. Atkinson, Ken Raj, and Soile Tapio.

J Proteome Res. 2017 Oct 6. doi: 10.1021/acs.jproteome.7b00536. Epub 2017 Sep 14. Copyright© 2017, American Chemical Society

Radiation-Induced Endothelial Inflammation Is Transferred via the Secretome to Recipient Cells in a STAT-Mediated Process

Jos Philipp,[†] Omid Azimzadeh,[†] Vikram Subramanian,[†] Juliane Merl-Pham,[‡] Donna Lowe,[§] Daniela Hladik,[†] Nadine Erbdinger,^{||} Svetlana Ktitareva,^{||} Claudia Fournier,^{||} Michael J. Atkinson,[†] Ken Raj,[§] and Soile Tapio^{*,†}

[†]Helmholtz Zentrum München - German Research Center for Environmental Health GmbH, Institute of Radiation Biology, D-85764 Neuherberg, Germany

[‡]Helmholtz Zentrum München - German Research Centre for Environmental Health, Research Unit Protein Science, D-80939 Munich, Germany

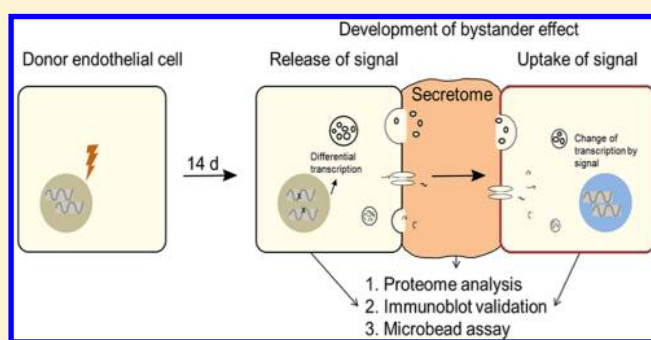
[§]Biological Effects Department, Centre for Radiation, Chemicals and Environmental Hazards, Public Health England, OX11 0RQ Chilton, United Kingdom

^{||}GSI Helmholtz Zentrum für Schwerionenforschung, 64291 Darmstadt, Germany

S Supporting Information

ABSTRACT: Radiation is the most common treatment of cancer. Minimizing the normal tissue injury, especially the damage to vascular endothelium, remains a challenge. This study aimed to analyze direct and indirect radiation effects on the endothelium by investigating mechanisms of signal transfer from irradiated to nonirradiated endothelial cells by means of secreted proteins. Human coronary artery endothelial cells (HCECest2) undergo radiation-induced senescence in vitro 14 days after exposure to 10 Gy X-rays. Proteomics analysis was performed on HCECest2 14 days after irradiation with X-ray doses of 0 Gy (control) or 10 Gy using label-free technology. Additionally, the proteomes of control and radiation-induced secretomes, and those of nonirradiated HCECest2 exposed for 24 h to secreted proteins of either condition were measured. Key changes identified by proteomics and bioinformatics were validated by immunoblotting, ELISA, bead-based multiplex assays, and targeted transcriptomics. The irradiated cells, their secretome, and the nonirradiated recipient cells showed similar inflammatory response, characterized by induction of interferon type I-related proteins and activation of the STAT3 pathway. These data indicate that irradiated endothelial cells may adversely affect nonirradiated surrounding cells via senescence-associated secretory phenotype. This study adds to our knowledge of the pathological background of radiation-induced cardiovascular disease.

KEYWORDS: senescence-associated secretory phenotype, X-ray irradiation, MHC-I class, proteomics, STAT, cardiovascular disease



INTRODUCTION

The vascular endothelium is a monolayer of cells lining all blood vessels in the body.¹ Well-functioning endothelial cells act in a paracrine, endocrine, and autocrine manner to modulate blood fluidity, inflammation, immune response, and vascular tone.² With aging, endothelial cells may enter senescence, an early pathophysiological state hallmarking cardiovascular disease (CVD).³

In spite of losing their replicative potential, senescent endothelial cells stay in a metabolically active state.^{4,5} They secrete a defined pattern of proteins comprising pro-inflammatory cytokines, chemokines, growth factors, and proteases, altogether called "senescence-associated secretory phenotype" (SASP).⁶ SASP is known to influence cell differentiation, cancer growth, cancer invasion, and promotion of endothelial cell invasion.^{4,7–9} It has been suggested that the SASP operates by activating interferon-related pathways,

associated with the release of interferon-inducible (IFI) proteins.¹⁰ SASP is known to spread inflammatory response and senescence to surrounding tissues^{11,12} and to contribute to age-dependent diseases such as CVD.^{5,13}

High and moderate doses of ionizing radiation are able to induce premature endothelial senescence in vitro^{14–19} and in vivo.²⁰ Thus, increased expression of intercellular and vascular adhesion molecules (ICAM1, ICAM2, VCAM1) and enhanced levels of senescence markers p16 and p21 have been found in endothelial cells isolated from murine heart 3–6 months after local irradiation with 8–16 Gy.^{20,21} A simultaneous increase in the levels of pro-inflammatory cytokines such as tumor necrosis factor alpha (TNF α), interleukin 1 alpha (IL-1 α), and interleukin 6 (IL-6) was detected in the serum of these mice.

Received: July 31, 2017

Published: August 29, 2017

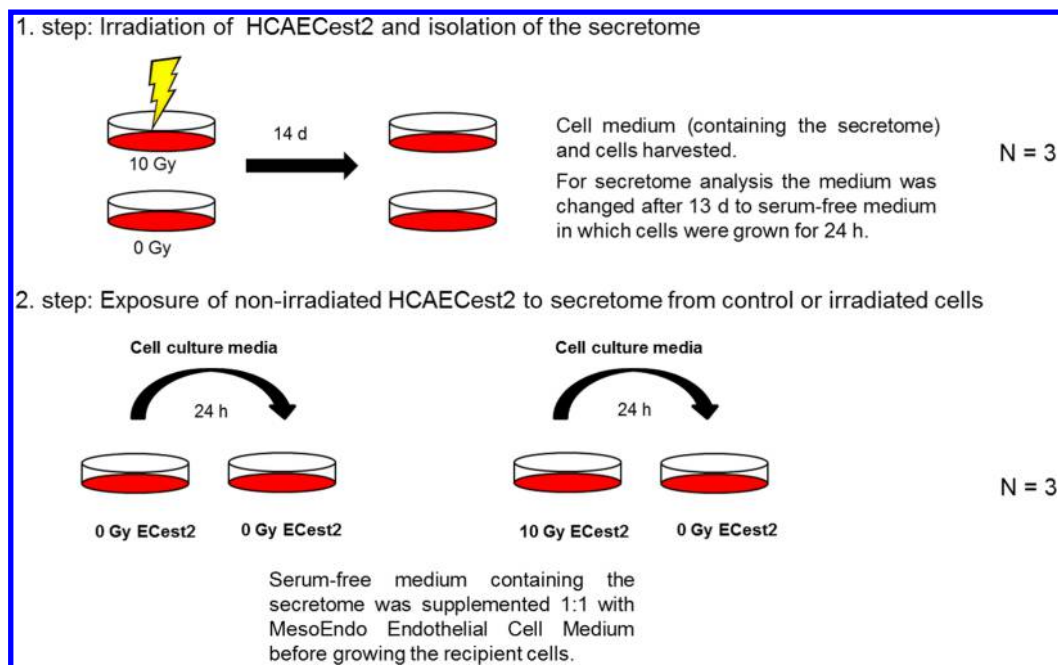


Figure 1. Workflow showing the experimental design of the study. Cells were not passaged, but media of the cells were changed every other day except over the weekend when 25% more media were provided to the cells. This was done by mixing conditioned media with fresh media with serum in a 1:1 relation. HCECest2 cells were irradiated with the dose of 10 Gy (X-ray) and isolated at day 14 for further analyses. For the secretome analysis, on the last transfer of media (day 13), the conditioned media was mixed 1:1 with serum-free media; the irradiated cells were grown for further 24 h in the serum-free media that was collected at day 14. For the recipient cell analysis, the serum-free conditioned media from the control or irradiated cells was diluted 1:1 with serum-containing media and transferred to the nonirradiated recipient HCECest2 cells cultured in parallel. The recipient cells were further cultured for 24 h and collected at day 14. All steps included a nonirradiated control.

This indicates that local irradiation is able to cause systemic pro-inflammatory alteration in the blood and thereby possibly influence the neighboring nonirradiated cells and tissues.²⁰ Indeed, local irradiation has been shown to induce systemic out-of-field (“bystander”) effects by activating the innate immune system to produce pro-inflammatory cytokines, leading to chronic inflammation.²² Partial lung radiation in rats induced increased expression of pro-inflammatory cytokines and ROS in the shielded lung volume adjacent but external to the targeted field.^{23–25}

The term “bystander effect” was coined in the early 1990s to describe effects occurring in cells that are not directly irradiated.²⁶ Studies investigating effects of radiation-induced SASP on neighboring “bystander” cells are scarce. Proteins secreted from radiation-induced senescent breast cancer cell line (MCF7) were analyzed by proteomics and by cytokine microarrays.^{27,28} These studies indicated that human umbilical vein endothelial cells (HUVEC) exposed to the radiation-induced secretome showed increased cell proliferation, invasion, migration, and wound healing activity. Xiao et al. showed immediate activation of the p38 pathway in HUVEC cocultured with irradiated macrophages.²⁹

In order to elucidate factors that lead to radiation-induced CVD it is important to know in detail how endothelial cells respond to radiation and how they communicate with the surrounding nonirradiated cells after the radiation injury. The goal of this study was to investigate molecules and biological pathways involved in this communication. We performed nonbiased label-free proteomics analysis of (i) irradiated endothelial cells, (ii) their secretome, and (iii) nonirradiated recipient (bystander) endothelial cells that were exposed to the radiation-induced secretome. Significant activation of the

STAT3 pathway was found in irradiated donor cells as well as nonirradiated recipient cells exposed to radiation-induced secretome.

EXPERIMENTAL SECTION

Materials

Ammonium bicarbonate (NH_4HCO_3) was obtained from Sigma (St. Louis, MO). Acetonitrile (ACN), formic acid (FA), and trifluoroacetic acid (TFA) were obtained from Roth (Karlsruhe, Germany). Iodoacetamide, tris- (hydroxymethyl) aminomethane (Tris), and sequencing-grade trypsin were obtained from Promega (Madison, WI). Cyano-4-hydroxycinnamic acid was obtained from Bruker Daltonik (Bremen, Germany). All solutions were prepared using HPLC grade water from Roth (Karlsruhe, Germany).

Cell Culture and Irradiation

Human telomerase-immortalized coronary artery endothelial cells (HCECest2) tested negative for mycoplasma were cultured at 37 °C with 5% CO_2 as described previously.¹⁹ The cells (1.8 million per plate) were seeded and grown in Human MesoEndo Endothelial Cell Medium containing fetal bovine serum (Cell Applications), exposed in a confluent state to X-ray doses of 0 Gy (control) or 10 Gy using AGO HS320/250 X-ray cabinet (250 kV, 13 mA, 1.5 mm Al, 1.2 mm Cu, 3 keV/ μm), and cultivated for 14 days before harvesting, a time point at which these cells have reached a radiation-induced senescent status.³⁰ Cells were not passaged, but media of the cells were changed every other day except over the weekend when 25% more media were provided to the cells. This was done by mixing conditioned medium with fresh medium with serum in a 1:1 relation.

For the secretome analysis, on the last medium transfer (day 13), the media was changed to serum-free media to remove albumin and isolated 24 h later by centrifugation at 10 000g for 10 min to remove all cells and cell debris.

To study the signal transfer to nonirradiated HCECest2, these were grown in the secreted medium from either control or irradiated cells diluted 1:1 with MesoEndo Endothelial Cell Medium with serum for 24 h before harvesting.⁶ After all cells were harvested, they were washed once using Hanks Balanced Salt Solution with 1.5 mM Mg²⁺ and 1 mM Ca²⁺ (HBSS⁺⁺) (Cell Applications, San Diego, U.S.A.) before storing at -70 °C. All media were stored at -70 °C. The workflow is shown in Figure 1.

Protein Lysis and Determination of Protein and RNA Concentration

All cell pellets were lysed with mirVana Paris Kit (Ambion, ThermoFisher Scientific, Darmstadt, Germany) according to manufacturer's instructions. Protein concentration was determined using the Bradford assay (Sigma-Aldrich, Taufkirchen, Germany). The analysis was performed at 595 nm on an Infinite M200 (Tecan GmbH, Crailsheim, Germany). RNA concentration was determined using NanoDrop (Peqlab Biotechnologie GmbH, Erlangen, Germany).

FASP Digest

Ten micrograms of cell lysate or 1 mL of serum-free medium containing the secretome was digested with a modified FASP procedure.³¹ Briefly, the proteins were reduced and alkylated using dithiothreitol and iodoacetamide, diluted with one volume of UA buffer (8 M urea in 0.1 M Tris/HCl pH 8.5) and centrifuged through a 30 kDa cutoff filter device (PALL, Port Washington, U.S.A.). Samples were washed three times with UA buffer and twice with 50 mM ammonium bicarbonate prior to proteolysis of the immobilized proteins on the filter for 2 h at room temperature using 1 µg of Lys-C (Wako Chemicals, Neuss, Germany) and for 16 h at 37 °C using 2 µg of trypsin (Promega, Mannheim, Germany). Tryptic peptides were collected by centrifugation (10 min at 14 000g), and the samples were acidified with 0.5% TFA and stored at -20 °C.

Mass Spectrometry

Before the samples were loaded, they were centrifuged for 5 min at 4 °C. LC-MS/MS analysis was performed on a QExactive HF mass spectrometer (Thermo Scientific) online coupled to Ultimate 3000 nano-RSLC (Thermo Scientific). Approximately 0.5 µg of digested sample was automatically injected and loaded onto the trap column at a flow rate of 30 µL/min in 3% ACN/0.1% FA. After 5 min, the peptides were eluted from the trap column and separated on the C18 analytical column (75 µm i.d. × 25 cm, Acclaim PepMap100 C18, 2 µm, 100 Å, Dionex) by a 90 min gradient from 5 to 25% ACN in 0.1% FA at 300 nL/min flow rate followed by a 5 min gradient from 25% to 40% ACN in 0.1% FA. Between each sample, the column was washed with 85% ACN for 5 min followed by equilibration at 3% ACN in 0.1% FA for 18 min. MS spectra were recorded at a resolution of 60 000 with an AGC target of 3×10^6 and a maximum injection time of 50 ms from 300 to 1500 *m/z*. From the MS scan, the 10 most abundant peptide ions were selected for fragmentation via HCD with a normalized collision energy of 27, an isolation window of 1.6 *m/z*, and a dynamic exclusion of 30 s. MS/MS spectra were recorded at a resolution of 15 000 with a AGC

target of 10^5 and a maximum injection time of 50 ms. Intensity threshold was set to 1×10^4 and unassigned charges, and charges of +1 and >8 were excluded.

Label-Free Proteomic Analysis

The acquired spectra were loaded to the Progenesis QI software (version 2.0, Nonlinear Dynamics) for label-free quantification and analyzed as described previously.^{32,33} Briefly, profile data of the MS and MS/MS scans were transformed to peak lists with respective peak *m/z* values, intensities, abundances (areas under the peaks), and *m/z* width. After reference selection, the retention times of the other samples were aligned by automatic alignment to a maximal overlay of all features. After exclusion of all features with only one charge or more than seven charges, all remaining MS/MS spectra were exported as Mascot generic file and used for peptide identification with Mascot (version 2.5.1) in the Ensembl Human protein database (release 83, 31 286 148 residues, 83 462 sequences). Search parameters used were: 10 ppm peptide mass tolerance and 20 mmu fragment mass tolerance, one missed cleavage allowed, carbamidomethylation was set as fixed modification, methionine oxidation and asparagine or glutamine deamidation were allowed as variable modifications. A Mascot-integrated decoy database search calculated an average false discovery of <1% when searches were performed with a Mascot percolator score cutoff of 13 and a significance threshold *p*. Peptide assignments were reimported into the Progenesis QI software, and the abundances of all peptides allocated to each protein were summed up. Resulting normalized protein abundances were used for calculation of fold-changes of proteins and calculation of significance values *p*. FDR-correction of *p*-values (*q*-values) was performed within the Progenesis QI software (Waters, Newcastle upon Tyne, U.K.).

Bioinformatics Analysis

To analyze the pathways associated with radiation-responsive proteins, all significantly deregulated proteins with their corresponding accession numbers were imported into Ingenuity Pathway Analysis (IPA, QIAGEN Redwood City, www.qiagen.com/ingenuity) or STRING-db (string-db.org).

Western Blotting

Fifteen micrograms of protein extract was loaded on 1D NuPAGE-4–12% Bis-Tris Gels (Novex, Life Technologies, Carlsbad, CA) of 1.5 mm thickness to separate the denatured proteins. Protein extracts were denatured in 4× Lämmli buffer for 5 min at 95 °C. Gel runs were performed for 2 h at 100 V constant. Gels were equilibrated to Towbin buffer (SERVA, Heidelberg, Germany) and blotted on a nitrocellulose membrane of 0.45 µm width (Amersham Hybond-ECL, GE Healthcare, Solingen, Germany) for 2 h at 120 V or for overnight at 10 V. After blotting, the membrane was stained with Ponceau solution (Sigma-Aldrich, Taufkirchen, Germany) for 10 min, washed and blocked for 1 h in 8% milk. Antibodies were used according to the manufacturer's instructions diluted in 5% milk. Immunoblot analysis was performed using the following antibodies, all from Cell Signaling Technology (Cambridge, U.K.): STAT3 (#9132), phospho-STAT3 (S727; #9134S), phospho-STAT3 (Y705; #), p16 INK4A (#4824), p21^{Waf1/Cip1} (12D1; #2947), SOD1 (#2770), or Santa Cruz Biotechnology (Heidelberg, Germany): STAT1 (E23; sc-346), ICAM1 (G-5; sc-8439) and GAPDH (sc-47724). The antibody against actin (A5441) was from Sigma-Aldrich (Taufkirchen,

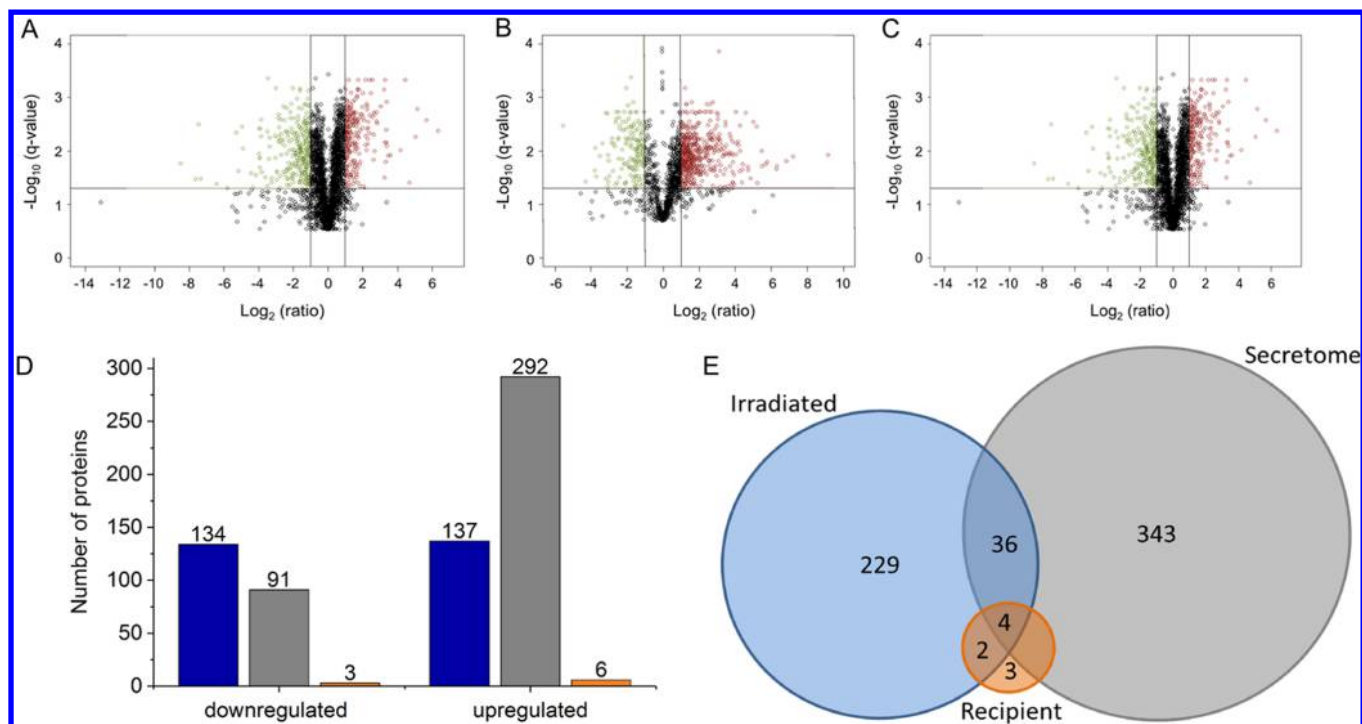


Figure 2. Volcano plots of the irradiated HCECest2 cells (A), the secretome (B), and the recipient HCECest2 cells (C) show the distribution of all quantified proteins (identification with ≥ 2 peptides; $q \leq 0.05$). Differentially regulated proteins (fold change ± 2.0) are marked as red or green circles corresponding to upregulated and downregulated proteins, respectively. The total number of up- and downregulated proteins is shown (D) in the irradiated cells (blue), the secretome (gray), and the recipient cells (orange). The Venn diagram shows the number of total and shared deregulated proteins in the irradiated cells (blue), the secretome (gray), and the recipient cells (orange) (E).

Germany). Membrane incubation was done overnight at 4 °C or for 2 h at room temperature, and detection was by incubation for 2 h with the appropriate horseradish-peroxidase-conjugated antirabbit or antimouse secondary antibodies at room temperature. The intensity of peroxidase signal determined by ECL Advance Western blotting detection kit (GE Healthcare) was measured using a chemiluminescence reader (Alpha Innotec, Biozym Scientific GmbH, Hessisch Oldendorf, Germany) with the software Flour Chem HD2 (Biozym). Blots were stripped using Stripping Buffer (0.2 M Glycine, 0.003 M SDS, 5.9×10^{-7} Tween20; pH of 2.4). Intensities were normalized to actin. Immunoblot intensities were analyzed with Gimp 2.8.16 (<https://www.gimp.org/>; 1997–2017; retrieved on Mar 28, 2017) and ImageJ 1.50f3.³⁴

Secretome Cytokine/Chemokine Analysis

For the ELISA cytokine/chemokine measurements, supernatants and cells were harvested, and the cell number for every sample was determined. The cytokine concentration in the whole supernatant was then corrected for the cell number of the respective sample, and the mean and standard deviation were calculated for all replicates. Every data point was based on three ELISA measurements allowing the inclusion of technical uncertainties. Normalization was carried out on the means and standard deviations compared to the control (0 Gy) of the respective time points.

For the micro bead assay, cytokine/chemokine panel containing interferon gamma (IFNG), IL-6, IL-8, and monocyte chemoattractant protein 1 (MCP-1) was used to quantify their secretion. The harvested medium was diluted 1:2 and centrifuged for 10 min at 10 000g. The multianalyte profiling was performed using the Milliplex MAP Kit (EMD Millipore Corporation, Billerica, MA) according to the

manufacturer's instructions and measured using a Bio-Rad Luminex 100 (Bio-Rad Laboratories, Puchheim, Germany). The analysis was done with the Bioplex Manager (Version 6.1, Bio-Rad). Standard curves were established in a concentration range of 14–23 000 pg/mL for IL-6, IL-8, and MCP-1 and 14–15 000 pg/mL for IFNG. The limits of detection varied from 3 pg/mL (LLOQ) to 10 000 pg/mL (ULOQ).

RT² Profiler Assay

RT² Profiler PCR Arrays (Oxidative Stress, PAHS-065Z, JAK/STAT Signaling Pathway, PAHS-039Y, and Interferon Type I Response, PAHS-016Z) (Qiagen) were used for validation following manufacturer's instructions. RNA (350 ng) was prepared with the RT² First Strand Kit (Qiagen, Hilden, Germany) using the Cyclone Gradient Cycler (Peqlab Biotechnologie GmbH, Erlangen, Germany). The real-time PCR was done on a StepOnePlus Real-time PCR System (Applied Biosystems, Waltham, MA). Fold change ($2^{(-\Delta\Delta Ct)}$) was the normalized gene expression ($2^{(-\Delta Ct)}$) in the test sample divided by the normalized gene expression ($2^{(-\Delta Ct)}$) in the control sample. Data was analyzed using the Data Analysis Center (Qiagen).

Statistical Analysis

Filtering criteria for proteomics analyses were the following: (i) significance for fold change (ratio irradiated to nonirradiated) ≥ 2.00 or ≤ 0.50 ; for recipient cells treated with the medium from control or irradiated cells an additional analysis using a fold change of ≥ 1.30 or ≤ 0.77 was allowed; (ii) FDR (q) ≤ 0.05 (Progenesis QI); and (iii) identification by at least 2 unique peptides.

Filtering criteria for targeted transcriptomics were (i) significance for fold change (ratio) > 2.00 or < 0.50 (ii) $p \leq 0.05$.

Table 1. Differentially Regulated Proteins Shared between the Irradiated Cells, the Secretome, and the Non-Irradiated Recipient (Bystander) Cells^a

name	description	localization/ IPA	biological function/STRING	fold change/A	fold change/B/C
ACO2	aconitase hydratase, mitochondrial	cytoplasm	catalyzes isomerization of citrate to isocitrate	2.3	3.6
AKAP12	A-kinase anchor protein 12	cytoplasm	mediates subcellular compartmentation of protein kinase A and C	3.1	2.7
CAPN2	calpain-2 catalytic subunit	cytoplasm	calcium-regulated nonlysosomal thiol protease catalyzing limited proteolysis of proteins involved in cytoskeletal remodeling and signal transduction	0.4	3.1
CD34	hematopoietic progenitor cell antigen CD34	plasma membrane	mediates attachment of stem cells to bone marrow extracellular matrix, presents carbohydrate ligands to selectin	2.5	2.9
CDH13	cadherin-13	plasma membrane	calcium-dependent cell adhesion protein, connection of cells	3.0	0.4
COL12A1	collagen alpha-1(XII) chain	extracellular space	interacts with type I collagen-containing fibrils	5.5	9
COL18A1	collagen alpha-1(XVIII) chain	extracellular space	may play a role in retinal structure and closure of neural tube	2.5	3.3
COL8A1	collagen alpha-1(VIII) chain	extracellular space	endothelial, migration and proliferation of vascular smooth muscle cells, atherogenesis	6.1	0.5
CTSA	cathepsin A	cytoplasm	carboxypeptidase, essential for activity of beta-galactosidase and neuraminidase	2.6	0.4
CTSS	cathepsin S	cytoplasm	thiol protease, removal of the invariant chain from MHC class II molecules	6.2	3.3
CYBSA	cytochrome b5	cytoplasm	electron carrier for membrane bound oxygenases, membrane-bound hemoprotein	2.7	6.3
DENR	density-regulated protein	other	translation initiation, involved in recruitment of aminoacylated initiator tRNA to P site of 40s ribosome, promotes release of tRNA and mRNA from recycled 40s subunits following ABCe1-mediated dissociation of ribosomal complexes into subunits	0.5	2.3
ECH1	delta(3,5)-delta(2,4)-dienoyl-CoA isomerase, mitochondrial	cytoplasm	peroxisomal, isomerization of 3-trans,5-cis-dienoyl-CoA to 2-trans,4-trans-dienoyl-CoA	2.6	2.5
ERAP1	endoplasmic reticulum aminopeptidase 1	extracellular space	peptide trimming for generation of HLA-class I binding peptides, prefers substrates of 9–16 residues, prefers Leu and hydrophobic C-termini	2.1	2.6
GAA	lysosomal alpha-glucosidase	cytoplasm	essential for degradation of glycogen to glucose in lysosomes	3.2	2.4
HADHA	trifunctional enzyme subunit alpha, mitochondrial	cytoplasm	mitochondrial beta-oxidation of long chain fatty acids	2.1	6.3
HADHB	trifunctional enzyme subunit beta, mitochondrial	cytoplasm	mitochondrial beta-oxidation of long chain fatty acids	2.7	3.1
HLA-A	HLA class I histocompatibility antigen	plasma membrane	involved in presentation of foreign antigens to immune system	3.6	4.0
HLA-B	HLA class I histocompatibility antigen	plasma membrane	involved in presentation of foreign antigens to immune system	6.9	12.8/2.3
HLA-C	HLA class I histocompatibility antigen	plasma membrane	involved in presentation of foreign antigens to immune system	8.2	6.0/2.2
ICAM1	intercellular adhesion molecule 1	plasma membrane	ligands for the leukocyte adhesion protein integrin alpha-L/beta-2, promotes assembly of endothelial apical cups	4.6	3.6
ISG15	ubiquitin-like protein ISG15	extracellular space	innate immune response via conjugation to a target protein (ISGylation) or action as a free protein	3.1	8.4/3.1
LOXL2	lysyl oxidase homologue 2	extracellular space	mediates post-translational oxidative deamination of lysine residues toward allysine, promotes cross-linking of extracellular matrix proteins by oxidative deamination of peptidyl lysine residues in precursors to fibrous collagen and elastin	2.1	0.4
MX1	interferon-induced GTP-binding protein Mx1	cytoplasm	interferon-induced dynamin-like GTPase with antiviral activity against a wide range of RNA viruses and some DNA viruses, targets are negative-stranded RNA viruses	10.3	11.2/8.6
MYL6	myosin light polypeptide 6	cytoplasm	component of smooth muscle and nonmuscle, regulatory light chain of myosin	0.3	6.8
OTUB1	OTU domain, ubiquitin aldehyde binding 1	cytoplasm	hydrolyase specifically removing Lys-48-linked conjugated ubiquitin from proteins. prevents degradation	0.4	2.3
PPP5C	serine/threonine-protein phosphatase 5, catalytic subunit	nucleus	dephosphorylates proteins involved in several signaling pathways (apoptosis, differentiation etc.)	0.5	2.1

Table 1. continued

name	description	localization/ IPA	biological function/STRING	fold change/A	fold change/B/C
PRDX6	peroxiredoxin-6	cytoplasm	redox regulation of the cell, reduces H ₂ O ₂ and short chain organic, fatty acid and phospholipid hydroperoxides	0.5	2.2
RALA	Ras-related protein RalA	cytoplasm	GTPase involved in cellular processes, such as gene expression, cell migration and proliferation, oncogenic transformation and membrane trafficking	2.3	2.2
RPL10	60S ribosomal protein L10	cytoplasm	translation and RNA binding	0.2	3.0
RPS12	40S ribosomal protein S12	cytoplasm	translation and RNA binding	0.4	2.4
SLIT2	Slit homologue 2 protein	extracellular space	molecular guidance in cellular migration, interaction with roundabout homologue receptors	0.2	0.2
STAT1	signal transducer and activator of transcription 1-alpha/beta	nucleus	response to interferons, other cytokines and growth factors. induces transcription by dimerization and translocation to nucleus	2.0	13.8
SYNPO	synaptopodin	cytoplasm	actin-associated protein, may modulate actin-based shape and motility	2.3	2.7
TAGLN	transgelin	cytoplasm	actin cross-linking/gelling protein, involved in calcium interactions, contractile properties may contribute to replicative senescence	3.9	6.1
THBS1	thrombospondin-1	extracellular space	adhesive glycoprotein mediating cell-to-cell and cell-to-matrix interactions, binds heparin, ligand for cd36 mediating antiangiogenic properties, involved in stress response	2.3	0.4
TMOD3	tropomodulin-3	cytoplasm	blocks elongation and depolymerization of actin filaments at pointed end	0.2	2.7
TPPI	tripeptidyl-peptidase 1	cytoplasm	lysosomal serine protease, may generate tripeptides from breakdown products	4.4	0.5
TSTA3	GDP-L-fucose synthase	plasma membrane	tissue-specific transplantation antigen P35B, catalyzes NADP-dependent conversion of GDP-4dehydro-6-deoxy-D-mannose to GDP-fructose, involved in epimerase and reductase reaction	0.4	3.8
TUBB	tubulin beta chain	cytoplasm	constituent of microtubules	0.5	2.1

^aThe fold changes are shown for the irradiated cells (A), the secretome (B), and the recipient cells (C). All 40 proteins are shared between the irradiated cells and the secretome; the four proteins also significantly deregulated in the recipient cells (HLA-B, HLA-C, ISG15, and MX1) are marked in bold. The deregulatory status is based on following criteria: (i) significance for fold change (ratio) >2.00 or <0.50; (ii) FDR (q) ≤ 0.05 (Progenesis Q1); and (iii) identification by at least two unique peptides.

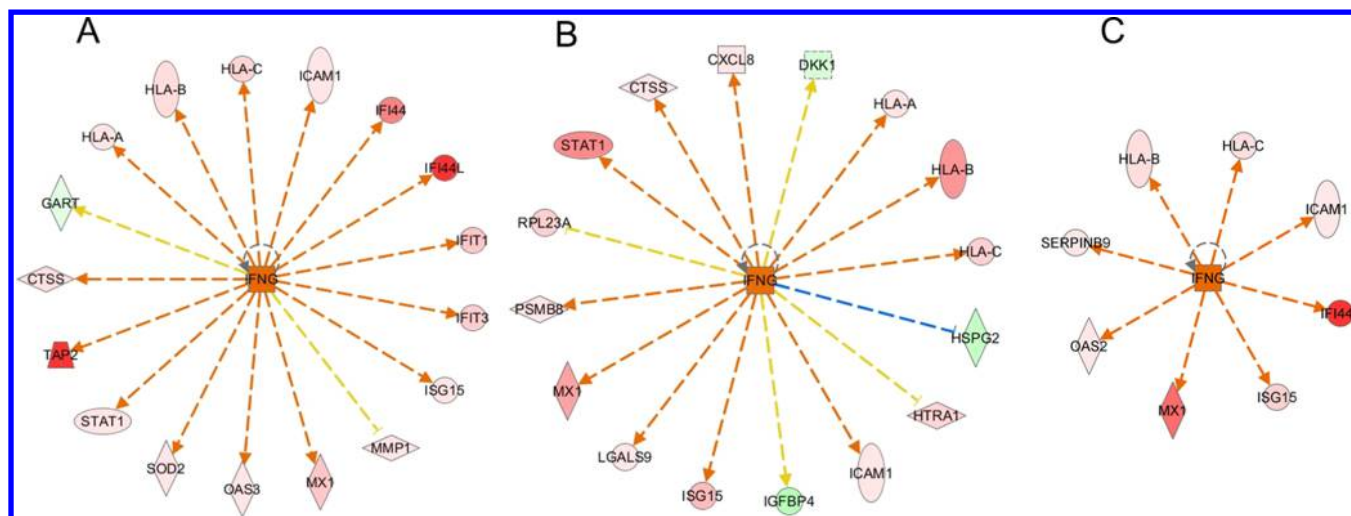


Figure 3. Analysis of predicted upstream regulators using IPA. Graphical representation of deregulated proteins with their upstream regulator INFG in the irradiated cells (A), in the secretome (B), and in the recipient cells (C) is shown (<http://www.INGENUITY.com>). The up- and downregulated proteins are marked in red and green, respectively (fold change ± 2.0 for A and B, fold change ± 1.3 for C). The orange color of the INFG node indicates activation. The protein IDs are available in Table-S1 (A), Table-S3 (B), and Table-S5 (C). The activation z-scores, *p* values, and numbers of target molecules are shown in Table-S8.

Immunoblotting significance criteria: Proteins showing altered expression compared to the control were considered to be significant if $p \leq 0.05$ (unpaired Student's *t* test). The error bars were calculated as standard error of the mean (SEM).

All experiments were performed using at least three biological replicates.

Data Availability

The raw MS data are available at the following: <http://dx.doi.org/doi:10.20348/STOREDB/1096/1136>

RESULTS

Irradiated Cells Are Morphologically Different from Control or Bystander Cells

Microscope images showed that nonirradiated control cells exhibited the normal “cobblestone” morphology while the irradiated cells showed a flattened, enlarged, and elongated morphology with stress fibers. In contrast, no difference was observed between cells exposed to medium from either control or irradiated cells (Figure-S1).

Irradiation Affects the Proteomes of the Irradiated Cells, Their Secretome, and Non-Irradiated Cells Treated with the Secretome

Proteome analyses of the irradiated cells, their secretome, and the recipient (bystander) cells were performed using label-free quantification in comparison to the corresponding non-irradiated control. Principal component analysis (PCA) based on all proteomic features showed a good separation of control and exposed groups in all three data sets, even in the recipient group (Figure-S2).

In the irradiated cells, 3028 proteins were identified of which 2008 were quantified. According to the filtering criteria (see [Statistical Analysis](#)), 271 of them were significantly differentially regulated. Among these, 137 were upregulated and 134 downregulated.

In the secretome, 1646 proteins were identified of which 1078 were quantified. Among these, 383 proteins were found to be significantly altered in their expression: 292 were upregulated and 91 downregulated.

In the recipient cells, 2926 proteins were identified of which 1963 were quantified. Out of these 9 were found to be significantly deregulated 6 proteins showing upregulation and 3 downregulation. Interestingly, the protein exhibiting the greatest reduction was angiotensin converting enzyme (ACE) (fold change: 0.36); the level of this protein was not significantly changed in the irradiated cells or the secretome. Similarly, the expression of von Willebrand factor (VWF) was significantly deregulated only in the recipient cells (fold change: 0.48). The protein showing the greatest increase was interferon-induced protein 44 like (IFI44L) (fold change: 12.05) that was also upregulated in the irradiated cells (fold change: 50.47) but not in the secretome; it is not reported to be a secretory protein.

The volcano plots of all quantified and significantly deregulated proteins are shown in Figure 2A–C. The secretome proteome showed the highest number of significantly deregulated proteins, whereas the recipient cells showed the smallest number of changes.

The total numbers of all deregulated proteins in the three data sets are shown in Figure 2D. All identified and significantly deregulated proteins from the irradiated cells, the secretome, and the recipient cells are listed in Tables-S1–S6.

There were 40 differentially regulated proteins that were shared between the irradiated cells and the secretome; four of these were also deregulated in the recipient cells (Figure 2E). The list of these proteins and their cellular localization is shown in Table 1. Most proteins were involved in extracellular activities and classified as secreted proteins.

Pathway Analysis Indicates the Activation of Type-I and Type-II-Interferon-Mediated Signaling in All Three Groups

The network of the 40 shared proteins between all three data sets was created using the STRING-db software (Figure-S3). The network consisted of four connected clusters. The largest cluster showed strongly interconnected proteins related to interferon signaling: signal transducer and activator of transcription 1 (STAT1); interferon-stimulated gene 15 (ISG15); MX dynamin like GTPase 1 (MX1); ICAM1; and human leukocyte antigens A, B, and C (HLA-A, -B, and -C). This

cluster was loosely connected to a subcluster of mitochondrial origin with proteins involved in lipid metabolism, especially fatty acid beta-oxidation. Further, a weak association was seen with collagen and ribosomal subclusters (Figure-S3).

All significantly differentially regulated proteins were further analyzed. IPA analysis of canonical pathways influenced by irradiation was performed in a z-score-dependent manner of all three groups (Table-S7). As none of the canonical pathways in the recipient group showed significance based on the z-score, the analysis was performed only in the irradiated cells and their secretome. Both groups showed significant changes in the interferon signaling and Gα12/13 signaling. In line with previous in vitro and in vivo data,^{20,35,36} irradiated cells showed radiation-induced changes in RhoA signaling.

To facilitate a deeper insight into the changes found in the recipient cells, a fold-change relaxation from ± 2 -fold to ± 1.3 -fold was allowed for this group as described and justified previously for label-free proteomics;³⁷ the other filtering criteria of $q \leq 0.05$ and two-unique-peptide identification were maintained. This increased the number of significantly deregulated proteins in the recipient cells from 9 to 23 of which 14 were significantly upregulated and 9 downregulated (Table-S6).

IPA analysis of predicted upstream regulators using a z-score filtering criteria of ± 2.0 , and the new relaxed filtering criteria for the recipient group proteins (± 1.3) revealed a predicted activation of IFNG in all three groups (Figure 3).

The list of all predicted upstream regulators is shown in Table-S8. Activated upstream regulators included several interferons of type I, especially in the irradiated cells. This group had the biggest impact on the proteome alterations in this study due to the large number of downstream deregulated proteins. In addition, an activation of toll-like receptors (TLR) 4, 7, and 9 was indicated with a predicted activation of TLR7 in all three groups. The upstream regulators that were predicted to be inhibited included mitogen-activated protein kinase 1 (MAPK1) (irradiated cells, secretome), Bruton tyrosine kinase (BTK) (irradiated and recipient cells), and interleukin 1 receptor antagonist (IL1RN) (irradiated cells) (Table-S8).

Targeted Transcriptomics Confirms the Activation of Type-I-Interferon-Mediated Signaling in Recipient Cells

In order to further investigate the predicted activation of interferon Type-I signaling in the recipient cells, a focused gene array analysis comprising 84 genes involved in this pathway was performed using GAPDH as the housekeeping gene for normalization. According to the filtering criteria (see Statistical Analysis), 7 genes were found significantly changed in expression, all showing upregulation. These were interferon alpha inducible proteins 6 and 27 (IFI6, IFI27), interferon induced protein with tetratricopeptide repeats 3 (IFIT3), MX dynamin like GTPases 1 and 2 (MX1, MX2), and 2'-5'-oligoadenylate synthetases 1 and 2 (OAS1, OAS2) (Table-S9). Of these, MX1 and OAS2 were also significantly upregulated at the level of protein expression (Table-S6). IFIT3 was also found to be upregulated at the protein level (14-fold), but as the identification was based only on one unique peptide, it did not pass the filtering criteria. The others were not identified in the proteomics analysis, probably due to very modest expression. The gene expression data confirmed the predicted activation of Type-I-interferon-mediated signaling in the recipient cells.

As JAK/STAT signaling is regulated by Type-I and -II interferons, the expression of the genes belonging to this pathway were investigated using pathway-focused transcriptomics assay. Of 84 genes involved in this pathway, three were found to be upregulated: Fc fragment of IgG receptor Ia (FCGR1A), ISG15 ubiquitin-like modifier (ISG15), and OAS1 (Table-S10). ISG15 was upregulated in both proteome and transcriptome analyses. As no significant changes in the expression of JAK genes was found, the activation of the JAK/STAT signaling was considered improbable. However, JAK-independent activation of STAT proteins could not be excluded.³⁸ Therefore, further studies using immunoblotting were performed (see section Western Blotting).

As the involvement of increased cellular ROS has been classically associated with the bystander effect,³⁹ the involvement of oxidative stress pathways was investigated in the recipient cells using a targeted gene array. Only aldehyde oxidase 1 (AOX1) was upregulated (Table-S11), suggesting no significant alteration in the oxidative stress level.

Irradiation Increases Cytokine/Chemokine Levels in the Endothelial Secretome

As the proteomics data from the irradiated and recipient cells indicated a possible influence of pro-inflammatory factors in the recipient cells, the levels of IL-6, IL-8, and MCP-1 were quantified in the secretome. A rapid (24 h) and significant increase of IL-6 and MCP-1 expression in the secretome of irradiated cells was observed while the level of IL-8 was significantly increased first at a later time point (1 week) (Figure-S4). At 2 weeks, corresponding to the time point when the recipient cells were exposed to the secreted proteins, the levels of IL-6, IL-8, and MCP-1 were all significantly upregulated in the secretome of irradiated cells compared to that of the nonirradiated ones (Figure 4). The IFNG level was below the detection limit of this assay (Figure 4).

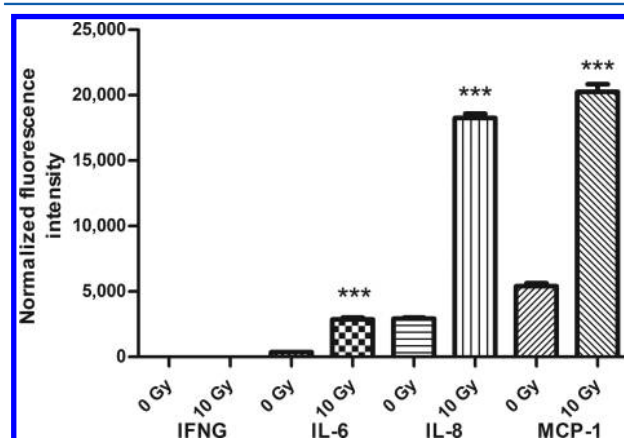


Figure 4. Cytokine/chemokine analysis of the secretome. The levels of the secretomal proteins IFNG, IL-6, IL-8, and MCP-1 are shown. The columns represent the average normalized fluorescence intensity in the secretome of irradiated vs nonirradiated cells. The error bars are calculated as SEM (t test; $*p < 0.05$; $n = 3$).

Immunoblotting Confirms the Induction of Inflammatory Response in the Recipient Cells

Immunoblotting was performed to validate proteins that were differentially regulated in the proteomics analysis. In addition, proteins important in cell cycle control and cellular senescence (p16, p21^{Cip1/Waf1}), and proteins responsive to inflammation

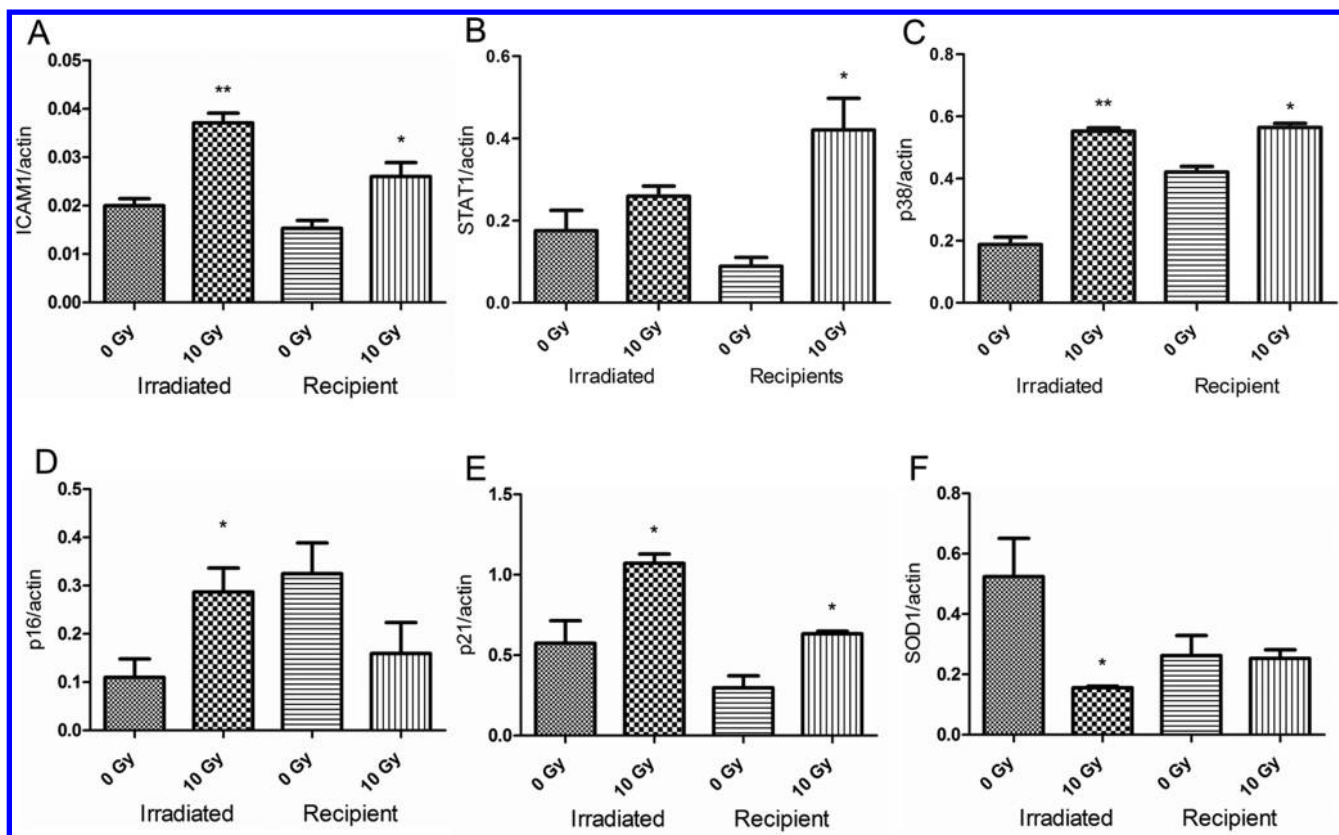


Figure 5. Immunoblot verification of protein changes in the irradiated and the recipient cells. The pro-inflammatory proteins ICAM1 (A), STAT1 (B), and p38 (C); the senescence/cell cycle regulatory proteins p16 (D) and p21^{Cip1/Waf1} (E); and the antioxidant protein SOD1 (F) are shown. The bars represent the relative expression after correction for background and normalization to actin. The error bars are calculated as SEM (*t* test; **p* < 0.05; *n* = 3).

(p38) or oxidative stress (SOD1) were investigated in both irradiated and recipient cells. The results are shown in Figure 5; the blots are shown in Figure-S5 and Figure-S6.

In accordance with the proteomics results, ICAM1 was significantly upregulated in both irradiated and recipient cells (Figure 5A). As ICAM1 expression is known to be induced by IL-6 in endothelial cells⁴⁰ this result further suggested cytokine-stimulated response in the recipients. Similarly, STAT1 expression is known to be induced by IL-6.⁴¹ It was found to be significantly upregulated in the recipient cells but not in the irradiated cells, where the increase in STAT1 level did not reach significance (Figure 5B).

Also the expression of p38 is known to be responsive to cytokines such as IL-6.⁴² Its level was highly increased in the irradiated cells and less but significantly upregulated in the recipient cells, again indicating inflammatory response in the bystander cells (Figure 5C).

Concerning the CDKN proteins p16 and p21^{Cip1/Waf1}, both were upregulated in the irradiated cells as expected due to the radiation-induced cellular senescence observed in these cells³⁰ but only p21^{Cip1/Waf1} was significantly upregulated in the recipient cells (Figure 5D,E).

The level of superoxide dismutase (SOD1) was down-regulated in the irradiated cells, probably due to radiation-induced oxidative stress. In line with the gene expression data (Table-S11), no significant change in the protein amount of SOD1 was seen in the recipients, again suggesting that alteration in the level of ROS is not involved in the bystander effect of this study (Figure 5F).

Phosphorylation (Y705) of STAT3 Beta Is Induced in the Irradiated and Recipient Cells

The expression and activation of STAT3 can be induced by IL-6 or INFG.⁴³ The levels of total STAT3 alpha and beta isoforms were tested by immunoblotting (Figure 6). In addition, the status of two phosphorylation sites (Y705, S727) present in both isoforms were investigated, but only the tyrosine-705 showed significant alteration (Figure 6 and data not shown). In the irradiated cells, the total level of the alpha isoform was significantly increased, while that of the beta isoform was decreased (Figure 6A). The ratio of phosphorylated to total protein was not changed in the case of STAT3 alpha but was increased in the case of STAT3 beta (Figure 6B). In the bystander cells, the expression of total alpha as well as total beta isoform was increased (Figure 6C), but similar to the irradiated cells, only the ratio of phosphorylated to total STAT3 beta was significantly increased (Figure 6D).

ICAM1 and STAT 3 Are Important Mediators of the Bystander Effect

In order to get a deeper insight into the character of the bystander effect observed in this study, a network analysis was performed of all molecules in the recipient cells with significant expression alterations, seen either at the gene level (fold change ± 2.0) or at the protein level (proteomics fold change ± 1.3 ; immunoblotting *p* ≤ 0.05). This network is shown in Figure 7. A strongly interconnected cluster of interferon-related inflammatory response genes/proteins is seen. This cluster is connected to other deregulated genes/proteins via ICAM1

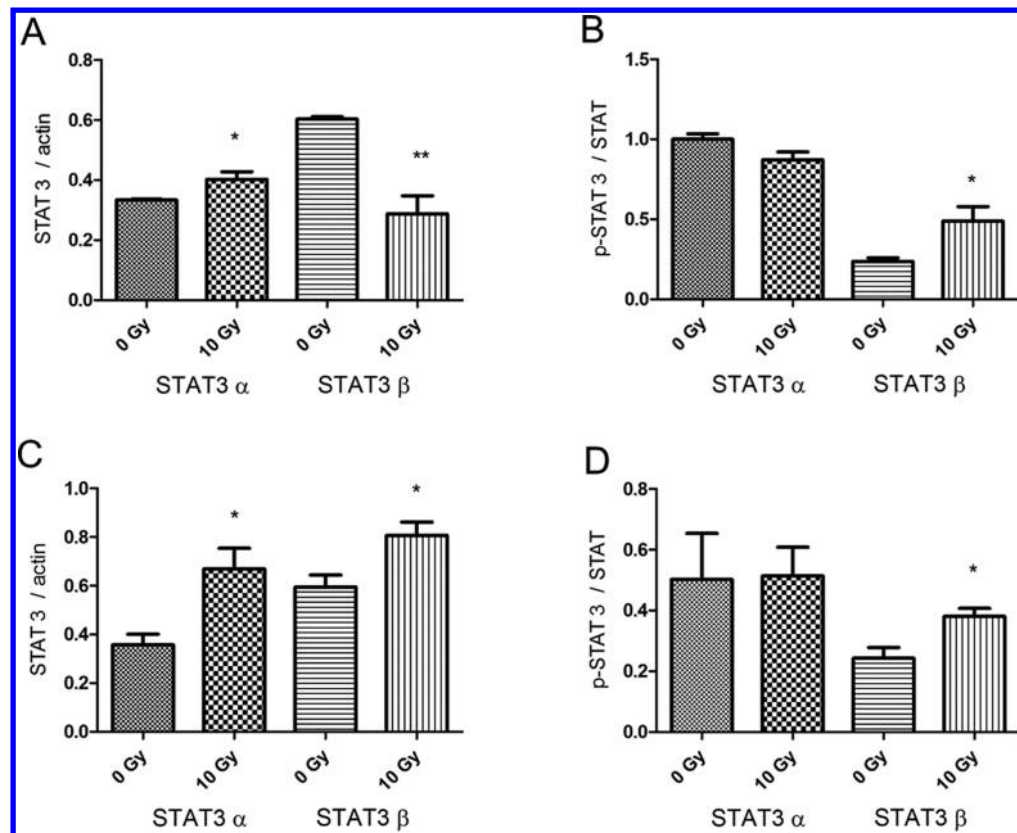


Figure 6. Immunoblot analysis of the STAT3 proteins. The relative expression of total STAT3 showing isoforms α and β in irradiated (A) and recipient cells (C) after background correction and normalization to actin. The expression of phospho-STAT3 (Y705) was calculated against the relative expression levels of the total STAT3 α and β isoforms in irradiated (B) and recipient cells (D). The error bars are calculated as SEM (t test; $*p < 0.05$; $n = 3$).

and STAT3 that suggests their central role in the bystander effect.

DISCUSSION

This is to our knowledge the first study to investigate radiation-induced proteome changes in irradiated cells, their corresponding secreted proteins, and their influence on nonirradiated recipient cells. As we aimed to elucidate possible transfer mechanisms of radiation-induced cardiovascular injury to the surrounding vascular tissue, human coronary artery endothelial cells were used as a model.

Interestingly, this study suggests that pro-inflammatory interferon-type I related proteins are involved in the transfer of information from the irradiated cells through the secretome to the recipient cells. The level of core proteins in this transfer process, MX1, ISG15, and HLA-proteins B and C, were significantly (at least 2-fold but up to 11-fold) augmented in all three proteomes studied here. The levels of MX1 and ISG15, but also that of STAT1 and IL-6 showing upregulation in this study, are known to be interferon-stimulated.⁴⁴

In accordance with our data, Furusawa et al. showed using gene expression analysis in irradiated HUVEC (2.5 Gy X-ray, 24 h) that the upregulated genes were associated with inflammatory responses, in particular with the type 1 interferon response.⁴⁵ Similar to our study, the MX1 level was found to be significantly upregulated in the irradiated cells.

A proteomic analysis of HUVEC infected by *Rickettsia conorii* bacteria has also shown induction of STAT1, MX1, and ISG15 indicating activation of interferon-STAT signaling pathways.⁴⁶

This suggests that the stress caused by bacterial or viral⁴⁷ invasion triggers a similar response as seen in this study in HCECest2 undergoing radiation-induced premature senescence.³⁰

Furthermore, normal and cancer cells that were induced into senescence by drugs also increased the levels of MX1, ISG15, STAT1, and IL-6⁴⁴, which was supportive of our findings.

The novel feature of this study is that these alterations are not restricted to the irradiated cells but can be passed to those exposed to the radiation-induced secreted proteins. The irradiated HCECest2 cells undoubtedly became senescent,³⁰ exhibited inflammatory features, and secreted pro-inflammatory cytokines. As all protein expression changes related to pro-inflammatory interferon-inducible proteins showed similar direction of deregulation in the irradiated and recipient cells (upregulation), it is reasonable to consider that the changes found in the recipients have also a pro-inflammatory character.

The transducing molecule from donor to the recipient may in this case be either IL-6 or IFNG. IFNG was not detectable in the secretome, probably due to its low abundance, but the amount of secreted IL-6 was greatly increased. IL-6 is known to induce the expression of several pro-inflammatory proteins such as ICAM1⁴⁰ and STAT3,⁴² which were detected in the recipient cells. Indeed, IL-6 response and IFNG-like response are distinct, but they both mediate a common set of core signals that can partly compensate each other.⁴³ The IL-6-induced activation of STAT3 can occur via p38,⁴² the expression of which was also significantly increased in the recipients.

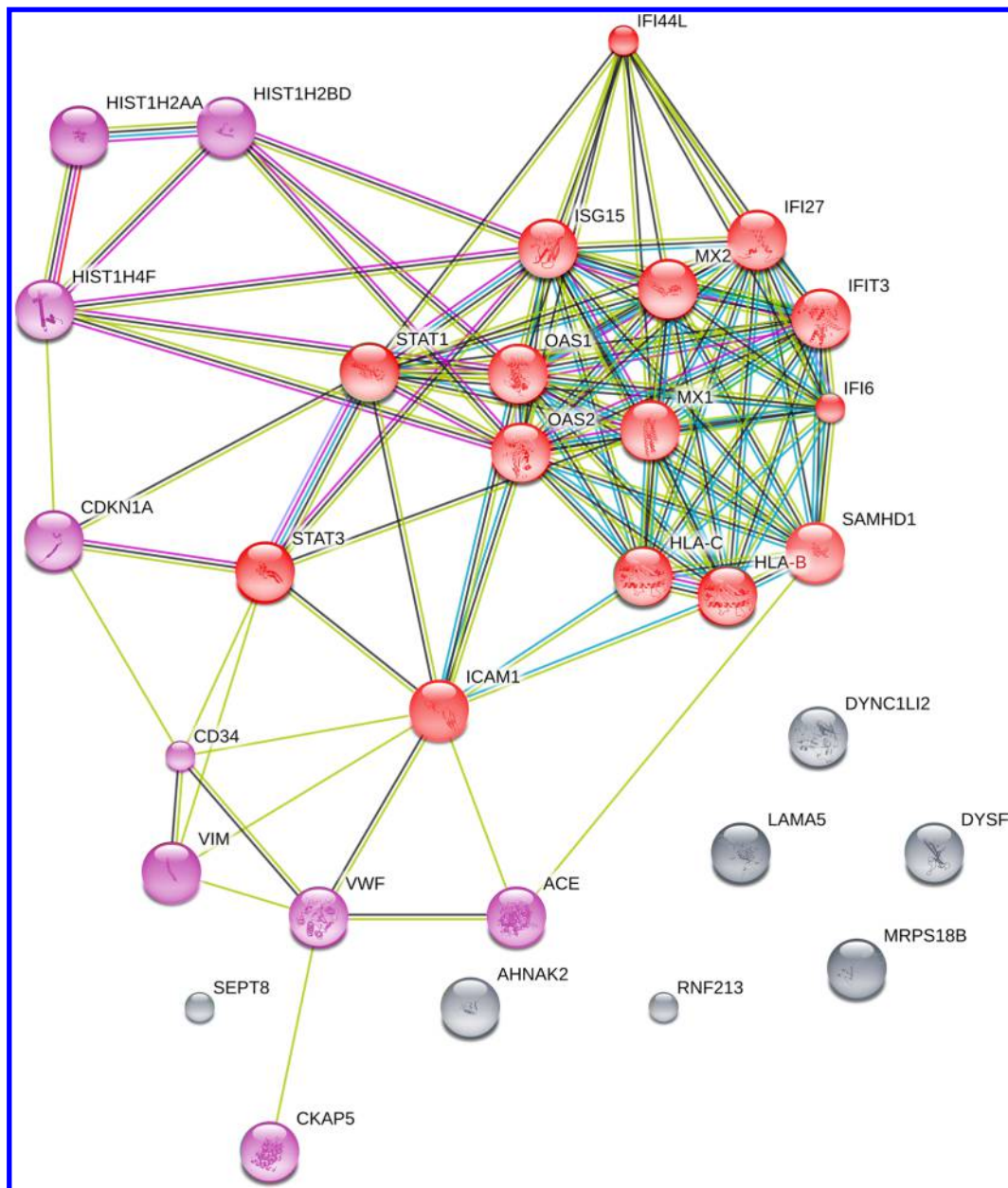


Figure 7. Interaction analysis of all significantly deregulated proteins in the recipient cells using the STRING-db. The interferon type I-related cluster is shown in red, and the proteins loosely interconnected to the main cluster are shown in purple. The proteins showing no interconnection are shown in gray. The significance of deregulation was based on the label-free proteomics analysis (fold change of ± 1.3 ; $q < 0.05$; $n = 3$), the immunoblotting (t test; $*p < 0.05$; $n = 3$), or the targeted gene array analysis (fold change of ± 2.0 ; $*p < 0.05$; $n = 3$).

STAT3 becomes activated after phosphorylation of tyrosine-705 in response to both IL-6 and interferons.⁴⁸ In addition, activation of STAT3 may occur via phosphorylation of serine-727 by MAPK⁴⁹ or through the src family of kinases.^{50,51} Our data show STAT3 phosphorylation at tyrosine-705 but not at serine-727 in both irradiated and recipient cells. This also supports the induction via IL-6 and/or IFNG. As we observe no expression changes in the JAK genes, this activation probably occurs in a JAK-independent manner.⁵²

STAT3 exists in two isoforms: the full-length STAT3 alpha and the truncated STAT3 beta. These isoforms have both distinct and overlapping functions that also vary in different tissues.^{53,54} The data concerning the function of these different isoforms in endothelial cells are very scarce. As activation of the beta isoform mitigated the development of atherosclerosis in

apolipoprotein E-deficient mice,⁵⁵ it was suggested to suppress rather than accelerate chronic inflammation in vasculature. Our data show an activation of the STAT3 beta isoform in both irradiated and recipient cells. It is difficult to interpret the activation of the beta isoform in the irradiated cells as being anti-inflammatory since these cells are in an inflammatory state. If similar mechanisms are valid also in the recipient cells, the outcome here would be pro-inflammatory as well. Taken together, more data are needed about the function of STAT3 isoforms in general and radiation-induced activation of the STAT3 in particular.

In accordance with the proteome profile of the irradiated cells, IL-6-STAT3 signaling has been associated with premature senescence.⁵⁶ We tested classical senescence markers p16 and p21^{Cip1/Waf1} also in the recipient cells. Although a significant 2-

fold increase was seen in the level of p21^{Cip1/Waf1}, it is questionable whether these cells express a full phenotype of premature senescence at this early time point after treatment. However, the increased expression of p21^{Cip1/Waf1} has been shown to precede the appearance of beta-galactosidase activity in chronically irradiated HUVEC.^{14,15} These cells showed no increase in the level of p16,^{14,15} similar to our results. The function of p21^{Cip1/Waf1} as a regulator of the cell cycle arrest could explain the increased expression, but as the recipient cells are not irradiated, no direct DNA damage is to be expected. Further, we observe no signs of increased oxidative stress in the recipients that could indirectly lead to DNA damage.

In spite of some similarities, the proteome response of the recipient cells differs from that of the irradiated cells or the secretome as more than half of the deregulated recipient proteins are unique to this group. In general, these data present several novel radiation-induced proteins including HLA-B and -C. They are part of the MHC-I antigen complex playing a key role in the immune system, particularly in the recognition of foreign intruders such as viruses and bacteria. This study suggests a crosstalk between ionizing radiation, innate immune response, and bystander effects.

CONCLUSIONS

Low-level persistent inflammatory condition is now understood to be a risk factor for CVD. In atomic bomb survivors, a dose-dependent increase in the levels of inflammatory markers has been found in the blood decades after the exposure, indicating a persistent radiation-induced inflammatory response.^{57,58} This may causally be related to increased risk for late-occurring CVD observed in this population.⁵⁹ The question of how persistent inflammation is maintained decades after radiation exposure remains to be answered. This study suggests that the irradiated cell population, by entering metabolically active premature senescent state, is able to affect its microenvironment via the production of inflammatory mediators and cause pro-inflammatory changes in the surrounding nonirradiated cell population. The surrounding bystander cells exhibit interferon type I response and activation of STAT signaling. Although further studies are needed, these data add to our knowledge of radiation-induced vascular damage and provide new targets for preventive measures in the future.

ASSOCIATED CONTENT

Supporting Information

The Supporting Information is available free of charge on the ACS Publications website at DOI: 10.1021/acs.jproteome.7b00536.

Typical microscope images showing cell morphology of HCECest2 endothelial cell line; principal component analysis (PCA) based on all proteomic features; network analysis by STRING-db of the shared differentially regulated proteins in the irradiated cells, the secretome, and the recipient cells; secretion of cytokines and chemokines by irradiated HCECest2; immunoblot verification of ICAM-1, STAT1, p16, p21^{Cip1/Waf1}, and SOD1; and immunoblot verification of p38, STAT3, and phospho-STAT3 (tyrosine-70S) (PDF)

All identified proteins in the irradiated cells; all significantly deregulated proteins in the irradiated cells; all identified proteins in the secretome; all significantly deregulated proteins in the secretome; all identified

proteins in the “bystander” recipient cells; all significantly deregulated proteins in the “bystander” recipient cells; IPA analysis of canonical pathways; IPA analysis of predicted upstream regulators; interferon signaling pathway gene array; JAK/STAT pathway gene array; and oxidative stress pathway gene array (XLS)

AUTHOR INFORMATION

Corresponding Author

*E-mail: soile.tapio@helmholtz-muenchen.de. Phone: +49-89-3187-3445. Fax: +49-89-3187-3378.

ORCID

Omid Azimzadeh: 0000-0001-8984-0388

Soile Tapio: 0000-0001-9860-3683

Notes

The authors declare no competing financial interest.

ACKNOWLEDGMENTS

We acknowledge the Core Facility Immunoanalytics of Helmholtz Zentrum München for assistance in acquiring the data with the Luminex platform. This research was supported by the Federal Ministry of Education and Research of Germany (Funding numbers: 02NUK038B, 02NUK045C) and the European Community's Seventh Framework Program (EURATOM) (# 295823 PROCARDIO). V.S. is recipient of a scholarship from the German Academic Exchange Service (DAAD).

ABBREVIATIONS

HCEC, human coronary artery endothelial cell; HUVEC, human umbilical vein endothelial cell; ROS, reactive oxygen species; CVD, cardiovascular disease; SASP, senescence-associated secretory phenotype; FASP, filter aided sample preparation; IPA, Ingenuity pathway analysis; FDR, false discovery rate; MHC, major histocompatibility complex

REFERENCES

- (1) Seals, D. R.; Jablonski, K. L.; Donato, A. J. Aging and vascular endothelial function in humans. *Clin. Sci.* **2011**, *120*, 357–75.
- (2) Davignon, J.; Ganz, P. Role of endothelial dysfunction in atherosclerosis. *Circulation* **2004**, *109*, III-27–III-32.
- (3) Bhayadia, R.; Schmidt, B. M.; Melk, A.; Homme, M. Senescence-Induced Oxidative Stress Causes Endothelial Dysfunction. *J. Gerontol., Ser. A* **2016**, *71*, 161–9.
- (4) Lasry, A.; Ben-Neriah, Y. Senescence-associated inflammatory responses: aging and cancer perspectives. *Trends Immunol.* **2015**, *36*, 217–28.
- (5) Pantsulaia, I.; Ciszewski, W. M.; Niewiarowska, J. Senescent endothelial cells: Potential modulators of immunosenescence and ageing. *Ageing Res. Rev.* **2016**, *29*, 13–25.
- (6) Rodier, F. Detection of the Senescence-Associated Secretory Phenotype (SASP). In *Cell Senescence: Methods and Protocols*; Galluzzi, L., Vitale, L., Kepp, O., Kroemer, G., Eds.; Humana Press: New York, 2013; p 538.
- (7) Coppe, J. P.; Kauser, K.; Campisi, J.; Beausejour, C. M. Secretion of vascular endothelial growth factor by primary human fibroblasts at senescence. *J. Biol. Chem.* **2006**, *281*, 29568–74.
- (8) Parrinello, S.; Coppe, J. P.; Krtolica, A.; Campisi, J. Stromal-epithelial interactions in aging and cancer: senescent fibroblasts alter epithelial cell differentiation. *J. Cell Sci.* **2005**, *118*, 485–496.
- (9) Liu, D.; Hornsby, P. J. Senescent human fibroblasts increase the early growth of xenograft tumors via matrix metalloproteinase secretion. *Cancer Res.* **2007**, *67*, 3117–26.

- (10) Baggetta, R.; De Andrea, M.; Gariano, G. R.; Mondini, M.; Ritta, M.; Caposio, P.; Cappello, P.; Giovarelli, M.; Gariglio, M.; Landolfo, S. The interferon-inducible gene IFI16 secretome of endothelial cells drives the early steps of the inflammatory response. *Eur. J. Immunol.* **2010**, *40*, 2182–9.
- (11) Prattichizzo, F.; De Nigris, V.; La Sala, L.; Procopio, A. D.; Olivieri, F.; Ceriello, A. "Inflammaging" as a Druggable Target: A Senescence-Associated Secretory Phenotype-Centered View of Type 2 Diabetes. *Oxid. Med. Cell. Longevity* **2016**, *2016*, Article No. 1810327.
- (12) Nelson, G.; Wordsworth, J.; Wang, C.; Jurk, D.; Lawless, C.; Martin-Ruiz, C.; von Zglinicki, T. A senescent cell bystander effect: senescence-induced senescence. *Aging Cell* **2012**, *11*, 345–9.
- (13) LeBrasseur, N. K.; Tchkonja, T.; Kirkland, J. L. Cellular Senescence and the Biology of Aging, Disease, and Frailty. *Nestle Nutr. Inst. Workshop Ser.* **2015**, *83*, 11–8.
- (14) Yentrapalli, R.; Azimzadeh, O.; Barjaktarovic, Z.; Sarioglu, H.; Wojcik, A.; Harms-Ringdahl, M.; Atkinson, M. J.; Haghdoost, S.; Tapio, S. Quantitative proteomic analysis reveals induction of premature senescence in human umbilical vein endothelial cells exposed to chronic low-dose rate gamma radiation. *Proteomics* **2013**, *13*, 1096–107.
- (15) Yentrapalli, R.; Azimzadeh, O.; Sriharshan, A.; Malinowsky, K.; Merl, J.; Wojcik, A.; Harms-Ringdahl, M.; Atkinson, M. J.; Becker, K. F.; Haghdoost, S.; Tapio, S. The PI3K/Akt/mTOR Pathway Is Implicated in the Premature Senescence of Primary Human Endothelial Cells Exposed to Chronic Radiation. *PLoS One* **2013**, *8*, e70024.
- (16) Dong, X.; Tong, F.; Qian, C.; Zhang, R.; Dong, J.; Wu, G.; Hu, Y. NEMO modulates radiation-induced endothelial senescence of human umbilical veins through NF-kappaB signal pathway. *Radiat. Res.* **2015**, *183*, 82–93.
- (17) Heo, J. I.; Kim, W.; Choi, K. J.; Bae, S.; Jeong, J. H.; Kim, K. S. XIAP-associating factor 1, a transcriptional target of BRD7, contributes to endothelial cell senescence. *Oncotarget* **2016**, *7*, 5118–30.
- (18) Kim, K. S.; Kim, J. E.; Choi, K. J.; Bae, S.; Kim, D. H. Characterization of DNA damage-induced cellular senescence by ionizing radiation in endothelial cells. *Int. J. Radiat. Biol.* **2014**, *90*, 71–80.
- (19) Lowe, D.; Raj, K. Premature aging induced by radiation exhibits pro-atherosclerotic effects mediated by epigenetic activation of CD44 expression. *Aging Cell* **2014**, *13*, 900–910.
- (20) Azimzadeh, O.; Sievert, W.; Sarioglu, H.; Merl-Pham, J.; Yentrapalli, R.; Bakshi, M. V.; Janik, D.; Ueffing, M.; Atkinson, M. J.; Multhoff, G.; Tapio, S. Integrative proteomics and targeted transcriptomics analyses in cardiac endothelial cells unravel mechanisms of long-term radiation-induced vascular dysfunction. *J. Proteome Res.* **2015**, *14*, 1203–19.
- (21) Sievert, W.; Tapio, S.; Breuninger, S.; Gaip, U.; Andratschke, N.; Trott, K. R.; Multhoff, G. Adhesion molecule expression and function of primary endothelial cells in benign and malignant tissues correlates with proliferation. *PLoS One* **2014**, *9*, e91808.
- (22) Formenti, S. C.; Demaria, S. Systemic effects of local radiotherapy. *Lancet Oncol.* **2009**, *10*, 718–26.
- (23) Khan, M. A.; Van Dyk, J.; Yeung, I. W.; Hill, R. P. Partial volume rat lung irradiation; assessment of early DNA damage in different lung regions and effect of radical scavengers. *Radiother. Oncol.* **2003**, *66*, 95–102.
- (24) Langan, A. R.; Khan, M. A.; Yeung, I. W.; Van Dyk, J.; Hill, R. P. Partial volume rat lung irradiation: the protective/mitigating effects of Eukarion-189, a superoxide dismutase-catalase mimetic. *Radiother. Oncol.* **2006**, *79*, 231–8.
- (25) Calveley, V. L.; Khan, M. A.; Yeung, I. W.; Vandyk, J.; Hill, R. P. Partial volume rat lung irradiation: temporal fluctuations of in-field and out-of-field DNA damage and inflammatory cytokines following irradiation. *Int. J. Radiat. Biol.* **2005**, *81*, 887–99.
- (26) Nagasawa, H.; Little, J. B. Bystander effect for chromosomal aberrations induced in wild-type and repair deficient CHO cells by low fluences of alpha particles. *Mutat. Res., Fundam. Mol. Mech. Mutagen.* **2002**, *508*, 121–9.
- (27) Hwang, H. J.; Jung, S. H.; Lee, H. C.; Han, N. K.; Bae, I. H.; Lee, M.; Han, Y. H.; Kang, Y. S.; Lee, S. J.; Park, H. J.; Ko, Y. G.; Lee, J. S. Identification of novel therapeutic targets in the secretome of ionizing radiation-induced senescent tumor cells. *Oncol. Rep.* **2016**, *35*, 841–50.
- (28) Han, N. K.; Kim, B. C.; Lee, H. C.; Lee, Y. J.; Park, M. J.; Chi, S. G.; Ko, Y. G.; Lee, J. S. Secretome analysis of ionizing radiation-induced senescent cancer cells reveals that secreted RKIP plays a critical role in neighboring cell migration. *Proteomics* **2012**, *12*, 2822–32.
- (29) Xiao, L.; Liu, W.; Li, J.; Xie, Y.; He, M.; Fu, J.; Jin, W.; Shao, C. Irradiated U937 cells trigger inflammatory bystander responses in human umbilical vein endothelial cells through the p38 pathway. *Radiat. Res.* **2014**, *182*, 111–21.
- (30) Lowe, D.; Raj, K. Premature aging induced by radiation exhibits pro-atherosclerotic effects mediated by epigenetic activation of CD44 expression. *Aging Cell* **2014**, *13*, 900–10.
- (31) Wisniewski, J. R.; Zougman, A.; Nagaraj, N.; Mann, M. Universal sample preparation method for proteome analysis. *Nat. Methods* **2009**, *6*, 359–62.
- (32) Hauck, S. M.; Dietter, J.; Kramer, R. L.; Hofmaier, F.; Zipplies, J. K.; Amann, B.; Feuchtinger, A.; Deeg, C. A.; Ueffing, M. Deciphering membrane-associated molecular processes in target tissue of auto-immune uveitis by label-free quantitative mass spectrometry. *Mol. Cell. Proteomics* **2010**, *9*, 2292–305.
- (33) Subramanian, V.; Seemann, I.; Merl-Pham, J.; Hauck, S. M.; Stewart, F. A.; Atkinson, M. J.; Tapio, S.; Azimzadeh, O. Role of TGF Beta and PPAR Alpha Signaling Pathways in Radiation Response of Locally Exposed Heart: Integrated Global Transcriptomics and Proteomics Analysis. *J. Proteome Res.* **2017**, *16*, 307–318.
- (34) Schneider, C. A.; Rasband, W. S.; Eliceiri, K. W. NIH Image to ImageJ: 25 years of image analysis. *Nat. Methods* **2012**, *9*, 671–5.
- (35) Sriharshan, A.; Boldt, K.; Sarioglu, H.; Barjaktarovic, Z.; Azimzadeh, O.; Hieber, L.; Zitzelsberger, H.; Ueffing, M.; Atkinson, M. J.; Tapio, S. Proteomic analysis by SILAC and 2D-DIGE reveals radiation-induced endothelial response: Four key pathways. *J. Proteomics* **2012**, *75*, 2319–30.
- (36) Barjaktarovic, Z.; Merl-Pham, J.; Azimzadeh, O.; Kempf, S. J.; Raj, K.; Atkinson, M. J.; Tapio, S. Low-dose radiation differentially regulates protein acetylation and histone deacetylase expression in human coronary artery endothelial cells. *Int. J. Radiat. Biol.* **2017**, *93*, 156–164.
- (37) Azimzadeh, O.; Azizova, T.; Merl-Pham, J.; Subramanian, V.; Bakshi, M. V.; Moseeva, M.; Zubkova, O.; Hauck, S. M.; Anastasov, N.; Atkinson, M. J.; Tapio, S. A dose-dependent perturbation in cardiac energy metabolism is linked to radiation-induced ischemic heart disease in Mayak nuclear workers. *Oncotarget* **2017**, *8*, 9067–9078.
- (38) Singh, R. Jak2-Independent Activation of Stat3 by Intracellular Angiotensin II in Human Mesangial Cells. *J. Signal Transduction* **2011**, *2011*, Article No. 257862.
- (39) Morgan, W. F.; Hartmann, A.; Limoli, C. L.; Nagar, S.; Ponnaiya, B. Bystander effects in radiation-induced genomic instability. *Mutat. Res., Fundam. Mol. Mech. Mutagen.* **2002**, *504*, 91–100.
- (40) Wung, B. S.; Ni, C. W.; Wang, D. L. ICAM-1 induction by TNFalpha and IL-6 is mediated by distinct pathways via Rac in endothelial cells. *J. Biomed. Sci.* **2005**, *12*, 91–101.
- (41) Sikorski, K.; Czerwoniec, A.; Bujnicki, J. M.; Wesoly, J.; Bluysen, H. A. STAT1 as a novel therapeutic target in pro-atherogenic signal integration of IFNgamma, TLR4 and IL-6 in vascular disease. *Cytokine Growth Factor Rev.* **2011**, *22*, 211–9.
- (42) Zauberman, A.; Zipori, D.; Krupsky, M.; Ben-Levy, R. Stress activated protein kinase p38 is involved in IL-6 induced transcriptional activation of STAT3. *Oncogene* **1999**, *18*, 3886–93.
- (43) Costa-Pereira, A. P.; Tininini, S.; Strobl, B.; Alonzi, T.; Schlaak, J. F.; Is'harc, H.; Gesualdo, L.; Newman, S. J.; Kerr, I. M.; Poli, V. Mutational switch of an IL-6 response to an interferon-gamma-like response. *Proc. Natl. Acad. Sci. U. S. A.* **2002**, *99*, 8043–7.

(44) Novakova, Z.; Hubackova, S.; Kosar, M.; Janderova-Rossmeislova, L.; Dobrovolna, J.; Vasicova, P.; Vancurova, M.; Horejsi, Z.; Hozak, P.; Bartek, J.; Hodny, Z. Cytokine expression and signaling in drug-induced cellular senescence. *Oncogene* **2010**, *29*, 273–84.

(45) Furusawa, Y.; Zhao, Q. L.; Hattori, Y.; Tabuchi, Y.; Iwasaki, T.; Nomura, T.; Kondo, T. Comprehensive and computational analysis of genes in human umbilical vein endothelial cells responsive to X-irradiation. *Genomics Data* **2016**, *8*, 126–30.

(46) Zhao, Y.; Valbuena, G.; Walker, D. H.; Gazi, M.; Hidalgo, M.; DeSousa, R.; Oteo, J. A.; Goetz, Y.; Brasier, A. R. Endothelial Cell Proteomic Response to Rickettsia conorii Infection Reveals Activation of the Janus Kinase (JAK)-Signal Transducer and Activator of Transcription (STAT)-Interferon Stimulated Gene (ISG)15 Pathway and Reprogramming Plasma Membrane Integrin/Cadherin Signaling. *Mol. Cell. Proteomics* **2016**, *15*, 289–304.

(47) Sadler, A. J.; Williams, B. R. Interferon-inducible antiviral effectors. *Nat. Rev. Immunol.* **2008**, *8*, 559–68.

(48) Wang, Y.; van Boxel-Dezaire, A. H.; Cheon, H.; Yang, J.; Stark, G. R. STAT3 activation in response to IL-6 is prolonged by the binding of IL-6 receptor to EGF receptor. *Proc. Natl. Acad. Sci. U. S. A.* **2013**, *110*, 16975–80.

(49) Tkach, M.; Roseblit, C.; Rivas, M. A.; Proietti, C. J.; Diaz Flaque, M. C.; Mercogliano, M. F.; Beguelin, W.; Maronna, E.; Guzman, P.; Gercovich, F. G.; Deza, E. G.; Elizalde, P. V.; Schillaci, R. p42/p44 MAPK-mediated Stat3Ser727 phosphorylation is required for progestin-induced full activation of Stat3 and breast cancer growth. *Endocr.-Relat. Cancer* **2013**, *20*, 197–212.

(50) Lim, C. P.; Cao, X. Structure, function, and regulation of STAT proteins. *Mol. BioSyst.* **2006**, *2*, 536–50.

(51) Silva, C. M. Role of STATs as downstream signal transducers in Src family kinase-mediated tumorigenesis. *Oncogene* **2004**, *23*, 8017–23.

(52) Kopantzev, Y.; Heller, M.; Swaminathan, N.; Rudikoff, S. IL-6 mediated activation of STAT3 bypasses Janus kinases in terminally differentiated B lineage cells. *Oncogene* **2002**, *21*, 6791–800.

(53) Maritano, D.; Sugrue, M. L.; Tininini, S.; Dewilde, S.; Strobl, B.; Fu, X.; Murray-Tait, V.; Chiarle, R.; Poli, V. The STAT3 isoforms alpha and beta have unique and specific functions. *Nat. Immunol.* **2004**, *5*, 401–9.

(54) Dewilde, S.; Vercelli, A.; Chiarle, R.; Poli, V. Of alphas and betas: distinct and overlapping functions of STAT3 isoforms. *Front. Biosci., Landmark Ed.* **2008**, *13*, 6501.

(55) Lee, J.; Baldwin, W. M., 3rd; Lee, C. Y.; Desiderio, S. Stat3beta mitigates development of atherosclerosis in apolipoprotein E-deficient mice. *J. Mol. Med. (Heidelberg, Ger.)* **2013**, *91*, 965–76.

(56) Kojima, H.; Inoue, T.; Kunimoto, H.; Nakajima, K. IL-6-STAT3 signaling and premature senescence. *JAKSTAT* **2013**, *2*, e25763.

(57) Hayashi, T.; Morishita, Y.; Kubo, Y.; Kusunoki, Y.; Hayashi, I.; Kasagi, F.; Hakoda, M.; Kyoizumi, S.; Nakachi, K. Long-term effects of radiation dose on inflammatory markers in atomic bomb survivors. *Am. J. Med.* **2005**, *118*, 83–6.

(58) Neriishi, K.; Nakashima, E.; DeLongchamp, R. R. Persistent subclinical inflammation among A-bomb survivors. *Int. J. Radiat. Biol.* **2001**, *77*, 475–82.

(59) Shimizu, Y.; Kodama, K.; Nishi, N.; Kasagi, F.; Suyama, A.; Soda, M.; Grant, E. J.; Sugiyama, H.; Sakata, R.; Moriwaki, H.; Hayashi, M.; Konda, M.; Shore, R. E. Radiation exposure and circulatory disease risk: Hiroshima and Nagasaki atomic bomb survivor data, 1950–2003. *Bmj* **2010**, *340*, b5349.

3.2 Data-independent acquisition mass spectrometry of irradiated mouse lung endothelial cells reveals a STAT-associated inflammatory response

3.2.1 Aim and Summary

In the case of breast cancer, the most common cancer in women, radiation therapy is still the method of choice (Sakorafas and Safioleas 2010). Inflammation of the lung and even fibrosis can occur as a long-term consequence of the high radiation doses used in the therapy (Chen, Wu, and Ning 2019; Aznar et al. 2018). It is therefore important to investigate the underlying mechanisms, especially the response in the lung endothelium immediately after the radiation, as aimed in this study. For this purpose, lung endothelial cells of female C57Bl/6 mice were isolated 24 hours after *in vivo* thorax irradiation with 10 Gy X-rays. We used sham-irradiated mice as control animals. Endothelial cells were isolated from the lung tissue of sham-irradiated and irradiated mice and cultured for six days. Global label-free proteome analysis was performed in a data-independent acquisition mass spectrometry. As a result 4,220 proteins were identified, of which 60 were significantly deregulated according to the following criteria: a fold change of ± 2.0 and a q-value of < 0.05 . A bioinformatics analysis revealed the induction of inflammatory proteins STAT1, IRF3, and 12 other proteins belonging to the type I interferon signaling pathway. The radiation-induced upregulation of STAT1 and its downstream-target ISG15 was confirmed by immunoblotting. Furthermore, the downregulation of the antioxidant proteins SOD1 and PRDX5 suggested a depletion in response to radiation-induced oxidative stress. Although the level of the cGAS protein was not significantly altered with irradiation the induction of many interferon-related proteins suggested an involvement of the JAK/STAT- and the cGAS/STING-pathways. Therefore, these pathways are potential targets in the prevention of radiation-induced pulmonary inflammation.

3.2.2 Contribution to the study

This study was conceived by Dr. Wolfgang Sievert from Radiation Immuno Oncology Group of the Technical University of Munich (TUM) and me. The mouse irradiation, the isolation of the endothelial cells and the cell culture was done by Wolfgang Sievert and me. This part of the work was carried out on the premises of TUM at

Campus Klinikum Rechts der Isar. The protein isolation, lysis, measurement of protein content, and the preparation for mass spectrometry analysis was done by me. The LC-MS/MS runs were performed by Dr. Fabian Metzger and Dr. Christine von Törne (Proteomics Core Facility, Research Unit Protein Science, HMGU). Statistical analysis was carried out by me with the advice from Dr. Herbert Braselmann (ZYTO, HMGU). Bioinformatics analysis was performed by me. The immunoblotting was carried out by me with technical advice from Dr. Anton Posch and Dr. Prabal Subedi. Daniela Hladik helped with the immunoblotting analysis. The figures and the first version of the manuscript were designed and written, respectively, by me. Prabal Subedi, Omid Azimzadeh, Prof. Dr. Gabriele Multhoff, Soile Tapio and Prof. Dr. Michael J. Atkinson provided me with advice, scientific discussions throughout the study and especially Soile Tapio did proofreading of the manuscript.

3.2.3 Publication

I presented in the data in an invited talk on September, 25th, 2018 at the Radiation Research Society Meeting in Chicago. The study was published as an original research paper on May, 2020 in the International Journal of Radiation Biology:

Reprinted with permission from:

Data independent acquisition mass spectrometry of irradiated mouse lung endothelial cells reveals a STAT-associated inflammatory response.

Jos Philipp, Wolfgang Sievert, Omid Azimzadeh, Christine von Toerne, Fabian Metzger, Anton Posch, Daniela Hladik, Prabal Subedi, Gabriele Multhoff, Michael J Atkinson, Soile Tapio.

Int J Radiat Biol., 2020 May, doi: 10.1080/09553002.2020.1712492. Epub 2020 Jan 21.




Data independent acquisition mass spectrometry of irradiated mouse lung endothelial cells reveals a STAT-associated inflammatory response

Jos Philipp, Wolfgang Sievert, Omid Azimzadeh, Christine von Toerne, Fabian Metzger, Anton Posch, Daniela Hladik, Prabal Subedi, Gabriele Multhoff, Michael J. Atkinson & Soile Tapio

To cite this article: Jos Philipp, Wolfgang Sievert, Omid Azimzadeh, Christine von Toerne, Fabian Metzger, Anton Posch, Daniela Hladik, Prabal Subedi, Gabriele Multhoff, Michael J. Atkinson & Soile Tapio (2020): Data independent acquisition mass spectrometry of irradiated mouse lung endothelial cells reveals a STAT-associated inflammatory response, *International Journal of Radiation Biology*, DOI: [10.1080/09553002.2020.1712492](https://doi.org/10.1080/09553002.2020.1712492)

To link to this article: <https://doi.org/10.1080/09553002.2020.1712492>

 [View supplementary material](#) 

 Accepted author version posted online: 08 Jan 2020.
Published online: 21 Jan 2020.

 [Submit your article to this journal](#) 

 Article views: 72

 [View related articles](#) 

 [View Crossmark data](#) 

Data independent acquisition mass spectrometry of irradiated mouse lung endothelial cells reveals a STAT-associated inflammatory response

Jos Philipp^a, Wolfgang Sievert^b, Omid Azimzadeh^a, Christine von Toerne^c, Fabian Metzger^c, Anton Posch^a, Daniela Hladik^a, Prabal Subedi^a, Gabriele Multhoff^{fb}, Michael J. Atkinson^a, and Soile Tapio^a

^aHelmholtz Zentrum München, German Research Center for Environmental Health GmbH, Institute of Radiation Biology, Neuherberg, Germany; ^bRadiation Immuno Oncology Group, Center for Translational Cancer Research (TranslaTUM), Munich, Germany; ^cHelmholtz Zentrum München, German Research Centre for Environmental Health GmbH, Research Unit Protein Science, Munich, Germany

ABSTRACT

Purpose: Pulmonary inflammation is an adverse consequence of radiation therapy in breast cancer. The aim of this study was to elucidate biological pathways leading to this pathology.

Materials and methods: Lung endothelial cells were isolated 24 h after thorax-irradiation (sham or 10 Gy X-ray) from female C57Bl/6 mice and cultivated for 6 days.

Results: Quantitative proteomic analysis of lung endothelial cells was done using data independent acquisition (DIA) mass spectrometry. The data were analyzed using Ingenuity Pathway Analysis and STRINGdb. In total, 4220 proteins were identified using DIA of which 60 were dysregulated in the irradiated samples (fold change ≥ 2.00 or ≤ 0.50 ; q -value < 0.05). Several (12/40) upregulated proteins formed a cluster of inflammatory proteins with STAT1 and IRF3 as predicted upstream regulators. The several-fold increased expression of STAT1 and STAT-associated ISG15 was confirmed by immunoblotting. The expression of antioxidant proteins SOD1 and PRXD5 was downregulated suggesting radiation-induced oxidative stress. Similarly, the phosphorylated (active) forms of STING and IRF3, both members of the cGAS/STING pathway, were downregulated.

Conclusions: These data suggest the involvement of JAK/STAT and cGas/STING pathways in the genesis of radiation-induced lung inflammation. These pathways may be used as novel targets for the prevention of radiation-induced lung damage.

ARTICLE HISTORY

Received 7 October 2019
Revised 11 December 2019
Accepted 2 January 2020

KEYWORDS

cGAS/STING pathway; endothelial cell; ionizing radiation; pulmonary inflammation; STAT1

Introduction

Breast cancer is the most common diagnosed cancer in women (Bray et al. 2018). Radiation therapy is an effective and often used treatment (Sakorafas and Safioleas 2010), whereby lung tissue unavoidably gets partially irradiated (Aznar et al. 2018). This results frequently in pulmonary inflammation possibly due to local release of cytokines and other pro-inflammatory molecules (Kainthola et al. 2017). The acute inflammatory response is orchestrated by alveolar epithelial cells, tissue residential macrophages, and endothelial cells of the pulmonary vasculature (Pate et al. 2010; Giridhar et al. 2015; Huang et al. 2017). The early induction of inflammation may cause persistent low-level inflammation that is characterized by endothelial dysfunction and senescence (Van der Meeren et al. 2003; Azimzadeh et al. 2015; Sievert et al. 2015; Baselet et al. 2019), finally leading to pneumonitis and fibrosis (Kainthola et al. 2017).

We previously used a human coronary artery endothelial cell line to study the biological mechanism of radiation-associated inflammation (Philipp et al. 2017). The endothelial cells entering radiation-induced premature senescence

showed increased expression of STAT-proteins. The JAK/STAT-pathway is prominent in the adaptive and innate immune response (Stark and Darnell 2012; Villarino et al. 2015). One of the key-players in the STAT cascade is STAT1, a transcription factor that induces expression of interferon (IFN)-related and other inflammatory genes (Au-Yeung et al. 2013; Trilling et al. 2013).

A potent inducer of STAT1 and other type I IFN-proteins is the so-called cGAS/STING-pathway, a component of the innate immune system that alerts the cell's immune system after detecting the presence of cytosolic DNA (Lam et al. 2014; Li and Chen 2018). In a convoluted cascade, the protein cGAS, activated by dsDNA, produces the second messenger cGAMP that binds and activates the adaptor protein STING that, in its turn, activates transcription factor IRF3 in a phosphorylation-dependent mechanism (Tao et al. 2016). This triggers the transcription of pro-inflammatory genes (Kato et al. 2017). Radiation-induced activation of the cGAS/STING-pathway followed by increased expression of STAT1 has been shown in different cancers (Weichselbaum et al. 2008; Deng et al. 2014; Woo et al. 2014).

An important player in converting acute inflammation into a chronic one is ISG15, a small secretory protein, the expression of which is induced by the JAK/STAT pathway (Fan et al. 2015; Megger et al. 2017). It covalently modifies cytoplasmic and nuclear proteins by ISGylation, similar to ubiquitination (Villarroya-Beltri et al. 2016). In a feedback loop, ISG15 is able to induce cytokine expression and augment inflammation by modulating the JAK/STAT proteins and stabilizing STAT1 (Malakhova et al. 2003; Fan et al. 2015; Przanowski et al. 2018).

The aim of this study was to investigate the mechanism of the radiation-induced inflammatory response in lung endothelium. For this purpose, we used label-free proteomics based on data-independent acquisition. Since irradiation creates DNA double strand breaks, our particular interest was to study the role of cGAS/STING pathway downstream of damaged DNA.

Materials and methods

Animals and irradiation

All experiments were approved by the responsible state agency (Regierung von Oberbayern, certificate no. 55.2-1-54-2532-191-14). They were in compliance with national law on animal experimentation and welfare and performed in accordance with institutional and ARRIVE guidelines. Female C57Bl/6 mice (Charles River Laboratories, Sulzfeld, Germany) aged 4–5 weeks were randomly allocated to the treatment groups (4 mice/group). Irradiation of the whole thorax was performed using a high-precision image-guided Small Animal Radiation Research Platform (SARRP, Xstrahl, Camberley, UK). The dosimetry was performed using a calibrated ionization chamber (International Atomic Energy Agency, Vienna, Austria; Technical Reports Series No. 398) and radiochromic films (Gafchromic EBT3, Ashland, Covington, KY), according to the manufacturer's recommendations. The mice were anesthetized by isoflurane/oxygen inhalation for the duration of the treatment. The thorax was first visualized by CBCT to identify the required radiation field (60-kV and 0.8-mA photons filtered with aluminum 1 mm). The software SARRP control and Muriplan were used to precisely target thorax and estimate the radiation dose, respectively (Sievert et al. 2018). A single dose of 10 Gy was delivered using a 220 kV and 13 mA X-ray beam filtered with copper (0.15 mm). Control mice received sham irradiation using CBCT. The mice were housed in single ventilated cages under pathogen-free conditions while experimentation. In total, 32 mice were used in this study.

Primary cell culture

Primary microvascular CD31-positive endothelial cells were isolated from the lung 24 h after irradiation as described in detail previously (Sievert et al. 2014). For each biological replicate, endothelial cells of four mice were pooled to increase the yield and seeded in gelatin (2%; Merck KGaA, Darmstadt, Germany)-coated ibidi[®] chamber (ibidi GmbH,

Gräfelfing, Germany) with EGM2 (PromoCell, Heidelberg, Germany) supplemented with 10% FCS, streptomycin (100 mg/ml) and penicillin (100 U/ml).

Protein lysis and determination of protein concentration

RIPA buffer (Pierce Biotechnology, Rockford, IL, USA) was used for cell lysis. Protease inhibitor (cComplete tablets) and phosphatase inhibitor (PhosSTOP, both Roche Diagnostics GmbH, Mannheim, Germany) were added prior to lysis. RIPA buffer was applied into slides that were shortly frozen (10 min, -20°C) to remove the adherent cells. The cells were washed out with RIPA buffer and the lysate was sonicated and centrifuged for 20 min at 4°C with 13,000g. Supernatants were collected and stored until further use at -80°C . Protein concentration was measured by BCA protein assay (Pierce Biotechnology) according to manufacturer's instructions. The analysis was performed at 562 nm on an Infinite M200 (Tecan GmbH, Crailsheim, Germany).

Sample preparation

Ten μg of protein lysate was subjected to tryptic digestion using a modified FASP protocol (Wisniewski et al. 2009; Grosche et al. 2016).

Mass spectrometry (MS) measurement

MS data were acquired in data-independent acquisition (DIA) mode on a Q Exactive (QE) high field (HF) mass spectrometer (Thermo Fisher Scientific GmbH, Bremen, Germany). Samples were automatically loaded to the online coupled RSLC (Ultimate 3000, Thermo Fisher Scientific GmbH) HPLC system. A nano trap column was used (300 μm inner diameter \times 5 mm, packed with Acclaim PepMap100 C18, 5 μm , 100 \AA ; LC Packings, Sunnyvale, CA) before separation by reversed phase chromatography (Acquity UPLC M-Class HSS T3 Column 75 μm ID \times 250 mm, 1.8 μm ; Waters, Eschborn, Germany) at 40°C . Peptides were eluted from the column at 250 nl/min using an acetonitrile (ACN) gradient (in 0.1% formic acid) from 3% to 40% over 105 min.

The hyper reaction monitoring (HRM) data independent acquisition (DIA) method consisted of a survey scan from 300 to 1500 m/z at 120,000 resolution and automatic gain control (AGC) target of 3×10^6 or 120 ms maximum injection time. Fragmentation was performed via higher-energy collisional dissociation (HCD) with a target value of 3×10^6 ions determined with predictive AGC. Precursor peptides were isolated with 17 variable windows spanning from 300 to 1500 m/z at 30,000 resolution with an AGC target of 3×10^6 and automatic injection time. The normalized collision energy was 28 and the spectra were recorded in profile type.

Spectral library

The spectral library was generated as described previously (Kappler et al. 2019). The final spectral library generated in Spectronaut contained 11,184 protein groups and 349,634 peptide precursors.

Spectronaut analysis and data processing

The DIA MS data for lung endothelial cell groups were analyzed using the Spectronaut 10 software applying default settings with the exceptions: quantification was limited to proteotypic peptides, data filtering was set to q -value 50% percentile, summing-up peptide abundances.

Immunoblotting

Five microgram of proteins lysate were loaded on 1D Bio-Rad Mini-Protean[®] TGX Stain-Free[™] 4-15% Gels (Bio-Rad Laboratories GmbH, Munich, Germany). Proteins were denatured in 1× Laemmli buffer for 5 min at 95 °C. Gel runs were performed for 2 h at 60–120 V. Blotting was performed using a Bio-Rad Trans-Blot[®] Turbo[™] Semi-dry transfer system. A predefined program of 1.3 A for 10 min was used to transfer also high-molecular weight proteins onto 0.2 μm nitrocellulose membrane (Bio-Rad Laboratories GmbH). For visualization of protein separation on the gel and control of transfer efficiency, the internal control Stain-free[™] technology was used after 1 min of activation time. Membranes were washed and blocked with 8% milk (milk powder, Carl Roth GmbH & Co KG, Karlsruhe, Germany, dissolved in 1× TBST) for 1 h. Antibodies were used according to manufacturer's instructions and diluted in 5% milk if not further specified. Following antibodies were purchased from Cell Signaling (Cell Signaling Technology Europe B.V., Frankfurt am Main, Germany): phospho STING (85735), phospho IRF3 (S396, 4947), cGAS (15102), phospho p38 MAPK (T180/Y182), (9211), p38 MAPK (9212), from Abcam (Abcam plc, Cambridge, UK): peroxiredoxin 5 (ab119712), from R&D Systems (R&D Systems, Inc., Abingdon, UK): STING (MAB7169) and from Santa Cruz (Santa Cruz Biotechnology, Inc., Heidelberg, Germany): SOD1 (sc-11407), STAT1 (sc-346), ISG15 (sc-166755).

Membranes were incubated with the primary antibody overnight at 4 °C. For detection, the blots were incubated for 2 h with the appropriate horseradish-peroxidase conjugated anti-rabbit or -mouse secondary antibody. Detection was performed by ECL Advance Western blotting detection kit (GE Healthcare GmbH, Solingen, Germany) quantified in a chemiluminescence reader ChemiDoc[™] MP (Bio-Rad Laboratories GmbH) with the appropriate ImageLab 6.0.1 software. Blots were stripped for reprobing maximally twice with Stripping Buffer (0.2 M Glycin, 0.003 M SDS, 1/100 Tween20, pH 2.4).

Protein band intensities obtained by chemiluminescence visualization were normalized by total protein staining based on Stainfree[™] technology (Rivero-Gutierrez et al. 2014).

The corresponding blots are shown in Supplementary Figure S1.

Bioinformatics analysis

To evaluate protein expression in the normalized dataset one-way ANOVA approach by limma package in R (<https://www.R-project.org/>) was used. Western blotting band intensity was analyzed by Student's t -test. IPA (Qiagen GmbH, Hilden, Germany) and STRING (Szklarczyk et al. 2019) (medium confidence, 0.400) were used to cluster and classify pathways.

Statistical analysis

Filtering criteria for proteomics analyses were the following: significance for fold change (ratio irradiated to sham-irradiated) ≥ 2.00 or ≤ 0.50 and a FDR (q) ≤ 0.05 (Benjamini–Hochberg). Immunoblotting significance criteria: Proteins showing altered expression compared to the control were considered to be significant if $p \leq .05$ (unpaired Student's t -test). The error bars were calculated as standard deviation.

All experiments were performed using at least three biological replicates. The principal component analysis (PCA) based on all proteomic features showed one outlier in the control group that was excluded from further experiments (Supplementary Figure S2).

Data availability

Raw files of MS runs are available under the following link: <http://dx.doi.org/doi:10.20348/STOREDB/1152/1212>.

Results

Proteomics analysis

For proteomics analysis, female C57Bl/6 mice were locally irradiated in the thorax (10 Gy). The mice were allowed to recover 24 h before the isolation of lung endothelial cells that were expanded by in vitro cultivation for 6 days. In general, within this time endothelial cells in culture start to show their typical flat morphology and all cells have a direct cell-to-cell contact.

In total, 4220 proteins were identified with at least one peptide using Spectronaut (Supplementary Table S1). Of those, 4208 proteins could be quantified by a fold change and p -value ($<.05$) (Supplementary Table S2). Using Benjamini–Hochberg corrected p -values (q -values) 589 proteins qualified for quantification (Supplementary Table S3). Of these, 60 were deregulated by a fold change of ≥ 2.00 or ≤ 0.50 (Table 1) with 40 proteins showing upregulation and 20 downregulation as illustrated in Figure 1(A). The corresponding Volcano plot is shown in Figure 1(B).

A supervised hierarchical clustering (heat map) established the separation of the four irradiated samples from the three non-irradiated controls (Figure 2(A)). A scatter plot

Table 1. All deregulated proteins with affiliations, gene names, fold changes, and *p*- and *q*-values. The proteins are ranked by the fold change from the highest to the lowest.

Accession	Protein	Gene	log Fc	2log Fc	<i>p</i> -value	Adj. <i>p</i> -value
Q9Z0E6	Guanylate-binding protein 1	Gbp2	3.96	15.58	.0011391	.02530007
Q64339	Ubiquitin-like protein ISG15	Isg15	3.86	14.52	3.09E-06	.00241664
P42225	Signal transducer and activator of transcription 1	Stat1	2.59	6.01	1.48E-07	.00062321
P97501	Dimethylalanine monooxygenase [N-oxide-forming] 3	Fmo3	2.53	5.79	.0005817	.01981294
Q60766	Immunity-related GTPase family M protein 1	Irgm1	2.35	5.12	.0000182	.00636871
O08573	Galectin-9	Lgals9	1.95	3.86	5.33E-06	.00281054
Q8R2Q8	Bone marrow stromal antigen 2	Bst2	1.88	3.68	3.38E-06	.00241664
Q2TB02	NF-kappa-B inhibitor delta	Nfkbid	1.80	3.49	.001678	.02787862
PODOV1	Interferon-activable protein 205-B	Mnda	1.79	3.45	.0010634	.02459538
Q9JIX9	Fas-activated serine/threonine kinase	Fastk	1.78	3.43	.0013952	.02612012
P01899	H-2 class I histocompatibility antigen, D-B alpha chain	H2-D1	1.75	3.37	.0000428	.00820035
P12388	Plasminogen activator inhibitor 2, macrophage	Serpib2	1.61	3.06	.0000093	.00356802
Q07797	Galectin-3-binding protein	Lgals3bp	1.49	2.82	.0022512	.03220337
P97864	Caspase-7	Casp7	1.42	2.68	.0012945	.02557735
P16460	Argininosuccinate synthase	Ass1	1.30	2.47	.0003561	.01776233
Q921H9	Cytochrome c oxidase assembly factor 7	Coa7	1.26	2.39	.0044726	.04123245
Q9CRB5	Prolactin-7C1	Prl7c1	1.24	2.36	.0041481	.0401213
Q62356	Follistatin-related protein 1	Fstl1	1.22	2.32	.0001823	.01617524
Q9Z207	Protein diaphanous homolog 3	Diaph3	1.21	2.32	.0015113	.02634191
Q07968	Coagulation factor XIII B chain	F13b	1.19	2.28	.0051197	.04321033
Q80YX1	Tenascin	Tnc	1.19	2.28	.0006075	.02034618
Q6GQT1	Alpha-2-macroglobulin-P	A2m	1.18	2.26	.0026677	.03395418
P59759	MKL/myocardin-like protein 2	Mkl2	1.17	2.25	.0026407	.03395418
Q9ER38	Torsin-3A	Tor3a	1.16	2.24	.000286	.0169972
Q91W10	Zinc transporter ZIP8	Slc39a8	1.15	2.27	.0044606	.04123245
Q3UTJ2	Sorbin and SH3 domain-containing protein 2	Sorbs2	1.11	2.15	.0009947	.02454703
P28665	Murinoglobulin-1	Mug1	1.10	2.14	.004914	.04225627
Q9Z1B3	1-phosphatidylinositol 4,5-bisphosphate phosphodiesterase beta-1	Plcb1	1.09	2.13	.0068384	.04916159
Q9ESY9	Gamma-interferon-inducible lysosomal thiol reductase	Ifi30	1.09	2.13	.0024718	.03325888
Q3UFX8	FERM domain-containing protein 8	Frmf8	1.09	2.13	.0005795	.01981294
Q32NZ6	Transmembrane channel-like protein 5	Tmc5	1.08	2.12	.0056118	.04474289
P01887	Beta-2-microglobulin	B2m	1.06	2.08	.00008	.01205033
P02463	Collagen alpha-1(IV) chain	Col4a1	1.06	2.08	.0027585	.03423763
P03958	Adenosine deaminase	Ada	1.05	2.07	.0000354	.00812031
P08122	Collagen alpha-2(IV) chain	Col4a2	1.05	2.07	.005521	.04444658
P29268	Connective tissue growth factor	Ctgf	1.03	2.04	.0000226	.00636871
Q9QUR7	Peptidyl-prolyl cis-trans isomerase NIMA-interacting 1	Pin1	1.03	2.04	.0031763	.03656709
Q61703	Inter-alpha-trypsin inhibitor heavy chain H2	Itih2	1.02	2.03	.0040255	.03969085
O08992	Syntenin-1	Sdcbp	1.01	2.02	.0001013	.01425062
Q61301	Catenin alpha-2	Ctnna2	1.01	2.01	.0014879	.02629629
Q8K2Z4	Condensin complex subunit 1	Ncapd2	-1.01	-2.01	.0006179	.0203716
Q91VN4	MICOS complex subunit Mic25	Chchd6	-1.03	-2.04	.0000773	.01205033
Q920L1	Fatty acid desaturase 1	Fads1	-1.09	-2.12	6.05E-06	.00283862
Q80VJ3	2'-deoxynucleoside 5'-phosphate N-hydrolase 1	Dnph1	-1.11	-2.15	.000099	.01425062
Q99JZ7	ERBB receptor feedback inhibitor 1	Errfi1	-1.13	-2.18	.0012971	.02557735
Q9D6Y9	1,4-alpha-glucan-branching enzyme	Gbe1	-1.18	-2.26	.0002708	.01698344
E9Q1P8	Interferon regulatory factor 2-binding protein 2	Irf2bp2	-1.18	-2.27	.0041393	.0401213
P62983	Ubiquitin-40S ribosomal protein S27a	Rps27a	-1.22	-2.33	.0003719	.01780657
P31324	cAMP-dependent protein kinase type II-beta regulatory subunit	Prkar2b	-1.23	-2.35	.0004285	.01888652
P83882	60S ribosomal protein L36a	Rpl36a	-1.26	-2.39	.0040918	.04001259
Q91WN1	DnaJ homolog subfamily C member 9	Dnajc9	-1.39	-2.62	.000205	.01617524
Q9D823	60S ribosomal protein L37	Rpl37	-1.41	-2.65	.0016353	.02749385
Q99J39	Malonyl-CoA decarboxylase, mitochondrial	Mlycd	-1.53	-2.89	.0003535	.01776233
P15864	Histone H1.2	Hist1h1c	-1.56	-2.95	.0068269	.04916159
P05063	Fructose-bisphosphate aldolase C	Aldoc	-1.59	-3.02	.0005435	.01975831
P43276	Histone H1.5	Hist1h1b	-1.62	-3.07	.0053081	.04375005
P17809	Solute carrier family 2, facilitated glucose transporter member 1	Slc2a1	-1.70	-3.24	.0005382	.01975831
P43277	Histone H1.3	Hist1h1d	-1.94	-3.83	.0045947	.04123245
P43275	Histone H1.1	Hist1h1a	-2.03	-4.08	.0028167	.03455388
Q8C3F2	Constitutive coactivator of PPAR-gamma-like protein 2	Fam120c	-2.32	-4.99	.0061685	.0465672

showing clear correlation within all samples in the two treatment groups, thereby supporting the used statistical tools, is shown in [Supplementary Figure S3](#).

Bioinformatics analysis

Protein interactions of the 60 deregulated proteins were investigated using the STRING database. Two main clusters

were seen: (i) a cluster consisting of pro-inflammatory proteins (light green) and (ii) a cluster representing proteins of ribosomal and histone origin (dark green) ([Figure 2\(B\)](#)). All proteins of the inflammatory cluster including STAT1, ISG15, and GBP2 were upregulated, while the members of the ribosome/histone cluster were downregulated ([Table 1](#)). The other deregulated proteins did not build clusters that could have been defined under any particular biological function ([Figure 2\(B\)](#), shown in gray).

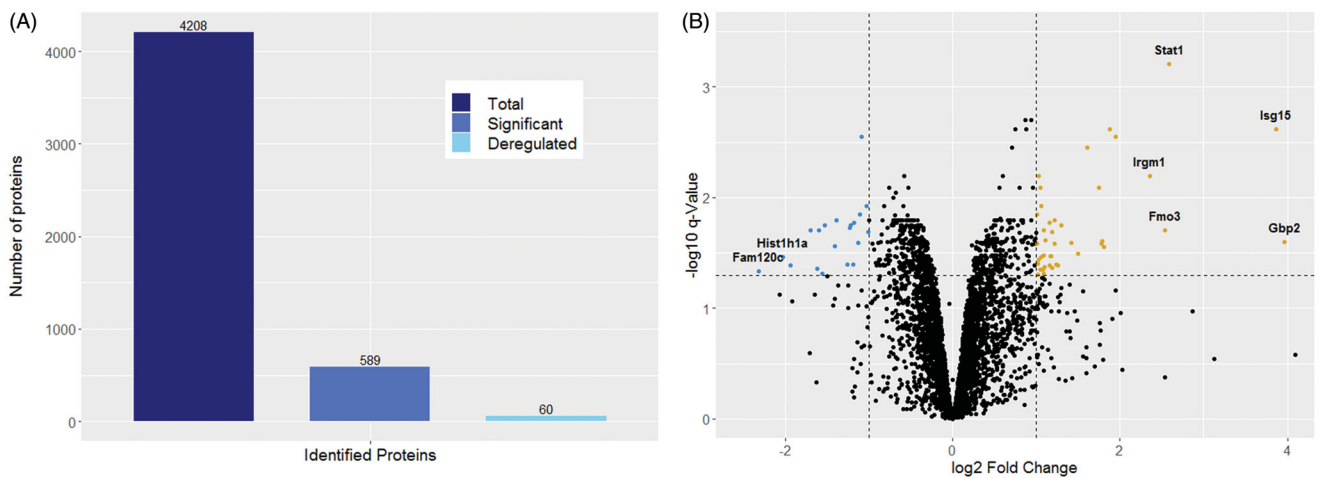


Figure 1. (A) Bar charts showing the deregulated proteins in mouse lung endothelial cells 7 days post irradiation. (B) Volcano plot displaying down- (blue) and up- (yellow) regulated proteins by $-\log_{10} q$ -value and \log_2 fold change.

All deregulated proteins were uploaded into IPA for upstream regulator prediction. The predicted upstream regulators, based on the activation z -score of >2 (IPA), were STAT1 and IRF3 (Figure 2(C)).

Immunoblotting validation

Immunoblotting was performed to validate the proteomics findings. Firstly, the expression of inflammatory proteins STAT1, ISG15, p38, and STAT3 was quantified. In accordance with the proteomics data, the level of STAT1 and ISG15 was significantly upregulated after irradiation (Figure 3(A,B)). The total amount of p38 or phospho-p38 (pp38) was not changed (Figure 3(C,D)). The ratio pp38/p38 showed tendency to upregulation that did not quite reach statistical significance ($p = .0502$) (Figure 3(E)). No changes were observed in the level of STAT3 (data not shown).

Since we previously observed a downregulation of oxidative stress markers in irradiated endothelial cells (Philipp et al. 2017), oxidative stress response was investigated (Figure 3(F–H)). The expression of antioxidative proteins SOD1 and PRXD5 (isoform 2) was downregulated after irradiation. This was probably due to radiation-induced increase in the reactive oxygen species levels.

To further investigate the radiation-induced enhancement of inflammatory markers, the key players of the cGAS/STING-pathway: STING, IRF3, and cGAS were tested (Figure 3(I–L)). In agreement with the proteomics data, the expression of total STING was not altered (Table S1). In contrast, the level of phospho-STING (S366) was significantly reduced in the irradiated samples. Similarly, the level of phospho-IRF3 (S396) showed radiation-induced decrease. Total IRF3 was not detectable by immunoblotting but was found unchanged in the proteomics analysis (Table S2). The level of the cGAS protein was not significantly altered with irradiation.

The expression of the p21Cip1/Waf1 protein, the upregulation of which has been seen in radiation-induced senescence in heart endothelial cells (Philipp et al. 2017) showed

no alteration in the lung endothelial cells one week post irradiation (data not shown).

Discussion

Irradiation is known to cause long-term damage in endothelial cells by inducing local and systemic inflammation (Azimzadeh et al. 2015; Mathias et al. 2015; Sievert et al. 2015) but the mechanism is largely unknown. In this study, proteomics analysis was performed using primary endothelial cells isolated from irradiated and sham-irradiated murine lung. Even though the cell isolation and in vitro culturing/expanding will affect the endothelial proteome to some extent, the irradiated cells and sham-irradiated controls will be affected in a similar way. We report here the comparative proteomic changes between these two states, not the absolute proteome. Furthermore, as endothelial cells from normal tissues such as the lung divide slowly compared to tumor endothelial cells (Sievert et al. 2014) we do not expect cultivation to alter the proteome to a great extent. The typical cell surface markers on endothelial cells derived from lung (CD31, CD105, CD144, CD34 CD54 CD102) did not change during the cultivation period [(Sievert et al. 2014) and data not shown].

We have shown previously that human coronary artery endothelial cells (HCECest2) are already in an inflammatory state two weeks post 10 Gy (X-ray) dose in vitro. The inflammatory response was reflected by increased levels of ISG15 (3.1-fold), p38 (2.9-fold), STAT1 (2.6-fold), and several IFN-induced proteins such as IFI44, IFI44L, IFIT1, and IFIT3 (Philipp et al. 2017). The results of this study, using primary endothelial cells from irradiated lung, are in line with the findings of the previous study. Radiation-associated inflammation was seen as significantly increased expression of Type I and Type II IFN-related proteins, especially ISG15, GBP2, IFI30, MNDA (IFI211) and, in particular, STAT1 (Table 1).

The phosphorylation of STAT1 is a transient process, increasing quickly but then decreasing over a period of some hours (Cheon and Stark 2009). In contrast, increased

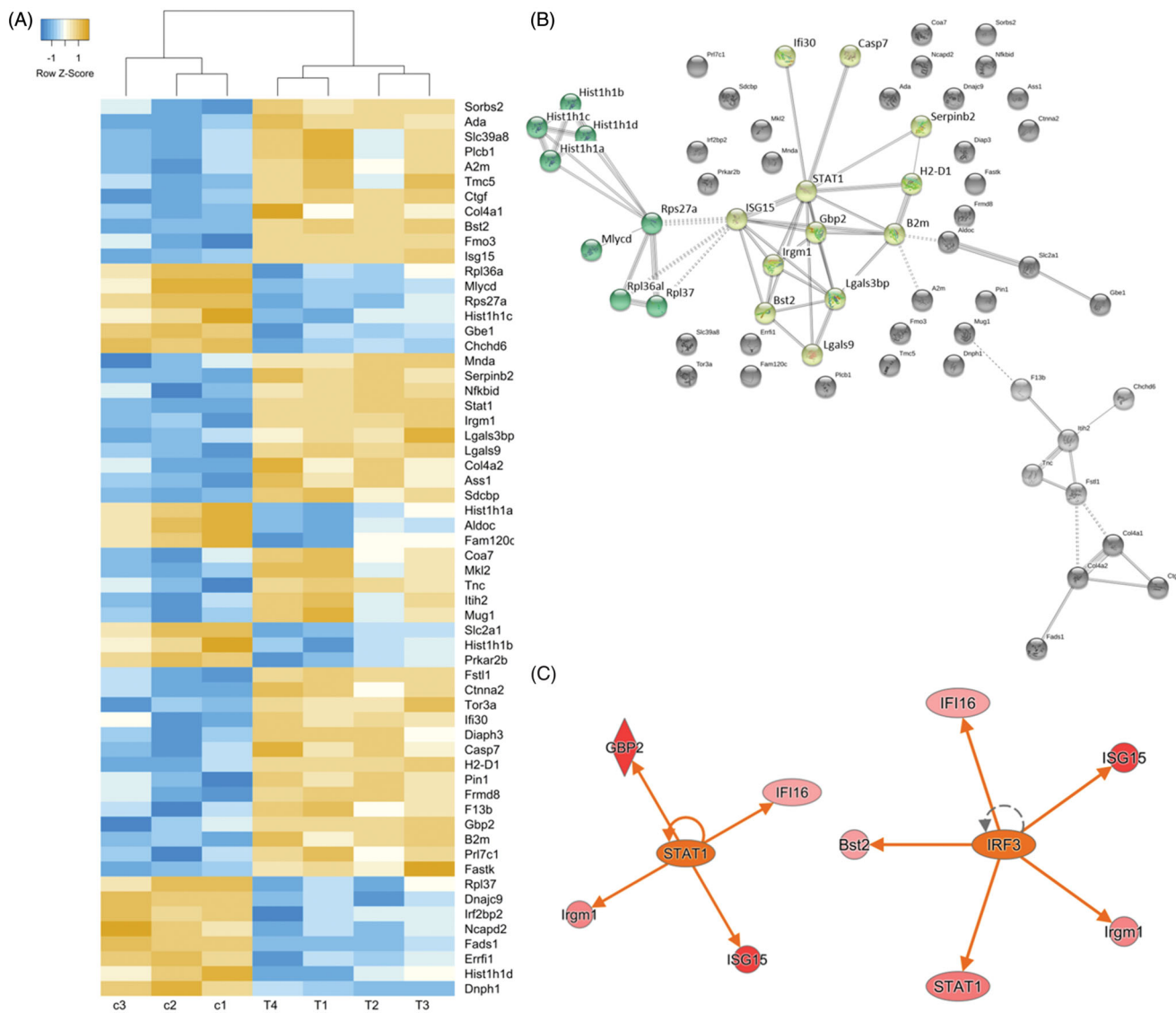


Figure 2. (A) A heat map showing the 60 deregulated proteins. Samples are distributed according to the average linkage hierarchical clustering (c, controls; T, irradiated samples). Z-scores are calculated by subtraction of the mean and dividing by the standard deviation for the deregulated proteins. (B) Interaction analysis of all significantly deregulated proteins using the STRING-db. The light green cluster represents the inflammatory cluster, the dark green cluster consists of ribosomal and histone proteins. The significance of deregulation was based on the label-free proteomics analysis (fold change ≥ 2.00 or ≤ 0.50 ; $q < 0.05$; $n = 3/4$). (C) Analysis of predicted upstream regulators using IPA. Graphical presentation of deregulated proteins with their upstream regulator STAT1 and IRF3 in the irradiated cells is shown (<http://www.INGENUITY.com>). The upregulated proteins are marked in red; the orange color of the STAT1 and IRF3 nodes indicates activation.

expression of non-phosphorylated STAT1, as found here, has been associated with prolonged expression of IFN-induced immune regulatory genes, including STAT1 itself (Cheon and Stark 2009; Yao et al. 2017). The p38 MAPK, the activation of which showed a positive trend in the irradiated cells ($p = .0502$), plays a critical role in Type I IFN-dependent transcriptional regulation but does not affect the phosphorylation status of STAT1 (Platanias 2003). A particular role in the maintenance of pro-inflammatory status has been given to ISG15 that was found to be strongly upregulated in this study. It is a secretory protein (Knight and Cordova 1991) that is able to induce IFN-gamma and IL-10 secretion (Bogunovic et al. 2012; Swaim et al. 2017) and thereby spread inflammation among endothelial cells in a paracrine manner (Philipp et al. 2017). In addition, the anti-inflammatory protein IRF2BPP2, important cofactor for revascularization (Ramalho-Oliveira et al. 2019), was

downregulated in irradiated endothelial cells (Table 1), further emphasizing the pro-inflammatory character of the proteomic response. Many of the IFN-related proteins found to be deregulated in this study have been shown to react in response to interferons but also to stay activated over time in fibroblasts (Megger et al. 2017).

One of the potential inducers of type I IFN-related inflammation is the cGAS/STING-pathway (Li and Chen 2018). Significant increase of interferon gamma-induced proteins 10 (IFI10) and 44 (IFI44) was seen in the lung of wild type mice 24 h after total body irradiation with 4.25 Gy but not in cGAS KO (knockout) or STING KO mice, emphasizing the role of this pathway in the early radiation-induced pulmonary inflammation (Gluck et al. 2017). While inflammation is an important process in the response to infection, uncontrolled and prolonged inflammation may have serious adverse consequences (Li and Chen 2018; Bai

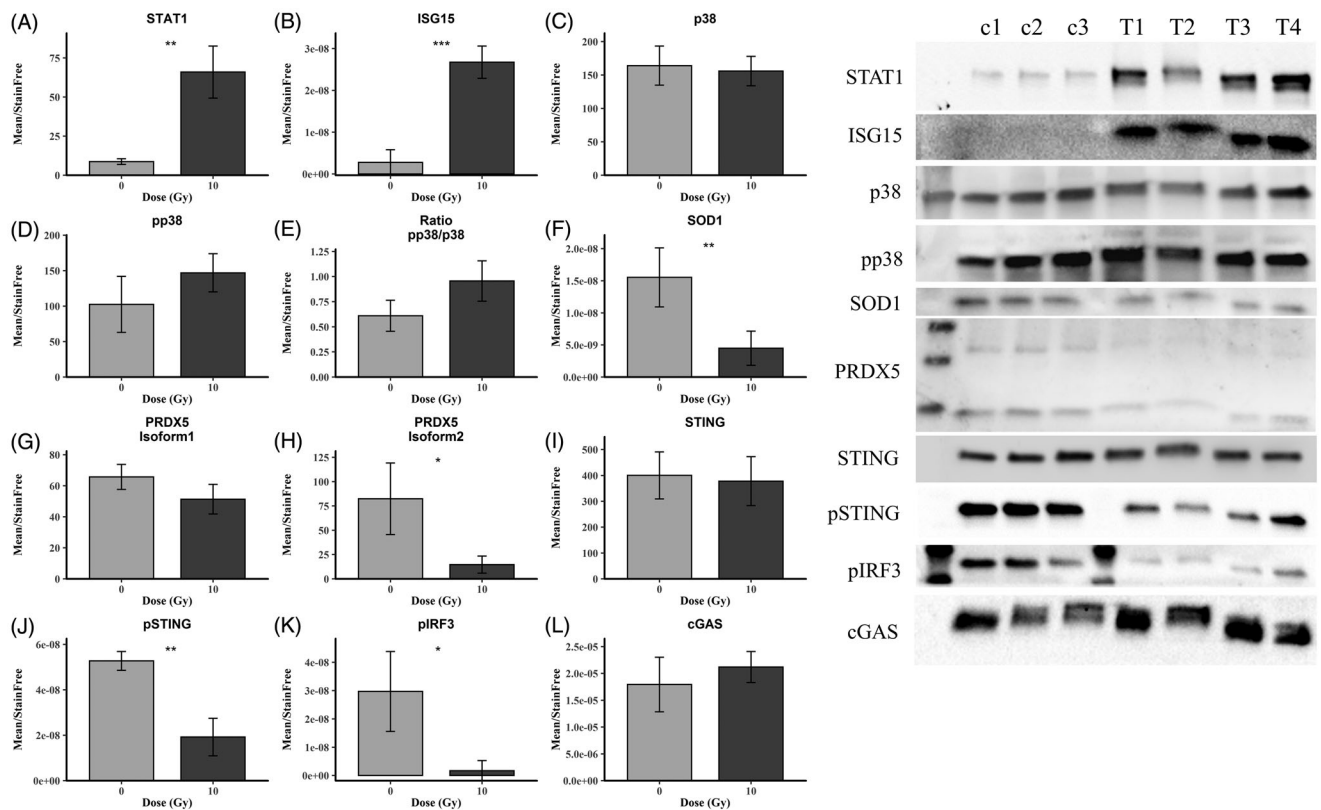


Figure 3. Immunoblot verification of protein changes in the irradiated cells. STAT1 (A), ISG15 (B), total p38 (C), phospho p38 (D); the ratio p38/phospho p38 (E), SOD1 (F), PRDX5 isoforms 1 (G) and 2 (H), STING (I), phospho STING (J), phospho IRF3 (K) and cGAS (L) are shown together with the immunoblots. The bars represent the relative expression after correction for background and normalization to stain free. The error bars are calculated as SD (*t*-test; **p* < .05, ***p* < .01, ****p* < .005; *n* = 3/4). C, control; T treated.

and Liu 2019). A number of negative feedback loops controlling the cGAS/STING pathway have been suggested (Ma and Damania 2016; Wu et al. 2017) but information concerning the induction and maintenance of the cGAS/STING pathway in radiation response is scarce. This study shows a significant reduction of the phosphorylated, transcriptionally active forms of STING and IRF3 in the irradiated lung endothelial cells compared to controls 7 days after the exposure, suggesting a possible negative feedback loop after initial induction of the cGAS/STING pathway. It has been shown previously that phosphorylated STING (S365) is able to bind to conserved, positively charged surfaces of IRF3, thereby recruiting IRF3 for its phosphorylation, dimerization, and translocation to the nucleus to induce the expression of IFN-dependent proteins (Liu et al. 2015). The bioinformatics analysis predicted activated IRF3 to be the transcriptional regulator of the changes observed in the irradiated proteome (Figure 2(C)), also indicating initial induction of this pathway. Taken together, a radiation-associated induction of the cGAS/STING pathway seems to be transient, while that of the STAT1-related pathway is persistent. However, more studies are needed to corroborate this.

In line with previous data (Azimzadeh et al. 2015, 2017; Philipp et al. 2017) we observed here a downregulation of antioxidative proteins (SOD1, PRDX5) in irradiated endothelial cells. Interestingly, a STAT-dependent positive feedback loop leading to a sustained interferon signature has been associated with increased ROS production in HUVECs (Kandhaya-Pillai et al. 2017) that could at least partly

explain the depletion of oxidative stress response proteins. In general, inflammation is known to be coupled to chronic oxidative stress in radiation-induced normal tissue injury (Zhao and Robbins 2009).

This study suggests that inhibition of STAT1 or ISG-15 could be used to prevent radiation-induced inflammatory response in the lung. However, both of these factors have been associated with tumor suppressor properties although there is no consensus whether these factors have pro-tumoral or a tumor suppressor effect (Villarroya-Beltri et al. 2017; Zhang and Liu 2017). In contrast, JAK1 inhibitors have no tumor suppressor properties and are being tested in clinical trials for the therapy of solid cancers including breast cancer (Beatty et al. 2019). JAK1 inhibitors have also been successfully used in cellular studies using alveolar macrophages isolated from chronic obstructive airway disease patients to inhibit STAT1 (Southworth et al. 2012); JAK/STAT pathway is known to be induced in the lung tissue of these patients (Yew-Booth et al. 2015). The efficient and safe use of JAK1 inhibitors suggests that this class of drugs could be used to prevent or treat radiation-induced pulmonary inflammation.

Conclusions

This study provides first evidence of the involvement of type I IFN-response and STAT1 and cGAS/STING pathways in particular in radiation-induced inflammation of the murine lung, greatly resembling the radiation response of human

heart endothelial cells (Philipp et al. 2017). The JAK/STAT pathway should be considered as future therapeutic target for potential prevention and treatment of pulmonary inflammation during radiation therapy.

Acknowledgments

The authors thank Dr. Herbert Braselmann for help and discussion in the statistics.

Disclosure statement

No potential conflict of interest was reported by the authors.

Funding

This research was funded by the Federal Ministry of Education and Research of Germany (BMBF) [02NUK038A (Wolfgang Sievert) and 02NUK038B (Jos Philipp)].

Notes on contributors

Jos Philipp (MSc) is a PhD student in the group of Radiation Proteomics at the Institute of Radiation Biology at HMGU. He investigates the effect of radiation-induced damages on endothelial cells of different origin.

Wolfgang Sievert (PhD) is a research scientist in the group of tumor imaging/radio-oncology/immunotherapy at Technical University Munich. His focus is radiation-induced endothelial damage.

Omid Azimzadeh (PhD) is an Adjunct Professor (Docent) of Radiation Biology and a research scientist at the Institute of Radiation Biology at HMGU. His research interests focus on the effects of radiation exposure on normal tissue with a specific emphasis on the myocardial and endothelial proteome response.

Christine von Toerne (PhD) is a group leader in the Research Unit Protein Science at HMGU, with a research focus on discovery proteomics for investigating cohort-based biomarker studies in the context of diabetes and complex diseases. Further, she is responsible for project management and quality controlled LC-MS/MS measurements in the Core Facility Proteomics at HMGU.

Fabian Metzger (PhD) is a postdoctoral researcher with the focus on targeted proteomics. He is responsible for project management and quality control at the Core Facility Proteomics, HMGU.

Anton Posch (PhD) is a guest scientist at the Institute of Radiation Biology (HMGU) and Federal Office for Radiation Protection with research interest in development of proteomics and immunoblotting.

Daniela Hladik (MSc) is a PhD student in the group of Radiation Proteomics at the Institute of Radiation Biology at HMGU. She investigates radiation-induced damages on the hippocampus.

Prabal Subedi (PhD) is a research scientist in the group of Radiation Proteomics at the Institute of Radiation Biology at HMGU. He investigates the role of extracellular vesicles in propagating radiation-induced leukemia.

Gabriele Multhoff (PhD) is the head of the group tumor imaging/radio-oncology/immunotherapy at Technical University Munich. Her research goal is the development of innovative immunological diagnostic and therapeutic methods related to heat shock proteins to target in combination with irradiation different cancer tissues.

Michael J. Atkinson (PhD) is the director of the Institute of Radiation Biology at the Helmholtz Zentrum München and Chair of Radiation Biology at the Technical University of Munich. His research goal is the improvement of radiation therapy by modulating the actions of radiation on tumor cells and non-cancerous tissues.

Soile Tapio (PhD) is an Adjunct Professor (Docent) of Radiation Biology. She leads the group of Radiation Proteomics at the Institute of Radiation Biology at HMGU. Her research topic is radiation-induced normal tissue damage in heart and brain.

References

- Au-Yeung N, Mandhana R, Horvath CM. 2013. Transcriptional regulation by STAT1 and STAT2 in the interferon JAK-STAT pathway. *Jakstat*. 2:e23931.
- Azimzadeh O, Sievert W, Sarioglu H, Merl-Pham J, Yentrapalli R, Bakshi MV, Janik D, Ueffing M, Atkinson MJ, Multhoff G, et al. 2015. Integrative proteomics and targeted transcriptomics analyses in cardiac endothelial cells unravel mechanisms of long-term radiation-induced vascular dysfunction. *J Proteome Res*. 14:1203–1219.
- Azimzadeh O, Subramanian V, Stander S, Merl-Pham J, Lowe D, Barjaktarovic Z, Moertl S, Raj K, Atkinson MJ, Tapio S. 2017. Proteome analysis of irradiated endothelial cells reveals persistent alteration in protein degradation and the RhoGDI and NO signaling pathways. *Int J Radiat Biol*. 90:920–928.
- Aznar MC, Duane FK, Darby SC, Wang Z, Taylor CW. 2018. Exposure of the lungs in breast cancer radiotherapy: a systematic review of lung doses published 2010–2015. *Radiother Oncol*. 126:148–154.
- Bai J, Liu F. 2019. The cGAS-cGAMP-STING pathway: a molecular link between immunity and metabolism. *Diabetes*. 68:1099–1108.
- Baselet B, Sonveaux P, Baatout S, Aerts A. 2019. Pathological effects of ionizing radiation: endothelial activation and dysfunction. *Cell Mol Life Sci*. 76:699–728.
- Beatty GL, Shahda S, Beck T, Uppal N, Cohen SJ, Donehower R, Gabayan AE, Assad A, Switzky J, Zhen H, et al. 2019. A Phase Ib/II study of the JAK1 inhibitor, itacitinib, plus nab-paclitaxel and gemcitabine in advanced solid tumors. *Oncologist*. 24:14–e10.
- Bogunovic D, Byun M, Durfee LA, Abhyankar A, Sanal O, Mansouri D, Salem S, Radovanovic I, Grant AV, Adimi P, et al. 2012. Mycobacterial disease and impaired IFN- γ immunity in humans with inherited ISG15 deficiency. *Science*. 337:1684–1688.
- Bray F, Ferlay J, Soerjomataram I, Siegel RL, Torre LA, Jemal A. 2018. Global cancer statistics 2018: GLOBOCAN estimates of incidence and mortality worldwide for 36 cancers in 185 countries. *CA Cancer J Clin*. 68:394–424.
- Cheon H, Stark GR. 2009. Unphosphorylated STAT1 prolongs the expression of interferon-induced immune regulatory genes. *Proc Natl Acad Sci U S A*. 106:9373–9378.
- Deng L, Liang H, Xu M, Yang X, Burnette B, Arina A, Li XD, Mauceri H, Beckett M, Darga T, et al. 2014. STING-dependent cytosolic DNA sensing promotes radiation-induced type I interferon-dependent antitumor immunity in immunogenic tumors. *Immunity*. 41:843–852.
- Fan JB, Miyauchi-Ishida S, Arimoto KI, Liu D, Yan M, Liu CW, Györfy B, Zhang DE. 2015. Type I IFN induces protein ISGylation to enhance cytokine expression and augments colonic inflammation. *Proc Natl Acad Sci U S A*. 112:14313–14318.
- Giridhar P, Mallick S, Rath GK, Julka PK. 2015. Radiation induced lung injury: prediction, assessment and management. *Asian Pac J Cancer Prev*. 16:2613–2617.
- Gluck S, Guey B, Gulen MF, Wolter K, Kang TW, Schmacke NA, Bridgeman A, Rehwinkel J, Zender L, Ablasser A. 2017. Innate immune sensing of cytosolic chromatin fragments through cGAS promotes senescence. *Nat Cell Biol*. 19:1061–1070.
- Grosche A, Hauser A, Lepper MF, Mayo R, von Toerne C, Merl-Pham J, Hauck SM. 2016. The proteome of native adult muller glial cells from murine retina. *Mol Cell Proteomics*. 15:462–480.

- Huang Y, Zhang W, Yu F, Gao F. 2017. The cellular and molecular mechanism of radiation-induced lung injury. *Med Sci Monit.* 23:3446–3450.
- Kainthola A, Haritwal T, Tiwari M, Gupta N, Parvez S, Tiwari M, Prakash H, Agrawala PK. 2017. Immunological aspect of radiation-induced pneumonitis, current treatment strategies, and future prospects. *Front Immunol.* 8:506.
- Kandhaya-Pillai R, Miro-Mur F, Alijotas-Reig J, Tchkonja T, Kirkland JL, Schwartz S. 2017. TNF α -senescence initiates a STAT-dependent positive feedback loop, leading to a sustained interferon signature, DNA damage, and cytokine secretion. *Aging.* 9:2411–2435.
- Kappler L, Hoene M, Hu C, von Toerne C, Li J, Bleher D, Hoffmann C, Böhm A, Kollipara L, Zischka H, et al. 2019. Linking bioenergetic function of mitochondria to tissue-specific molecular fingerprints. *Am J Physiol Endocrinol Metab.* 317:E374–E387.
- Kato K, Omura H, Ishitani R, Nureki O. 2017. Cyclic GMP-AMP as an endogenous second messenger in innate immune signaling by cytosolic DNA. *Annu Rev Biochem.* 86:541–566.
- Knight E Jr, Cordova B. 1991. IFN-induced 15-kDa protein is released from human lymphocytes and monocytes. *J Immunol.* 146:2280–2284.
- Lam E, Stein S, Falck-Pedersen E. 2014. Adenovirus detection by the cGAS/STING/TBK1 DNA sensing cascade. *J Virol.* 88:974–981.
- Li T, Chen ZJ. 2018. The cGAS-cGAMP-STING pathway connects DNA damage to inflammation, senescence, and cancer. *J Exp Med.* 215:1287–1299.
- Liu S, Cai X, Wu J, Cong Q, Chen X, Li T, Du F, Ren J, Wu YT, Grishin NV, et al. 2015. Phosphorylation of innate immune adaptor proteins MAVS, STING, and TRIF induces IRF3 activation. *Science.* 347:aaa2630.
- Ma Z, Damania B. 2016. The cGAS-STING defense pathway and its counteraction by viruses. *Cell Host Microbe.* 19:150–158.
- Malakhova OA, Yan M, Malakhov MP, Yuan Y, Ritchie KJ, Kim KI, Peterson LF, Shuai K, Zhang DE. 2003. Protein ISGylation modulates the JAK-STAT signaling pathway. *Genes Dev.* 17:455–460.
- Mathias D, Mitchel RE, Barclay M, Wyatt H, Bugden M, Priest ND, Whitman SC, Scholz M, Hildebrandt G, Kamprad M, et al. 2015. Low-dose irradiation affects expression of inflammatory markers in the heart of ApoE $-/-$ mice. *PLoS One.* 10:e0119661.
- Megger DA, Philipp J, Le-Trilling VTK, Sitek B, Trilling M. 2017. Deciphering of the human interferon-regulated proteome by mass spectrometry-based quantitative analysis reveals extent and dynamics of protein induction and repression. *Front Immunol.* 8:1139.
- Pate M, Damarla V, Chi DS, Negi S, Krishnaswamy G. 2010. Endothelial cell biology: role in the inflammatory response. *Adv Clin Chem.* 52:109–130.
- Philipp J, Azimzadeh O, Subramanian V, Merl-Pham J, Lowe D, Hladik D, Erbelinger N, Kitarova S, Fournier C, Atkinson MJ, et al. 2017. Radiation-induced endothelial inflammation is transferred via the secretome to recipient cells in a STAT-mediated process. *J Proteome Res.* 16:3903–3916.
- Platanias LC. 2003. The p38 mitogen-activated protein kinase pathway and its role in interferon signaling. *Pharmacol Ther.* 98:129–142.
- Przanowski P, Loska S, Cysewski D, Dabrowski M, Kaminska B. 2018. ISGylation increases stability of numerous proteins including Stat1, which prevents premature termination of immune response in LPS-stimulated microglia. *Neurochem Int.* 112:227–233.
- Ramalho-Oliveira R, Oliveira-Vieira B, Viola J. 2019. IRF2BP2: a new player in the regulation of cell homeostasis. *J Leukoc Biol.* 106:717–723.
- Rivero-Gutierrez B, Anzola A, Martinez-Augustin O, de Medina FS. 2014. Stain-free detection as loading control alternative to Ponceau and housekeeping protein immunodetection in Western blotting. *Anal Biochem.* 467:1–3.
- Sakorafas GH, Safioleas M. 2010. Breast cancer surgery: an historical narrative. Part III. From the sunset of the 19th to the dawn of the 21st century. *Eur J Cancer Care (Engl).* 19:145–166.
- Sievert W, Stangl S, Steiger K, Multhoff G. 2018. Improved overall survival of mice by reducing lung side effects after high-precision heart irradiation using a small animal radiation research platform. *Int J Radiat Oncol Biol Phys.* 101:671–679.
- Sievert W, Tapio S, Breuninger S, Gaipf U, Andratschke N, Trott KR, Multhoff G. 2014. Adhesion molecule expression and function of primary endothelial cells in benign and malignant tissues correlates with proliferation. *PLoS One.* 9:e91808.
- Sievert W, Trott KR, Azimzadeh O, Tapio S, Zitzelsberger H, Multhoff G. 2015. Late proliferating and inflammatory effects on murine microvascular heart and lung endothelial cells after irradiation. *Radiother Oncol.* 117:376–381.
- Southworth T, Metryka A, Lea S, Farrow S, Plumb J, Singh D. 2012. IFN- γ synergistically enhances LPS signalling in alveolar macrophages from COPD patients and controls by corticosteroid-resistant STAT1 activation. *Br J Pharmacol.* 166:2070–2083.
- Stark GR, Darnell JE. Jr. 2012. The JAK-STAT pathway at twenty. *Immunity.* 36:503–514.
- Swaim CD, Scott AF, Canadeo LA, Huibregtse JM. 2017. Extracellular ISG15 signals cytokine secretion through the LFA-1 integrin receptor. *Mol Cell.* 68:581–590.e585.
- Szklarczyk D, Gable AL, Lyon D, Junge A, Wyder S, Huerta-Cepas J, Simonovic M, Doncheva NT, Morris JH, Bork P, et al. 2019. STRING v11: protein-protein association networks with increased coverage, supporting functional discovery in genome-wide experimental datasets. *Nucleic Acids Res.* 47:D607–D613.
- Tao J, Zhou X, Jiang Z. 2016. cGAS-cGAMP-STING: the three musketeers of cytosolic DNA sensing and signaling. *IUBMB Life.* 68:858–870.
- Trilling M, Bellora N, Rutkowski AJ, de Graaf M, Dickinson P, Robertson K, Prazeres da Costa O, Ghazal P, Friedel CC, Alba MM, et al. 2013. Deciphering the modulation of gene expression by type I and II interferons combining 4sU-tagging, translational arrest and in silico promoter analysis. *Nucleic Acids Res.* 41:8107–8125.
- Van der Meeren A, Vandamme M, Squiban C, Gaugler MH, Mouthon MA. 2003. Inflammatory reaction and changes in expression of coagulation proteins on lung endothelial cells after total-body irradiation in mice. *Radiat Res.* 160:637–646.
- Villarino AV, Kanno Y, Ferdinand JR, O'Shea JJ. 2015. Mechanisms of Jak/STAT signaling in immunity and disease. *J Immunol.* 194:21–27.
- Villarroya-Beltri C, Baixauli F, Mittelbrunn M, Fernández-Delgado I, Torralba D, Moreno-Gonzalo O, Baldanta S, Enrich C, Guerra S, Sánchez-Madrid F. 2016. ISGylation controls exosome secretion by promoting lysosomal degradation of MVB proteins. *Nat Commun.* 7:13588.
- Villarroya-Beltri C, Guerra S, Sanchez-Madrid F. 2017. ISGylation – a key to lock the cell gates for preventing the spread of threats. *J Cell Sci.* 130:2961–2969.
- Weichselbaum RR, Ishwaran H, Yoon T, Nuyten DSA, Baker SW, Khodarev N, Su AW, Shaikh AY, Roach P, Kreike B, et al. 2008. An interferon-related gene signature for DNA damage resistance is a predictive marker for chemotherapy and radiation for breast cancer. *Proc Natl Acad Sci USA.* 105:18490–18495.
- Wisniewski JR, Zougman A, Nagaraj N, Mann M. 2009. Universal sample preparation method for proteome analysis. *Nat Methods.* 6:359–362.
- Woo SR, Fuertes MB, Corrales L, Spranger S, Furdyna MJ, Leung MYK, Duggan R, Wang Y, Barber GN, Fitzgerald KA, et al. 2014. STING-dependent cytosolic DNA sensing mediates innate immune recognition of immunogenic tumors. *Immunity.* 41:830–842.
- Wu X, Yang J, Na T, Zhang K, Davidoff AM, Yuan BZ, Wang Y. 2017. RIG-I and IL-6 are negative-feedback regulators of STING induced by double-stranded DNA. *PLoS One.* 12:e0182961.
- Yao K, Chen Q, Wu Y, Liu F, Chen X, Zhang Y. 2017. Unphosphorylated STAT1 represses apoptosis in macrophages during Mycobacterium tuberculosis infection. *J Cell Sci.* 130:1740–1751.
- Yew-Booth L, Birrell MA, Lau MS, Baker K, Jones V, Kilty I, Belvisi MG. 2015. JAK-STAT pathway activation in COPD. *Eur Respir J.* 46:843–845.
- Zhang Y, Liu Z. 2017. STAT1 in cancer: friend or foe?. *Discov Med.* 24:19–29.
- Zhao W, Robbins ME. 2009. Inflammation and chronic oxidative stress in radiation-induced late normal tissue injury: therapeutic implications. *CMC.* 16:130–143.

3.3 Radiation response in HCECest2 revealed a central role for cGAS/STING pathway in the development of chronic inflammation

3.3.1 Aim and Summary

Radiation-induced inflammation is known to affect endothelial cells and damage the endothelial barrier whereby, the separation between blood and tissue is no longer warranted (Guipaud et al. 2018). This increases the risk for developing atherosclerosis and later on CVD. My previous studies showed radiation-induced inflammation in a human endothelial cell line and primary mouse lung microvascular endothelial cells. Therefore, the aim of this study was to investigate the initiation of the endothelial inflammation and pathways and proteins associated with it. In addition, this study investigated a possible dose threshold at which the inflammatory response is no longer observed. For this purpose, human coronary artery endothelial cell line (HCECest2) was irradiated with doses of 0, 0.25, 0.5, and 2 to 10 Gy ($^{60}\text{Co-}\gamma$) and harvested after 4 h, 24 h, 48 h and one week post-radiation. Label-free global proteome analysis was performed in a data-independent acquisition mode. The data were validated by statistical approaches and immunoblotting. Whereas low- and moderate doses induced mainly time-related effects, high-dose treatments (2 and 10 Gy) led to the activation of DNA-damage repair, inflammation, and oxidative stress pathways. The DNA-damage response was activated early and accompanied by the expression of proteins related to the cGAS/STING-pathway and the type I interferon response. The upregulation of the latter increased in a time- and dose-dependent manner. Strongest effects were seen in 10 Gy irradiated samples after one week. At this dose and time point the proteins STING, STAT1, ICAM1, and ISG15 were upregulated several fold. This suggested a slowly developing inflammatory state strongly dependent on the radiation dose *in vitro*.

3.3.2 Contribution to the study

This study was conceived by me. The irradiation and cell culture was carried out with the help of Stefanie Winkler (ISB, HMGU). Cell harvest, protein isolation, lysis, measurement of protein content and the preparation for mass spectrometry analysis was done by me. The LC-MS/MS runs were performed by Dr. Christine von Törne

(PROT, HMGU). Statistical analysis was done by Dr. Ronan Le Gleut from the Institute of Computational Biology, HMGU, and by me with the advice from Prabal Subedi and Omid Azimzadeh. The bioinformatics analysis and immunoblotting were carried out by me with the help from Prabal Subedi. The figures and the manuscript were designed and written, respectively, by me. Prabal Subedi, Omid Azimzadeh, Soile Tapio and Michael J. Atkinson provided me with advice, scientific discussions throughout the study and especially Dr. Soile Tapio did proofreading of the manuscript.

3.3.3 Publication

The study was published as an original research paper on 27th of October, 2020 in the Journal Proteomes:

Publication is distributed by Creative Commons Attribution License (CC BY 4.0):



Radiation Response of Human Cardiac Endothelial Cells Reveals a Central Role of the cGAS-STING Pathway in the Development of Inflammation.

Jos Philipp, Ronan Le Gleut, Christine von Toerne, Prabal Subedi, Omid Azimzadeh, Michael J Atkinson, Soile Tapio.

Proteomes, 2020 Oct. 26; 8(4): E30. doi: 10.3390/proteomes8040030.

Article

Radiation Response of Human Cardiac Endothelial Cells Reveals a Central Role of the cGAS-STING Pathway in the Development of Inflammation

Jos Philipp ¹, Ronan Le Gleut ², Christine von Toerne ³, Prabal Subedi ^{1,4} , Omid Azimzadeh ¹ , Michael J. Atkinson ^{1,5} and Soile Tapio ^{1,*} 

¹ Institute of Radiation Biology, Helmholtz Center Munich, German Research Center for Environmental Health GmbH, 85764 Neuherberg, Germany; jos.philipp@rub.de (J.P.); psubedi@bfs.de (P.S.); omid.azimzadeh@helmholtz-muenchen.de (O.A.); atkinson@helmholtz-muenchen.de (M.J.A.)

² Institute of Computational Biology, Helmholtz Center Munich, German Research Center for Environmental Health GmbH, 85764 Neuherberg, Germany; ronan.legleut@helmholtz-muenchen.de

³ Research Unit Protein Science, Helmholtz Center Munich, German Research Center for Environmental Health GmbH, 85764 Neuherberg, Germany; vontorne@helmholtz-muenchen.de

⁴ Federal Office for Radiation Protection, BfS, 85764 Neuherberg, Germany

⁵ Chair of Radiation Biology, Technical University of Munich, 80333 Munich, Germany

* Correspondence: soile.tapio@helmholtz-muenchen.de; Tel.: +49-89-3187-3445

Received: 2 September 2020; Accepted: 19 October 2020; Published: 26 October 2020



Abstract: Radiation-induced inflammation leading to the permeability of the endothelial barrier may increase the risk of cardiovascular disease. The aim of this study was to investigate potential mechanisms in vitro at the level of the proteome in human coronary artery endothelial cells (HCECest2) that were exposed to radiation doses of 0, 0.25, 0.5, 2.0 and 10 Gy (60Co- γ). Proteomics analysis was performed using mass spectrometry in a label-free data-independent acquisition mode. The data were validated using bioinformatics and immunoblotting. The low- and moderate-dose-irradiated samples (0.25 Gy, 0.5 Gy) showed only scarce proteome changes. In contrast, an activation of DNA-damage repair, inflammation, and oxidative stress pathways was seen after the high-dose treatments (2 and 10 Gy). The level of the DNA damage response protein DDB2 was enhanced early at the 10 Gy dose. The expression of proteins belonging to the inflammatory response or cGAS-STING pathway (STING, STAT1, ICAM1, ISG15) increased in a dose-dependent manner, showing the strongest effects at 10 Gy after one week. This study suggests a connection between the radiation-induced DNA damage and the induction of inflammation which supports the inhibition of the cGAS-STING pathway in the prevention of radiation-induced cardiovascular disease.

Keywords: ionizing radiation; proteomics; inflammation; cGAS-STING-pathway; DDB2; endothelial cells; STAT1; data-independent acquisition

1. Introduction

Endothelial cells form the inner single-cell layer surrounding every blood vessel, thus representing the barrier between blood and the tissues underneath. Endothelial cells are responsible for taking up nutrients and delivering waste products to the blood, thereby protecting the tissue, communicating with immune cells and controlling the blood flow [1]. Signal mechanisms induced by external stressors such as ionizing radiation, chemicals or pathogenic agents trigger an acute inflammatory immune response that functions in a paracrine, endocrine and/or autocrine manner [2–5]. The initial signaling cascades include the activation of endothelial signaling molecules like nitric oxide or adhesion molecules but also inflammatory proteins. In the case of ionizing radiation, both the radiation dose and the time

elapsing after the exposure influence the inflammatory outcome [6,7]. In the worst case, the initial acute inflammation may progress to a chronic one [8–11]. Sustained low-level inflammation is a risk factor for cardiovascular disease by promoting atherosclerotic plaque formation, rupture and finally thrombosis [12].

High-throughput “omics” technologies such as proteomics enable a deeper understanding of biological processes on different levels and scales [13]. This has the advantage to display not only single pathways but to observe changes in several pathways simultaneously within one measurement. In radiation biology, dose- and time-dependent measurements are necessary to reveal changes in the proteome leading to morphological and functional alterations at a cellular level. In endothelial cells, due to their complex barrier forming system, it is particularly relevant to investigate whole processes taking place after radiation exposure.

In endothelial cells, low and moderate doses (<0.5 Gy) may attenuate an ongoing inflammatory process [14,15]. If the cells are not in an inflammatory state at the time of irradiation, both pro- and anti-inflammatory effects or no radiation influence on inflammatory parameters have been reported [16–19] whereas high doses are clearly pro-inflammatory [20–23]. At high doses (>0.5 Gy), endothelial cells express and release cytokines such as IL-6, IL-8, MCP1, and type I interferon-related proteins to attract immune cells [24,25]. In addition, other pro-inflammatory proteins, especially intracellular and vascular adhesion molecules like ICAM1, VCAM1 and PECAM1 are increasingly present at the cell surface [26]. This leads to the attachment and infiltration of immune cells into the surrounding tissue and later on to senescence [23].

DNA damage caused by radiation exposure results in the accumulation of cytosolic DNA that is recognized by the cGAS-STING pathway [27,28] alerting the cell's immune system [29,30]. In a complex cascade, cGAS generates the second messenger cGAMP that activates the adaptor protein STING which, in its turn, activates the transcription factor IRF3 in a phosphorylation-dependent mechanism [31]. This triggers the induction of type I interferon-related pro-inflammatory immune response [32]. Recent research has provided strong evidence that cGAS also has an essential role in promoting cellular senescence via the senescence-associated secretory phenotype, SASP [2,24,33], thereby connecting DNA damage, inflammation and senescence [30,34].

Previously, we reported a pro-inflammatory radiation response in human coronary artery endothelial cell line (HCECest2) and primary murine lung endothelial cells after a dose of 10 Gy X-ray [24,34]. In both cases, a strong inflammatory reaction based on the activation of signal transducer and the activator of transcription 1 (STAT1), a transcription factor that induces the expression of interferon (IFN)-related and other inflammatory genes, was observed [35,36]. Consequently, a strong upregulation of ubiquitin-like protein ISG15 was observed in both studies where the pro-inflammatory phenotype appeared relatively late in the *in vitro* conditions, 14 and 10 days after the radiation exposure in the two studies, respectively.

Based on our previous results and the fact that STAT1 is known to be activated by the cGAS-STING pathway [37], we hypothesized that this pathway could be activated by ionizing radiation in endothelial cells from early on to trigger the pro-inflammatory response. However, we preferred to look at the global proteome changes rather than only some selected proteins not to miss any previously less defined components of the inflammatory pathway. Furthermore, the proteomic approach used in this study could work as a data source for several future publications. In this study, however, we focused on a continuation of our previous work examining the associated proteins of the cGAS-STING pathway, a task that can hardly be performed using immunoblotting only. Therefore, we investigated the dose- and time-dependent alterations in the endothelial proteome globally but with a particular focus on the cGAS-STING pathway. This systematic analysis using the newest proteomics methods was necessary since the initiation and progression of radiation-induced inflammatory response in endothelial cells is poorly understood. Gaining more information about the inflammatory processes in endothelial cells could open the door for new possibilities in the prevention and alleviation of radiation-associated cardiovascular disease.

2. Materials and Methods

2.1. Cell Culture and Irradiation

Human telomerase-immortalized coronary artery endothelial cells (HCECest2) obtained from Dr. Ken Raj, were cultured at 37 °C and 5% CO₂ as described previously [23]. Cells were grown in Human MesoEndo Cell Growth Medium Kit (Cell Applications, Inc., San Diego, CA, USA) until confluency. Cells were irradiated with a Caesium-137 source (HWM-D-2000, dose rate 400 mGy/min) with γ -doses of 0 Gy (sham irradiation), 0.25, 0.5, 2 and 10 Gy and were harvested after 4, 24, 48 h and one week. During the experiment, the cells were not passaged but every two days a new medium was applied. Time- and radiation-dependent cell morphology changes were recorded by taking microscopic images using Keyence BZ-9000 (Keyence Corporation, Neu-Isenburg, Germany) with a 4 \times /0.20 objective. The cells were harvested by removing the medium, washing twice with ice-cold phosphate buffered saline, scraping and centrifugation at 300 \times g for 5 min. The supernatant was discarded and the cell pellets frozen at -80 °C until further use. Four biological replicates of each time and dose point were made. The replicates were cultivated at different time points. The work flow is shown in Figure 1.

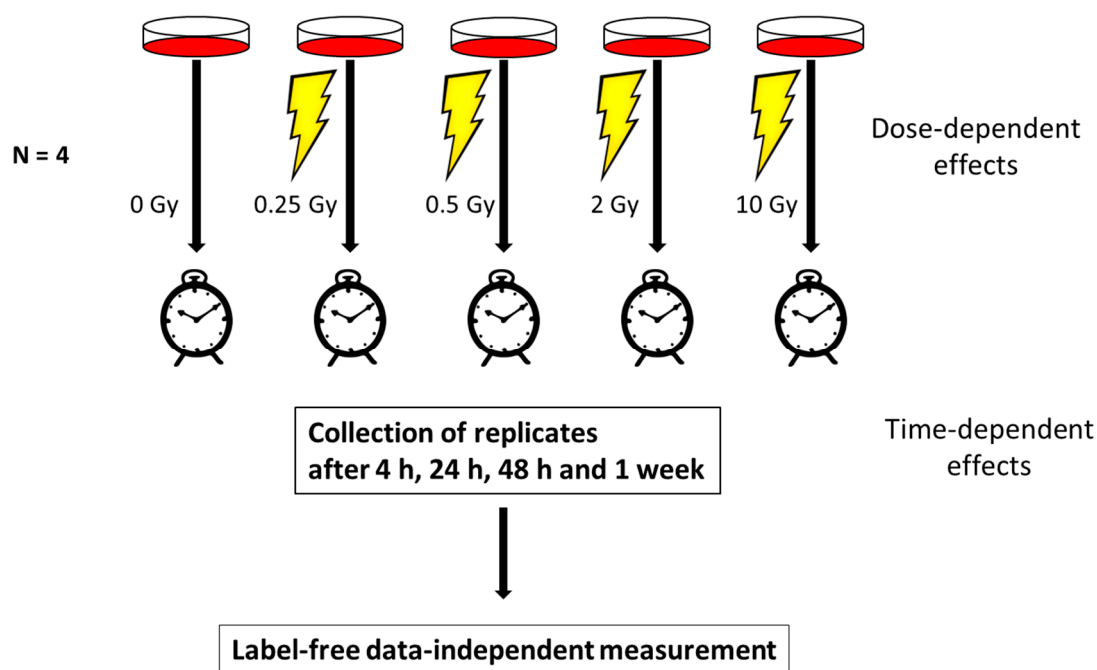


Figure 1. The work flow of the study showing the experimental design. Human coronary artery endothelial cells (HCAECs) were irradiated with 0, 0.25, 0.5, 2 or 10 Gy. At 4, 24, 48 h and 1 week, the cells were harvested and analyzed using a data-independent proteomics approach. The proteome changes in all irradiated samples were normalized to the sham-irradiated sample collected at the corresponding time point to investigate the dose-dependent effects. The proteome changes at different time points were normalized to the corresponding sample collected at 4 h.

2.2. Cell Lysis and Sample Preparation

All cell pellets were lysed with RIPA buffer (Thermo Fisher Scientific, Schwerte, Germany) containing phosphatase inhibitor (PhosStop, Roche Applied Science, Penzberg, Germany) and protease inhibitor (cOmpleteTM, Roche, Darmstadt, Germany) following the manufacturer's instructions. Protein concentration was determined using the PierceTM BCA Protein Assay Kit (Thermo Fisher Scientific) according to the manufacturer's instructions. Sample preparation was done using FASP digest [38].

2.3. Mass Spectrometry (MS)

MS data were acquired in data-independent acquisition (DIA) mode on a Q Exactive (QE) high field (HF) mass spectrometer (Thermo Fisher Scientific) as described previously [39] with the following changes: peptides were eluted from column at 250 nl/min using an increasing acetonitrile (ACN) concentration (in 0.1% formic acid) from 3% to 41% over a 105 min gradient. Precursor peptides were isolated with 37 variable windows spanning from 300 to 1650 m/z at 30,000 resolution with an AGC target of 3e6 and automatic injection time.

2.4. Spectral Library, Spectronaut Analysis and Data Processing

Selected LC–MS/MS DDA data encompassing 80 raw files were analyzed using Proteome Discoverer (Version 2.1, Thermo Fisher Scientific) using Byonic (Version 2.0, Proteinmetrics, San Carlos, CA, USA) search engine node maintaining 1% peptide and protein false discovery rate (FDR) threshold. The peptide spectral library was generated in Spectronaut (Version 10, Biognosys, Schlieren, Switzerland) with default settings using the Proteome Discoverer result file. Spectronaut was equipped with the SwissProt human database (Release 2017.02, 20,194 sequences, www.uniprot.org) with a few spiked proteins (e.g., Biognosys iRT peptide sequences). The final spectral library generated in Spectronaut contained 11,505 protein groups and 417,843 peptide precursors. Mastermix containing peptides from all treatments was used to obtain the same quality in all measurements. The DIA MS data were analyzed using the Spectronaut 12 software as described previously [34].

2.5. Statistical Analysis

For the statistical analysis, the R software (version 3.52.0, GNU General Public License, Boston, MA, USA) was used. The “normalized” abundances were filtered for proteins identified with more than one unique peptide. The vsn R package (version 3.52.0) [40] was then used for an affine transformation and a generalized log₂ transformation of the protein expression. Two-dimension reduction techniques, UMAP [41] and t-SNE [42], were then applied on the transformed data, which helped us to identify a strong batch effect due to the 4 replicates. The differential expression analysis was run using the R package LIMMA (version 3.40.2) [43] using a generalized linear mixed model including the interaction between the different doses and time points, as fixed effects and the replicates as a random effect to account for the similarities within the replicates. The significance of protein deregulation was based on the label-free proteomics analysis (fold change of ± 1.3 ; Storey-corrected p -value $q < 0.05$ [44]; $n = 4$) and immunoblotting (t -test; $p < 0.05$; $n = 3$).

2.6. Bioinformatics

Proteins were grouped based on the time and dose. Grouped proteins were further investigated for pathway affiliation using ingenuity pathway analysis (IPA, Qiagen, Inc., Hilden, Germany, <https://www.qiagenbioinformatics.com/products/ingenuitypathway-analysis>).

2.7. Immunoblotting

Immunoblotting was done as described previously [35]. The following antibodies were purchased from Merck Millipore: cGAS (ABF124) and from Santa Cruz (Santa Cruz Biotechnology, Inc., Heidelberg, Germany): STAT1 (sc-346), ISG15 (sc-166755), ICAM1 (sc-8435).

2.8. Data Availability

The MS proteomics data were deposited to the ProteomeXchange Consortium via the PRIDE [45] partner repository with the dataset identifier PXD020735.

3. Results

3.1. Radiation Dose and Time Effects on the Proteome

Proteome analysis of the irradiated cells at different time points and irradiation doses was performed label-free and in a data-independent acquisition mode to also identify low abundant proteins. In total, 4060 proteins were identified. The dataset was statistically analyzed for the radiation dose (Tables S1–S4) and time (Tables S6–S10).

Time-dependent effects were measured against the 4 h time point, the first time point with proteomics data. A large number of proteins were found to be deregulated in a time-dependent manner, especially at 2 and 10 Gy, with 516 and 1087 deregulated proteins, respectively (Figure 2A). In addition, 227 and 188 deregulated proteins were found for the 0.25 and 0.5 Gy dose points, respectively.

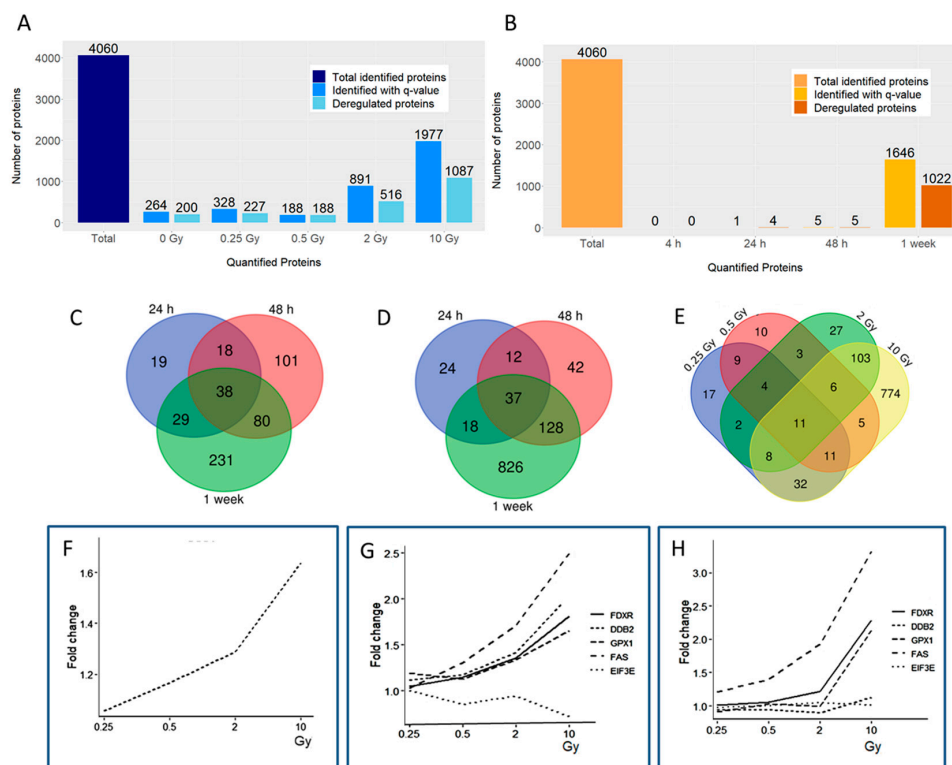


Figure 2. The alterations in the human coronary artery endothelial cell line (HCECest2) cell proteome with time and radiation dose. **(A)** The total number of all identified proteins (dark blue), the number of all quantified ($q \leq 0.05$) proteins (blue) and the number of significantly differentially regulated ($q \leq 0.05$; fold change ± 1.3) proteins (light blue) at each time point compared to the 4 h time point are shown. **(B)** The total number of all identified proteins (light orange), the number of all quantified ($q \leq 0.05$) proteins (orange) and the number of significantly differentially regulated ($q \leq 0.05$; fold change ± 1.3) proteins (dark orange) at each radiation dose compared to the 0 Gy control are shown. **(C)** Venn diagram illustrating the number of shared deregulated proteins between the three time points at 2 Gy. **(D)** Venn diagram illustrating the number of shared deregulated proteins between the three time points at 10 Gy. **(E)** Venn diagram illustrating the number of shared deregulated proteins between the four radiation doses at the 1 week time point. **(F)** The level of DDB2 (DNA damage-binding protein 2) at different radiation doses 24 h post-exposure is shown. **(G)** The level of deregulated proteins FDXR (ferredoxin reductase), DDB2, GPX1 (glutathione peroxidase 1), FAS (tumor necrosis factor receptor superfamily member 6), and EIF3 (eukaryotic translation initiation factor 3 subunit E) at different radiation doses 48 h post-exposure is shown. **(H)** The level of deregulated proteins FDXR, DDB2, GPX1, FAS, and EIF3 at different radiation doses 1 week post-exposure is shown.

The radiation, in contrast, only marginally affected the protein expression at the early time points (Figure 2B). No proteins were deregulated at 4 h post-radiation compared to the control (0 Gy). Similarly, the number of deregulated proteins 24 and 48 h post-radiation, being one and five proteins, respectively, was low (Figure 2B). Nevertheless, a strong radiation effect with 1022 deregulated proteins at all doses was observed after one week (Figure 2B). At 10 Gy, 950 proteins were deregulated using the fold change of ± 1.3 that we then used for all time points and radiation doses. Increasing the fold change to ± 1.5 or ± 2.0 decreased the number of deregulated proteins at 10 Gy to 413 and 67, respectively.

The clear increase in the number of deregulated proteins in a time-dependent manner is illustrated in the Venn diagrams at 2 (Figure 2C) and at 10 Gy (Figure 2D). The Venn diagram illustrating the number of shared deregulated proteins between the four radiation doses was shown in Figure 2E. The number of deregulated proteins changed with the radiation dose as follows: 94 (5.7% of all quantified proteins) were deregulated at 0.25 Gy, 59 (3.6%) at 0.5 Gy, 164 (10.0%) at 2 Gy, and 950 (57.7%) proteins at 10 Gy. Only 11 proteins were deregulated at every radiation dose. Most shared proteins (128) were found between the two higher doses (Figure 2E).

Only one protein, DNA damage-binding protein 2 (DDB2), was significantly deregulated (2, 10 Gy) at 24 h showing upregulation (Figure 2F). It was also upregulated at 48 h (10 Gy), similar to the proteins ferredoxin reductase (FDXR), glutathione peroxidase 1 (GPX1), and tumor necrosis factor receptor superfamily member 6 (FAS) (Figure 2G). The only downregulated protein at 48 h was the elongation factor EIF3E (10 Gy). After one week, DDB2 and EIF3E were no longer deregulated but the proteins FDXR, GPX1 and FAS all remained upregulated (Figure 2H). When clustering the proteins deregulated after one week, most proteins at the lower doses of 0.25 and 0.5 Gy showed a similar direction of deregulation that was inverted at the higher doses of 2 and 10 Gy (Figure S1). In addition, the deregulated proteins at 0.25 and 0.5 Gy clustered together as did those at 2 and 10 Gy (Figure S1).

The ingenuity pathway analysis (IPA) showed that the most important altered molecular function as a function of the radiation dose was the inflammatory response (Table S5). The first three functional categories with the lowest *p*-value and the highest number of proteins all include the term inflammation (Table S5).

3.2. The Expression of Proteins Involved in DNA Repair, Oxidative Stress and Inflammatory Response

To further analyze the radiation-affected pathways, the expressions of proteins involved in DNA repair, inflammatory response, and oxidative stress was investigated in more detail.

The expression of the DNA-repair proteins DDB1 and DDB2 was upregulated at the highest dose of 10 Gy at 24 and 48 h time point, then declining after one week (Figure 3A,B), indicating radiation-induced DNA damage.

Then, we investigated the level of proteins of the cGAS-STING-pathway. As the cGAS protein was not present in the proteomics data, probably due to its low abundance, the expression of its downstream targets was examined. Additionally, alterations in the protein expression associated with the type I interferon response that are known to be induced by the upregulation of STING [46] were studied. The expression of STING was markedly upregulated at 10 Gy from the 48 h time point onwards (Figure 3C). The STIM1 protein that is known to co-localize with STING in the endoplasmic reticulum was also upregulated at 2 and 10 Gy after one week (Figure 3D). As previously shown, the type I interferon response in endothelial cells is activated by irradiation [24,35]. Similar to our previous studies, the expression of ISG15, a type I interferon-related protein, was highly upregulated after 2 and 10 Gy at the 1 week time point (Figure 3E). In a similar fashion, the level of ICAM1 was also upregulated after 1 week at the dose of 10 Gy (Figure 3F). STAT1, a key player of the type I Interferon response, was upregulated at 2 and 10 Gy 1 week post-radiation (Figure 3G). In contrast, the expression of the cGAS downstream target TBK1 did not change significantly (Figure 3H). Additional inflammatory proteins such as interferon-induced GTP-binding proteins MX1 and MX2, proteins of the oligoadenylate synthetase (OAS) family and proteins of the IFIT family that are known to be induced in

response to the type I Interferon-related activation, did not show significant time- or dose-dependent expression changes (Figure S2).

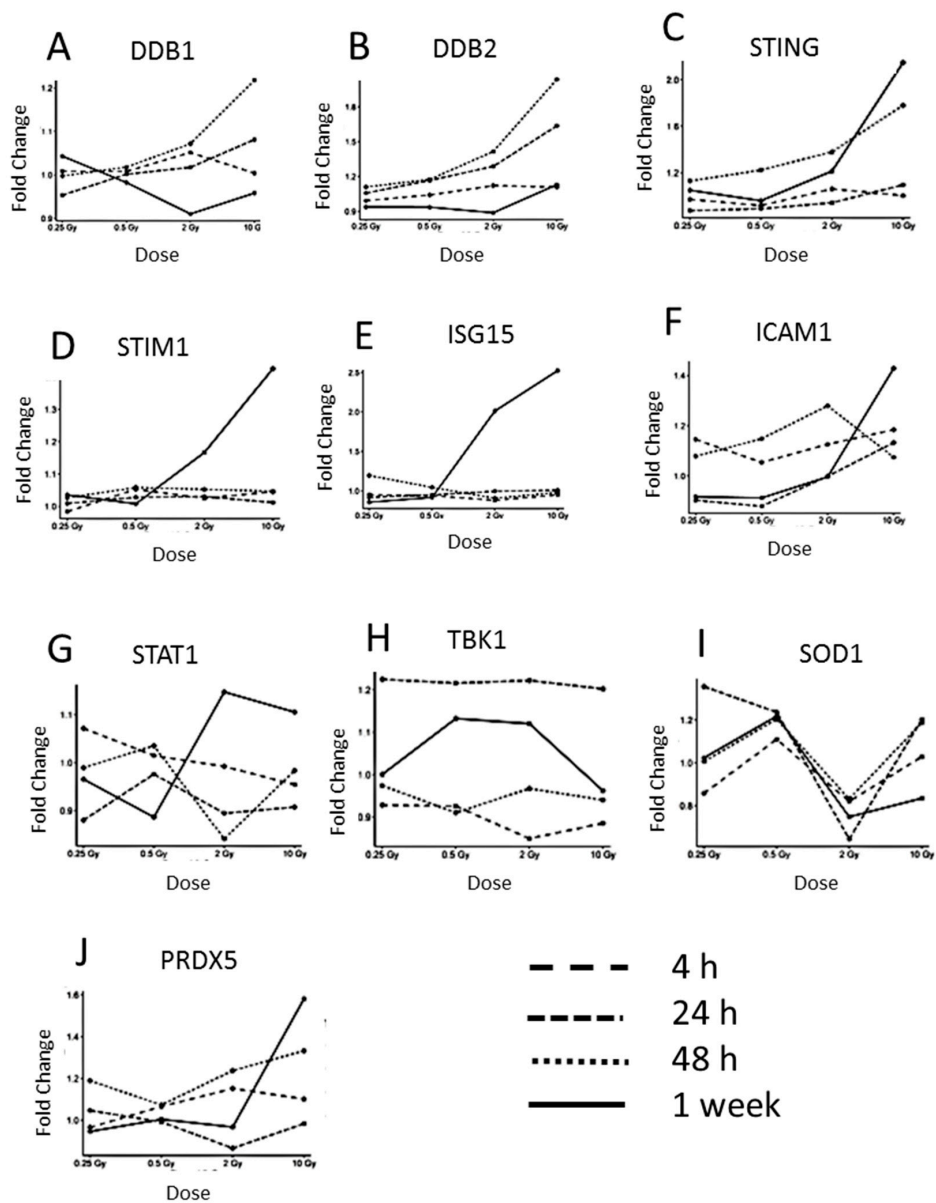


Figure 3. The dose-dependent alteration in the expression of proteins belonging to functionally different groups: DNA repair pathway, inflammatory response, and oxidative stress. (A) The level of DDB1 (DNA damage-binding protein 1), (B) DDB2 (DNA damage-binding protein 2), (C) STING (stimulator of interferon genes protein), (D) STIM1 (stromal interaction molecule 1), (E) ISG15 (ubiquitin-like protein ISG15), (F) ICAM1 (intercellular adhesion molecule 1), (G) STAT1 (signal transducer and activator of transcription 1), (H) TBK1 (serine/threonine-protein kinase TBK1), (I) SOD1 (superoxide dismutase (Cu-Zn)), and (J) PRDX5 (peroxiredoxin-5, mitochondrial) is shown after 4, 24, 48 h, and 1 week.

Inflammation is linked to increased oxidative stress in cardiovascular disease [47]. In order to monitor the possible changes in the oxidative stress response, the levels of superoxide dismutase 1 (SOD1) and peroxiredoxin 5 (PRDX5) were investigated (Figure 3I,J). The expression of SOD1 was not deregulated in a dose-dependent manner. In contrast, PRDX5 was upregulated after 1 week at the dose of 10 Gy.

In addition to the DNA repair, inflammatory and oxidative stress proteins, we found a large number of mitochondrial proteins differentially regulated, especially members of the respiratory complex I 1 week post-radiation (Tables S4 and S5). These, as well as mitochondrial antiviral-signaling protein (MAVS), were upregulated emphasizing the role of mitochondria in the endothelial radiation response.

3.3. Immunoblotting Validation 1 Week Post-Radiation

Methodological validation of the proteomics data was performed using immunoblotting (Figure 4). Proteins involved in the cGAS-STING pathway or inflammatory response were tested. After one week, a significant upregulation for ISG15 was found at 10 Gy (Figure 4A), whereas cGAS was significantly upregulated at 0.5 and 2 Gy, but interestingly, not at 10 Gy (Figure 4B). STAT1 showed two bands in the blotting. The upper band was significantly upregulated only at 2 Gy but the lower band showed upregulation both at 2 and 10 Gy (Figure 4C,D), in accordance with the proteomics data. The immunoblots are shown in Figure 4E.

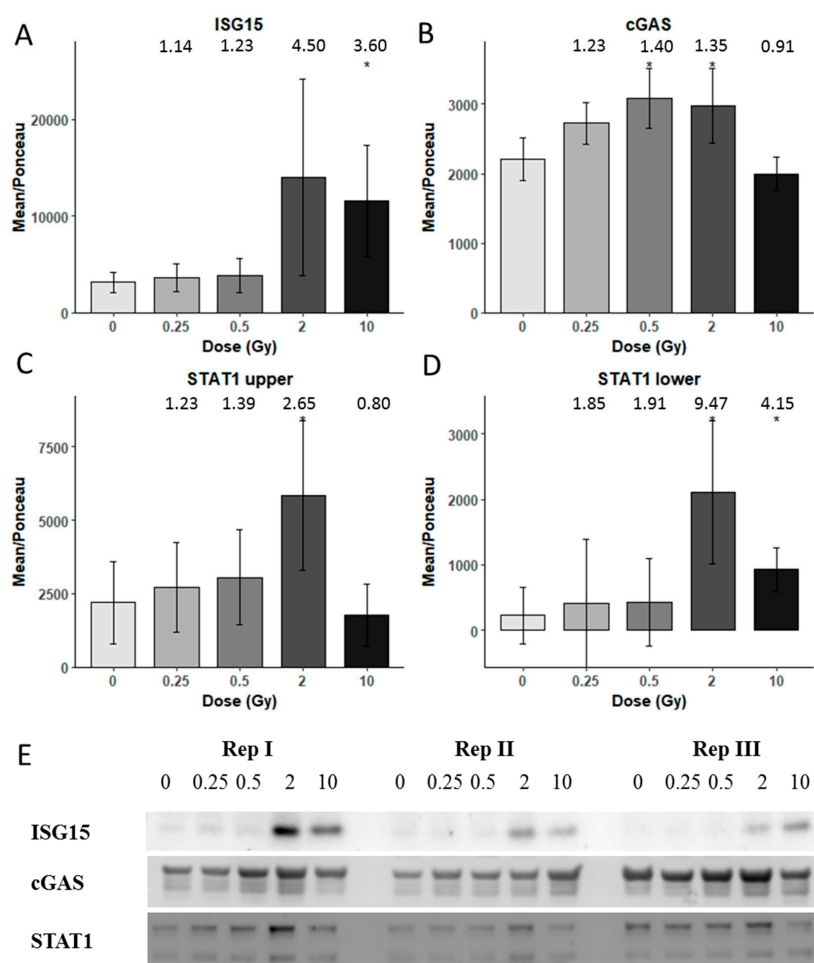


Figure 4. Immunoblot verification of the protein changes in the irradiated HCECest2 cells 1 week after radiation exposure. (A) The expression of ISG15 (ubiquitin-like protein ISG15), (B) cGAS (cyclic GMP-AMP synthase), (C) STAT1 (signal transducer and activator of transcription 1) upper band, (D) STAT1 lower band is shown. The bars represent the relative expression after correction for background and normalization to Ponceau. The error bars are calculated as the SEM (*t* test; * *p* < 0.05; *n* = 3). (E) The visualization of protein bands is shown.

The time-dependent expression changes of ICAM1 were tested with immunoblotting (Figure S3). The level of ICAM1 was increased after one week independently of the radiation dose and even in the control.

4. Discussion

In the standard radiation therapy for treating breast cancer, the applied dose varies from 0.1 to 20 Gy in the left anterior descending artery [48], and a similar average dose exposure to the lung was reported [49]. Considering the increasing risk for vascular and cardiac disease in breast cancer survivors, it is important to investigate the endothelial response to a range of different radiation doses [50,51]. In this study, we investigated a dose- and time-related response of endothelial cells after irradiation with doses ranging from 0.25 to 10 Gy over one week. These doses correspond to the cardiac doses received in radiation therapy, depending on the location of the tumor.

Previously, we saw the induction of pro-inflammatory proteins two weeks post-radiation in HCECest2 cells [24] and one week post-radiation in primary mouse lung endothelial cells [35]; both studies used a radiation dose of 10 Gy. In addition, long-term studies (16 weeks) performed in cardiac endothelial cells isolated from mice exposed to local heart radiation (16 Gy) revealed an induction of inflammation by assessing global proteome changes or selected surface markers [9,10]. Using the same cell line as in this study, the increased adhesion of monocytes and the release of pro-inflammatory cytokines (interleukins 6 and 8) was shown already at the dose of 2 Gy X-rays [52]. This effect became significant seven days after the exposure. At lower radiation doses, the induction of inflammatory response is contradictory [16–19], although significant changes in other processes such as NO signaling or protein degradation have been observed already at the dose of 0.5 Gy *in vitro*, especially after 14 days [17].

These previous studies are in agreement with the data presented here. The doses of 0.25 Gy and 0.5 Gy triggered some proteomic changes after one week but these alterations did not contribute to the inflammatory response. Interestingly, the results from cellular studies are in accordance with the epidemiological data suggesting a threshold dose for the induction of radiation-induced cardiovascular disease of about 0.5 Gy [53,54] with only a scarce number of studies showing an increased risk at doses slightly lower than that [55,56].

At 24 and 48 h, the 2 and 10 Gy doses increased the expression of DDB2 significantly, indicating an induction of the DNA repair process. DDB2 is one of the best radiation biomarkers not only in the human blood but also in different types of cells [57–60]. However, to the best of our knowledge, this is the first study to find a radiation-associated increase in DDB2 in endothelial cells. DDB2 is regulated by p38MAPK and p53 [61,62]. It was found to be one of the 16 blood biomarkers of aging revealing a role not only in the radiation response but also in the pathology of senescence [63].

Also indicating DNA damage is the dose-dependent upregulation of the FDXR protein, also known as ferredoxin reductase. As DDB2, it has been shown to be highly upregulated by ionizing radiation at the transcriptional level, making it one of the most reliable radiation biomarkers in the human blood [64–67]. This p53-regulated flavoprotein, the first enzyme in the mitochondrial P450 system, also responds also to other DNA-damaging agents rather than ionizing radiation but to a lesser extent [68].

It is well known that ionizing radiation and other DNA-damaging agents are able to induce the expression of type I interferons and other cytokines [69–75]. A relatively new observation is the essential role of the cGAS-STING pathway in this process, even in non-cancerous cells and tissues [24,35,76]. Our present study showed that cGAS was markedly upregulated at 2 Gy one week post-radiation. At 10 Gy, in contrast to STING which was upregulated about two-fold, the level of cGAS was not changed. Although this result was somewhat surprising, it supported our previous data with primary lung endothelial cells where no cGAS upregulation was seen at 10 Gy [35]. In addition to STING, also its counterpart STIM1 that interacts with STING by inactivating it [46] was upregulated at 10 Gy one week after irradiation, indicating a possible negative feedback loop to regulate the

STING level. Furthermore, the MAVS protein was significantly upregulated at 2 and 10 Gy one week post-radiation. Similar to STING, MAVS has recently been shown to be necessary for radiation-induced Type I interferon signaling [77]. Then, STING forms a complex with TBK1 allowing its activation by autophosphorylation [78]. This type of activation may explain why we see no changes in TBK1 protein level. TBK1 phosphorylates interferon regulatory transcription factor 3 (IRF3). Phosphorylated IRF3 dissociates from its adapter proteins and in a dimerized form enters the nucleus to induce the expression of interferons [32,79].

One of the target proteins of the type I Interferon response is ISG15, which we found to be significantly upregulated after one week (2 and 10 Gy) in agreement with our previous data [24,35]. ISG15 causes ISGylation, a process yet incompletely understood. However, ISGylation has been shown to increase the stability of proteins such as STAT1, preventing a termination of the inflammatory response [80]. Accordingly, the level of STAT1 was significantly increased in the 2 and 10 Gy-treated samples after one week. As shown by us and by others, the ISG15 protein can function as a secreted cytokine allowing the spreading and maintenance of the pro-inflammatory and senescent phenotype [24,81]. The interaction network of the proteins in the cGAS-STING pathway is illustrated in Figure 5.

Interestingly, a large number of proteins changed their expression with time. It has been shown previously that culture conditions strongly influence the expression pattern of several inflammatory proteins increasing the levels of cytokines but decreasing the level of endothelial nitric oxide synthase (eNOS) the function of which is necessary for the vascular tone [82–84]. Proteins such as ICAM1, STAT1, and STING were upregulated in the time course of this experiment. However, time-dependent changes were not totally independent of the radiation dose since we found most such alterations in the irradiated cells. Both of these factors, the time and the radiation dose, seem to be necessary for the development of inflammatory response in cardiac endothelial cells.

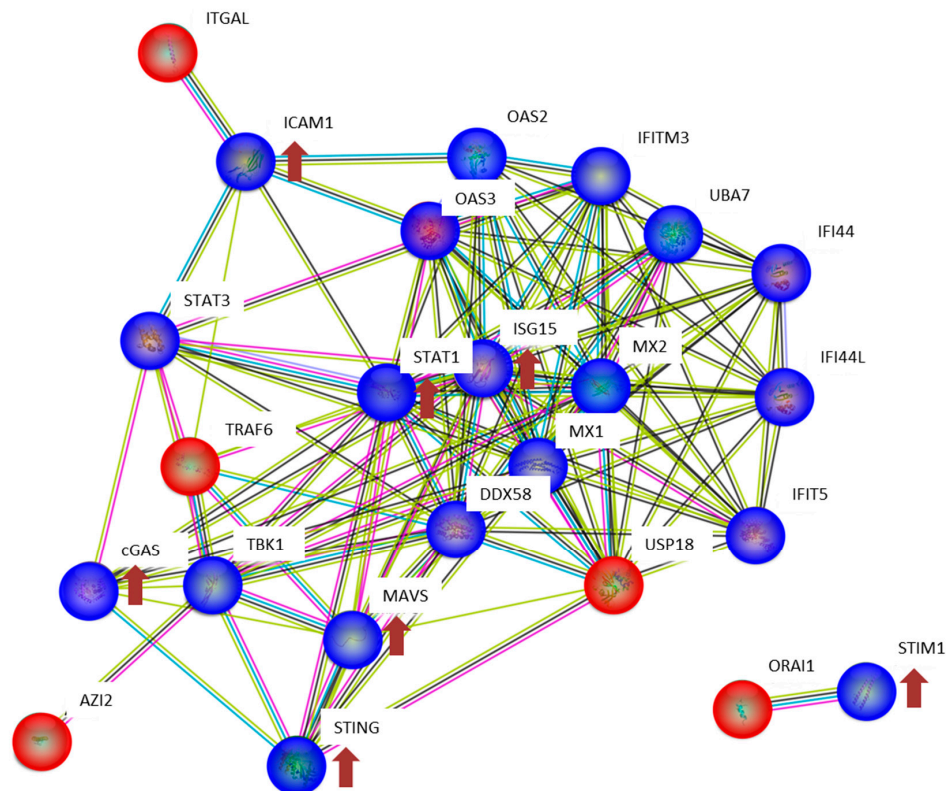


Figure 5. Interaction analysis of the cGAS-STING network using the STRING-db (string-db.org). Direct interactions between the proteins identified in HCECest2 cells one week after irradiation using proteomics or immunoblotting are shown in blue, predicted interactions (one step relaxation in STRING-db) are shown in red. Significantly differentially regulated proteins and the direction of deregulation are shown by red arrows. The significance of deregulation was based on the label-free proteomics analysis (fold change of ± 1.3 ; $q < 0.05$; $n = 4$) and immunoblotting (t -test; $p < 0.05$; $n = 3$). The lines between the proteins have the following color code: the red line indicates the presence of fusion evidence, the green line indicates neighborhood evidence, blue line indicates co-occurrence evidence, the purple line indicates experimental evidence, the yellow line indicates text mining evidence, the light blue indicates line database evidence, and the black line indicates co-expression evidence. The abbreviations and full names of the network proteins are as follows: AZI2: 5-azacytidine-induced protein 2; cGAS: cyclic GMP-AMP synthase; DDX58: antiviral innate immune response receptor RIG-I; ICAM1: intercellular adhesion molecule 1; IFI44: interferon-induced protein 44; IFI44L: interferon-induced protein 44-like; IFIT5: interferon-induced protein with tetratricopeptide repeats 5; IFITM3: interferon-induced transmembrane protein 3; ISG15: ubiquitin-like protein ISG15; ITGAL: integrin alpha-L; MAVS: mitochondrial antiviral-signaling protein; MX1: interferon-induced GTP-binding protein Mx1; MX2: interferon-induced GTP-binding protein Mx2; OAS2: 2'-5'-oligoadenylate synthase 2; OAS3: 2'-5'-oligoadenylate synthase 3; ORAI1: calcium release-activated calcium channel protein 1; STAT1: signal transducer and activator of transcription 1-alpha/beta; STAT3: signal transducer and activator of transcription 3; STING: stimulator of interferon genes protein; STIM1: stromal interaction molecule 1; TBK1: serine/threonine-protein kinase TBK1; TRAF6: TNF receptor-associated factor 6; UBA7: ubiquitin-like modifier-activating enzyme 7; USP18: Ubl carboxyl-terminal hydrolase 18.

5. Conclusions

This systematic investigation using the newest proteomics technology provides insights in the molecular changes in endothelial cells after the exposure to a range of radiation doses. This data set contains such a large amount of information that it cannot be all included in one study. Based on our previous results, we followed here particular pathways that are known to be induced by irradiation or

characteristic for cardiovascular disease, namely inflammatory response, DNA damage, and oxidative stress. The pro-inflammatory state was seen at 2 and 10 Gy as an activation of the cGAS-STING pathway, especially one week after the radiation exposure. At the lower doses of 0.25 and 0.5 Gy, no radiation-induced inflammation could be observed. This study supports the recent effort to develop inhibitors of the cGAS-STING pathway as anti-inflammatory agents [85] that could be used in the prevention and alleviation of radiation-induced cardiovascular disease.

Limitations of the Study

In this study, we used only one dose rate, namely 400 mGy/min. This relatively low dose rate allowed us to give small doses such as 0.25 Gy accurately. In addition, irradiating the cells with the total dose of 10 Gy took 25 min, which was still possible within the time frame of the experiment. However, we cannot exclude possible additional effects on the proteome if we had used a different dose rate.

The large SEM values that we discovered when using immunoblotting may be due to the fact that we used real biological replicates, meaning that the cells between the different replicates were cultivated at different time points. The cells were irradiated as a confluent monolayer as described before [24] and although all cell cultures were initiated using the same cell number, they may have been at slightly different stages at the time of irradiation.

Biological variation is obviously a limitation of the cell culture model that we used here. However, in order to investigate the large number of doses and time points as in this study, it would have been difficult to use an animal model. To deal with the limitations and exclude a possible effect of contaminants, we followed the cell cultures irradiated with different radiation doses at different time points by taking microscope images (Figure S6). Although we found time-dependent proteome changes even in the sham-irradiated controls, we could not observe any morphological changes (Figure S6). The dose of 10 Gy induced the most marked morphological changes: The cell density started to decrease at the same time as the cell size turned bigger (24 h post-irradiation). In addition, the cobblestone monolayer pattern, typical for endothelial cell cultures and as seen in the sham-irradiated, 0.25 and 0.5 Gy irradiated cells, was lost beginning after 48 h at 10 Gy. At day five, the cell density of the 2 Gy irradiated cells also started to decrease.

Although we observe changes in the proteome that indicate DNA damage and inflammatory response after the high-dose radiation, we did not measure these end points directly. The protein changes can only suggest this being the case which is a limitation of this study.

Supplementary Materials: The following are available online at <http://www.mdpi.com/2227-7382/8/4/30/s1>, Figure S1: Heat map of all significantly deregulated (1022) proteins in HCECest2 cell line 1 week after different radiation doses; Figure S2: Expression of inflammatory proteins as a function of radiation dose or time; Figure S3: Ponceau staining as the loading control of the immunoblot analysis for Figure 4; Figure S4: Immunoblot verification of ICAM1 levels as a function of time in HCECest2 cells; Figure S5: Ponceau stainings as the loading controls for the immunoblot analysis for Figure S4; Figure S6: Radiation-induced cell morphology changes of the endothelial cell line HCECest2; Table S1: All the identified, quantified, and deregulated proteins at different radiation doses compared to the sham-irradiated control at 4 h; Table S2: All the identified, quantified, and deregulated proteins at different radiation doses compared to the sham-irradiated control at 24 h; Table S3: All the identified, quantified, and deregulated proteins at the different radiation doses compared to the sham-irradiated control at 48 h; Table S4: All the identified, quantified, and deregulated proteins at different radiation doses compared to the sham-irradiated control at one week; Table S5: IPA pathway analysis and molecular functions for the radiation effect at one week; Table S6: All the identified, quantified, and deregulated proteins at different time points compared to the 4 h time point in the sham-irradiated control; Table S7: All the identified, quantified, and deregulated proteins at the different time points compared to the 4 h time point in 0.25 Gy irradiated samples; Table S8: All the identified, quantified, and deregulated proteins at the different time points compared to the 4 h time point in the 0.5 Gy irradiated samples; Table S9: All the identified, quantified, and deregulated proteins at the different time points compared to the 4 h time point in the 2 Gy irradiated samples; Table S10: All the identified, quantified, and deregulated proteins at different time points compared to the 4 h time point in 10 Gy irradiated samples; Table S11: Ingenuity pathway analysis and molecular functions for each time and dose point.

Author Contributions: Conceptualization, J.P. and S.T.; methodology, J.P., R.L.G. and C.v.T.; software, J.P., R.L.G., P.S. and O.A.; validation, J.P.; formal analysis, J.P., R.L.G. and C.v.T.; investigation, J.P., M.J.A. and S.T.; resources,

S.T., M.J.A.; data curation, J.P., R.L.G. and C.v.T.; writing—original draft preparation, J.P.; writing—review and editing, J.P., R.L.G., C.v.T., P.S., O.A., M.J.A. and S.T.; visualization, J.P. and S.T.; supervision, M.J.A. and S.T.; project administration, S.T.; funding acquisition, J.P. and S.T. All authors have read and agreed to the published version of the manuscript.

Funding: This research was funded by the Federal Ministry of Education and Research of Germany (BMBF), grant number 02NUK038B to J.P. and S.T.

Acknowledgments: We thank Stefanie Winkler for technical assistance in culturing the cells.

Conflicts of Interest: The authors declare no conflict of interest.

References

1. Krüger-Genge, A.; Blocki, A.; Franke, R.P.; Jung, F. Vascular endothelial cell biology: An update. *Int. J. Mol. Sci.* **2019**, *20*, 4411. [[CrossRef](#)] [[PubMed](#)]
2. Kim, K.S.; Kim, J.E.; Choi, K.J.; Bae, S.; Kim, D.H. Characterization of DNA damage-induced cellular senescence by ionizing radiation in endothelial cells. *Int. J. Radiat. Biol.* **2014**, *90*, 71–80. [[CrossRef](#)] [[PubMed](#)]
3. Bhayadia, R.; Schmidt, B.M.; Melk, A.; Homme, M. Senescence-induced oxidative stress causes endothelial dysfunction. *J. Gerontol. A Biol. Sci. Med. Sci.* **2016**, *71*, 161–169. [[CrossRef](#)] [[PubMed](#)]
4. Cancel, L.M.; Ebong, E.E.; Mensah, S.; Hirschberg, C.; Tarbell, J.M. Endothelial glycocalyx, apoptosis and inflammation in an atherosclerotic mouse model. *Atherosclerosis* **2016**, *252*, 136–146. [[CrossRef](#)] [[PubMed](#)]
5. Guipaud, O.; Jaillet, C.; Clément-Colmou, K.; François, A.; Supiot, S.; Milliat, F. The importance of the vascular endothelial barrier in the immune-inflammatory response induced by radiotherapy. *Br. J. Radiol.* **2018**, *91*, 20170762. [[CrossRef](#)]
6. Draeger, E.; Sawant, A.; Johnstone, C.; Koger, B.; Becker, S.; Vujaskovic, Z.; Jackson, I.L.; Poirier, Y. A Dose of Reality: How 20 years of incomplete physics and dosimetry reporting in radiobiology studies may have contributed to the reproducibility crisis. *Int. J. Radiat. Oncol. Biol. Phys.* **2020**, *106*, 243–252. [[CrossRef](#)]
7. Jordan, B.R. The Hiroshima/Nagasaki survivor studies: Discrepancies between results and general perception. *Genetics* **2016**, *203*, 1505–1512. [[CrossRef](#)]
8. Papiez, A.; Azimzadeh, O.; Azizova, T.; Moseeva, M.; Anastasov, N.; Smida, J.; Tapio, S.; Polanska, J. Integrative multiomics study for validation of mechanisms in radiation-induced ischemic heart disease in Mayak workers. *PLoS ONE* **2018**, *13*, e0209626. [[CrossRef](#)]
9. Azimzadeh, O.; Sievert, W.; Sarioglu, H.; Merl-Pham, J.; Yentrapalli, R.; Bakshi, M.V.; Janik, D.; Ueffing, M.; Atkinson, M.J.; Multhoff, G.; et al. Integrative proteomics and targeted transcriptomics analyses in cardiac endothelial cells unravel mechanisms of long-term radiation-induced vascular dysfunction. *J. Proteome Res.* **2015**, *14*, 1203–1219. [[CrossRef](#)]
10. Sievert, W.; Trott, K.R.; Azimzadeh, O.; Tapio, S.; Zitzelsberger, H.; Multhoff, G. Late proliferating and inflammatory effects on murine microvascular heart and lung endothelial cells after irradiation. *Radiation Oncol.* **2015**, *117*, 376–381. [[CrossRef](#)]
11. Hayashi, T.; Kusunoki, Y.; Hakoda, M.; Morishita, Y.; Kubo, Y.; Maki, M.; Kasagi, F.; Kodama, K.; Macphee, D.G.; Kyoizumi, S. Radiation dose-dependent increases in inflammatory response markers in A-bomb survivors. *Int. J. Radiat. Biol.* **2003**, *79*, 129–136. [[CrossRef](#)]
12. Chen, Y.C.; Huang, A.L.; Kyaw, T.S.; Bobik, A.; Peter, K. Atherosclerotic plaque rupture: Identifying the straw that breaks the camel's back. *Arterioscler. Thromb. Vasc. Biol.* **2016**, *36*, e63–e72. [[CrossRef](#)] [[PubMed](#)]
13. Karahalil, B. Overview of systems biology and omics technologies. *Curr. Med. Chem.* **2016**, *23*, 4221–4230. [[CrossRef](#)]
14. Shan, Y.X.; Jin, S.Z.; Liu, X.D.; Liu, Y.; Liu, S.Z. Ionizing radiation stimulates secretion of pro-inflammatory cytokines: Dose-response relationship, mechanisms and implications. *Radiat. Environ. Biophys.* **2007**, *46*, 21–29. [[CrossRef](#)]
15. Frey, B.; Hehlgans, S.; Rödel, F.; Gaipl, U.S. Modulation of inflammation by low and high doses of ionizing radiation: Implications for benign and malignant diseases. *Cancer Lett.* **2015**, *368*, 230–237. [[CrossRef](#)]
16. Cervelli, T.; Panetta, D.; Navarra, T.; Andreassi, M.G.; Basta, G.; Galli, A.; Salvadori, P.A.; Picano, E.; Del Turco, S. Effects of single and fractionated low-dose irradiation on vascular endothelial cells. *Atherosclerosis* **2014**, *235*, 510–518. [[CrossRef](#)] [[PubMed](#)]

17. Azimzadeh, O.; Subramanian, V.; Stander, S.; Merl-Pham, J.; Lowe, D.; Barjaktarovic, Z.; Moertl, S.; Raj, K.; Atkinson, M.J.; Tapio, S. Proteome analysis of irradiated endothelial cells reveals persistent alteration in protein degradation and the RhoGDI and NO signalling pathways. *Int. J. Radiat. Biol.* **2017**, *93*, 920–928. [[CrossRef](#)] [[PubMed](#)]
18. Ebrahimian, T.G.; Beugnies, L.; Surette, J.; Priest, N.; Gueguen, Y.; Gloaguen, C.; Benderitter, M.; Jourdain, J.R.; Tack, K. Chronic exposure to external low-dose gamma radiation induces an increase in anti-inflammatory and anti-oxidative parameters resulting in atherosclerotic plaque size reduction in ApoE(-/-) Mice. *Radiat. Res.* **2018**, *189*, 187–196. [[CrossRef](#)]
19. Baselet, B.; Belmans, N.; Coninx, E.; Lowe, D.; Janssen, A.; Michaux, A.; Tabury, K.; Raj, K.; Quintens, R.; Benotmane, M.A.; et al. Functional gene analysis reveals cell cycle changes and inflammation in endothelial cells irradiated with a single X-ray dose. *Front. Pharmacol.* **2017**, *8*, 213. [[CrossRef](#)]
20. Baselet, B.; Sonveaux, P.; Baatout, S.; Aerts, A. Pathological effects of ionizing radiation: Endothelial activation and dysfunction. *Cell. Mol. Life Sci.* **2019**, *76*, 699–728. [[CrossRef](#)]
21. Boström, M.; Kalm, M.; Eriksson, Y.; Bull, C.; Ståhlberg, A.; Björk-Eriksson, T.; Hellström Erkenstam, N.; Blomgren, K. A role for endothelial cells in radiation-induced inflammation. *Int. J. Radiat. Biol.* **2018**, *94*, 259–271. [[CrossRef](#)] [[PubMed](#)]
22. Halle, M.; Hall, P.; Tornvall, P. Cardiovascular disease associated with radiotherapy: Activation of nuclear factor kappa-B. *J. Intern. Med.* **2011**, *269*, 469–477. [[CrossRef](#)]
23. Lowe, D.; Raj, K. Premature aging induced by radiation exhibits pro-atherosclerotic effects mediated by epigenetic activation of CD44 expression. *Aging Cell* **2014**, *13*, 900–910. [[CrossRef](#)] [[PubMed](#)]
24. Philipp, J.; Azimzadeh, O.; Subramanian, V.; Merl-Pham, J.; Lowe, D.; Hladik, D.; Erbelinger, N.; Ktitareva, S.; Fournier, C.; Atkinson, M.J.; et al. Radiation-induced endothelial inflammation is transferred via the secretome to recipient cells in a stat-mediated process. *J. Proteome Res.* **2017**, *16*, 3903–3916. [[CrossRef](#)]
25. Meeren, A.V.; Bertho, J.M.; Vandamme, M.; Gaugler, M.H. Ionizing radiation enhances IL-6 and IL-8 production by human endothelial cells. *Mediat. Inflamm.* **1997**, *6*, 185–193. [[CrossRef](#)]
26. Sievert, W.; Tapio, S.; Breuninger, S.; Gaipf, U.; Andratschke, N.; Trott, K.R.; Multhoff, G. Adhesion molecule expression and function of primary endothelial cells in benign and malignant tissues correlates with proliferation. *PLoS ONE* **2014**, *9*, e91808. [[CrossRef](#)]
27. Margolis, S.R.; Wilson, S.C.; Vance, R.E. Evolutionary origins of cGAS-STING signaling. *Trends Immunol.* **2017**, *38*, 733–743. [[CrossRef](#)]
28. Durante, M.; Formenti, S.C. Radiation-induced chromosomal aberrations and immunotherapy: Micronuclei, Cytosolic DNA, and interferon-production pathway. *Front. Oncol.* **2018**, *8*, 192. [[CrossRef](#)]
29. Lam, E.; Stein, S.; Falck-Pedersen, E. Adenovirus detection by the cGAS/STING/TBK1 DNA sensing cascade. *J. Virol.* **2014**, *88*, 974–981. [[CrossRef](#)]
30. Li, T.; Chen, Z.J. The cGAS-cGAMP-STING pathway connects DNA damage to inflammation, senescence, and cancer. *J. Exp. Med.* **2018**, *215*, 1287–1299. [[CrossRef](#)] [[PubMed](#)]
31. Tao, J.; Zhou, X.; Jiang, Z. cGAS-cGAMP-STING: The three musketeers of cytosolic DNA sensing and signaling. *IUBMB Life* **2016**, *68*, 858–870. [[CrossRef](#)] [[PubMed](#)]
32. Sun, L.; Wu, J.; Du, F.; Chen, X.; Chen, Z.J. Cyclic GMP-AMP synthase is a cytosolic DNA sensor that activates the type I interferon pathway. *Science* **2013**, *339*, 786–791. [[CrossRef](#)]
33. Lafargue, A.; Degorre, C.; Corre, I.; Alves-Guerra, M.C.; Gaugler, M.H.; Vallette, F.; Pecqueur, C.; Paris, F. Ionizing radiation induces long-term senescence in endothelial cells through mitochondrial respiratory complex II dysfunction and superoxide generation. *Free Radic. Biol. Med.* **2017**, *108*, 750–759. [[CrossRef](#)]
34. Philipp, J.; Sievert, W.; Azimzadeh, O.; von Toerne, C.; Metzger, F.; Posch, A.; Hladik, D.; Subedi, P.; Multhoff, G.; Atkinson, M.J.; et al. Data independent acquisition mass spectrometry of irradiated mouse lung endothelial cells reveals a STAT-associated inflammatory response. *Int. J. Radiat. Biol.* **2020**, *96*, 642–650. [[CrossRef](#)]
35. Au-Yeung, N.; Mandhana, R.; Horvath, C.M. Transcriptional regulation by STAT1 and STAT2 in the interferon JAK-STAT pathway. *JAKSTAT* **2013**, *2*, e23931. [[CrossRef](#)] [[PubMed](#)]
36. Trilling, M.; Bellora, N.; Rutkowski, A.J.; de Graaf, M.; Dickinson, P.; Robertson, K.; Prazeres da Costa, O.; Ghazal, P.; Friedel, C.C.; Albà, M.M.; et al. Deciphering the modulation of gene expression by type I and II interferons combining 4sU-tagging, translational arrest and in silico promoter analysis. *Nucleic Acids Res.* **2013**, *41*, 8107–8125. [[CrossRef](#)]

37. Kreienkamp, R.; Graziano, S.; Coll-Bonfill, N.; Bedia-Diaz, G.; Cybulla, E.; Vindigni, A.; Dorsett, D.; Kubben, N.; Batista, L.F.Z.; Gonzalo, S. A Cell-Intrinsic Interferon-like Response Links Replication Stress to Cellular Aging Caused by Progerin. *Cell Rep.* **2018**, *22*, 2006–2015. [[CrossRef](#)]
38. Wisniewski, J.R.; Zougman, A.; Nagaraj, N.; Mann, M. Universal sample preparation method for proteome analysis. *Nat. Methods* **2009**, *6*, 359–362. [[CrossRef](#)]
39. Kappler, L.; Hoene, M.; Hu, C.; von Toerne, C.; Li, J.; Bleher, D.; Hoffmann, C.; Bohm, A.; Kollipara, L.; Zischka, H.; et al. Linking bioenergetic function of mitochondria to tissue-specific molecular fingerprints. *Am. J. Physiol. Endocrinol. Metab.* **2019**, *317*, E374–E387. [[CrossRef](#)]
40. Huber, W.; von Heydebreck, A.; Sultmann, H.; Poustka, A.; Vingron, M. Variance stabilization applied to microarray data calibration and to the quantification of differential expression. *Bioinformatics* **2002**, *18* (Suppl. 1), S96–S104. [[CrossRef](#)] [[PubMed](#)]
41. McInnes, L.; Healy, J. UMAP: Uniform manifold approximation and projection for dimension reduction. *arXiv* **2018**, arXiv:1802.03426.
42. van der Maaten, L.J.P.; Hinton, G.E. Visualizing high-dimensional data using t-SNE. *J. Mach. Learn. Res.* **2008**, *9*, 2579–2605.
43. Phipson, B.; Lee, S.; Majewski, I.J.; Alexander, W.S.; Smyth, G.K. Robust hyperparameter estimation protects against hypervariable genes and improves power to detect differential expression. *Ann. Appl. Stat.* **2016**, *10*, 946–963. [[CrossRef](#)]
44. Storey, J. A direct approach to false discovery rates. *J. R. Stat. Soc.* **2002**, *64*, 479–498. [[CrossRef](#)]
45. Perez-Riverol, Y.; Csordas, A.; Bai, J.; Bernal-Llinares, M.; Hewapathirana, S.; Kundu, D.J.; Inuganti, A.; Griss, J.; Mayer, G.; Eisenacher, M.; et al. The PRIDE database and related tools and resources in 2019: Improving support for quantification data. *Nucleic Acids Res.* **2019**, *47*, D442–D450. [[CrossRef](#)]
46. Srikanth, S.; Woo, J.S.; Wu, B.; El-Sherbiny, Y.M.; Leung, J.; Chupradit, K.; Rice, L.; Seo, G.J.; Calmettes, G.; Ramakrishna, C.; et al. The Ca(2+) sensor STIM1 regulates the type I interferon response by retaining the signaling adaptor STING at the endoplasmic reticulum. *Nat. Immunol.* **2019**, *20*, 152–162. [[CrossRef](#)]
47. Garcia, N.; Zazueta, C.; Aguilera-Aguirre, L. Oxidative stress and inflammation in cardiovascular disease. *Oxid. Med. Cell. Longev.* **2017**, *2017*, 5853238. [[CrossRef](#)]
48. Wennstig, A.K.; Garmo, H.; Isacson, U.; Gagliardi, G.; Rintelä, N.; Lagerqvist, B.; Holmberg, L.; Blomqvist, C.; Sund, M.; Nilsson, G. The relationship between radiation doses to coronary arteries and location of coronary stenosis requiring intervention in breast cancer survivors. *Radiat. Oncol.* **2019**, *14*, 40. [[CrossRef](#)]
49. Aznar, M.C.; Duane, F.K.; Darby, S.C.; Wang, Z.; Taylor, C.W. Exposure of the lungs in breast cancer radiotherapy: A systematic review of lung doses published 2010–2015. *Radiother. Oncol.* **2018**, *126*, 148–154. [[CrossRef](#)]
50. Hooning, M.J.; Botma, A.; Aleman, B.M.; Baaijens, M.H.; Bartelink, H.; Klijn, J.G.; Taylor, C.W.; van Leeuwen, F.E. Long-term risk of cardiovascular disease in 10-year survivors of breast cancer. *J. Natl. Cancer Inst.* **2007**, *99*, 365–375. [[CrossRef](#)]
51. Wennstig, A.K.; Wadsten, C.; Garmo, H.; Fredriksson, I.; Blomqvist, C.; Holmberg, L.; Nilsson, G.; Sund, M. Long-term risk of ischemic heart disease after adjuvant radiotherapy in breast cancer: Results from a large population-based cohort. *Breast Cancer Res.* **2020**, *22*, 10. [[CrossRef](#)] [[PubMed](#)]
52. Baselet, B.; Azimzadeh, O.; Erbeltinger, N.; Bakshi, M.V.; Dettmering, T.; Janssen, A.; Ktitareva, S.; Lowe, D.J.; Michaux, A.; Quintens, R.; et al. Differential impact of single-dose Fe ion and X-Ray irradiation on endothelial cell transcriptomic and proteomic responses. *Front. Pharmacol.* **2017**, *8*, 570. [[CrossRef](#)] [[PubMed](#)]
53. Little, M.P.; Tawn, E.J.; Tzoulaki, I.; Wakeford, R.; Hildebrandt, G.; Paris, F.; Tapio, S.; Elliott, P. A systematic review of epidemiological associations between low and moderate doses of ionizing radiation and late cardiovascular effects, and their possible mechanisms. *Radiat. Res.* **2008**, *169*, 99–109. [[CrossRef](#)] [[PubMed](#)]
54. Little, M.P.; Tawn, E.J.; Tzoulaki, I.; Wakeford, R.; Hildebrandt, G.; Paris, F.; Tapio, S.; Elliott, P. Review and meta-analysis of epidemiological associations between low/moderate doses of ionizing radiation and circulatory disease risks, and their possible mechanisms. *Radiat. Environ. Biophys.* **2010**, *49*, 139–153. [[CrossRef](#)]
55. Gillies, M.; Richardson, D.B.; Cardis, E.; Daniels, R.D.; O’Hagan, J.A.; Haylock, R.; Laurier, D.; Leuraud, K.; Moissonnier, M.; Schubauer-Berigan, M.K.; et al. Mortality from circulatory diseases and other non-cancer outcomes among nuclear workers in France, the United Kingdom and the United States (INWORKS). *Radiat. Res.* **2017**, *188*, 276–290. [[CrossRef](#)] [[PubMed](#)]

56. Little, M.P.; Zablotska, L.B.; Brenner, A.V.; Lipshultz, S.E. Circulatory disease mortality in the Massachusetts tuberculosis fluoroscopy cohort study. *Eur. J. Epidemiol.* **2016**, *31*, 287–309. [[CrossRef](#)]
57. Amundson, S.A.; Fornace, A.J., Jr. Microarray approaches for analysis of cell cycle regulatory genes. *Methods Mol. Biol.* **2004**, *241*, 125–141.
58. Kis, E.; Szatmári, T.; Keszei, M.; Farkas, R.; Esik, O.; Lumniczky, K.; Falus, A.; Sáfrány, G. Microarray analysis of radiation response genes in primary human fibroblasts. *Int. J. Radiat. Oncol. Biol. Phys.* **2006**, *66*, 1506–1514. [[CrossRef](#)]
59. Tilton, S.C.; Markillie, L.M.; Hays, S.; Taylor, R.C.; Stenoien, D.L. Identification of differential gene expression patterns after acute exposure to high and low doses of low-let ionizing radiation in a reconstituted human skin tissue. *Radiat. Res.* **2016**, *186*, 531–538. [[CrossRef](#)]
60. Balázs, K.; Kis, E.; Badie, C.; Bogdándi, E.N.; Candéias, S.; Garcia, L.C.; Dominczyk, I.; Frey, B.; Gaipf, U.; Jurányi, Z.; et al. Radiotherapy-induced changes in the systemic immune and inflammation parameters of head and neck cancer patients. *Cancers* **2019**, *11*, 1324. [[CrossRef](#)]
61. Hwang, B.J.; Ford, J.M.; Hanawalt, P.C.; Chu, G. Expression of the p48 xeroderma pigmentosum gene is p53-dependent and is involved in global genomic repair. *Proc. Natl. Acad. Sci. USA* **1999**, *96*, 424–428. [[CrossRef](#)] [[PubMed](#)]
62. Zhao, Q.; Barakat, B.M.; Qin, S.; Ray, A.; El-Mahdy, M.A.; Wani, G.; Arafa, E.-S.; Mir, S.N.; Wang, Q.E.; Wani, A.A. The p38 mitogen-activated protein kinase augments nucleotide excision repair by mediating DDB2 degradation and chromatin relaxation. *J. Biol. Chem.* **2008**, *283*, 32553–32561. [[CrossRef](#)] [[PubMed](#)]
63. Nakamura, S.; Kawai, K.; Takeshita, Y.; Honda, M.; Takamura, T.; Kaneko, S.; Matoba, R.; Matsubara, K. Identification of blood biomarkers of aging by transcript profiling of whole blood. *Biochem. Biophys. Res. Commun.* **2012**, *418*, 313–318. [[CrossRef](#)] [[PubMed](#)]
64. Badie, C.; Kabacik, S.; Balagurunathan, Y.; Bernard, N.; Brengues, M.; Faggioni, G.; Greither, R.; Lista, F.; Peinnequin, A.; Poyot, T.; et al. Laboratory intercomparison of gene expression assays. *Radiat. Res.* **2013**, *180*, 138–148. [[CrossRef](#)]
65. Jen, K.Y.; Cheung, V.G. Transcriptional response of lymphoblastoid cells to ionizing radiation. *Genome Res.* **2003**, *13*, 2092–2100. [[CrossRef](#)]
66. Hall, J.; Jeggo, P.A.; West, C.; Gomolka, M.; Quintens, R.; Badie, C.; Laurent, O.; Aerts, A.; Anastasov, N.; Azimzadeh, O.; et al. Ionizing radiation biomarkers in epidemiological studies—An update. *Mutat. Res.* **2017**, *771*, 59–84. [[CrossRef](#)]
67. O'Brien, G.; Cruz-Garcia, L.; Majewski, M.; Grepl, J.; Abend, M.; Port, M.; Tichý, A.; Sirak, I.; Malkova, A.; Donovan, E.; et al. FDXR is a biomarker of radiation exposure in vivo. *Sci. Rep.* **2018**, *8*, 684. [[CrossRef](#)]
68. Rothkamm, K.; Beinke, C.; Romm, H.; Badie, C.; Balagurunathan, Y.; Barnard, S.; Bernard, N.; Boulay-Greene, H.; Brengues, M.; De Amicis, A.; et al. Comparison of established and emerging biodosimetry assays. *Radiat. Res.* **2013**, *180*, 111–119. [[CrossRef](#)]
69. Fenech, M.; Morley, A.A. Cytokinesis-block micronucleus method in human lymphocytes: Effect of in vivo ageing and low dose X-irradiation. *Mutat. Res.* **1986**, *161*, 193–198. [[CrossRef](#)]
70. Schlegel, R.; MacGregor, J.T.; Everson, R.B. Assessment of cytogenetic damage by quantitation of micronuclei in human peripheral blood erythrocytes. *Cancer Res.* **1986**, *46*, 3717–3721.
71. Coppé, J.P.; Kauser, K.; Campisi, J.; Beauséjour, C.M. Secretion of vascular endothelial growth factor by primary human fibroblasts at senescence. *J. Biol. Chem.* **2006**, *281*, 29568–29574. [[CrossRef](#)]
72. Rodier, F.; Coppe, J.P.; Patil, C.K.; Hoeijmakers, W.A.; Munoz, D.P.; Raza, S.R.; Freund, A.; Campeau, E.; Davalos, A.R.; Campisi, J. Persistent DNA damage signalling triggers senescence-associated inflammatory cytokine secretion. *Nat. Cell Biol.* **2009**, *11*, 973–979. [[CrossRef](#)]
73. Brzostek-Racine, S.; Gordon, C.; Van Scoy, S.; Reich, N.C. The DNA damage response induces IFN. *J. Immunol.* **2011**, *187*, 5336–5345. [[CrossRef](#)] [[PubMed](#)]
74. Kondo, T.; Kobayashi, J.; Saitoh, T.; Maruyama, K.; Ishii, K.J.; Barber, G.N.; Komatsu, K.; Akira, S.; Kawai, T. DNA damage sensor MRE11 recognizes cytosolic double-stranded DNA and induces type I interferon by regulating STING trafficking. *Proc. Natl. Acad. Sci. USA* **2013**, *110*, 2969–2974. [[CrossRef](#)] [[PubMed](#)]
75. Härtlova, A.; Erttmann, S.F.; Raffi, F.A.; Schmalz, A.M.; Resch, U.; Anugula, S.; Lienenklaus, S.; Nilsson, L.M.; Kröger, A.; Nilsson, J.A.; et al. DNA damage primes the type I interferon system via the cytosolic DNA sensor STING to promote anti-microbial innate immunity. *Immunity* **2015**, *42*, 332–343. [[CrossRef](#)]

76. Du, S.; Chen, G.; Yuan, B.; Hu, Y.; Yang, P.; Chen, Y.; Zhao, Q.; Zhou, J.; Fan, J.; Zeng, Z. DNA sensing and associated type 1 interferon signaling contributes to progression of radiation-induced liver injury. *Cell. Mol. Immunol.* **2020**. [[CrossRef](#)]
77. Ranoa, D.R.; Parekh, A.D.; Pitroda, S.P.; Huang, X.; Darga, T.; Wong, A.C.; Huang, L.; Andrade, J.; Staley, J.P.; Satoh, T.; et al. Cancer therapies activate RIG-I-like receptor pathway through endogenous non-coding RNAs. *Oncotarget* **2016**, *7*, 26496–26515. [[CrossRef](#)]
78. Ma, X.; Helgason, E.; Phung, Q.T.; Quan, C.L.; Iyer, R.S.; Lee, M.W.; Bowman, K.K.; Starovasnik, M.A.; Dueber, E.C. Molecular basis of Tank-binding kinase 1 activation by transautophosphorylation. *Proc. Natl. Acad. Sci. USA* **2012**, *109*, 9378–9383. [[CrossRef](#)]
79. Chen, Q.; Sun, L.; Chen, Z.J. Regulation and function of the cGAS-STING pathway of cytosolic DNA sensing. *Nat. Immunol.* **2016**, *17*, 1142–1149. [[CrossRef](#)]
80. Przanowski, P.; Loska, S.; Cysewski, D.; Dabrowski, M.; Kaminska, B. ISGylation increases stability of numerous proteins including Stat1, which prevents premature termination of immune response in LPS-stimulated microglia. *Neurochem. Int.* **2018**, *112*, 227–233. [[CrossRef](#)]
81. Bogunovic, D.; Boisson-Dupuis, S.; Casanova, J.L. ISG15: Leading a double life as a secreted molecule. *Exp. Mol. Med.* **2013**, *45*, e18. [[CrossRef](#)] [[PubMed](#)]
82. Schröder, S.; Juerß, D.; Kriesen, S.; Manda, K.; Hildebrandt, G. Immunomodulatory properties of low-dose ionizing radiation on human endothelial cells. *Int. J. Radiat. Biol.* **2019**, *95*, 23–32. [[CrossRef](#)] [[PubMed](#)]
83. Schröder, S.; Kriesen, S.; Paape, D.; Hildebrandt, G.; Manda, K. Modulation of inflammatory reactions by low-dose ionizing radiation: Cytokine release of murine endothelial cells is dependent on culture conditions. *J. Immunol. Res.* **2018**, *2018*, 2856518. [[CrossRef](#)] [[PubMed](#)]
84. Wang, H.; Segaran, R.C.; Chan, L.Y.; Aladresi, A.A.M.; Chinnathambi, A.; Alharbi, S.A.; Sethi, G.; Tang, F.R. Gamma radiation-induced disruption of cellular junctions in HUVECs is mediated through affecting MAPK/NF- κ B inflammatory pathways. *Oxid. Med. Cell. Longev.* **2019**, *2019*, 1486232. [[CrossRef](#)] [[PubMed](#)]
85. Sheridan, C. Drug developers switch gears to inhibit STING. *Nat. Biotechnol.* **2019**, *37*, 199–201. [[CrossRef](#)]

Publisher's Note: MDPI stays neutral with regard to jurisdictional claims in published maps and institutional affiliations.



© 2020 by the authors. Licensee MDPI, Basel, Switzerland. This article is an open access article distributed under the terms and conditions of the Creative Commons Attribution (CC BY) license (<http://creativecommons.org/licenses/by/4.0/>).

4. Conclusion and Discussion

The research on endothelial cells considering irradiation-induced vascular damage has gained attention in the last years. Although endothelial cells play a pivotal role in CVD (Baselet et al. 2019), still the knowledge about the endothelial function is very general in nature. Due to the heterogeneity of endothelial cells of different origin (Aird 2007) each tissue endothelium should be investigated separately.

In the standard breast cancer radiation therapy it is unavoidable that also the normal tissue like heart and lung is exposed to radiation to some extent. For example, the left anterior descending artery may receive X-ray doses between 0.1-20 Gy (Wennstig et al. 2019) that is comparable to the average dose to the lungs (Aznar et al. 2018). Considering the increasing risk of vascular and cardiac diseases associated with irradiation, the investigation of the influence of different radiation doses on the heart and lung endothelium is of high relevance. Nevertheless, high doses of more than 2 Gy have been more extensively studied in different human cell lines and mice than the lower doses. Most prominent findings at high doses are the development of cellular senescence in endothelial cells (Yentrapalli, Azimzadeh, Barjaktarovic, et al. 2013) and the secretion of pro-inflammatory cytokines and chemokines by senescent cells (Meeren et al. 1997). The mechanisms for the development of radiation-induced senescence and inflammation are rather unknown. Therefore, the presented work was conducted to elucidate mechanisms responsible for endothelial inflammation and senescence after high dose radiation. In addition, the research focus was to investigate low-dose irradiation as a possible trigger of these two parameters, particularly the existence of a possible threshold dose under which these effects can't be observed. Proteomics enables the discovery of multifaceted radiation response on the protein level and makes it possible to study inflammation and senescence simultaneously. In this thesis, a link between senescence, innate immune response, and DNA damage is suggested.

4.1 Direct irradiation damage on endothelial cells

As mentioned previously, the radiation damage on endothelial cells is difficult to assess directly due to the low proliferation rate *in vivo* and access to irradiated human material. However, we know from several *in vitro* studies (Lowe and Raj 2014; Haimovitz-Friedman et al. 1994; Lafargue et al. 2017) and a few available *in vivo* studies (Paris 2001; Hamada et al. 2020) that radiation damage is associated with an increased rate of apoptosis and therefore leakage-related malfunctions within the endothelial barrier. In addition, leukocytes and monocytes become adhesive to the endothelial layer (Mollà et al. 2003) leading to their penetration. After high dose radiation of 90 Gy (X-ray) using the mouse ear as a model (SKH-1/h), the diameter of veins and arteries was enhanced with simultaneously increased red blood velocity (Goertz et al. 2015). This might be a consequence of the cells undergoing senescence and cell death and the cohesion among the surviving cells. Senescent endothelial cells increase their size as observed by us and others after high dose irradiation (Lowe and Raj 2014; Philipp et al. 2017; Philipp, Le Gleut, et al. 2020). The enlarged endothelial cell body has been described at atherosclerotic plaques (Tokunaga, Fan, and Watanabe 1989). As we have observed, this occurs prematurely after high dose irradiation of > 2 Gy γ -irradiation within the first week post radiation (Philipp, Le Gleut, et al. 2020). In addition to a greater cell surface area, Lowe and Raj (Lowe and Raj 2014) observed an increased monocyte adhesion resulting in plaques using human coronary artery endothelial cell line in cell culture (X-ray, 10 Gy). The increased cell size and enhanced adhesion of monocytes display a potential risk for developing atherosclerosis and might therefore lead to CVD vessel sites receiving high radiation doses as in the radiation therapy.

4.2 Irradiation-induced inflammation

Irradiation causes long-term damage to endothelial cells by triggering local and systemic inflammation (Azimzadeh et al. 2015; Sievert et al. 2015). In the most conducted studies, very high radiation doses of at least 8 Gy were used. However, as mentioned before, the left anterior descending artery may receive variable X-ray doses between 0.1-20 Gy depending on the site (Wennstig et al. 2019) and the same is true for the lung doses (Aznar et al. 2018). A dose-dependent increase in

inflammatory markers has been observed in the blood of atomic bomb survivors in Japan long after the exposure (Hayashi et al. 2003) including people exposed to relatively low total body doses of 0.1 Gy, suggesting that irradiation causes a persistent inflammation even at a relatively low doses if the affects large body volumes. Hence, it is necessary to investigate not only the effects of high-dose radiation, but also the role of lower radiation doses in the induction and development of inflammatory responses. At the moment there is still a big gap in the knowledge between the immediate effects of irradiation and the development of the disease such as CVD. The work carried out here attempts to provide some answers to these remaining questions and offers indications of how the inflammatory reactions after irradiation may arise.

4.2.1 Innate immune response via cGAS/STING-pathway

Our recent data suggests that there is a connection between irradiation and inflammation: the cGAS/STING-pathway (Philipp, Sievert, et al. 2020; Philipp, Le Gleut, et al. 2020). As described in the introduction this pathway is activated by the occurrence of dsDNA in the cytosol. It is part of the innate immune response and triggers the self-defense of the cell. A look at the phylogenetic tree shows how conserved and therefore important this pathway is. Here it becomes clear that cGAS and STING are present not only in all mammals but also in many invertebrates (X. Wu et al. 2014). Its evolutionary development refers to the defense against invading pathogens with the detection of microbial and viral DNA (Lam, Stein, and Falck-Pedersen 2014). Irradiation is known to cause dsDNA breaks in the nucleus and in the mitochondria resulting in the leakage of dsDNA fragments to the cytosol (Mackenzie et al. 2017; West et al. 2015). We have shown that, in case of endothelial cells, the cytosolic DNA sensing by cGAS is upregulated by high radiation doses (X-ray, 10 Gy) in human coronary artery endothelial cell line (Philipp, Le Gleut, et al. 2020) but also in mouse primary endothelial cells received from the irradiated lung (Philipp, Sievert, et al. 2020). The induction of cGAS not only depends on the presence of the cytosolic dsDNA but also on the length of the cytosolic dsDNA fragments. The longer the dsDNA fragments, the stronger the response (Luecke et al. 2017). This may explain the sensitivity of cGAS for radiation-

induced DNA damage, since small amounts of short DNA might get cleared by nucleases but especially high-dose radiation is known to produce large amounts of long fragments, enough for full cGAS activation. We have shown that, similarly to cGAS, STING is upregulated even after the dose of 2 Gy γ -irradiation (Philipp, Le Gleut, et al. 2020). This elevation of cGAS and STING protein levels triggers a protein signaling cascade *via* TBK1 and IRF3 and finally leads to the transcriptional activation of various proteins of the type I interferon response (Du et al. 2020). In this signaling cascade, the protein STING is the linchpin of the whole pathway. It can activate either IRF3 as we have observed or NF κ B both leading to the transcription of type I interferon response (Dou et al. 2017). However, it is not well understood which transcription factor is activated for which purpose. Nevertheless, the control of STING expression is important to prevent a chronic activation of inflammation, as observed in several autoimmune diseases (Ahn et al. 2012; Liu et al. 2014). For controlling purposes, STING has several negative regulators. One of those is STIM1 known to inactivate STING (Srikanth et al. 2019). We have observed an upregulation of STIM1 a week after the cells had been irradiated with the 10 Gy X-ray dose in primary mouse lung endothelial cells (Philipp, Sievert, et al. 2020) as well as after 10 Gy γ -irradiation in the human coronary artery endothelial cell line (Philipp, Le Gleut, et al. 2020). However, in our hands this did not lead to downregulation of STING. In addition to STIM1, other regulators acting *via* a negative feedback loop might be needed to prevent the permanent activation of STING and subsequent downstream pathways. Since STING is known as a chronic inducer of the type I interferon response (West et al. 2015), it might be a good target for pre-radiation treatment to prevent chronic inflammation of the normal tissue after radiation therapy. The palmitoylation inhibitor 2-bromopalmitate could therefore be used to inhibit the STING activation and therefore the chronic induction of inflammation (Mukai et al. 2016). Summarizing, the cGAS/STING pathway is needed for initiation of the type I interferon response after irradiation and plays therefore a pivotal role in the radiation-induced inflammatory response.

4.2.2 Type I Interferon response and its consequences

Recently, it has been suggested that similarly to the cGAS/STING-pathway, AT-rich dsDNA fragments including promoter regions might be transcribed and the corresponding cytosolic RNA could then be detected by the MAVS-dependent RNA sensing pathway (Feng et al. 2020). Also in this case, an initiation of the type I interferon response has been observed (Belgnaoui, Paz, and Hiscott 2011). We have found the MAVS protein significantly upregulated at 2 and 10 Gy one week post γ -irradiation (Philipp, Le Gleut, et al. 2020). Since the pathways of MAVS-dependent RNA sensing and cGAS/STING overlap correspond from the transcription factors IRF3 and NF κ B on, the induction of the type I interferon response might be altered by both pathways.

In addition, we have shown that radiation-induced endothelial response includes upregulation of proteins such as STAT1, MX1 and ISG15 (Philipp et al. 2017), all of which are also involved in the endothelial antiviral response (Zhao et al. 2016). This is supported by the finding that 2.5 Gy X-ray irradiation leads to the upregulation of gene expression corresponding to those inflammatory proteins in HUVECs after 24 hours (Furusawa et al. 2016). This further suggests the induction of host defense against invading pathogens after irradiation.

In addition to the promotion of the antiviral proteins, we have observed a significant upregulation of HLA-B and -C proteins of the MHC-I class (Philipp et al. 2017; Philipp, Le Gleut, et al. 2020) and the analog H2-D1 in mouse (Philipp, Sievert, et al. 2020). All of these proteins are involved in the immune reaction as they are presenting peptides on the cell surface to immune cells and thereby regulate the immune response (Markus et al. 1988). As such they are upregulated by interferons and cytokines. Furthermore, in cooperation with integrin β 4 these proteins are involved in migration and proliferation (X. Zhang, Rozengurt, and Reed 2010). Our data suggest an active role of endothelial cells overexpressing these components in the radiation-induced immune response.

Our data also highlight a role of secretory proteins in the radiation-associated immune response. According to our data, proteins like the interleukins IL-6 and IL-8, ISG15 and MCP1 are increasingly secreted in a para- and endocrine manner (Meeren et al. 1997; Bevilacqua et al. 1985; Schröder et al. 2019; Philipp et al. 2017;

Philipp, Sievert, et al. 2020; Philipp, Le Gleut, et al. 2020). This displays a warning signal also similar to that after pathogen detection.

In parallel, the expression pattern of the type I interferon response suggests also a direct involvement of interferons in the signaling cascades (Costa-Pereira et al. 2002). However, we could not verify this due to their low abundance (Philipp et al. 2017). The immediate role of interferons is closely connected to spreading of the inflammatory signal, recruiting immune cells and warning associated cells. The increased expression of interferon signaling one and two weeks post-irradiation that we have observed after high radiation doses (X-ray, 10 Gy) is an indication of chronic inflammation. Similar permanent increase in the level of cell adhesion molecules has been shown after high dose irradiation in mice (Sievert et al. 2015). We and others also have shown that ICAM1 and other cell adhesion molecules are triggered by the cGAS/STING-pathway on one hand (Mao et al. 2017; Philipp, Sievert, et al. 2020; Philipp, Le Gleut, et al. 2020), and by interferons and interleukins on the other hand (Megger et al. 2017; Watson et al. 1996). Such a persistent inflammatory response may be actuated by either the cGAS/STING-pathway or interferons most probably both. Therefore, it is highly relevant to investigate the type I interferon response in long term clinical and cellular studies to further elucidate the role of the central players. This would enable a preventive anti-inflammatory treatment after radiation exposure targeting especially the vasculature since endothelial dysfunction is a major consequence of persistent inflammation. Additionally, the role of secreted proteins as investigated here (Philipp et al. 2017; Philipp, Sievert, et al. 2020; Philipp, Le Gleut, et al. 2020) has to be assessed in more detail. Proteomics is an excellent method of choice to investigate type I interferon response to irradiation for better understanding of the underlying and subsequent effects.

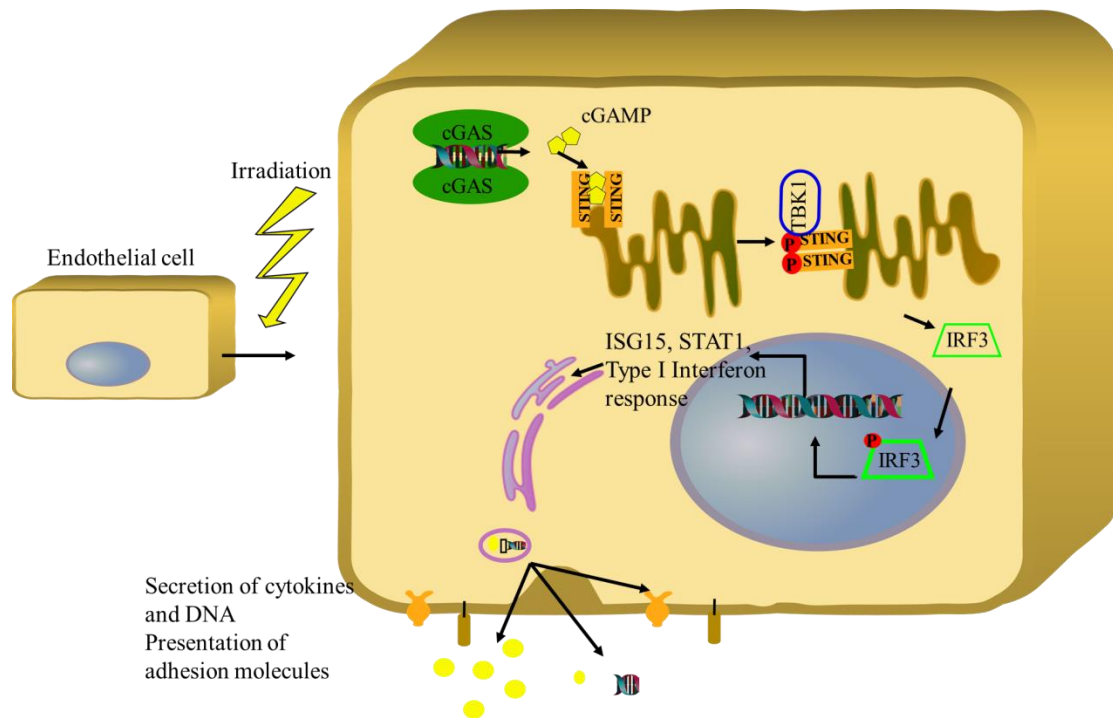


Figure 8: Response of endothelial cells on irradiation. Ionizing radiation induces DNA double strand breaks resulting in dsDNA fragments in the cytoplasm. The protein cGAS recognizes the dsDNA fragments initiating a cascade by producing cGAMP after dimerization. The protein STING is activated by cGAMP and gets phosphorylated by TBK1. The phosphorylated STING in turn leads to the phosphorylation of IRF3 that translocates to the nucleus and initiates transcription of type I interferon responsive genes. Some target proteins are secreted or presented on the cell surface.

4.2.3 Role of STAT1 and STAT3

Within the type I interferon response the STAT-proteins 1 and 3 play a pivotal role in inducing and maintaining the inflammatory state. These proteins are known to be induced by the JAK/STAT-pathway (Stark and Darnell 2012). So far, little is known about their role in the radiation response of endothelial cells but the studies conducted in this thesis highlight their importance. Clearly, STAT1 is upregulated by irradiation in our data (Philipp et al. 2017; Philipp, Le Gleut, et al. 2020) but the mechanism remains unclear. We suggest that induction by the JAK/STAT and the cGAS/STING-pathways could be responsible for this. On one hand, STING induces the production of type I interferon proteins by the TBK1-IRF3 cascade (Basit et al. 2020). Furthermore, dsDNA triggers the activation of JAK/STAT, and in particular STAT1 in human B-cell line (Dong, Guanjun et al. 2015), which also induces the type I interferon response. In turn, STAT1 is actively involved in the transcription of the

STING protein in wild type black 6 bone marrow derived macrophages (F. Ma et al. 2015) thereby, strengthening the response of the activated STING-TBK1-IRF3 axis. On the other hand the induced type I interferon response leads to the activation of the JAK/STAT-pathway activating STAT1 and downstream interferon responsive gene expression (Mogensen 2019). Anyhow, the induction of STAT1 seems not to be phosphorylation dependent and might function as a potential positive regulator of the type I interferon response. Upregulated non-phosphorylated STAT1 can act in a similar fashion to phosphorylated STAT1 (Cheon and Stark 2009), which dimerizes and translocates to the nucleus for transcriptional induction. Thus, STAT1 is able to positively regulate its own expression but also the type I interferon response.

STAT3 is able to act in a similar way (Sgrignani et al. 2015). However, STAT3 can also be activated by IL-6 (Y. Wang et al. 2013) since its permanent activation relies on the association of the IL-6 receptor with the epidermal growth factor receptor (Y. Wang et al. 2013). STAT3 expression can also be modulated by the p38/MAP kinase (Zauberman et al. 1999). We observed upregulation of both isomers of STAT3 (α , β) in the bystander cells of the first study (Philipp et al. 2017). In the irradiated donor cells only the α -isoform was upregulated, the β -isoform being downregulated. The β -isoform has been shown to be anti-inflammatory (Lee et al. 2013). Therefore, this could be an indication of chronic inflammation in the directly irradiated cells two weeks after the exposure that is not yet present in the bystander cells that were analyzed 24 hours after the exposure to the irradiated secretome. The β -isoform of STAT3 is a potential clinical target due to its anti-inflammatory character (Raddatz et al. 2020).

The STAT1 and STAT3 protein have the potential to amplify the type I interferon response towards a persistent inflammation. Obviously much more focus should be put on the STAT proteins in the future studies.

4.2.4 ISG15 a potential biomarker for radiation-induced inflammation?

One of the type I interferon responsive proteins is ISG15. It was found strongly upregulated by radiation in all three studies described here (Philipp et al. 2017; Philipp, Sievert, et al. 2020; Philipp, Le Gleut, et al. 2020). It is relevant for a

translational modification called ISGylation (Villarroya-Beltri, Guerra, and Sánchez-Madrid 2017) and was found to positively enhance the JAK/STAT-pathway (Malakhova 2003) as well as act in a cytokine-like manner (Bogunovic, Boisson-Dupuis, and Casanova 2013). In addition, it is able to bind to type I interferon proteins (Giannakopoulos et al. 2005) and enhance the production of inflammatory cytokines by the p38/MAPK pathway by preventing the protein degradation (Fan et al. 2015). On the contrary, some clinical evidence indicate the role of ISG15 as a negative regulator of type I interferon response (Xianqin Zhang et al. 2015). Furthermore, it is also involved in DNA damage response and high levels of ISG15, intrinsic or induced by interferon-beta, accelerate DNA replication fork progression, leading to ample DNA damage and chromosomal aberrations (Raso et al. 2020). In this way, ISG15 could contribute to the endothelial dysfunction by increasing genomic instability of endothelial cells. This is in accordance with the observation that ISG15 and also STAT1 contribute to increased resistance to radiation and chemotherapy in cancer cell lines (Weichselbaum et al. 2008). Furthermore, ISG15 could function as a potential biomarker for radiation-induced inflammation. We have shown here (Philipp et al. 2017) that especially irradiated endothelial cells might secrete large amounts after high radiation doses suggesting a role as a biomarker for particularly vascular inflammation.

4.3 Bystander effects in human endothelial coronary artery endothelial cells after irradiation

As mentioned before and as found by us, irradiated endothelial cells have a particular profile of secreted proteins (Bogunovic, Boisson-Dupuis, and Casanova 2013; Schröder et al. 2019; Philipp et al. 2017). These proteins can function in endocrine and paracrine manner in neighboring cells but also in cells that are located further away. Our proteomic analysis of the secreted proteins verified the release of IL-6 and other cytokines into the supernatant in human coronary artery endothelial cells two weeks after high dose irradiation (X-ray, 10 Gy). The supernatant when applied to non-irradiated cells was able to induce a bystander effect resembling that seen in directly irradiated cells (Philipp et al. 2017). It has been shown on the surface of the endothelial cell IL-6 and other cytokines can bind to receptors triggering the

p38/MAPK-pathway finally activating STAT3 (Zauberman et al. 1999). Other studies investigated cell-cell contacts and could observe an induction of the p38/MAPK-pathway in endothelial cells by irradiated macrophages (Xiao et al. 2014). However, most of the bystander effects are mediated *via* gap junctions in a paracrine manner. In this manner, NO, ROS and other chemical substances (Ramadan et al. 2020; Feine et al. 2012) but also cGAMP, the second messenger between cGAS and STING, can be transferred through these channels connecting endothelial cells (Ablasser et al. 2013). This transport mechanism enables communication and due to its passive and fast nature, the signals can spread rapidly across the whole vessel. This enables control of vasoconstriction and vasodilation but also leads to spreading of radiation-induced damage in the bystander cells.

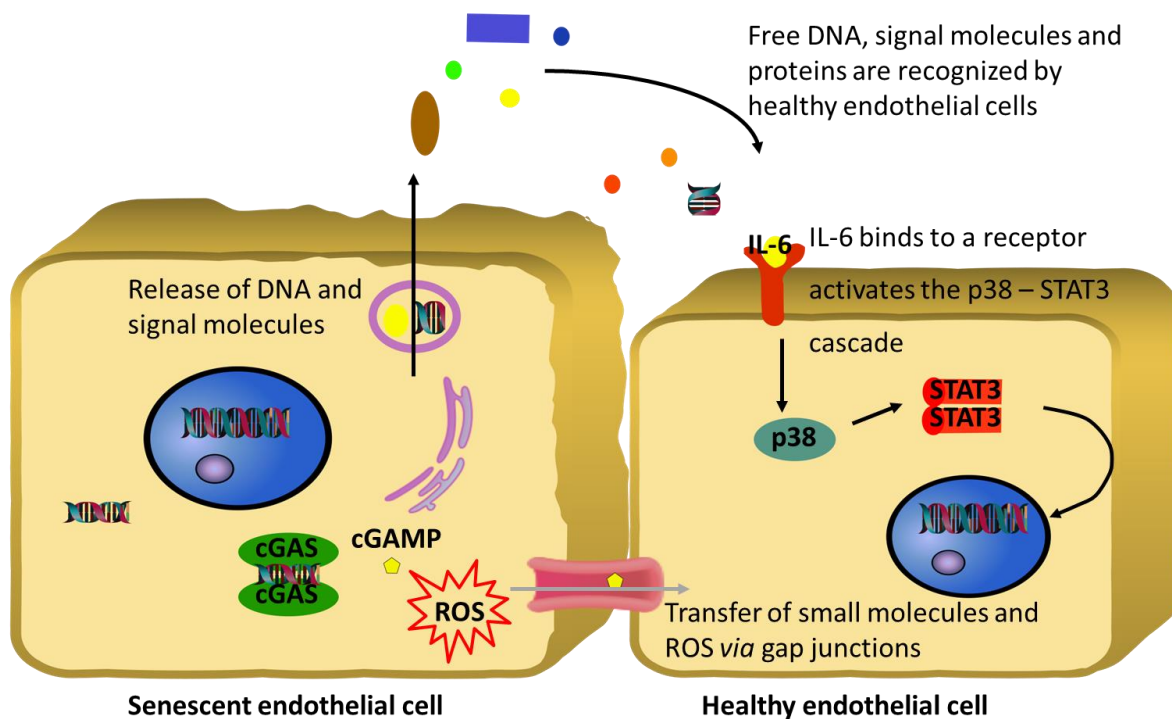


Figure 9: A damaged endothelial cell in a senescent state as a consequence of irradiation. After initiation of apoptosis the cell produces great amounts of signaling molecules such as IL-6 and DNA fragments that become released. IL-6 is then recognized by a receptor on an intact endothelial cell inducing a signaling cascade of p38/STAT3. STAT3 is translocated to the nucleus to initiate a type I interferon response. Furthermore, second messengers as cGAMP and ROS might influence directly neighboring endothelial cells by gap junction-mediated transport.

4.4 Irradiation induces senescence by chronic inflammation

Radiation-induced inflammation can lead to senescence if the inflammation persists. The senescent state of a cell is characterized by secretory proteins (SASP) that we analyzed using proteomics in the first study (Lasry and Ben-Neriah 2015; Philipp et al. 2017). Furthermore, senescent endothelial cells present surface markers after irradiation like CD44 (Lowe and Raj 2014) and adhesion molecules such as ICAM1 (Sievert et al. 2015). Chronic inflammatory response causes premature senescence even after low doses and dose rates (Baselet et al. 2017; Yentrapalli, Azimzadeh, Barjaktarovic, et al. 2013) but also high doses (Lowe and Raj 2014; Philipp et al. 2017) strongly suggesting that irradiation is able to trigger premature senescence in endothelial cells. We found in the first study elevated levels of senescence markers showing cell cycle arrest such as p16 and p21 in irradiated endothelial cells (Philipp et al. 2017) but not in the bystander cells 24 hours after exposing them to the SASP from irradiated cells. This suggests that no immediate cell cycle arrest is induced in the bystander cells by the transferred media. However, the activation of the IL-6/STAT3-pathway that we also observe in the bystander cells (Philipp et al. 2017) has previously been shown to be a senescence trigger (Kojima et al. 2013) suggesting that the SASP released by irradiated endothelial cells can also induce senescence in healthy non-irradiated bystander cells. The reason why we could not observe this in the first study was probably the relatively short time frame (24 hours) that we used for the read out.

The elevation of p16 and p21 is followed by β -galactosidase activity, a biomarker of senescence, in irradiated cells (Yentrapalli, Azimzadeh, Barjaktarovic, et al. 2013; Yentrapalli, Azimzadeh, Sriharshan, et al. 2013; Dimri et al. 1995).

When senescent cells underwent apoptosis, increasing levels of free DNA were measured (Rostami et al. 2020). The consequence of radiation-induced senescence is endothelial dysfunction (Azimzadeh et al. 2015), that is causally associated with many CVD-related diseases. Proteomics and other “omics” methods are powerful tools to study endothelial senescence in detail (Yentrapalli et al. 2015).

4.5 Oxidative stress after irradiation

In the second study (Philipp, Sievert, et al. 2020) the expression of oxidative stress proteins was investigated. These proteins are necessary to dismantle ROS (Fig. 2). SOD1 and PRDX5 were downregulated one week after irradiation (X-ray, 10 Gy) (Philipp, Sievert, et al. 2020). SOD1 downregulation was also found in another study using the same mouse strain (C57BL/6J) but a higher radiation dose on the whole lung of 12 Gy (X-ray). In contrast, C3H/ HeJ mice, which are more resistant to lung fibrosis showed the opposite regulation of SOD1 (Ao et al. 2008) suggesting that expression of oxidative stress proteins is tissue- and strain-dependent. The reason for the downregulation might be depletion due to high ROS levels after irradiation. After two weeks we observed no deregulation of these proteins in a human endothelial cell line (Philipp et al. 2017). Posttranslational mechanisms such as acetylation have been shown to regulate SOD1 activity (Banks et al. 2017).

The function of oxidative stress proteins is not only to neutralize ROS but also to activate receptors (Mondola et al. 2016) and binding to other proteins (Skoko, Attaran, and Neumann 2019). Non-active isoforms of PRDX5 which lack the catalytic center still contain peptide structures that bind specifically to receptors of the HLA class I family (Sensi et al. 2009). This suggests that these splicing variants might be autocrine promoters of an inflammatory response. Furthermore, SOD1 deficiency has been shown to lead to hyperoxidized inactive peroxiredoxins 2 and 3 (Homma et al. 2015). These additional functions of the oxidative stress proteins might become relevant with increasing ROS levels as observed after high-dose radiation (J. Ma, Wang, and Mostafavi 2018; Wardman 2009). Therefore, it is necessary to investigate oxidation effects and their regulation after irradiation.

4.6 Low dose effects on endothelial cells

There are some data showing that low doses (< 0.5 Gy) may have an anti-inflammatory effect *in vitro* (Hildebrandt et al. 2002; Roedel et al. 2002) and *in vivo* (Hildebrandt, J. Jahns, M. Hindemith 2000; Schaeue et al. 2005) (all X-ray). Nevertheless, it is very difficult to study these effects *in vitro* as culture conditions modify the measured effect (Schröder et al. 2018). The anti-inflammatory effect of

low dose irradiation has been shown previously mainly in endothelial cells that are stimulated to an inflammatory state using TNF- α (Rödel et al. 2004). However, it was shown recently that the enhanced expression of pro-inflammatory marker proteins occurred even in non-stimulated endothelial cells in a time-dependent manner (30 min up to 48 hours) after low-dose irradiation (X-ray, 0.05 Gy to 0.5 Gy) but the stimulation of the cells with TNF- α enhanced the release considerably for all tested proteins (IL-8, G-CSF, PDGF-BB) (Baselet et al. 2017). We found in our third study (Philipp, Le Gleut, et al. 2020) using non-stimulated endothelial cells no anti-inflammatory effects of low radiation doses. On the other hand, we did not find inflammatory effects either at these doses (γ , 0.25 and 0.5 Gy). In contrast, Baselet et al. used the same cells and found a slight increase in the expression of IL-6 and CCL2 (Baselet et al. 2017). However, these proteins are too low abundant to be seen with proteomics (Philipp, Le Gleut, et al. 2020). In addition, Baselet et al. found an increase in senescence associated β -galactosidase activity two weeks after 0.05 Gy and a decrease in inflammatory protein expression (IL-6, CCL2). An increase of the anti-inflammatory IL-10 has been found in a long term study on BALB/cJ mice (Jangiam et al. 2018). In this study, IL-10 was increased in the bone marrow at the dose of 0.05 Gy γ -irradiation but not at a dose of 0.1 Gy after six months.

Long term studies performed in the cohort of atomic bomb survivors in Japan show linearly increasing risk for CVD even at 0.1 Gy (Jordan 2016) suggesting no anti-inflammatory effects in the case of whole body irradiation at this dose range. However, the lower the dose the more difficult it is to show a statistically significant effect, which becomes even more relevant if only certain areas of the body are irradiated.

Some data suggest that the dose rate seems to be more relevant for anti-inflammatory impact than the dose alone, particularly in endothelial cells. In an *in vitro* study a lower dose rate (γ , 6 mGy/h vs 1 Gy/min) was associated with an increased expression of anti-inflammatory and antioxidant genes in human aorta endothelial cells (Vieira Dias et al. 2018). This was supported by findings in an ApoE $-/-$ mouse model (Ebrahimian et al. 2018). In this study, the mice were exposed to very low dose rates similar to those in the contaminated areas of Fukushima and Chernobyl. Antioxidant and anti-inflammatory effects were found in

the irradiated mice but not in the control group after eight months (γ , 28 $\mu\text{Gy/h}$). In addition, the irradiated mice had decreased atherosclerotic plaque size compared to the non-irradiated controls. Taken together, these data highlight the necessity of further studies using low doses and dose rates. In addition, such studies need a large number of animals in order to estimate the effects of low-dose radiation in a statistically significant manner.

4.7 How DNA damage, senescence and inflammation come together

Our studies have clearly suggested a link between DNA damage, inflammation and senescence in endothelial cells. Direct or indirect radiation-induced DNA damage produces fragments of dsDNA of nuclear and mitochondrial origin that may leak into the cytoplasm. These fragments are recognized by the cGAS/STING-pathway leading to an induction of the innate immune and type I interferon response (Philipp, Sievert, et al. 2020; Philipp, Le Gleut, et al. 2020). This response might include positive feedback loops within the immune response as well as SASP associated proteins, which are released to the surrounding (Lasry and Ben-Neriah 2015; Philipp et al. 2017). The activation of the cGAS/STING-pathway and the induction of the type I interferon response as a consequence of irradiation indicate a falsely activated host defense reaction. The irradiated cell triggers also the production of warning signals that are received by non-affected bystander cells by secreting proteins like interleukins but also ISG15 (Philipp et al. 2017). This results in a large-area impact in the tissue. Within the affected tissue, a part of the irradiated endothelial cell population undergoes premature senescence, release SASP and become dysfunctional. Cells that undergo apoptosis, release DNA fragments into the surrounding media that further induce the innate immune and type I interferon response in a vicious circle (Rostami et al. 2020) finally producing a chronic inflammation. The inflammatory state is possibly maintained by the STAT-proteins that successively induce type I interferon response in a positive feedback loop (Cheon and Stark 2009).

All in all, chronic inflammatory state is a risk factor for CVD and cancer. Hence, it is of great importance to further investigate radiation-induced inflammatory response and search for potential preventive and treatment options. Inhibiting the spreading of

the pro-inflammatory signals to the surrounding tissue might be the most promising and most challenging goal.

Bibliography

- Ablasser, Andrea, Jonathan L. Schmid-Burgk, Inga Hemmerling, Gabor L. Horvath, Tobias Schmidt, Eicke Latz, and Veit Hornung. 2013. "Cell Intrinsic Immunity Spreads to Bystander Cells via the Intercellular Transfer of CGAMP." *Nature* 503 (7477): 530–34. <https://doi.org/10.1038/nature12640>.
- Ades, Edwin W, Francisco J Candal, Robert A Swerlick, Velma G George, Susan. Summers, Diane C Bosse, and Thomas J Lawley. 1992. "HMEC-1: Establishment of an Immortalized Human Microvascular Endothelial Cell Line." *Journal of Investigative Dermatology* 99 (6): 683–90. <https://doi.org/10.1111/1523-1747.ep12613748>.
- Ahn, J., D. Gutman, S. Saijo, and G. N. Barber. 2012. "STING Manifests Self DNA-Dependent Inflammatory Disease." *Proceedings of the National Academy of Sciences* 109 (47): 19386–91. <https://doi.org/10.1073/pnas.1215006109>.
- Aird, William C. 2007. "Phenotypic Heterogeneity of the Endothelium: I. Structure, Function, and Mechanisms." *Circulation Research* 100 (2): 158–73. <https://doi.org/10.1161/01.RES.0000255691.76142.4a>.
- Andersen, Jens S., Birte Svensson, and Peter Roepstorff. 1996. "Electrospray Ionization and Matrix Assisted Laser Desorption/Ionization Mass Spectrometry: Powerful Analytical Tools in Recombinant Protein Chemistry." *Nature Biotechnology* 14 (4): 449–57. <https://doi.org/10.1038/nbt0496-449>.
- Ao, Xiaoping, David M. Lubman, Mary A. Davis, Xianying Xing, Feng-Ming Kong, Theodore S. Lawrence, and Ming Zhang. 2008. "Comparative Proteomic Analysis of Radiation-Induced Changes in Mouse Lung: Fibrosis-Sensitive and -Resistant Strains." *Radiation Research* 169 (4): 417–25. <https://doi.org/10.1667/RR1173.1>.
- Atkins, Peter. 2010. *Physical Chemistry*. 9th ed. Oxford: Oxford University Press.
- Azimzadeh, Omid, Tamara Azizova, Juliane Merl-Pham, Vikram Subramanian, Mayur V. Bakshi, Maria Moseeva, Olga Zubkova, et al. 2017. "A Dose-Dependent Perturbation in Cardiac Energy Metabolism Is Linked to Radiation-Induced Ischemic Heart Disease in Mayak Nuclear Workers." *Oncotarget* 8 (6): 9067–78. <https://doi.org/10.18632/oncotarget.10424>.
- Azimzadeh, Omid, Wolfgang Sievert, Hakan Sarioglu, Juliane Merl-Pham, Ramesh Yentrapalli, Mayur V. Bakshi, Dirk Janik, et al. 2015. "Integrative Proteomics and Targeted Transcriptomics Analyses in Cardiac Endothelial Cells Unravel Mechanisms of Long-Term Radiation-Induced Vascular Dysfunction." *Journal of Proteome Research* 14 (2): 1203–19. <https://doi.org/10.1021/pr501141b>.
- Azizova, T. V., E. Batistatou, E. S. Grigorieva, R. McNamee, R. Wakeford, H. Liu, F. de Vocht, and R. M. Agius. 2018. "An Assessment of Radiation-Associated Risks of Mortality from Circulatory Disease in the Cohorts of Mayak and Sellafield Nuclear Workers." *Radiation Research* 189 (4): 371. <https://doi.org/10.1667/RR14468.1>.
- Azizova, Tamara, Ksenia Briks, Maria Bannikova, and Evgeniya Grigoryeva. 2019. "Hypertension Incidence Risk in a Cohort of Russian Workers Exposed to Radiation at the Mayak Production

- Association Over Prolonged Periods." *Hypertension* 73 (6): 1174–84.
<https://doi.org/10.1161/HYPERTENSIONAHA.118.11719>.
- Azizova, Tamara V., Maria V. Bannikova, Evgeniya S. Grigorieva, Yaroslava P. Bagaeva, and Elena V. Azizova. 2016. "Risk of Lower Extremity Arterial Disease in a Cohort of Workers Occupationally Exposed to Ionizing Radiation over a Prolonged Period." *Radiation and Environmental Biophysics* 55 (2): 147–59. <https://doi.org/10.1007/s00411-016-0645-6>.
- Azizova, Tamara V, Evgeniya S Grigoryeva, Richard G E Haylock, Maria V Pikulina, and Maria B Moseeva. 2015. "Ischaemic Heart Disease Incidence and Mortality in an Extended Cohort of Mayak Workers First Employed in 1948–1982." *The British Journal of Radiology* 88 (1054): 20150169. <https://doi.org/10.1259/bjr.20150169>.
- Aznar, Marianne C., Frances K. Duane, Sarah C. Darby, Zhe Wang, and Carolyn W. Taylor. 2018. "Exposure of the Lungs in Breast Cancer Radiotherapy: A Systematic Review of Lung Doses Published 2010–2015." *Radiotherapy and Oncology* 126 (1): 148–54.
<https://doi.org/10.1016/j.radonc.2017.11.022>.
- Baker, John E., John E. Moulder, and John W. Hopewell. 2011. "Radiation as a Risk Factor for Cardiovascular Disease." *Antioxidants & Redox Signaling* 15 (7): 1945–56.
<https://doi.org/10.1089/ars.2010.3742>.
- Banks, Courtney J., Nathan W. Rodriguez, Kyle R. Gashler, Rushika R. Pandya, Jeffrey B. Mortenson, Matthew D. Whited, Erik J. Soderblom, et al. 2017. "Acylation of Superoxide Dismutase 1 (SOD1) at K122 Governs SOD1-Mediated Inhibition of Mitochondrial Respiration." *Molecular and Cellular Biology* 37 (20): e00354-17, /mcb/37/20/e00354-17.atom. <https://doi.org/10.1128/MCB.00354-17>.
- Bar-Ad, Voichita, Emily Hubley, Adam Luginbuhl, David Cognetti, Joseph Curry, Amy S Harrison, Jennifer M Johnson, et al. 2019. "Single Institution Implementation of Permanent 131Cs Interstitial Brachytherapy for Previously Irradiated Patients with Resectable Recurrent Head and Neck Carcinoma." *Journal of Contemporary Brachytherapy* 11 (3): 227–34.
<https://doi.org/10.5114/jcb.2019.85778>.
- Barjaktarovic, Zarko, Dominik Schmaltz, Alena Shyla, Omid Azimzadeh, Sabine Schulz, Julia Haagen, Wolfgang Dörr, et al. 2011. "Radiation-Induced Signaling Results in Mitochondrial Impairment in Mouse Heart at 4 Weeks after Exposure to X-Rays." Edited by Marianne Koritzinsky. *PLoS ONE* 6 (12): e27811. <https://doi.org/10.1371/journal.pone.0027811>.
- Baselet, Bjorn, Niels Belmans, Emma Coninx, Donna Lowe, Ann Janssen, Arlette Michaux, Kevin Tabury, et al. 2017. "Functional Gene Analysis Reveals Cell Cycle Changes and Inflammation in Endothelial Cells Irradiated with a Single X-Ray Dose." *Frontiers in Pharmacology* 8 (April): 213. <https://doi.org/10.3389/fphar.2017.00213>.
- Baselet, Bjorn, Pierre Sonveaux, Sarah Baatout, and An Aerts. 2019. "Pathological Effects of Ionizing Radiation: Endothelial Activation and Dysfunction." *Cellular and Molecular Life Sciences* 76 (4): 699–728. <https://doi.org/10.1007/s00018-018-2956-z>.
- Basit, Abdul, Min-Guk Cho, Eui-Yun Kim, Dohyeong Kwon, Suk-Jo Kang, and Jae-Ho Lee. 2020. "The CGAS/STING/TBK1/IRF3 Innate Immunity Pathway Maintains Chromosomal Stability

- through Regulation of P21 Levels.” *Experimental & Molecular Medicine*, April.
<https://doi.org/10.1038/s12276-020-0416-y>.
- Beckman, Joshua A, Avni Thakore, Barbara H Kalinowski, Jay R Harris, and Mark A Creager. 2001. “Radiation Therapy Impairs Endothelium-Dependent Vasodilation in Humans.” *Journal of the American College of Cardiology* 37 (3): 761–65. [https://doi.org/10.1016/S0735-1097\(00\)01190-6](https://doi.org/10.1016/S0735-1097(00)01190-6).
- Belgnaoui, S Mehdi, Suzanne Paz, and John Hiscott. 2011. “Orchestrating the Interferon Antiviral Response through the Mitochondrial Antiviral Signaling (MAVS) Adapter.” *Current Opinion in Immunology* 23 (5): 564–72. <https://doi.org/10.1016/j.coi.2011.08.001>.
- Bevilacqua, M P, J S Pober, M E Wheeler, R S Cotran, and M A Gimbrone. 1985. “Interleukin 1 Acts on Cultured Human Vascular Endothelium to Increase the Adhesion of Polymorphonuclear Leukocytes, Monocytes, and Related Leukocyte Cell Lines.” *Journal of Clinical Investigation* 76 (5): 2003–11. <https://doi.org/10.1172/JCI112200>.
- Boaventura, Paula, Cecília Durães, Adélia Mendes, Natália Rios Costa, Inês Chora, Sara Ferreira, Emanuel Araújo, et al. 2018. “Is Low-Dose Radiation Exposure a Risk Factor for Atherosclerotic Disease?” *Radiation Research* 189 (4): 418–24.
<https://doi.org/10.1667/RR14942.1>.
- Bogunovic, Dusan, Stéphanie Boisson-Dupuis, and Jean-Laurent Casanova. 2013. “ISG15: Leading a Double Life as a Secreted Molecule.” *Experimental & Molecular Medicine* 45 (4): e18–e18.
<https://doi.org/10.1038/emm.2013.36>.
- Bondarenko, Pavel V., Dirk Chelius, and Thomas A. Shaler. 2002. “Identification and Relative Quantitation of Protein Mixtures by Enzymatic Digestion Followed by Capillary Reversed-Phase Liquid Chromatography–Tandem Mass Spectrometry.” *Analytical Chemistry* 74 (18): 4741–49. <https://doi.org/10.1021/ac0256991>.
- Bruderer, Roland, Oliver M. Bernhardt, Tejas Gandhi, Saša M. Miladinović, Lin-Yang Cheng, Simon Messner, Tobias Ehrenberger, et al. 2015. “Extending the Limits of Quantitative Proteome Profiling with Data-Independent Acquisition and Application to Acetaminophen-Treated Three-Dimensional Liver Microtissues.” *Molecular & Cellular Proteomics* 14 (5): 1400–1410.
<https://doi.org/10.1074/mcp.M114.044305>.
- BUND, Landesverband Rheinland-Pfalz. 2020. “Lebenszyklus und Generationenfolge des Schwalbenschwanzes im Jahresverlauf.” <https://www.bund-rlp.de/themen/tiere-pflanzen/schmetterlinge/besondere-schmetterlinge/schwalbenschwanz/>. June 10, 2020.
- Carnicer, A., M. Sans-Merce, S. Baechler, I. Barth, L. Donadille, P. Ferrari, M. Fulop, et al. 2011. “Hand Exposure in Diagnostic Nuclear Medicine with 18F- and 99mTc-Labelled Radiopharmaceuticals - Results of the ORAMED Project.” *Radiation Measurements* 46 (11): 1277–82. <https://doi.org/10.1016/j.radmeas.2011.07.019>.
- Cervelli, Tiziana, Daniele Panetta, Teresa Navarra, Maria Grazia Andreassi, Giuseppina Basta, Alvaro Galli, Piero A. Salvadori, Eugenio Picano, and Serena Del Turco. 2014. “Effects of

- Single and Fractionated Low-Dose Irradiation on Vascular Endothelial Cells." *Atherosclerosis* 235 (2): 510–18. <https://doi.org/10.1016/j.atherosclerosis.2014.05.932>.
- Chance, B, H Sies, and A Boveris. 1979. "Hydroperoxide Metabolism in Mammalian Organs." *Physiological Reviews* 59 (3): 527–605. <https://doi.org/10.1152/physrev.1979.59.3.527>.
- Chen, Zhongjie, Zhiqiang Wu, and Wen Ning. 2019. "Advances in Molecular Mechanisms and Treatment of Radiation-Induced Pulmonary Fibrosis." *Translational Oncology* 12 (1): 162–69. <https://doi.org/10.1016/j.tranon.2018.09.009>.
- Cheon, H., and G. R. Stark. 2009. "Unphosphorylated STAT1 Prolongs the Expression of Interferon-Induced Immune Regulatory Genes." *Proceedings of the National Academy of Sciences* 106 (23): 9373–78. <https://doi.org/10.1073/pnas.0903487106>.
- Costa-Pereira, A. P., S. Tininini, B. Strobl, T. Alonzi, J. F. Schlaak, H. Is'harc, I. Gesualdo, S. J. Newman, I. M. Kerr, and V. Poli. 2002. "Mutational Switch of an IL-6 Response to an Interferon- like Response." *Proceedings of the National Academy of Sciences* 99 (12): 8043–47. <https://doi.org/10.1073/pnas.122236099>.
- Darby, Sarah C., Marianne Ewertz, Paul McGale, Anna M. Bennet, Ulla Blom-Goldman, Dorthe Brønnum, Candace Correa, et al. 2013. "Risk of Ischemic Heart Disease in Women after Radiotherapy for Breast Cancer." *New England Journal of Medicine* 368 (11): 987–98. <https://doi.org/10.1056/NEJMoa1209825>.
- Dimri, G. P., X. Lee, G. Basile, M. Acosta, G. Scott, C. Roskelley, E. E. Medrano, M. Linskens, I. Rubelj, and O. Pereira-Smith. 1995. "A Biomarker That Identifies Senescent Human Cells in Culture and in Aging Skin in Vivo." *Proceedings of the National Academy of Sciences* 92 (20): 9363–67. <https://doi.org/10.1073/pnas.92.20.9363>.
- Dong, Guanjun, You, Ming, Ding, Liang, Fan, Hongye, Liu, Fei, Ren, Deshan, and Hou, Yayi. 2015. "STING Negatively Regulates Double-Stranded DNA-Activated JAK1-STAT1 Signaling via SHP-1/2 in B Cells." *Molecules and Cells* 38 (5): 441–51. <https://doi.org/10.14348/MOLCELLS.2015.2359>.
- Dou, Zhixun, Kanad Ghosh, Maria Grazia Vizioli, Jiajun Zhu, Payel Sen, Kirk J. Wangenstein, Johayra Simithy, et al. 2017. "Cytoplasmic Chromatin Triggers Inflammation in Senescence and Cancer." *Nature* 550 (7676): 402–6. <https://doi.org/10.1038/nature24050>.
- Du, Shisuo, Genwen Chen, Baoying Yuan, Yong Hu, Ping Yang, Yixing Chen, Qianqian Zhao, Jian Zhou, Jia Fan, and Zhaochong Zeng. 2020. "DNA Sensing and Associated Type 1 Interferon Signaling Contributes to Progression of Radiation-Induced Liver Injury." *Cellular & Molecular Immunology*, March. <https://doi.org/10.1038/s41423-020-0395-x>.
- Early Breast Cancer Trialists' Collaborative Group (EBCTCG). 2005. "Effects of Radiotherapy and of Differences in the Extent of Surgery for Early Breast Cancer on Local Recurrence and 15-Year Survival: An Overview of the Randomised Trials." *The Lancet* 366 (9503): 2087–2106. [https://doi.org/10.1016/S0140-6736\(05\)67887-7](https://doi.org/10.1016/S0140-6736(05)67887-7).
- Ebrahimian, T. G., L. Beugnie, J. Surette, N. Priest, Y. Gueguen, C. Gloaguen, M. Benderitter, J. R. Jourdain, and K. Tack. 2018. "Chronic Exposure to External Low-Dose Gamma Radiation Induces an Increase in Anti-Inflammatory and Anti-Oxidative Parameters Resulting in

- Atherosclerotic Plaque Size Reduction in ApoE^{-/-} Mice." *Radiation Research* 189 (2): 187–96. <https://doi.org/10.1667/RR14823.1>.
- Edgell, C. J., C. C. McDonald, and J. B. Graham. 1983. "Permanent Cell Line Expressing Human Factor VIII-Related Antigen Established by Hybridization." *Proceedings of the National Academy of Sciences* 80 (12): 3734–37. <https://doi.org/10.1073/pnas.80.12.3734>.
- Egawa, Gyohei, Satoshi Nakamizo, Yohei Natsuaki, Hiromi Doi, Yoshiki Miyachi, and Kenji Kabashima. 2013. "Intravital Analysis of Vascular Permeability in Mice Using Two-Photon Microscopy." *Scientific Reports* 3 (1): 1932. <https://doi.org/10.1038/srep01932>.
- Endemann, D. H. 2004. "Endothelial Dysfunction." *Journal of the American Society of Nephrology* 15 (8): 1983–92. <https://doi.org/10.1097/01.ASN.0000132474.50966.DA>.
- Escher, Claudia, Lukas Reiter, Brendan MacLean, Reto Ossola, Franz Herzog, John Chilton, Michael J. MacCoss, and Oliver Rinner. 2012. "Using IRT, a Normalized Retention Time for More Targeted Measurement of Peptides." *PROTEOMICS* 12 (8): 1111–21. <https://doi.org/10.1002/pmic.201100463>.
- Fajardo, L. F., J. R. Stewart, and K. E. Cohn. 1968. "Morphology of Radiation-Induced Heart Disease." *Archives of Pathology* 86 (5): 512–19.
- Fan, Jun-Bao, Sayuri Miyauchi-Ishida, Kei-ichiro Arimoto, Dan Liu, Ming Yan, Chang-Wei Liu, Balázs Györfy, and Dong-Er Zhang. 2015. "Type I IFN Induces Protein ISGylation to Enhance Cytokine Expression and Augments Colonic Inflammation." *Proceedings of the National Academy of Sciences* 112 (46): 14313–18. <https://doi.org/10.1073/pnas.1505690112>.
- Feine, Ilan, Iddo Pinkas, Yoram Salomon, and Avigdor Scherz. 2012. "Local Oxidative Stress Expansion through Endothelial Cells – A Key Role for Gap Junction Intercellular Communication." Edited by Masuko Ushio-Fukai. *PLoS ONE* 7 (7): e41633. <https://doi.org/10.1371/journal.pone.0041633>.
- Feng, Xu, Anthony Tubbs, Chunchao Zhang, Mengfan Tang, Sriram Sridharan, Chao Wang, Dadi Jiang, et al. 2020. "ATR Inhibition Potentiates Ionizing Radiation-induced Interferon Response via Cytosolic Nucleic Acid-sensing Pathways." *The EMBO Journal* 39 (14). <https://doi.org/10.15252/embj.2019104036>.
- Florey. 1966. "The Endothelial Cell." *BMJ* 2 (5512): 487–90. <https://doi.org/10.1136/bmj.2.5512.487>.
- Friedrich Lottspeich, and Joachim W. Engels. 2006. *Bioanalytik*. 2. Munich: Spektrum Akademischer Verlag.
- Fulton, R. J., R. L. McDade, P. L. Smith, L. J. Kienker, and J. R. Kettman. 1997. "Advanced Multiplexed Analysis with the FlowMetrix System." *Clinical Chemistry* 43 (9): 1749–56.
- Furchgott, Robert F., and John V. Zawadzki. 1980. "The Obligatory Role of Endothelial Cells in the Relaxation of Arterial Smooth Muscle by Acetylcholine." *Nature* 288 (5789): 373–76. <https://doi.org/10.1038/288373a0>.
- Furusawa, Yukihiro, Qing-Li Zhao, Yuichi Hattori, Yoshiaki Tabuchi, Toshiyasu Iwasaki, Takaharu Nomura, and Takashi Kondo. 2016. "Comprehensive and Computational Analysis of Genes in Human Umbilical Vein Endothelial Cells Responsive to X-Irradiation." *Genomics Data* 8 (June): 126–30. <https://doi.org/10.1016/j.gdata.2016.05.007>.

- Gaugler, Marie-Hélène, Michel Neunlist, Stéphanie Bonnaud, Philippe Aubert, Marc Benderitter, and François Paris. 2007. "Intestinal Epithelial Cell Dysfunction Is Mediated by an Endothelial-Specific Radiation-Induced Bystander Effect." *Radiation Research* 167 (2): 185–93. <https://doi.org/10.1667/RR0702.1>.
- Gerhardt, Teresa, and Klaus Ley. 2015. "Monocyte Trafficking across the Vessel Wall." *Cardiovascular Research* 107 (3): 321–30. <https://doi.org/10.1093/cvr/cvv147>.
- Ghitescu, L., Z. Galis, M. Simionescu, and N. Simionescu. 1988. "Differentiated Uptake and Transcytosis of Albumin in Successive Vascular Segments." *Journal of Submicroscopic Cytology and Pathology* 20 (4): 657–69.
- Giannakopoulos, Nadia V., Jiann-Kae Luo, Vladimir Papov, Weiguo Zou, Deborah J. Lenschow, Barbara S. Jacobs, Ernest C. Borden, Jun Li, Herbert W. Virgin, and Dong-Er Zhang. 2005. "Proteomic Identification of Proteins Conjugated to ISG15 in Mouse and Human Cells." *Biochemical and Biophysical Research Communications* 336 (2): 496–506. <https://doi.org/10.1016/j.bbrc.2005.08.132>.
- Goertz, O., C. Poettgen, A. Akbari, J. Kolbenschlag, S. Langer, M. Lehnhardt, M. Stuschke, and L. von der Lohe. 2015. "New Model for Long-Term Investigations of Cutaneous Microcirculatory and Inflammatory Changes Following Irradiation." *Journal of Radiation Research* 56 (3): 456–61. <https://doi.org/10.1093/jrr/rru124>.
- Grosche, Antje, Alexandra Hauser, Marlen Franziska Lepper, Rebecca Mayo, Christine von Toerne, Juliane Merl-Pham, and Stefanie M. Hauck. 2016. "The Proteome of Native Adult Müller Glial Cells From Murine Retina." *Molecular & Cellular Proteomics* 15 (2): 462–80. <https://doi.org/10.1074/mcp.M115.052183>.
- Groschner, Lukas N., Markus Waldeck-Weiermair, Roland Malli, and Wolfgang F. Graier. 2012. "Endothelial Mitochondria—Less Respiration, More Integration." *Pflügers Archiv - European Journal of Physiology* 464 (1): 63–76. <https://doi.org/10.1007/s00424-012-1085-z>.
- Guipaud, Olivier, Cyprien Jaillet, Karen Clément-Colmou, Agnès François, Stéphane Supiot, and Fabien Milliat. 2018. "The Importance of the Vascular Endothelial Barrier in the Immune-Inflammatory Response Induced by Radiotherapy." *The British Journal of Radiology*, April, 20170762. <https://doi.org/10.1259/bjr.20170762>.
- Haimovitz-Friedman, A, C C Kan, D Ehleiter, R S Persaud, M McLoughlin, Z Fuks, and R N Kolesnick. 1994. "Ionizing Radiation Acts on Cellular Membranes to Generate Ceramide and Initiate Apoptosis." *The Journal of Experimental Medicine* 180 (2): 525–35. <https://doi.org/10.1084/jem.180.2.525>.
- Halcox, Julian P.J. 2012. "Endothelial Dysfunction." In *Primer on the Autonomic Nervous System*, 319–24. Elsevier. <https://doi.org/10.1016/B978-0-12-386525-0.00066-4>.
- Hallahan, D., J. Kuchibhotla, and C. Wyble. 1996. "Cell Adhesion Molecules Mediate Radiation-Induced Leukocyte Adhesion to the Vascular Endothelium." *Cancer Research* 56 (22): 5150–55.
- Hamada, Nobuyuki, Ki-ichiro Kawano, Farina Mohamad Yusoff, Kyoji Furukawa, Ayumu Nakashima, Makoto Maeda, Hiroshi Yasuda, Tatsuya Maruhashi, and Yukihito Higashi. 2020. "Ionizing

- Irradiation Induces Vascular Damage in the Aorta of Wild-Type Mice." *Cancers* 12 (10): 3030. <https://doi.org/10.3390/cancers12103030>.
- Han, Xiang- Bei, Yan Tan, Yan- Qiu Fang, and Feng Li. 2018. "Protective Effects of Celastrol against γ Irradiation- induced Oxidative Stress in Human Umbilical Vein Endothelial Cells." *Experimental and Therapeutic Medicine*, June. <https://doi.org/10.3892/etm.2018.6270>.
- Havaki, Sophia, Athanassios Kotsinas, Efsthios Chronopoulos, Dimitris Kletsas, Alexandros Georgakilas, and Vassilis G. Gorgoulis. 2015. "The Role of Oxidative DNA Damage in Radiation Induced Bystander Effect." *Cancer Letters* 356 (1): 43–51. <https://doi.org/10.1016/j.canlet.2014.01.023>.
- Hawkins, E, and R Cumming. 1990. "Enhanced Chemiluminescence for Tissue Antigen and Cellular Viral DNA Detection." *Journal of Histochemistry & Cytochemistry* 38 (3): 415–19. <https://doi.org/10.1177/38.3.1689340>.
- Hayashi, T., Y. Kusunoki, M. Hakoda, Y. Morishita, Y. Kubo, M. Maki, F. Kasagi, K. Kodama, D. G. Macphee, and S. Kyoizumi. 2003. "Radiation Dose-Dependent Increases in Inflammatory Response Markers in A-Bomb Survivors." *International Journal of Radiation Biology* 79 (2): 129–36. <https://doi.org/10.1080/0955300021000038662>.
- Hayflick, L. 1965. "The Limited in Vitro Lifetime of Human Diploid Cell Strains." *Experimental Cell Research* 37 (3): 614–36. [https://doi.org/10.1016/0014-4827\(65\)90211-9](https://doi.org/10.1016/0014-4827(65)90211-9).
- Henzel, W. J., J. T. Stults, C. A. Hsu, and D. W. Aswad. 1989. "The Primary Structure of a Protein Carboxyl Methyltransferase from Bovine Brain That Selectively Methylates L-Isoaspartyl Sites." *The Journal of Biological Chemistry* 264 (27): 15905–11.
- Hernandez-Segura, Alejandra, Jamil Nehme, and Marco Demaria. 2018. "Hallmarks of Cellular Senescence." *Trends in Cell Biology* 28 (6): 436–53. <https://doi.org/10.1016/j.tcb.2018.02.001>.
- Hildebrandt, G., L. Maggiorella, F. Rödel, V. Rödel, D. Willis, and K.-R. Trott. 2002. "Mononuclear Cell Adhesion and Cell Adhesion Molecule Liberation after X-Irradiation of Activated Endothelial Cells in Vitro." *International Journal of Radiation Biology* 78 (4): 315–25. <https://doi.org/10.1080/09553000110106027>.
- Hildebrandt, J. Jahns, M. Hindemith, G. 2000. "Effects of Low Dose Radiation Therapy on Adjuvant Induced Arthritis in Rats." *International Journal of Radiation Biology* 76 (8): 1143–53. <https://doi.org/10.1080/09553000050111613>.
- Hinz, John M., N. Alice Yamada, Edmund P. Salazar, Robert S. Tebbs, and Larry H. Thompson. 2005. "Influence of Double-Strand-Break Repair Pathways on Radiosensitivity throughout the Cell Cycle in CHO Cells." *DNA Repair* 4 (7): 782–92. <https://doi.org/10.1016/j.dnarep.2005.03.005>.
- Hobson, B, and J Denekamp. 1984. "Endothelial Proliferation in Tumours and Normal Tissues: Continuous Labelling Studies." *British Journal of Cancer* 49 (4): 405–13. <https://doi.org/10.1038/bjc.1984.66>.
- Homma, Takujiro, Satoshi Okano, Jaeyong Lee, Junitsu Ito, Noriyuki Otsuki, Toshihiro Kurahashi, Eun Sil Kang, Osamu Nakajima, and Junichi Fujii. 2015. "SOD1 Deficiency Induces the

- Systemic Hyperoxidation of Peroxiredoxin in the Mouse." *Biochemical and Biophysical Research Communications* 463 (4): 1040–46. <https://doi.org/10.1016/j.bbrc.2015.06.055>.
- Hooning, M. J., A. Botma, B. M. P. Aleman, M. H. A. Baaijens, H. Bartelink, J. G. M. Klijn, C. W. Taylor, and F. E. van Leeuwen. 2007. "Long-Term Risk of Cardiovascular Disease in 10-Year Survivors of Breast Cancer." *JNCI Journal of the National Cancer Institute* 99 (5): 365–75. <https://doi.org/10.1093/jnci/djk064>.
- Hoorelbeke, Delphine, Elke Decrock, Maarten De Smet, Marijke De Bock, Benedicte Descamps, Valérie Van Haver, Tinneke Delvaeye, et al. 2020. "Cx43 Channels and Signaling via IP3/Ca2+, ATP, and ROS/NO Propagate Radiation-Induced DNA Damage to Non-Irradiated Brain Microvascular Endothelial Cells." *Cell Death & Disease* 11 (3): 194. <https://doi.org/10.1038/s41419-020-2392-5>.
- Hopewell, J. W. 1975. "Early and Late Changes in the Functional Vascularity of the Hamster Cheek Pouch after Local X-Irradiation." *Radiation Research* 63 (1): 157–64.
- Hoyer, Leon W., Rene P. de los Santos, and John R. Hoyer. 1973. "Antihemophilic Factor Antigen. LOCALIZATION IN ENDOTHELIAL CELLS BY IMMUNOFLUORESCENT MICROSCOPY." *Journal of Clinical Investigation* 52 (11): 2737–44. <https://doi.org/10.1172/JCI107469>.
- Hu, Qizhi, Robert J. Noll, Hongyan Li, Alexander Makarov, Mark Hardman, and R. Graham Cooks. 2005. "The Orbitrap: A New Mass Spectrometer." *Journal of Mass Spectrometry: JMS* 40 (4): 430–43. <https://doi.org/10.1002/jms.856>.
- Ishikawa, Hiroki, and Glen N. Barber. 2008. "STING Is an Endoplasmic Reticulum Adaptor That Facilitates Innate Immune Signalling." *Nature* 455 (7213): 674–78. <https://doi.org/10.1038/nature07317>.
- Iyer, R., B. E. Lehnert, and R. Svensson. 2000. "Factors Underlying the Cell Growth-Related Bystander Responses to Alpha Particles." *Cancer Research* 60 (5): 1290–98.
- Jaffe, Eric A. 1987. "Cell Biology of Endothelial Cells." *Human Pathology* 18 (3): 234–39. [https://doi.org/10.1016/S0046-8177\(87\)80005-9](https://doi.org/10.1016/S0046-8177(87)80005-9).
- Jaffe, Eric A., Ralph L. Nachman, Carl G. Becker, and C. Richard Minick. 1973. "Culture of Human Endothelial Cells Derived from Umbilical Veins. IDENTIFICATION BY MORPHOLOGIC AND IMMUNOLOGIC CRITERIA." *Journal of Clinical Investigation* 52 (11): 2745–56. <https://doi.org/10.1172/JCI107470>.
- Jangiam, Witawat, Chatchanok Udomtanakunchai, Paiboon Reungpatthanaphong, Montree Tungjai, Louise Honikel, Chris R. Gordon, and Kanokporn Noy Rithidech. 2018. "Late Effects of Low-Dose Radiation on the Bone Marrow, Lung, and Testis Collected From the Same Exposed BALB/CJ Mice." *Dose-Response* 16 (4): 155932581881503. <https://doi.org/10.1177/1559325818815031>.
- Jones, C. H. 1887. "Note Concerning the Endothelium of the Small Cerebral Arteries." *Journal of Anatomy and Physiology* 21 (Pt 4): 672–73.
- Jordan, Bertrand R. 2016. "The Hiroshima/Nagasaki Survivor Studies: Discrepancies Between Results and General Perception." *Genetics* 203 (4): 1505–12. <https://doi.org/10.1534/genetics.116.191759>.

- Kawamura, Kasumi, Fei Qi, and Junya Kobayashi. 2018. "Potential Relationship between the Biological Effects of Low-Dose Irradiation and Mitochondrial ROS Production." *Journal of Radiation Research* 59 (suppl_2): ii91–97. <https://doi.org/10.1093/jrr/rxx091>.
- Keehan, S., M. L. Taylor, R. L. Smith, L. Dunn, T. Kron, and R. D. Franich. 2016. "DOSE AND GAMMA-RAY SPECTRA FROM NEUTRON-INDUCED RADIOACTIVITY IN MEDICAL LINEAR ACCELERATORS FOLLOWING HIGH-ENERGY TOTAL BODY IRRADIATION." *Radiation Protection Dosimetry* 172 (4): 327–32. <https://doi.org/10.1093/rpd/ncv480>.
- Kelleher, Neil L., Sean V. Taylor, David Grannis, Cynthia Kinsland, Hsiu-Ju Chiu, Tadhg P. Begley, and Fred W. McLafferty. 1998. "Efficient Sequence Analysis of the Six Gene Products (7-74 KDA) from the Escherichia Coli Thiamin Biosynthetic Operon by Tandem High-Resolution Mass Spectrometry." *Protein Science* 7 (8): 1796–1801. <https://doi.org/10.1002/pro.5560070815>.
- Kettle, E. H. 1918. "Tumours Arising from Endothelium." *Proceedings of the Royal Society of Medicine* 11 (Pathol_Sect): 19–34. <https://doi.org/10.1177/003591571801101102>.
- Kibria, G, D Heath, P Smith, and R Biggar. 1980. "Pulmonary Endothelial Pavement Patterns." *Thorax* 35 (3): 186–91. <https://doi.org/10.1136/thx.35.3.186>.
- Kojima, Hirotada, Toshiaki Inoue, Hiroyuki Kunimoto, and Koichi Nakajima. 2013. "IL-6-STAT3 Signaling and Premature Senescence." *JAK-STAT* 2 (4): e25763. <https://doi.org/10.4161/jkst.25763>.
- Komarova, Yulia, and Asrar B. Malik. 2010. "Regulation of Endothelial Permeability via Paracellular and Transcellular Transport Pathways." *Annual Review of Physiology* 72 (1): 463–93. <https://doi.org/10.1146/annurev-physiol-021909-135833>.
- Krüger-Genge, Blocki, Franke, and Jung. 2019. "Vascular Endothelial Cell Biology: An Update." *International Journal of Molecular Sciences* 20 (18): 4411. <https://doi.org/10.3390/ijms20184411>.
- Lafargue, Audrey, Charlotte Degorre, Isabelle Corre, Marie-Clotilde Alves-Guerra, Marie-Hélène Gaugler, François Vallette, Claire Pecqueur, and François Paris. 2017. "Ionizing Radiation Induces Long-Term Senescence in Endothelial Cells through Mitochondrial Respiratory Complex II Dysfunction and Superoxide Generation." *Free Radical Biology and Medicine* 108 (July): 750–59. <https://doi.org/10.1016/j.freeradbiomed.2017.04.019>.
- Lam, E., S. Stein, and E. Falck-Pedersen. 2014. "Adenovirus Detection by the CGAS/STING/TBK1 DNA Sensing Cascade." *Journal of Virology* 88 (2): 974–81. <https://doi.org/10.1128/JVI.02702-13>.
- Lasry, Audrey, and Yinon Ben-Neriah. 2015. "Senescence-Associated Inflammatory Responses: Aging and Cancer Perspectives." *Trends in Immunology* 36 (4): 217–28. <https://doi.org/10.1016/j.it.2015.02.009>.
- Lee, Jihyun, William M. Baldwin, Chih-Yuan Lee, and Stephen Desiderio. 2013. "Stat3 β Mitigates Development of Atherosclerosis in Apolipoprotein E-Deficient Mice." *Journal of Molecular Medicine* 91 (8): 965–76. <https://doi.org/10.1007/s00109-013-1013-5>.

- Li, Xin, Chang Shu, Guanghui Yi, Catherine T. Chaton, Catherine L. Shelton, Jiasheng Diao, Xiaobing Zuo, C. Cheng Kao, Andrew B. Herr, and Pingwei Li. 2013. "Cyclic GMP-AMP Synthase Is Activated by Double-Stranded DNA-Induced Oligomerization." *Immunity* 39 (6): 1019–31. <https://doi.org/10.1016/j.immuni.2013.10.019>.
- Little, Mark P. 2016. "Radiation and Circulatory Disease." *Mutation Research/Reviews in Mutation Research* 770 (October): 299–318. <https://doi.org/10.1016/j.mrrev.2016.07.008>.
- Little, Mark P., Tamara V. Azizova, Dimitry Bazyka, Simon D. Bouffler, Elisabeth Cardis, Sergey Chekin, Vadim V. Chumak, et al. 2012. "Systematic Review and Meta-Analysis of Circulatory Disease from Exposure to Low-Level Ionizing Radiation and Estimates of Potential Population Mortality Risks." *Environmental Health Perspectives* 120 (11): 1503–11. <https://doi.org/10.1289/ehp.1204982>.
- Liu, Yin, Adriana A. Jesus, Bernadette Marrero, Dan Yang, Suzanne E. Ramsey, Gina A. Montealegre Sanchez, Klaus Tenbrock, et al. 2014. "Activated STING in a Vascular and Pulmonary Syndrome." *New England Journal of Medicine* 371 (6): 507–18. <https://doi.org/10.1056/NEJMoa1312625>.
- López-Otín, Carlos, Maria A. Blasco, Linda Partridge, Manuel Serrano, and Guido Kroemer. 2013. "The Hallmarks of Aging." *Cell* 153 (6): 1194–1217. <https://doi.org/10.1016/j.cell.2013.05.039>.
- Lowe, Donna, and Kenneth Raj. 2014. "Premature Aging Induced by Radiation Exhibits Pro-Atherosclerotic Effects Mediated by Epigenetic Activation of CD44 Expression." *Aging Cell* 13 (5): 900–910. <https://doi.org/10.1111/ace1.12253>.
- Ludwig, Christina, Ludovic Gillet, George Rosenberger, Sabine Amon, Ben C Collins, and Ruedi Aebersold. 2018. "Data-independent Acquisition-based SWATH - MS for Quantitative Proteomics: A Tutorial." *Molecular Systems Biology* 14 (8). <https://doi.org/10.15252/msb.20178126>.
- Luecke, Stefanie, Andreas Holleufer, Maria H Christensen, Kasper L Jønsson, Gerardo A Boni, Lambert K Sørensen, Mogens Johannsen, Martin R Jakobsen, Rune Hartmann, and Søren R Paludan. 2017. "cGAS Is Activated by DNA in a Length-dependent Manner." *EMBO Reports* 18 (10): 1707–15. <https://doi.org/10.15252/embr.201744017>.
- Ma, Feng, Bing Li, Yongxin Yu, Shankar S Iyer, Mingyu Sun, and Genhong Cheng. 2015. "Positive Feedback Regulation of Type I Interferon by the Interferon-stimulated Gene STING." *EMBO Reports* 16 (2): 202–12. <https://doi.org/10.15252/embr.201439366>.
- Ma, Jun, Furong Wang, and Mehran Mostafavi. 2018. "Ultrafast Chemistry of Water Radical Cation, H₂O^{•+}, in Aqueous Solutions." *Molecules (Basel, Switzerland)* 23 (2). <https://doi.org/10.3390/molecules23020244>.
- Mackenzie, Karen J., Paula Carroll, Carol-Anne Martin, Olga Murina, Adeline Fluteau, Daniel J. Simpson, Nelly Olova, et al. 2017. "CGAS Surveillance of Micronuclei Links Genome Instability to Innate Immunity." *Nature* 548 (7668): 461–65. <https://doi.org/10.1038/nature23449>.
- Malakhova, O. A. 2003. "Protein ISGylation Modulates the JAK-STAT Signaling Pathway." *Genes & Development* 17 (4): 455–60. <https://doi.org/10.1101/gad.1056303>.

- Mao, Yun, Wei Luo, Lin Zhang, Weiwei Wu, Liangshuai Yuan, Hao Xu, Juhee Song, et al. 2017. "STING–IRF3 Triggers Endothelial Inflammation in Response to Free Fatty Acid-Induced Mitochondrial Damage in Diet-Induced Obesity." *Arteriosclerosis, Thrombosis, and Vascular Biology* 37 (5): 920–29. <https://doi.org/10.1161/ATVBAHA.117.309017>.
- Markus, B. H., Y. L. Colson, J. J. Fung, A. Zeevi, and R. J. Duquesnoy. 1988. "HLA Antigen Expression on Cultured Human Arterial Endothelial Cells." *Tissue Antigens* 32 (5): 241–53. <https://doi.org/10.1111/j.1399-0039.1988.tb01663.x>.
- Marsac, Kara E., Pamela C. Burnley, Christopher T. Adcock, Daniel A. Haber, Russell L. Malchow, and Elisabeth M. Hausrath. 2016. "Modeling Background Radiation Using Geochemical Data: A Case Study in and around Cameron, Arizona." *Journal of Environmental Radioactivity* 165 (December): 68–85. <https://doi.org/10.1016/j.jenvrad.2016.07.012>.
- Martin, G. M., C. A. Sprague, and C. J. Epstein. 1970. "Replicative Life-Span of Cultivated Human Cells. Effects of Donor's Age, Tissue, and Genotype." *Laboratory Investigation; a Journal of Technical Methods and Pathology* 23 (1): 86–92.
- Masselon, C., G. A. Anderson, R. Harkewicz, J. E. Bruce, L. Pasa-Tolic, and R. D. Smith. 2000. "Accurate Mass Multiplexed Tandem Mass Spectrometry for High-Throughput Polypeptide Identification from Mixtures." *Analytical Chemistry* 72 (8): 1918–24. <https://doi.org/10.1021/ac991133+>.
- Matoba, Tetsuya, Hiroaki Shimokawa, Mikio Nakashima, Yoji Hirakawa, Yasushi Mukai, Katsuya Hirano, Hideo Kanaide, and Akira Takeshita. 2000. "Hydrogen Peroxide Is an Endothelium-Derived Hyperpolarizing Factor in Mice." *Journal of Clinical Investigation* 106 (12): 1521–30. <https://doi.org/10.1172/JCI10506>.
- McEver, R P, J H Beckstead, K L Moore, L Marshall-Carlson, and D F Bainton. 1989. "GMP-140, a Platelet Alpha-Granule Membrane Protein, Is Also Synthesized by Vascular Endothelial Cells and Is Localized in Weibel-Palade Bodies." *Journal of Clinical Investigation* 84 (1): 92–99. <https://doi.org/10.1172/JCI114175>.
- McRobb, Lucinda S., Vivienne S. Lee, Margaret Simonian, Zhenjun Zhao, Santhosh George Thomas, Markus Wiedmann, Jude V. Amal Raj, et al. 2017. "Radiosurgery Alters the Endothelial Surface Proteome: Externalized Intracellular Molecules as Potential Vascular Targets in Irradiated Brain Arteriovenous Malformations." *Radiation Research* 187 (1): 66. <https://doi.org/10.1667/RR14518.1>.
- Meeren, A. V., J. M. Bertho, M. Vandamme, and M. H. Gaugler. 1997. "Ionizing Radiation Enhances IL-6 and IL-8 Production by Human Endothelial Cells." *Mediators of Inflammation* 6 (3): 185–93. <https://doi.org/10.1080/09629359791677>.
- Megger, Dominik A., Thilo Bracht, Helmut E. Meyer, and Barbara Sitek. 2013. "Label-Free Quantification in Clinical Proteomics." *Biochimica et Biophysica Acta (BBA) - Proteins and Proteomics* 1834 (8): 1581–90. <https://doi.org/10.1016/j.bbapap.2013.04.001>.
- Megger, Dominik A., Jos Philipp, Vu Thuy Khanh Le-Trilling, Barbara Sitek, and Mirko Trilling. 2017. "Deciphering of the Human Interferon-Regulated Proteome by Mass Spectrometry-Based

- Quantitative Analysis Reveals Extent and Dynamics of Protein Induction and Repression.” *Frontiers in Immunology* 8 (September): 1139. <https://doi.org/10.3389/fimmu.2017.01139>.
- Min, Jeong-Ki, Young-Myeong Kim, Sung Wan Kim, Min-Chul Kwon, Young-Yun Kong, In Koo Hwang, Moo Ho Won, Jaerang Rho, and Young-Guen Kwon. 2005. “TNF-Related Activation-Induced Cytokine Enhances Leukocyte Adhesiveness: Induction of ICAM-1 and VCAM-1 via TNF Receptor-Associated Factor and Protein Kinase C-Dependent NF-KB Activation in Endothelial Cells.” *The Journal of Immunology* 175 (1): 531–40. <https://doi.org/10.4049/jimmunol.175.1.531>.
- Mogensen, Trine H. 2019. “IRF and STAT Transcription Factors - From Basic Biology to Roles in Infection, Protective Immunity, and Primary Immunodeficiencies.” *Frontiers in Immunology* 9 (January): 3047. <https://doi.org/10.3389/fimmu.2018.03047>.
- Mollà, Meritxell, Meritxell Gironella, Rosa Miquel, Victoria Tovar, Pablo Engel, Albert Biete, Josep M Piqué, and Julián Panés. 2003. “Relative Roles of ICAM-1 and VCAM-1 in the Pathogenesis of Experimental Radiation-Induced Intestinal Inflammation.” *International Journal of Radiation Oncology*Biophysics*Physics* 57 (1): 264–73. [https://doi.org/10.1016/S0360-3016\(03\)00523-6](https://doi.org/10.1016/S0360-3016(03)00523-6).
- Moncada, S., E.A. Higgs, and J.R. Vane. 1977. “HUMAN ARTERIAL AND VENOUS TISSUES GENERATE PROSTACYCLIN (PROSTAGLANDIN X), A POTENT INHIBITOR OF PLATELET AGGREGATION.” *The Lancet* 309 (8001): 18–21. [https://doi.org/10.1016/S0140-6736\(77\)91655-5](https://doi.org/10.1016/S0140-6736(77)91655-5).
- Moncada, S., and J.R. Vane. 1981. “Prostacyclin and Blood Coagulation:” *Drugs* 21 (6): 430–37. <https://doi.org/10.2165/00003495-198121060-00002>.
- Mondola, Paolo, Simona Damiano, Anna Sasso, and Mariarosaria Santillo. 2016. “The Cu, Zn Superoxide Dismutase: Not Only a Dismutase Enzyme.” *Frontiers in Physiology* 7: 594. <https://doi.org/10.3389/fphys.2016.00594>.
- Morgan, William F., and Marianne B. Sowa. 2007. “Non-Targeted Bystander Effects Induced by Ionizing Radiation.” *Mutation Research/Fundamental and Molecular Mechanisms of Mutagenesis* 616 (1–2): 159–64. <https://doi.org/10.1016/j.mrfmmm.2006.11.009>.
- Mukai, Kojiro, Hiroyasu Konno, Tatsuya Akiba, Takefumi Uemura, Satoshi Waguri, Toshihide Kobayashi, Glen N. Barber, Hiroyuki Arai, and Tomohiko Taguchi. 2016. “Activation of STING Requires Palmitoylation at the Golgi.” *Nature Communications* 7 (1): 11932. <https://doi.org/10.1038/ncomms11932>.
- Nagasawa, H., and J. B. Little. 1992. “Induction of Sister Chromatid Exchanges by Extremely Low Doses of Alpha-Particles.” *Cancer Research* 52 (22): 6394–96.
- Narita, Masashi, Sabrina Nuñez, Edith Heard, Masako Narita, Athena W. Lin, Stephen A. Hearn, David L. Spector, Gregory J. Hannon, and Scott W. Lowe. 2003. “Rb-Mediated Heterochromatin Formation and Silencing of E2F Target Genes during Cellular Senescence.” *Cell* 113 (6): 703–16. [https://doi.org/10.1016/S0092-8674\(03\)00401-X](https://doi.org/10.1016/S0092-8674(03)00401-X).
- NCI Dictionaries. 2020. “Definition of Endothelial Cell - NCI Dictionary of Cancer Terms - National Cancer Institute.” Text/html. Definition of Endothelial Cell - NCI Dictionary of Cancer Terms -

- National Cancer Institute. January 23, 2020.
<https://www.cancer.gov/publications/dictionaries/cancer-terms/def/endothelial-cell>.
- Neriishi, K., E. Nakashima, and R. R. Delongchamp. 2001. "Persistent Subclinical Inflammation among A-Bomb Survivors." *International Journal of Radiation Biology* 77 (4): 475–82.
<https://doi.org/10.1080/09553000010024911>.
- Osman, R., L. Pardo, J. Banfelder, A. P. Mazurek, L. Shvartzman, R. Strauss, and H. Weinstein. 1991. "Molecular Mechanisms of Radiation Induced Dna Damage: H-Addition to Bases, Direct Ionization and Double Strand Break." *Free Radical Research Communications* 13 (1): 465–67. <https://doi.org/10.3109/10715769109145819>.
- Paris, F. 2001. "Endothelial Apoptosis as the Primary Lesion Initiating Intestinal Radiation Damage in Mice." *Science* 293 (5528): 293–97. <https://doi.org/10.1126/science.1060191>.
- Philipp, Jos, Omid Azimzadeh, Vikram Subramanian, Juliane Merl-Pham, Donna Lowe, Daniela Hladik, Nadine Erbelinger, et al. 2017. "Radiation-Induced Endothelial Inflammation Is Transferred via the Secretome to Recipient Cells in a STAT-Mediated Process." *Journal of Proteome Research* 16 (10): 3903–16. <https://doi.org/10.1021/acs.jproteome.7b00536>.
- Philipp, Jos, Ronan Le Gleut, Christine von Toerne, Prabal Subedi, Omid Azimzadeh, Michael J. Atkinson, and Soile Tapio. 2020. "Radiation Response of Human Cardiac Endothelial Cells Reveals a Central Role of the CGAS-STING Pathway in the Development of Inflammation." *Proteomes* 8 (4): 30. <https://doi.org/10.3390/proteomes8040030>.
- Philipp, Jos, Wolfgang Sievert, Omid Azimzadeh, Christine von Toerne, Fabian Metzger, Anton Posch, Daniela Hladik, et al. 2020. "Data Independent Acquisition Mass Spectrometry of Irradiated Mouse Lung Endothelial Cells Reveals a STAT-Associated Inflammatory Response." *International Journal of Radiation Biology*, January, 1–9.
<https://doi.org/10.1080/09553002.2020.1712492>.
- Pouget, Jean-Pierre, and Stephen J. Mather. 2001. "General Aspects of the Cellular Response to Low- and High-LET Radiation." *European Journal of Nuclear Medicine* 28 (4): 541–61.
<https://doi.org/10.1007/s002590100484>.
- Raddatz, Michael A., Tessa Huffstater, Matthew R. Bersi, Bradley I. Reinfeld, Matthew Z. Madden, Sabrina E. Booton, W. Kimryn Rathmell, et al. 2020. "Macrophages Promote Aortic Valve Cell Calcification and Alter STAT3 Splicing." *Arteriosclerosis, Thrombosis, and Vascular Biology* 40 (6). <https://doi.org/10.1161/ATVBAHA.120.314360>.
- Ramadan, Raghda, Els Vromans, Dornatien Chuo Anang, Ines Goetschalckx, Delphine Hoorelbeke, Elke Decrock, Sarah Baatout, Luc Leybaert, and An Aerts. 2020. "Connexin43 Hemichannel Targeting With TAT-Gap19 Alleviates Radiation-Induced Endothelial Cell Damage." *Frontiers in Pharmacology* 11 (March): 212. <https://doi.org/10.3389/fphar.2020.00212>.
- Raso, Maria Chiara, Nikola Djoric, Franziska Walser, Sandra Hess, Fabian Marc Schmid, Sibylle Burger, Klaus-Peter Knobloch, and Lorenza Penengo. 2020. "Interferon-Stimulated Gene 15 Accelerates Replication Fork Progression Inducing Chromosomal Breakage." *Journal of Cell Biology* 219 (8): e202002175. <https://doi.org/10.1083/jcb.202002175>.

- Ratikan, Josephine A., Ewa D. Micewicz, Michael W. Xie, and Dörthe Schae. 2015. "Radiation Takes Its Toll." *Cancer Letters* 368 (2): 238–45. <https://doi.org/10.1016/j.canlet.2015.03.031>.
- Reinders, Janny G., Ben J.M. Heijmen, Manouk J.J. Olofsen-van Acht, Wim L.J. van Putten, and Peter C. Levendag. 1999. "Ischemic Heart Disease after Mantlefield Irradiation for Hodgkin's Disease in Long-Term Follow-Up." *Radiotherapy and Oncology* 51 (1): 35–42. [https://doi.org/10.1016/S0167-8140\(99\)00026-2](https://doi.org/10.1016/S0167-8140(99)00026-2).
- Riederer, Isabelle, Wolfgang Sievert, Günther Eissner, Michael Molls, and Gabriele Multhoff. 2010. "Irradiation-Induced Up-Regulation of HLA-E on Macrovascular Endothelial Cells Confers Protection against Killing by Activated Natural Killer Cells." Edited by Nils Cordes. *PLoS ONE* 5 (12): e15339. <https://doi.org/10.1371/journal.pone.0015339>.
- Rivero-Gutiérrez, B., A. Anzola, O. Martínez-Augustin, and F. Sánchez de Medina. 2014. "Stain-Free Detection as Loading Control Alternative to Ponceau and Housekeeping Protein Immunodetection in Western Blotting." *Analytical Biochemistry* 467 (December): 1–3. <https://doi.org/10.1016/j.ab.2014.08.027>.
- Rödel, Franz, Ulrich Schaller, Stefan Schultze-Mosgau, Horst-Ulrich Beuscher, Ludwig Keilholz, Martin Herrmann, Reinhard Voll, Rolf Sauer, and Guido Hildebrandt. 2004. "The Induction of TGF-Beta(1) and NF-KappaB Parallels a Biphasic Time Course of Leukocyte/Endothelial Cell Adhesion Following Low-Dose X-Irradiation." *Strahlentherapie Und Onkologie: Organ Der Deutschen Röntgengesellschaft ... [et Al]* 180 (4): 194–200. <https://doi.org/10.1007/s00066-004-1237-y>.
- Rodier, Francis, and Judith Campisi. 2011. "Four Faces of Cellular Senescence." *The Journal of Cell Biology* 192 (4): 547–56. <https://doi.org/10.1083/jcb.201009094>.
- Rodier, Francis, Jean-Philippe Coppé, Christopher K. Patil, Wieteke A. M. Hoeijmakers, Denise P. Muñoz, Saba R. Raza, Adam Freund, Eric Campeau, Albert R. Davalos, and Judith Campisi. 2009. "Persistent DNA Damage Signalling Triggers Senescence-Associated Inflammatory Cytokine Secretion." *Nature Cell Biology* 11 (8): 973–79. <https://doi.org/10.1038/ncb1909>.
- Roedel, F., N. Kley, H. U. Beuscher, G. Hildebrandt, L. Keilholz, P. Kern, R. Voll, M. Herrmann, and R. Sauer. 2002. "Anti-Inflammatory Effect of Low-Dose X-Irradiation and the Involvement of a TGF-β 1 -Induced down-Regulation of Leukocyte/Endothelial Cell Adhesion." *International Journal of Radiation Biology* 78 (8): 711–19. <https://doi.org/10.1080/09553000210137671>.
- Rostami, Ariana, Meghan Lambie, Caberry W. Yu, Vuk Stambolic, John N. Waldron, and Scott V. Bratman. 2020. "Senescence, Necrosis, and Apoptosis Govern Circulating Cell-Free DNA Release Kinetics." *Cell Reports* 31 (13): 107830. <https://doi.org/10.1016/j.celrep.2020.107830>.
- Sakorafas, G.H., and Michael Safioleas. 2010. "Breast Cancer Surgery: An Historical Narrative. Part III. From the Sunset of the 19th to the Dawn of the 21st Century." *European Journal of Cancer Care* 19 (2): 145–66. <https://doi.org/10.1111/j.1365-2354.2008.01061.x>.
- Schae, Dörthe, Jutta Jahns, Guido Hildebrandt, and Klaus-Rüdiger Trott. 2005. "Radiation Treatment of Acute Inflammation in Mice." *International Journal of Radiation Biology* 81 (9): 657–67. <https://doi.org/10.1080/09553000500385556>.

- Schey, Kevin L., J. Matthew Luther, and Kristie L. Rose. 2015. "Proteomics Characterization of Exosome Cargo." *Methods* 87 (October): 75–82. <https://doi.org/10.1016/j.ymeth.2015.03.018>.
- Schneider, Caroline A, Wayne S Rasband, and Kevin W Eliceiri. 2012. "NIH Image to ImageJ: 25 Years of Image Analysis." *Nature Methods* 9 (7): 671–75. <https://doi.org/10.1038/nmeth.2089>.
- Schröder, Sabine, Dajana Juerß, Stephan Kriesen, Katrin Manda, and Guido Hildebrandt. 2019. "Immunomodulatory Properties of Low-Dose Ionizing Radiation on Human Endothelial Cells." *International Journal of Radiation Biology* 95 (1): 23–32. <https://doi.org/10.1080/09553002.2018.1486515>.
- Schröder, Sabine, Stephan Kriesen, Daniel Paape, Guido Hildebrandt, and Katrin Manda. 2018. "Modulation of Inflammatory Reactions by Low-Dose Ionizing Radiation: Cytokine Release of Murine Endothelial Cells Is Dependent on Culture Conditions." *Journal of Immunology Research* 2018 (June): 1–13. <https://doi.org/10.1155/2018/2856518>.
- Sensi, M., G. Pietra, A. Molla, G. Nicolini, C. Vegetti, I. Bersani, E. Millo, et al. 2009. "Peptides with Dual Binding Specificity for HLA-A2 and HLA-E Are Encoded by Alternatively Spliced Isoforms of the Antioxidant Enzyme Peroxiredoxin 5." *International Immunology* 21 (3): 257–68. <https://doi.org/10.1093/intimm/dxn141>.
- Serrano, Manuel, Athena W Lin, Mila E McCurrach, David Beach, and Scott W Lowe. 1997. "Oncogenic Ras Provokes Premature Cell Senescence Associated with Accumulation of P53 and P16INK4a." *Cell* 88 (5): 593–602. [https://doi.org/10.1016/S0092-8674\(00\)81902-9](https://doi.org/10.1016/S0092-8674(00)81902-9).
- Sgrignani, Jacopo, Simon Olsson, Dariusz Ekonomiuk, Davide Genini, Rolf Krause, Carlo V. Catapano, and Andrea Cavalli. 2015. "Molecular Determinants for Unphosphorylated STAT3 Dimerization Determined by Integrative Modeling." *Biochemistry* 54 (35): 5489–5501. <https://doi.org/10.1021/bi501529x>.
- Shan, Yu-Xing, Shun-Zi Jin, Xiao-Dong Liu, Yang Liu, and Shu-Zheng Liu. 2007. "Ionizing Radiation Stimulates Secretion of Pro-Inflammatory Cytokines: Dose–Response Relationship, Mechanisms and Implications." *Radiation and Environmental Biophysics* 46 (1): 21–29. <https://doi.org/10.1007/s00411-006-0076-x>.
- Shay, J. 1991. "A Role for Both RB and P53 in the Regulation of Human Cellular Senescence*1." *Experimental Cell Research* 196 (1): 33–39. [https://doi.org/10.1016/0014-4827\(91\)90453-2](https://doi.org/10.1016/0014-4827(91)90453-2).
- Shimizu, Y., K. Kodama, N. Nishi, F. Kasagi, A. Suyama, M. Soda, E. J Grant, et al. 2010. "Radiation Exposure and Circulatory Disease Risk: Hiroshima and Nagasaki Atomic Bomb Survivor Data, 1950-2003." *BMJ* 340 (jan14 1): b5349–b5349. <https://doi.org/10.1136/bmj.b5349>.
- Sievert, Wolfgang, Soile Tapio, Stephanie Breuninger, Udo Gaipl, Nicolaus Andratschke, Klaus-Rüdiger Trott, and Gabriele Multhoff. 2014. "Adhesion Molecule Expression and Function of Primary Endothelial Cells in Benign and Malignant Tissues Correlates with Proliferation." Edited by Alan Graham Pockley. *PLoS ONE* 9 (3): e91808. <https://doi.org/10.1371/journal.pone.0091808>.
- Sievert, Wolfgang, Klaus-Rüdiger Trott, Omid Azimzadeh, Soile Tapio, Horst Zitzelsberger, and Gabriele Multhoff. 2015. "Late Proliferating and Inflammatory Effects on Murine Microvascular

- Heart and Lung Endothelial Cells after Irradiation." *Radiotherapy and Oncology* 117 (2): 376–81. <https://doi.org/10.1016/j.radonc.2015.07.029>.
- Simonetto, Cristoforo, Tamara V. Azizova, Zarko Barjaktarovic, Johann Bauersachs, Peter Jacob, Jan Christian Kaiser, Reinhard Meckbach, Helmut Schöllnberger, and Markus Eidemüller. 2017. "A Mechanistic Model for Atherosclerosis and Its Application to the Cohort of Mayak Workers." Edited by Xianwu Cheng. *PLOS ONE* 12 (4): e0175386. <https://doi.org/10.1371/journal.pone.0175386>.
- Skoko, John J., Shireen Attaran, and Carola A. Neumann. 2019. "Signals Getting Crossed in the Entanglement of Redox and Phosphorylation Pathways: Phosphorylation of Peroxiredoxin Proteins Sparks Cell Signaling." *Antioxidants (Basel, Switzerland)* 8 (2). <https://doi.org/10.3390/antiox8020029>.
- Slany, Astrid, Andrea Bileck, Dominique Kreutz, Rupert L. Mayer, Besnik Muqaku, and Christopher Gerner. 2016. "Contribution of Human Fibroblasts and Endothelial Cells to the Hallmarks of Inflammation as Determined by Proteome Profiling." *Molecular & Cellular Proteomics* 15 (6): 1982–97. <https://doi.org/10.1074/mcp.M116.058099>.
- Sriharshan, Arundhathi, Karsten Boldt, Hakan Sarioglu, Zarko Barjaktarovic, Omid Azimzadeh, Ludwig Hieber, Horst Zitzelsberger, Marius Ueffing, Michael J. Atkinson, and Soile Tapio. 2012. "Proteomic Analysis by SILAC and 2D-DIGE Reveals Radiation-Induced Endothelial Response: Four Key Pathways." *Journal of Proteomics* 75 (8): 2319–30. <https://doi.org/10.1016/j.jprot.2012.02.009>.
- Srikanth, Sonal, Jin Seok Woo, Beibei Wu, Yasser M. El-Sherbiny, Jennifer Leung, Koollawat Chupradit, Laura Rice, et al. 2019. "The Ca²⁺ Sensor STIM1 Regulates the Type I Interferon Response by Retaining the Signaling Adaptor STING at the Endoplasmic Reticulum." *Nature Immunology* 20 (2): 152–62. <https://doi.org/10.1038/s41590-018-0287-8>.
- Stark, George R., and James E. Darnell. 2012. "The JAK-STAT Pathway at Twenty." *Immunity* 36 (4): 503–14. <https://doi.org/10.1016/j.immuni.2012.03.013>.
- Stewart, Fiona Anne, Sylvia Heeneman, Johannes te Poele, Jacqueline Kruse, Nicola S. Russell, Marion Gijbels, and Mat Daemen. 2006. "Ionizing Radiation Accelerates the Development of Atherosclerotic Lesions in ApoE^{-/-} Mice and Predisposes to an Inflammatory Plaque Phenotype Prone to Hemorrhage." *The American Journal of Pathology* 168 (2): 649–58. <https://doi.org/10.2353/ajpath.2006.050409>.
- Storey, John D. 2002. "A Direct Approach to False Discovery Rates." *Journal of the Royal Statistical Society: Series B (Statistical Methodology)* 64 (3): 479–98. <https://doi.org/10.1111/1467-9868.00346>.
- Tapio, Soile, Mark P. Little, Jan Christian Kaiser, Nathalie Impens, Nobuyuki Hamada, Alexandros G. Georgakilas, David Simar, and Sisko Salomaa. 2021. "Ionizing Radiation-Induced Circulatory and Metabolic Diseases." *Environment International* 146 (January): 106235. <https://doi.org/10.1016/j.envint.2020.106235>.

- Thomas, P. A., B. L. Tracy, T. Ping, M. Wickstrom, N. Sidhu, and L. Hiebert. 2003. "Relative Biological Effectiveness (RBE) of ^{210}Po Alpha-Particles versus X-Rays on Lethality in Bovine Endothelial Cells." *International Journal of Radiation Biology* 79 (2): 107–18.
- Tiruppathi, Chinnaswamy, Wei Song, Magnus Bergenfeldt, Phillip Sass, and Asrar B. Malik. 1997. "Gp60 Activation Mediates Albumin Transcytosis in Endothelial Cells by Tyrosine Kinase-Dependent Pathway." *Journal of Biological Chemistry* 272 (41): 25968–75.
<https://doi.org/10.1074/jbc.272.41.25968>.
- Tokunaga, O., J. L. Fan, and T. Watanabe. 1989. "Atherosclerosis- and Age-Related Multinucleated Variant Endothelial Cells in Primary Culture from Human Aorta." *The American Journal of Pathology* 135 (6): 967–76.
- Turrens, J. F. 2003. "Mitochondrial Formation of Reactive Oxygen Species." *The Journal of Physiology* 552 (2): 335–44. <https://doi.org/10.1113/jphysiol.2003.049478>.
- Vieira Dias, Juliana, Celine Gloaguen, Dimitri Kereselidze, Line Manens, Karine Tack, and Teni G Ebrahimian. 2018. "Gamma Low-Dose-Rate Ionizing Radiation Stimulates Adaptive Functional and Molecular Response in Human Aortic Endothelial Cells in a Threshold-, Dose-, and Dose Rate-Dependent Manner." *Dose-Response* 16 (1): 155932581875523.
<https://doi.org/10.1177/1559325818755238>.
- Villarroya-Beltri, Carolina, Susana Guerra, and Francisco Sánchez-Madrid. 2017. "ISGylation – a Key to Lock the Cell Gates for Preventing the Spread of Threats." *Journal of Cell Science* 130 (18): 2961–69. <https://doi.org/10.1242/jcs.205468>.
- Vogt, M., C. Haggblom, J. Yeargin, T. Christiansen-Weber, and M. Haas. 1998. "Independent Induction of Senescence by P16INK4a and P21CIP1 in Spontaneously Immortalized Human Fibroblasts." *Cell Growth & Differentiation: The Molecular Biology Journal of the American Association for Cancer Research* 9 (2): 139–46.
- Vozenin, M.-C., J.H. Hendry, and C.L. Limoli. 2019. "Biological Benefits of Ultra-High Dose Rate FLASH Radiotherapy: Sleeping Beauty Awoken." *Clinical Oncology* 31 (7): 407–15.
<https://doi.org/10.1016/j.clon.2019.04.001>.
- Wagner, Rudolph. 1839. *Erläuterungstafeln zur Physiologie und Entwicklungsgeschichte : mit vorzüglicher Rücksicht auf seine Lehrbücher über Physiologie und vergleichende Anatomie*. Leipzig: Leopold Voss.
- Wang, E. 1995. "Senescent Human Fibroblasts Resist Programmed Cell Death, and Failure to Suppress Bcl2 Is Involved." *Cancer Research* 55 (11): 2284–92.
- Wang, Y., A. H. H. van Boxel-Dezaire, H. Cheon, J. Yang, and G. R. Stark. 2013. "STAT3 Activation in Response to IL-6 Is Prolonged by the Binding of IL-6 Receptor to EGF Receptor." *Proceedings of the National Academy of Sciences* 110 (42): 16975–80.
<https://doi.org/10.1073/pnas.1315862110>.
- Wang, Yingying, Marjan Boerma, and Daohong Zhou. 2016. "Ionizing Radiation-Induced Endothelial Cell Senescence and Cardiovascular Diseases." *Radiation Research* 186 (2): 153–61.
<https://doi.org/10.1667/RR14445.1>.

- Ward, J.F. 1988. "DNA Damage Produced by Ionizing Radiation in Mammalian Cells: Identities, Mechanisms of Formation, and Reparability." In *Progress in Nucleic Acid Research and Molecular Biology*, 35:95–125. Elsevier. [https://doi.org/10.1016/S0079-6603\(08\)60611-X](https://doi.org/10.1016/S0079-6603(08)60611-X).
- Wardman, P. 2009. "The Importance of Radiation Chemistry to Radiation and Free Radical Biology (The 2008 Silvanus Thompson Memorial Lecture)." *The British Journal of Radiology* 82 (974): 89–104. <https://doi.org/10.1259/bjr/60186130>.
- Wasinger, Valerie C., Stuart J. Cordwell, Anne Cerpa-Poljak, Jun X. Yan, Andrew A. Gooley, Marc R. Wilkins, Mark W. Duncan, Ray Harris, Keith L. Williams, and Ian Humphery-Smith. 1995. "Progress with Gene-Product Mapping of the Mollicutes: *Mycoplasma Genitalium*." *Electrophoresis* 16 (1): 1090–94. <https://doi.org/10.1002/elps.11501601185>.
- Watson, C., S. Whittaker, N. Smith, A. J. Vora, D. C. Dumonde, and K. A. Brown. 1996. "IL-6 Acts on Endothelial Cells to Preferentially Increase Their Adherence for Lymphocytes." *Clinical and Experimental Immunology* 105 (1): 112–19. <https://doi.org/10.1046/j.1365-2249.1996.d01-717.x>.
- Weichselbaum, R. R., H. Ishwaran, T. Yoon, D. S. A. Nuyten, S. W. Baker, N. Khodarev, A. W. Su, et al. 2008. "An Interferon-Related Gene Signature for DNA Damage Resistance Is a Predictive Marker for Chemotherapy and Radiation for Breast Cancer." *Proceedings of the National Academy of Sciences* 105 (47): 18490–95. <https://doi.org/10.1073/pnas.0809242105>.
- Wennstig, Anna-Karin, Hans Garmo, Ulf Isacson, Giovanna Gagliardi, Niina Rintelä, Bo Lagerqvist, Lars Holmberg, Carl Blomqvist, Malin Sund, and Greger Nilsson. 2019. "The Relationship between Radiation Doses to Coronary Arteries and Location of Coronary Stenosis Requiring Intervention in Breast Cancer Survivors." *Radiation Oncology* 14 (1): 40. <https://doi.org/10.1186/s13014-019-1242-z>.
- Wennstig, Anna-Karin, Charlotta Wadsten, Hans Garmo, Irma Fredriksson, Carl Blomqvist, Lars Holmberg, Greger Nilsson, and Malin Sund. 2020. "Long-Term Risk of Ischemic Heart Disease after Adjuvant Radiotherapy in Breast Cancer: Results from a Large Population-Based Cohort." *Breast Cancer Research* 22 (1): 10. <https://doi.org/10.1186/s13058-020-1249-2>.
- West, A. Phillip, William Khoury-Hanold, Matthew Staron, Michal C. Tal, Cristiana M. Pineda, Sabine M. Lang, Megan Bestwick, et al. 2015. "Mitochondrial DNA Stress Primes the Antiviral Innate Immune Response." *Nature* 520 (7548): 553–57. <https://doi.org/10.1038/nature14156>.
- Wiśniewski, Jacek R, Alexandre Zougman, Nagarjuna Nagaraj, and Matthias Mann. 2009. "Universal Sample Preparation Method for Proteome Analysis." *Nature Methods* 6 (5): 359–62. <https://doi.org/10.1038/nmeth.1322>.
- Wu, J., L. Sun, X. Chen, F. Du, H. Shi, C. Chen, and Z. J. Chen. 2013. "Cyclic GMP-AMP Is an Endogenous Second Messenger in Innate Immune Signaling by Cytosolic DNA." *Science* 339 (6121): 826–30. <https://doi.org/10.1126/science.1229963>.
- Wu, Nz, Ba Ross, C Gulledege, B Klitzman, R Dodge, and Mw Dewhirst. 1994. "Differences in Leucocyte-Endothelium Interactions between Normal and Adenocarcinoma Bearing Tissues

- in Response to Radiation." *British Journal of Cancer* 69 (5): 883–89.
<https://doi.org/10.1038/bjc.1994.171>.
- Wu, Xiaomei, Fei-Hua Wu, Xiaoqiang Wang, Lilin Wang, James N. Siedow, Weiguo Zhang, and Zhen-Ming Pei. 2014. "Molecular Evolutionary and Structural Analysis of the Cytosolic DNA Sensor CGAS and STING." *Nucleic Acids Research* 42 (13): 8243–57.
<https://doi.org/10.1093/nar/gku569>.
- Xiao, Linlin, Weili Liu, Jitao Li, Yuexia Xie, Mingyuan He, Jiamei Fu, Wensen Jin, and Chunlin Shao. 2014. "Irradiated U937 Cells Trigger Inflammatory Bystander Responses in Human Umbilical Vein Endothelial Cells through the P38 Pathway." *Radiation Research* 182 (1): 111–21.
<https://doi.org/10.1667/RR13736.1>.
- Yamada, Michiko, Kumiko Naito, Fumiyoshi Kasagi, Naomi Masunari, and Gen Suzuki. 2005. "Prevalence of Atherosclerosis in Relation to Atomic Bomb Radiation Exposure: An RERF Adult Health Study." *International Journal of Radiation Biology* 81 (11): 821–26.
<https://doi.org/10.1080/09553000600555504>.
- Yentrapalli, Ramesh, Omid Azimzadeh, Zarko Barjaktarovic, Hakan Sarioglu, Andrzej Wojcik, Mats Harms-Ringdahl, Michael J. Atkinson, Siamak Haghdoost, and Soile Tapio. 2013. "Quantitative Proteomic Analysis Reveals Induction of Premature Senescence in Human Umbilical Vein Endothelial Cells Exposed to Chronic Low-Dose Rate Gamma Radiation." *PROTEOMICS* 13 (7): 1096–1107. <https://doi.org/10.1002/pmic.201200463>.
- Yentrapalli, Ramesh, Omid Azimzadeh, Anne Kraemer, Katharina Malinowsky, Hakan Sarioglu, Karl-Friedrich Becker, Michael J. Atkinson, Simone Moertl, and Soile Tapio. 2015. "Quantitative and Integrated Proteome and MicroRNA Analysis of Endothelial Replicative Senescence." *Journal of Proteomics* 126 (August): 12–23. <https://doi.org/10.1016/j.jprot.2015.05.023>.
- Yentrapalli, Ramesh, Omid Azimzadeh, Arundhathi Sriharshan, Katharina Malinowsky, Juliane Merl, Andrzej Wojcik, Mats Harms-Ringdahl, et al. 2013. "The PI3K/Akt/MTOR Pathway Is Implicated in the Premature Senescence of Primary Human Endothelial Cells Exposed to Chronic Radiation." Edited by Gayle E. Woloschak. *PLoS ONE* 8 (8): e70024.
<https://doi.org/10.1371/journal.pone.0070024>.
- Zauberman, A, D Zipori, M Krupsky, and R Ben-Levy. 1999. "Stress Activated Protein Kinase P38 Is Involved in IL-6 Induced Transcriptional Activation of STAT3." *Oncogene* 18 (26): 3886–93.
<https://doi.org/10.1038/sj.onc.1202738>.
- Zhang, X., E. Rozengurt, and E. F. Reed. 2010. "HLA Class I Molecules Partner with Integrin 4 to Stimulate Endothelial Cell Proliferation and Migration." *Science Signaling* 3 (149): ra85–ra85.
<https://doi.org/10.1126/scisignal.2001158>.
- Zhang, Xianqin, Dusan Bogunovic, Béatrice Payelle-Brogard, Véronique Francois-Newton, Scott D. Speer, Chao Yuan, Stefano Volpi, et al. 2015. "Human Intracellular ISG15 Prevents Interferon- α/β over-Amplification and Auto-Inflammation." *Nature* 517 (7532): 89–93.
<https://doi.org/10.1038/nature13801>.
- Zhao, Yingxin, Gustavo Valbuena, David H. Walker, Michal Gazi, Marylin Hidalgo, Rita DeSousa, Jose Antonio Oteo, Yenny Goetz, and Allan R. Brasier. 2016. "Endothelial Cell Proteomic

Response to *Rickettsia Conorii* Infection Reveals Activation of the Janus Kinase (JAK)-Signal Transducer and Activator of Transcription (STAT)-Interferon Stimulated Gene (ISG)15 Pathway and Reprogramming Plasma Membrane Integrin/Cadherin Signaling.” *Molecular & Cellular Proteomics* 15 (1): 289–304. <https://doi.org/10.1074/mcp.M115.054361>.

Zhou, H., M. Suzuki, G. Randers-Pehrson, D. Vannais, G. Chen, J. E. Trosko, C. A. Waldren, and T. K. Hei. 2001. “Radiation Risk to Low Fluences of Alpha Particles May Be Greater than We Thought.” *Proceedings of the National Academy of Sciences of the United States of America* 98 (25): 14410–15. <https://doi.org/10.1073/pnas.251524798>.